17610

NATIONAL LIBRARY
OTTAWA

CANADA

BIBLIOTHÈQUE NATIONALE
OTTAWA

NAME OF AUTHOR........Edward C. McRoberts........

TITLE OF THESIS........Stability of Slopes in Permafrost........

....

....

UNIVERSITY........ALBERTA........

DEGREE FOR WHICH THESIS WAS PRESENTED........~~1973~~ Ph.D.

YEAR THIS DEGREE GRANTED........1973........

Permission is hereby granted to THE NATIONAL LIBRARY OF CANADA to microfilm this thesis and to lend or sell copies of the film.

The author reserves other publication rights, and neither the thesis nor extensive extracts from it may be printed or otherwise reproduced without the author's written permission.

(Signed)........Edward C McRoberts........

PERMANENT ADDRESS:

Dept of Civil Eng
U of A
Edmonton Alta

DATED........5 Oct........1973

NL-91 (10-68)

THE UNIVERSITY OF ALBERTA

STABILITY OF SLOPES IN PERMAFROST

by

© EDWARD CHARLES MCROBERTS

A THESIS
SUBMITTED TO THE FACULTY OF GRADUATE STUDIES
AND RESEARCH IN PARTIAL FULFILMENT OF THE
REQUIREMENTS FOR THE DEGREE OF
DOCTOR OF PHILOSOPHY

DEPARTMENT OF CIVIL ENGINEERING
EDMONTON, ALBERTA
FALL, 1973

THE UNIVERSITY OF ALBERTA

FACULTY OF GRADUATE STUDIES AND RESEARCH

The undersigned certify that they have read, and recommend to the Faculty of Graduate Studies and Research for acceptance, a thesis entitled "STABILITY OF SLOPES IN PERMAFROST" submitted by Edward Charles McRoberts in partial fulfilment of the requirements for the degree of Doctor of Philosophy in Civil Engineering.

....
N.R. Morgenstern, Supervisor

Thomson
....
S. Thomson

....
D.M. Cruden

....
D. Gill

J. R. Mackay
....
J.R. Mackay, External Examiner

Date: 5 October 73

ABSTRACT

This thesis is concerned with two major geotechnical aspects of landslides in periglacial regions: the classification of mass movements in soil; and a quantitative understanding of the mechanics of failure.

A study of landslides in the Mackenzie River Valley, NWT, based on a detailed inspection of aerial photographs and field exploration undertaken by boat, fixed-wing and helicopter traverses coupled with a drilling programme has given considerable insight into the possible range of landslide types. With this foundation, and complemented by a geotechnical appreciation of the pertinent literature, landslides have been subdivided, in a descriptive classification, into the categories of fall, flow and slide-dominated movements.

Periglacial landslides can be considered mechanistically in three groups; that is, in thawing, freezing and frozen soils. The most impressive and best-documented landslides are associated with the onset of thaw and are described as solifluction, skin flows and bi-modal flows. Factors affecting the thaw of frozen soils have been studied and a mechanistic interpretation of low angle slope movements has been gained by coupling thaw-consolidation theory with an infinite slope limit equilibrium analysis. The study of the behaviour of soils at high void ratios has been extended by considering a theory of sedimentation which has been modified to account for sedimentation-consolidation and thaw-sedimentation. Parametric studies using experimentally-observed flow laws in ice and frozen soils emphasize the possibility of creep in frozen soils. Other studies on large landslides such as block and MR slides confirm that shear failure can occur through frozen soil and conventional stability analyses with suitable shear strengths can account for limiting equilibrium conditions. Certain aspects of the load-deformation response of frozen soil have been reviewed in detail and yield valuable insight into mass movement mechanisms. In freezing soils it is possible to create instability in saturated coarse-grained soils when pore water is expelled from an advancing ice-water interface. Instability results from excess pore pressures set up due to the impeded drainage of expelled water. This phenomenon is also possible in fine-grained soils which expel rather than attract water at higher stress levels.

Some engineering considerations of landslides in the Mackenzie River Valley have been presented by synthesizing the observations of landslide types and occurrence with the proposed mass-movement mechanisms. Special attention has been given to the initiating and sustaining mechanisms.

ACKNOWLEDGEMENTS

It is impossible to give full credit to all the people and organizations who gave assistance in the preparation of this thesis. Singled out for my particular thanks are: Dr. N.R. Morgenstern, my advisor, for his interest, counsel and guidance; the remainder of my oral committee for their assistance at various times; Messrs. W.D. Roggensack and D. Pufhal for their able and willing help during the field programme; Dr. J.F. Nixon, for his aid in the field and his assistance in the preparation of Appendix C; the Geologic Survey of Canada, Mackenzie Valley Pipeline Research Limited and Canadian Arctic Gas Systems Limited for providing funds for field exploration; and, finally, the Izaak Walton Killam Memorial Fellowships, the National Research Council of Canada and the Department of Civil Engineering, University of Alberta for providing scholarships and financial assistance.

TABLE OF CONTENTS

Page

Release Form (i)

Title Page (ii)

Approval Sheet (iii)

Abstract (iv)

Acknowledgements (vi)

Table of Contents (vii)

List of Tables (ix)

List of Figures (x)

List of Plates (xiv)

CHAPTER I THE SINGULAR NATURE OF PERIGLACIAL MASS-MOVEMENTS

1.1 Introduction 1

1.2 The Study Area in relation to the Periglacial Region 2

1.3 Scope of the Thesis 3

1.4 A Review of Periglacial mass-movements 4

CHAPTER II THE LANDSLIDES AND THE ENGINEERING GEOLOGY OF THE STUDY AREA

2.1 Landslide Classification 45

2.2 Quaternary Geology 59

2.3 Permafrost Conditions 64

2.4 Geotechnical Considerations 71

2.5 Observations on Terrain Disturbance 75

CHAPTER III THAW-DOMINATED MASS-MOVEMENTS

3.1 Introduction 93

3.2 Some Aspects of the Thaw of Soils 94

3.3 Instability Mechanisms in Thawing Soils 105

3.4 The Ablation Problem 122

3.5 Other Processes in Thawing Slopes 126

Page

CHAPTER IV INSTABILITY IN FREEZING SOILS

4.1 The Phenomenon of Pore Water Expulsion in Freezing Soils 151

4.2 Mathematical Models 158

4.3 Some Consequences of Pore Water Expulsion 164

4.4 The Importance of Freezing in Solifluction 167

CHAPTER V MASS-MOVEMENTS IN FROZEN SOILS

5.1 Introduction 178

5.2 Secondary Creep Model 182

5.3 Mass-movements due to Shear Displacements 193

CHAPTER VI SOME ENGINEERING CONSIDERATIONS OF LANDSLIDES IN THE MACKENZIE RIVER VALLEY

6.1 The Initiation of Landslides 219

6.2 The Continuing Degradation of Frozen Slopes 227

6.3 Stabilization of Landslides 231

CHAPTER VII CONCLUDING REMARKS 234

BIBLIOGRAPHY 239

APPENDIX A FIELD OBSERVATIONS

A.1 Observations on Landslides in the Vicinity of the Mackenzie River Mile 205 to 660 249

A.2 Observations on Permafrost Conditions in Relation to Landslides 275

APPENDIX B BOREHOLE LOGS AND GEOTECHNICAL TEST DATA 306

APPENDIX C THE SEDIMENTATION OF SOIL

C.1 Introduction 323

C.2 Development of the Theory of Sedimentation 327

C.3 Experimental Verification of Sedimentation 334

C.4 Sedimentation Consolidation 336

C.5 Thaw-sedimentation 341

APPENDIX D THE SOLUTION FOR THE FLOW SPECIFIED SEEPAGE PROBLEM 366

LIST OF TABLES

Table		Page
1.1	Comparison of solifluction terminology	31
1.2	Pliestocene solifluction slopes	32
1.3	Some reported solifluction slopes	33
1.4	Frost heave, potential frost creep and recorded movements, Northern Norway	38
1.5	Slope angle and index properties, Mesters Vig	39
1.6	Comparison of failed and predicted solifluction slope angles	40
1.7	Summary of flows	41
2.1	Summary of skin flows	83
2.2	Summary of bi-modal flows	84
2.3	Summary of MR flows	85
2.4	Summary of block slides	86
2.5	Summary of MR slides	87
2.6	Summary of ice wedge occurrence	88
3.1	Albedo of various surfaces	129
3.2	Ratio of components of the energy balance	130
3.3	Some values of net radiation and incoming solar radiation	131
3.4	Case histories for rate of thaw	132
3.5	Summary of sedimentation tests	133
3.6	Summary of critical depths	134
3.7	Summary of the rate of movements of headscarps in bi-modal flows	135
4.1	Freezing data on Ottawa Sand	170
4.2	Freezing tests on Russian soils	171
4.3	Expulsion/attraction tests in Devon Silt	172
5.1	Summary of long-term frozen shear strengths	205
5.2	Summary of shear strength test information for frozen Mountain River soils	206
B.1	Index properties	307
B.2	Field water contents: summer survey	308
B.3	Summary of grain size characteristics for all boreholes	309
C.1	Soils considered in sedimentation theory	344

LIST OF FIGURES

Figure		Page
1.1	Location of the study area	44
2.1	Landslide classification	89
2.2	Results of field piezometer tests	90
2.3	Permafrost distribution adjacent to a high river bank	91
2.4	Typical gully formation adjacent to flow landslides	92
3.1	Ground surface temperatures in the Mesters Vig	136
3.2	Rate of thaw for sinusoidal surface temperature	137
3.3	Effect of T_s on rate of thaw	138
3.4	Measured rates of thaw	139
3.5	Comparison of measured and predicted rates of thaw	142
3.6	Depth of thaw under organic covers	143
3.7	Infinite slope analysis formulation	145
3.8	Solution to the infinite slope analysis in terms of the ratio R	146
3.9	Solution to the infinite slope analysis in terms of T_s and c_v	147
3.10	Void ratio versus effective stress, permeability and coefficient of consolidation for Fort Norman silt	148
3.11	Characteristic hindered settling and post-sedimentation settlement behaviour	149
3.12	Graphical solution to the ablation problem	150
4.1	Closed and open system freezing tests	173
4.2	Two-dimensional freezing problem	174
4.3	Solution to the flow specified problem	175
4.4	Comparison with a finite element solution	176
4.5	Solution to a typical freezing problem	177
5.1	The flow law for ice	207
5.2	Solution to the infinite slope creep problem	208
5.3	The flow law for ice compared with secondary creep rates in soil	209
5.4	Unconfined long-term strength data for Sault Ste. Marie Clay	210
5.5	Unconfined long-term strength data for a fat clay	211

LIST OF FIGURES (Continued)

Figure		Page
5.6	Stress-strain relationships for frozen Mountain River silts	212
5.7	Long-term strength for Mountain River silt	213
5.8	Frictional response of frozen soil	214
5.9	Long-term frictional response	215
5.10	Unconfined long-term strength tests	216
5.11	Mountain River slide cross-section	217
5.12	Results of slope stability calculations	218
6.1	Methods of initiation of bi-modal flows	233
A.1	Mile 205 - 285	280
A.2	Fort Simpson landslide	281
A.3	Fort Simpson landslide	282
A.4	Mile 285 - 315	283
A.5	Mile 313 - 355	283
A.6	Mile 355 - 394	284
A.7	Mile 394 - 426	284
A.8	Mile 440 - 491	285
A.9	Mile 455 - 470	286
A.10	Mile 470 - 488	287
A.11	Big Smith Creek landslide	288
A.12	Old Fort Point landslide	289
A.13	Old Fort Point landslide, sketch plan	290
A.14	Mile 497 - 565	291
A.15	Fort Norman landslide	292
A.16	Little Norman landslide	293
A.17	Sans Sault Rapids area	294
A.18	Hanna Island landslide	295
A.19	Mountain River: site plan	296
A.20	Mountain River: profile	297
A.21	Hanna River landslide	298
A.22	Hume River Site HU1: site plan	299

LIST OF FIGURES (Continued)

Figure Page

A.23 Hume River Site HU1: profile 300

A.24 Hume River Site HU2 301

B.1 Mountain River M1 borehole log 310

B.2 Hume HU1-1 borehole log 311

B.3 Hume HU1-2 borehole log 312

B.4 Hume HU1-3 borehole log 313

B.5 Water (ice) content versus depth for M1 314

B.6 Water (ice) content versus depth for HU1-1 315

B.7 Water (ice) content versus depth for HU1-2 316

B.8 Water (ice) content versus depth for HU1-3 317

B.9 Plasticity chart for Mackenzie River clays 318

B.10 Liquid limit versus % clay fraction Mackenzie River clays 319

B.11 Grain Size curves: summer survey 320

B.12 Grain Size curves: Mountain River site 321

B.13 Grain Size curves: frozen strength samples 321

B.14 Void ratio versus permeability and effective stress for Mountain River silt 322

C.1 Characteristics of hindered settling sedimentation 345

C.2 Sedimentation mode: concave down flux plot 346

C.3 Sedimentation mode: concave up flux plot 347

C.4 Normalized flux plot: Richardson-Zaki relationship 348

C.5 Generalized sedimentation modes for hindered settling 349

C.6 Hindered settling for Devon Sand 350

C.7 Hindered settling for grit 351

C.8 Hindered settling for Fort Norman Silt 352

C.9 Hindered settling for Devon Silt 353

C.10 Richardson-Zaki correlations 354

C.11 Richardson-Zaki correlations 355

C.12 Normalized flux plot: Fort Norman Silt 356

C.13 Normalized flux plot: Devon Silt 356

C.14 Normalized flux plots 357

C.15 The sedimentation-consolidation problem 358

LIST OF FIGURES (Continued)

Figure		Page
C.16	Solution for the excess pore pressures in a sedimented soil at the completion of sedimentation	359
C.17	Hindered settling and subsequent consolidation: Fort Norman Silt	360
C.18	Consolidation due to head imbalance: Fort Norman Silt	361
C.19	Hindered settling	362
C.20	Consolidation due to head imbalance	362
C.21	Hindered settling stirred Fort Norman silt	363
C.22	Comparison of observed and predicted settlement and pore pressures, Fort Norman silt	364
C.23	The thaw-sedimentation problem	365

LIST OF PLATES

Plate		Page
1	Fort Simpson landslide, an MR flow	302
2	Skin flows near the Wrigley River	302
3	Big Smith Creek landslide, a bi-modal flow	302
4	Old Fort Point landslide, a bi-modal flow	303
5	Ice Buttress landslide, a bi-modal flow	303
6	Fort Norman landslide, a bi-modal flow	303
7	Block slide at Mile 655	304
8	Hanna Island landslide, a bi-modal flow	304
9	Mountain River landslide, an MR slide	304
10	Falls on the Mountain River	305
11	Hume River, site HU1-1	305
12	Hume River, site HU1-1	305

CHAPTER I

THE SINGULAR NATURE
OF PERIGLACIAL MASS MOVEMENTS

1.1 Introduction

With the burgeoning pressure of economic need the cold regions of the world are now beginning to be exploited in earnest. This accelerating rate of development coupled with an increased awareness of environmental effects is making new demands on the geotechnical profession. In particular, the requirement for a basic understanding of the processes and mechanisms of mass movement is now of vital importance in order that design and development can continue apace. This thesis is, therefore, concerned with both an investigation of the mechanics of mass movement in the so-called periglacial environment and the classification of observed landslide types.

A geotechnical appraisal of the range of periglacial mass movements encountered in the cold regions of the world quickly concludes that most of the landslide forms encountered are unique to that area. The landslides are singular when compared with the types of mass movement forms encountered in other regions in that they cannot be completely described using conventional geotechnical practice. The peculiar features of these mass movements, found in Alpine, Sub-arctic and Arctic Regions, have attracted the attention of investigators for many years and an extensive literature has been built up describing the greater part of these unique phenomena. The main part of this literature describes in qualitative terms the processes encountered while, on the other hand, less information of a quantitative nature can be found. In turn, much of it has been gathered without due regard to the nature of the mass movement mechanisms effecting the processes observed.

This thesis seeks to answer the demand for a detailed and quantitative understanding by identifying a range of possible mass movement mechanisms and by comparing them with reported phenomenon and with landslide types observed during the course of field exploration. We shall see that there are many aspects of slobe stability in freezing, thawing or frozen soils that established geotechnical practice in unfrozen or long-thawed soils cannot predict. Further, it will become evident that while possible mechanisms have been identified there are significant gaps in our knowledge that must be studied before complete and confident recommendations can be made for quantitative design procedures.

1.2 The Study Area in Relation to the Periglacial Region.

Given the vast extent of those areas that, today, can be called periglacial it was necessary to focus attention on a study area that was both representative yet readily accessible so that a realistic range of actual slope processes could be studied in the field.

It is first useful, however, to briefly consider what is meant by the term periglacial. It has been pointed out by Bird (1967) that the definition of this term has not been consistent. The term was originally used to refer to areas lying near the margins of Pleistocene ice and was extended by Embleton and King (1968, p. 448) to describe a zone peripheral to glacial ice, past or present. Both Bird and Carson and Kirkby (1972) find merit in describing the periglacial zone as being coincident with permafrost regions. Bird suggests that a better practical boundary is obtained from vegetation and that the periglacial zone includes the arctic tundra zone of the boreal forest. Therefore, the periglacial region can be seen to be a useful term for the cold regions of the world and is used in this sense in this thesis.

The study area that was chosen for consideration is situated in the vicinity of the Mackenzie River between Fort Simpson, Mile 205, and north to above the Ramparts at Mile 660. This area is within the discontinuous permafrost zone as defined by Brown (1970) and is completely within the Boreal Forest zone. As such it is not entirely representative of the complete periglacial environment but, nevertheless, has proved to be an adequately representative area for field study. The study area is shown on Fig 1.1.

The study area was first examined in detail on aerial photographs during the fall of 1971 and flown over briefly during September 1971. A detailed field reconnaissance was undertaken by a river-based operation, supplemented by helicopter surveys, during the summer of 1972 and a detailed field drilling programme was conducted during March, 1973. The observations made during the course of the field exploration are essentially confined to non-bedrock slopes and in particular to the glaciolacustrine or glacial lake basin (GLB)* soils found in all parts of the study area.

1.3 Scope of the Thesis

The primary aim of this thesis is to investigate possible mass movement failure mechanisms for landslides in periglacial regions. However, in order to acquire detailed first-hand knowledge of actual slope processes it was necessary to derive a working classification of landslides within the study area. Therefore, the proposed classification as well as the attendant observations on landslide morphology, permafrost conditions and allied geotechnical considerations form a significant part of this thesis.

The periglacial mass movement literature is reviewed in the remainder of Chapter I and an engineering classification of the landslides of the study area presented in Chapter II. Both the review of the periglacial literature and the engineering classification derived have been developed using a purely descriptive classification. The most trying aspect of a review of the periglacial landslide literature is the almost endless proliferation and mixing of descriptive and mechanistic terms. Considerable debate centres around the use of genetic or mechanistic terms used to catalogue the various processes and for this reason the review of Chapter I and the classification presented in Chapter II are based on a descriptive framework. Furthermore, the review in Chapter I is developed under the headings of solifluction, flow, slide and falls; a distinction which anticipates the classification presented in Chapter II.

---

* This abbreviation will be used throughout the thesis.

The remainder of Chapter II concerns itself with aspects of the engineering geology of the study area.

The next three chapters, III, IV and V, describe mass movement mechanisms for thawing, freezing and frozen soils and compare the models derived with the landslide phenomena observed in Chapters I and II.

Chapter VI discusses the initiation and occurrence of landslides in periglacial regions and Chapter VII presents some conclusions.

1.4 A Review of Periglacial Mass Movements

1.4.1 Solifluction

(i) Introduction

This section seeks to present a review of the salient geotechnical features of solifluction mass movements and is restricted to those case histories in which either quantitative information is reported or where detailed qualitative observations are given. Many difficulties and contradictions arise in the description and classification of active layer mass movement processes and they have been reviewed by Washburn (1967) who differentiates between solifluction and frost creep. He considers frost creep as

> "the ratchet-like downslope movement of particles as the result of frost heaving of the ground and subsequent settling upon thawing, the heaving being predominantly normal to the slope and the settling more nearly vertical."

However, there is no succinct definition of solifluction given by Washburn who, in fact, finds merit in the use of the term gelifluction or congelifluction to distinguish from solifluction which, in his view, should not be limited to cold climate phenomena. It is apparent from a review of the literature that these difficulties in terminology arise from an unfortunate mixing of descriptive classification and of proposed mass movement mechanisms. For geotechnical purposes it is argued that solifluction is an established term for a type of mass movement common to cold regions that can be pictorially described without recourse to mechanistic arguments.

Creep is also considered by many to be an important aspect of shallow periglacial mass movement. Carson and Kirkby (1972) distinquish between continuous creep operating under the direct action of shear stress and seasonal creep caused by various processes in a zone of seasonal fluctuations. In cold regions continuous creep stems from the inherent rheologic properties of frozen or thawing soil while seasonal creep is equivalent to frost creep.

Although there is general agreement as to what periglacial features constitute solifluction there is a wide range of terminology used in describing these features. Table 1.1 presents a summary of some of the terms used in the various classifications for arctic, sub-arctic and alpine regions. Capps (1919 and 1940) describing slow soil flows in the Kantishna Region of Alaska notes that these mass movements are large and numerous only in permafrost regions, that movement is restricted to the thawing active layer, and that slow flows are restricted to soils having large water contents. Although Capps points out that there are gradational phases between any form of movement he isolates certain forms of solifluction movements, Table 1.1. Striped slopes are found on high slopes with little or scanty vegetation and results in a smooth rounded slope profile with a striped arrangement of rock particles and vegetation along lines of downslope movement. A second type results when soil movements are constrained by vegetation and is described as follows:

> " After the superficial layer of muck and soil has thawed the semi-fluid mass tends to sag down the hillside stretching the turf into a flat, bulbous form. As the turf is tenacious and feltlike, however, it stretches but does not break ...... In this way a hillside may be entirely covered by mammillary lobes, closely grouped and constantly creeping downhill."

Capps reports that the lobes vary in size from small flows with lobes a few feet in height and width at the front edge to large movements with 8 to 10 ft high scarps and with frontal widths up to several hundred feet. At some locations a hillside may be covered by many small separate lobes. Another variety appears as long wavelike terraces with successive waves appearing one above the other and these movements are common on slopes as low as 10°.

Sigafoos and Hopkins (1952) describe solifluction forms in Northern Alaska and identify features described as solifluction terraces (soil or altiplanation terraces), solifluction lobes and stripes.

In a review of mass wasting processes on Victoria Island in the Canadian Arctic, Washburn (1947) isolates features described as solifluction sheets, lobes, streams and stripes, co-existing on a solifluction slope. Some solifluction sheets lack distinct upper and lower margins whereas in others well-defined lower margins occur where encroaching sheets move out over stationary soils. In some cases these frontal segments are nearly straight while others are lobate. Washburn finds that solifluction streams occur when soil movements become laterally confined and that many streams can grade into a sheet. In turn, many sheets are characterized by stripes trending in the direction of the steepest available slope. Active stripes have been noted on slopes as low as 5° to 6°. Washburn concludes that:

> "Characteristically, solifluction slopes present an assemblage of forms, and frequently the assemblage is so complicated that it becomes practically impossible to single out the component parts. Thus, solifluction sheets or streams are found singly or together and with or without solifluction fronts, lobes, and stripes; but either singly or together they enter into the make-up of a solifluction slope."

Subsequent to his field work in the Canadian Arctic, Washburn (1956) presented a classification of solifluction movements by delineating features on a descriptive basis, Table 1.1. Steps are patterned ground where a series of terraces can be found one on top of the other. Non-sorted steps have a vegetation covered embankment while sorted steps have a border of stones. Sorted stripes are formed by lines of stones and finer soils while non-sorted stripes describe alternating lines of vegetated and relatively bare ground.

Adopting a descriptive terminology based on the parameters used by Washburn (1956), Benedict (1970) describes solifluction features found in the high alpine environment of the Colorado Front Range, Table 1.1.

(ii) Quantitative Aspects of Solifluction Movements

A peculiar feature of solifluction movements is instability on low angle slopes. Evidence of these low angle movements exists in the fossil features of the Pleistocene periglacial zone and some typical case histories are noted in Table 1.2. Many active features have been observed in contemporary periglacial areas and movements have been observed on low slopes, Table 1.3.

Knowledge of the rate of solifluction movements can be of interest and have been the subject of much active field measurement. Movement rates on both low and high angle slopes from arctic, sub-arctic and alpine environments in a variety of soil types are presented in Table 1.3. Large downslope movements have also been inferred for certain fossil solifluction slopes, Table 1.2. Many authors attribute the movements to a combination of frost creep, creep and solifluction. Velocity profiles have been measured at a variety of sites and, characteristically, they have a concave downslope profile (see Carson and Kirkby, 1972).

There is a tendency among some authors to seek a relationship between rates of movement and some function of the slope angle. Washburn (1967) reports a linear relation between annual movement and the size of the slope angle. Although the relationship is presented as being a good fit among average measurements the apparent standard deviation is high. Higashi and Corte (1971) conducted model experiments on solifluction and report a linear relation between movement and the tangent squared of the slope angle. There is no apparent justification for these relationships.

The process of frost creep has been the subject of considerable investigation as it is amenable to direct field measurement. The theoretical, or potential, frost creep downslope movement, D, results when a soil surface freezes and heaves, perpendicular to the slope, a distance H, and can be related by:

$$D = H \tan \theta \tag{1.1}$$

where θ is the slope angle

The actual frost creep equals the potential if, on thaw, the soils settle vertically. However, as pointed out by Carson and Kirkby (1972) the heaved soil seldom settles vertically but has an apparent upslope component of movement and both Washburn (1967) and Benedict (1970) note retrograde movements that considerably lessen the total movement that can be attributed to frost creep.

Field measurements of frost creep also suggest that its importance may be overstated. Williams (1966) infers the amount of heave, H, required to account for recorded downslope movements using

Eq 1.1. He finds that the frost heave required, H, to account for the measured displacement, D, unrealistically high when compared to the observed ice stratigraphy and rejects the likelihood of frost creep in accounting for observed winter movements. Washburn (1967) reports an average winter movement of 1.2 cm occurring on a slope of 2.5°. Eq 1.1 predicts a required heave of 28 cm but vertical deformations of this order of magnitude are not reported. Jahn (1961) considering frost heave on a 4° slope in Spitsbergen finds that the measured heave of 15 cm predicts a movement of 1 cm which is considerably less that the total downslope movement of 3 cm measured during spring thaw. A comparison of frost heave, potential frost creep calculated by Eq 1.1 and recorded movements for solifluction slopes in Northern Norway is given in Table 1.4, and it can be seen that total measured downslope movements are greater than movements that can be attributed to frost creep. Benedict (1970) measures both frost heave and downslope winter movements on a solifluction lobe of known angle and finds that actual movements are at least double winter movements.

Winter excavations in a solifluction lobe on Garry Island show that numerous horizontal to vertical ice veins ranging from a fraction to several mm in thickness cut across the frozen active layer (Kerfoot and Mackay, 1972). It is also noted that the curvature of tubes installed to monitor slope movements have a marked tendency to kink or bend at the base of the active layer and it is suggested that downslope movement is aided considerably by the freeze-thaw of these ice veins.

(iii) Soil Characteristics

Movements due to solifluction or frost creep are favoured in fine-grained soils. Jahn (1960), commenting on the relative lack of movement on rock slopes on Spitsbergen, notes that the slopes lack fine material which is indispensible for solifluction movements. Benedict (1970), Washburn (1967) and Chandler (1972) all present detailed documentation on the large percentage of fine-grained soils involved in slow downslope movements.

Washburn (1947) comments on well-developed solifluction sheets moving downslope and engulfing old strand lines and notes the significant difference in soil composition between the till-like solifluction sheet with abundant clay and silt and the well-sorted beach debris. As the climatic conditions will be essentially identical for both segments of the slope, the effect of soil composition is evident. A comparison of slope angle and index properties for slopes in the Mesters Vig, Greenland, is presented in Table 1.5, drawn from data in Washburn (1967). It can be seen that a tendency towards lower slope angle exists in those slopes with increased fines.

The intense sorting action characteristic of periglacial environments also aids slope movement. Separation of coarse and fine-grained soils conditions the slope by concentrating the finer-grained, more frost or thaw susceptible, soil at depth. As pointed out by Corte (1963) both vertical and horizontal sorting can occur. Corte (1963, p.132) presents an excellent photograph of the intense vertical sorting that has occurred in the active layer in Thule, Greenland. Washburn (1967) notes that at sites ES7 and ES8 that the top several centimeters are coarse and have boulder concentrations and that the fines increase with depth.

The consequences of horizontal sorting apparently causes the sorted stripes common to some solifluction slopes and the concentration of fines favouring slope movement processes result in the relatively greater movement of the finer soil as noted by Benedict (1970).

(iv) The Importance of Freeze and Thaw

It is generally agreed that solifluction movements occur during the spring thaw and that water is "involved" in these movements. It is generally agreed, usually implicitly but also explicitly, that this water comes from the thawing of frozen ground. It is also agreed, albeit for a wide variety of reasons, that the freeze-thaw cycling of a periglacial zone is vital to solifluction.

Paterson (1940), discussing the importance of freeze and thaw on solifluction, concludes:

> "it appears, therefore, that the decisive factor is the amount of soaking of the ground, and that the extensive occurrence of solifluction in cold regions is due to the greater tendency to earth-soaking during a thaw succeeding a period of intensive frost when water is held up as ice."

Taber (1943), as a result of his earlier work in frost susceptibility, comments on the consequences of ice segregation on freeze back and the resulting instability on thaw. A description of the instability of solifluction slopes during thaw given by Washburn (1947) can hardly be improved on:

> "The completely saturated condition of a solifluction slope during the spring thaw is the most important factor in movements. In the spring, when excavations were made in solifluction fronts, water invariably trickled down over the exposure. Trenches cut into the surface of a lobe collapsed at the sides and formed a runway for miniature mudflows. A completely saturated condition also characterizes the upper portions of a solifluction sheet. On June 17, solifluction slopes on the southwest side of Mount Pelly sparkled with water, especially where the vegetation was thick, and apparently firm ground on the summit plateau was so soft and capable of flowage that the writer sank to his ankles in the stoney, clayey mass .... By July 9, this area was quite firm underfoot."

Barnett (1966), in a study of certain slope forms in the Canadian Arctic, feels that downslope movements are confined to the spring thaw season. Similar studies by Smith (1960) in South Georgia; Rapp (1960 and 1962) in the Karkevagge area of Sweden; Harris (1972) in Northern Norway, and Jahn (1961) in Spitsbergen, also emphasize the importance of the thaw season in controlling solifluction movements.

The importance and association of freeze and thaw in solifluction movements stems from characteristic properties of the fine-grained soils common to solifluction slopes. During the freezing cycle the fine-grained soils bulk and develop ice lenses as water is attracted to the freezing front. On the completion of freeze back the active layer of the zone of seasonal frost penetration has then undergone a net increase in volume, as witnessed by the amount of heave that can be measured. Then, during the following thaw cycle, instability results because of the characteristic mechanical properties of low permeability and high compressibility of the fine grained soil. The detailed mechanisms of instability will be considered later and we shall, for now, follow Jahn (1970) and Benedict (1970) in noting that this process of volume increase is vital in conditioning a slope for solifluction movements during spring thaw. Benedict (1970) states that:

> "Although much of the alpine region is saturated during the spring thaw significant solifluction occurs only in areas where the water table remains high enough during the fall freeze to permit thick ice-lense development."

As the result of many years of observations in Greenland, Washburn (1967) notes that solifluction movements during the spring thaw were greater in those sites that were wet and saturated during the preceding autumn freeze-back. As these sites were in frost susceptible soils with 30 to 45% fines it is felt that bulking or ice lensing contributed to the solifluction movements. The importance of moisture migration to the freezing front is also reviewed by Jahn (1970). Harris (1972) notes that movement rates are higher in sites where soils are saturated during thaw.

Although many workers dwell on the importance of snow melt and atmospheric water sources in influencing solifluction, it is felt that the main influence is indirect. While summer rainfall or snow melt may increase the rate of thaw or increase the stress imbalance in a thawing slope the dominant influence of wet summer conditions is to contribute to saturated conditions at the onset of freeze back. These saturated conditions, therefore, ensure an adequate water supply for frost heaving. The presence of an impermeable frozen layer in permafrost terrain contributes to this conditioning. Washburn (1947) is partly aware of this distinction and comments that although melt water from snow may aid solifluction there is no reason to believe that it is a requisite condition for solifluction. However, Washburn also applies the same argument to the water derived from ice lenses, and we shall see in a later chapter that ice lenses exert an important control on stability during the thaw cycle.

(v) Mechanics of Solifluction

We have seen that solifluction occurs predominantly in fine-grained soils on low angle slopes and that movements are primarily restricted to the spring thaw period. Representative mechanisms must then account for these factors in a quantitative manner.

A wealth of geotechnical experience in temperate regions suggests that it is entirely appropriate to consider the stability of long shallow solifluction slopes using the infinite slope analysis. It is well-known that, in this case, by applying a statical balance of forces the factor of safety of a slope, F_s, becomes:

$$F_s = \frac{\gamma' \tan \phi'}{\gamma \tan \theta} \quad (1.2)$$

where γ'/γ is the ratio of effective to total unit weight and is generally about 1/2

ϕ' is the angle of shearing resistance in terms of effective stress ($c' = 0$)

θ is the slope angle

As solifluction slopes can undergo large displacements, it is appropriate to introduce a residual value for the strength parameter in Eq 1.2. Eq 1.2 then predicts that slopes should be stable at angles less than given by the following expression:

$$\tan \theta = \frac{\gamma' \tan \phi'_r}{\gamma} \quad (1.3)$$

However, it is found that when conventional limit equilibrium analysis is applied to actual solifluction slopes, movement or unstable slopes are found on slope angles much less than predicted by Eq 1.3. Field investigation on fossil solifluction slopes and on active slopes in contemporary periglacial areas indicate that movements can occur on slopes at angles considerably less than predicted. A summary of available quantitative case histories is given in Table 1.6 and it can be seen that the failed angle is considerably less than the predicted angle using Eq 1.3.

Eq 1.2 has been developed using the maximum hydrostatic pore pressure condition of parallel to the slope seepage in conjunction with the lowest possible residual angle. Assuming that it is appropriate to use a residual angle derived from conventional testing practice, then excess pore pressures are required to account for low angle movements. Expressing the pore pressure, Pw, in terms of the ratio:

$$r_u = \frac{P_w}{\gamma Z} \quad (1.4)$$

where γZ is the total stress

it is possible to express the amount of excess pore pressure required to predict failure by Eq 1.2, see Table 1.6. Noting that for most conditions $r_u = 0.5$ is a measure of the maximum hydrostatic pore pressure, the relative amount of excess pore pressure required to induce failure is apparent in Table 1.6.

Weeks (1969) and Chandler (1970) invoke a mechanism of differential freezing and ice-blocked drainage to account for excess pore pressure and which is identical to a mechanism of ice block drainage already suggested by Siple (1952). Although this mechanism is possible it will not explain movements during spring thaw, which, as has been shown, are the most significant in contempory periglacial areas. Furthermore, during freeze back of typical fine-grained solifluction soils, pore water tensions, or at least pressures less than hydrostatic, can be expected due to ice lense formation processes and it has been noted that bulking and ice lensing is vital to solifluction movements. Therefore, although excess pore pressure resolves the problem, it is unlikely that the ice-blocked drainage process is a dominant mechanism.

Excess pore pressures have been measured in the field, in an active solifluction slope in Spitsbergen by Chandler (1972). Using open standpipe piezometers r_u values of from 0.60 to 0.84 were measured at depths of from 0.2 to 0.58 m. These values compare favourably with the required values given in Table1.6for this site. In addition to the ice-blocked drainage mechanism discussed above, Chandler (1972) also suggests that permeability contrasts within the slope profile can contribute to artesian conditions.

A process that is unique to thawing ground phenomena and which resolves this paradox of movement on low angle slopes within the concept of limit equilibrium is what has come to be termed thaw consolidation. The concept of consolidation in thawing soils was formulated in a correct manner by Morgenstern and Nixon (1971), and applied to the prediction of thaw slope stability by McRoberts (1972). The theory, which will be developed in a later chapter, predicts that excess pore pressures can be generated during the thaw of fine-grained soils. When frozen ground thaws, water is released; settlements develop as the water is squeezed from the ground and, if water is generated at a rate exceeding the discharge capacity of the soil, excess pore pressures may be set-up. The prediction of instability on low angle slopes results from the input of excess pore pressures due to thaw consolidation which, in turn, reduces effective stress and thus the available shear strength along a slip plane.

Many aspects of thaw consolidation theory have been confirmed by laboratory testing and positive excess pore water pressures have been measured in the laboratory on natural soil samples (Nixon, 1973). Excess pore pressures have been recorded in the field under an instrumented oil pipe thaw test and thaw consolidation theory accurately predicts the measured pore pressures (Nixon, 1973).

Taber (1943) has discussed in qualitative terms the basic ideas involved in thaw consolidation (see also Sec 1.4.2) and Williams (1959) is aware of the implications and comments that:

> "it is often tacitly assumed that, in thawing of soil where considerable water accumulation has occurred at freezing, conditions of hydrostatic excess pressure will arise generally and contribute in considerable measure to instability."

However, he rejects the importance of this phenomena based on the results of pore pressure measurements that record tensions in the recently thawed soil of active solifluction slopes (Williams, 1959 and 1966). For one site movement is documented on a 22-1/2° slope and Eq 1.3 would require a residual angle of some 45° to account for instability with full hydrostatic pore pressure conditions. As a lower residual angle might be considered appropriate pore water sub-pressures are consistent with movements on this high angle slope. Tensiometers have also been used by Harris (1972) to study pore pressure conditions in a non-permafrost site in Northern Norway. For all the sites studied, positive pressures indicating saturated conditions are noted until thaw, which is observed with thermistor strings, is completely over. Immediately after thaw, tensions build up rapidly, either due to desaturation or downwards flow, and it might be expected that similar conditions apply to the sites studied by Williams.

A mechanism of true lubricated flow of soil layers is proposed by Carson and Kirkby (1972) which is similar to thaw consolidation. The authors comment on the importance of slow freezing in which large amounts of water are drawn up into the soil and the subsequent effect of rapid thaw in some way producing instability.

Low angle solifluction movements, on the other hand, present no conceptual problems to those investigators who emphasize the so-called flow aspect of solifluction. Mass movements are based on a concept of viscous flowage and as the solifluction slope is, in some manner, changed into a viscous liquid, it then follows that movement may occur on low angle slopes.

Bird (1967), in reviewing the mechanics of solifluction, favours a viscous flowage process and suggests that:

> "in spring, melt water from snow and ice melts
> the soil until the cohesive strength fails
> and viscous flow occurs."

Embelton and King (1968) qualitatively describe a movement process due to the flow of water-saturated debris and Washburn

(1967) comments that:

> "The Atterberg limit is an important parameter in the solifluction and significant solifluction probably occurs only at moisture values exceeding the liquid limit."

These comments on the role of the liquid limit in defining the onset of solifluction are reasonable but not because soil water contents near the liquid limit define the loss of cohesive strength. Rather, the observed loss of shear strength near the liquid limit is due to the low effective stresses that must co-exist with the high void ratio in situ in a solifluction slope.

Apart from these statements describing qualitatively a flow process, no mention is made of the specific type of constitutive relation governing flow. The reader is left to imagine the form of the rheologic model and the author is not aware of any attempts to quantify observed viscous flow in thawing soils.

The actual processes by which a viscous liquid of soil slurry can be created and sustained are considered in a later chapter. Briefly, it can be noted that if thaw proceeds at a sufficient rate the effective stresses in a thawing soil can be maintained by thaw-sedimentation processes which result if the velocity of the advancing thaw-front exceeds the velocity of fall of soil particles. As effective stresses are then always zero, the only shear strength that can be mobilized is due to the inherent rheologic properties of the soil-water mixture.

The process of frost creep described earlier is often invoked to account for solifluction movements. It has been shown that magnitude of movements ascribed to frost creep demand frost heave movements that are far greater than those measured and that movements that might be attributed to frost creep are much less significant than thaw-dominated spring movements. Carson and Kirkby (1972), after reviewing the importance of frost creep suggest that frost creep appears to be a simplification of the mechanisms involved and that it is inadequate in accounting for observed movements.

The possibility that some winter movements are influenced by the deformation of frozen ground is suggested by Washburn (1967). He applies the constitutive relationship between shear stress and shear strain rate given by Wahrhaftig and Cox (1959) to a 14° slope in the Mesters Vig but, as the predicted rate of 12 cm/yr exceeds observed winter movements, discounts the importance of frost creep. However, as the Mesters Vig slopes may not have high overall ice contents the rates predicted are an upper boundary. As there is some evidence in both the Mesters Vig and other sites that observed winter movements cannot be completely accounted for by frost creep, creep movements in ice-rich frozen soils may be a reasonable mechanism.

1.4.2 Flow Landslides

(i) Description

Certain forms of periglacial mass movements can be considered under the category of flow landslides. While flows and solifluction mass movements are felt to have many common failure mechanisms the difference in appearance is marked making the distinction between the two forms mandatory. Mass movements, considered herein as flows, are variously described in the literature as mudflows, earthflows, rapid viscous flows, mudslumps, tundra mudflows and so forth. Considering these forms of periglacial landslides it is possible, on a purely descriptive basis, to identify two broad categories of flow landslides. Anticipating the terminology derived for use in the study area and keeping in mind that the distinction may not be made in all cases due to incomplete documentation, flow landslides are subdivided into skin and bi-modal flows. Skin flows develop with a marked planar shape while bi-modal flows is a term used to describe flows developing with a definite bi-angular profile. A summary of representative periglacial flow landslides is given in Table 1.7 and where possible a discrimination is made as to sub-type. The reader is referred to the detailed description of skin and bi-modal flows given in Chapter 2.

Skin flows begin as a thin detachment of vegetation and mineral soil moving out in a planar fashion over the permafrost table (for example: Capps, 1919; Eakin, 1919; Sigafoos and Hopkins, 1952; Wahrahftig and Birman, 1954; Mackay and Mathews, 1973). Skin flows have been reported along the Mackenzie River by Hardy and Morrison (1972) who note a form of surface scouring initiated by brush fires and who comment that forest fires can precipitate surface movements on quite flat slopes. Hughes (1970) comments on the frequency of detachment failures caused by the movement of the active layer over underlying permafrost. Long ribbon-like skin flows are reported by Isaacs and Code (1972) as are similar landslides called active layer glides reported by Mackay and Mathews (1973).

Bi-modal flows, unlike skin flows, develop with a marked bi-angular profile which, as will be discussed in later sections, is caused by different processes at work in the same landslide. Bi-modal flows have a steep headscarp portion and a much lower angle tongue area.

Bi-modal flows are, for the most part, reported in the higher arctic tundra regions. Headscarps are reported containing significant percentages of either or both massive ground ice and ice wedges and the headscarps in active flows are bare of vegetation except for small overhangs of moss cover (see Lamothe and St. Onge, 1961). Headscarps can be observed back-sapping at considerable rates, see Sec 3.4. Kerfoot (1969) has given a detailed description of the characteristic development of the headscarp profile during the thaw season.

The tongue portion of some bi-modal flows is more a stream of liquid-like mud (Washburn, 1947; Lamothe and St. Onge, 1961;

Mackay, 1966) while in other flows the colluvial debris can retain soil-like characteristics (Bird, 1967; Wahrahftig and Birman, 1954).

Hughes (1972) describes a retrogressive flow seated in the ice-rich glaciolacustrine sediments found along the Mackenzie River Valley. The flow landslide is apparently a bi-modal type as are flow landslides reported by Heginbottom (1971) in the Inuvik, N.W.T. area.

The distinction between bi-angular or planar profile is sometimes difficult. For example, when a skin flow moves out suddenly a steep but relatively shallow headscarp may be abandoned by the downslope movement and a weak bi-angular profile created. This bi-angular profile can, however, be further developed by additional movements in the recently bared headscarp area.

Cuts made artificially in ice-rich soils can also result in the formation of what are essentially bi-modal flows. Documented evidence of melting highway cuts in Northern Alaska has been reported by Smith and Berg (1972), who note that rapid headscarp recession due to thaw results when cuts are made in ice-rich soils.

(ii) The Importance of Vegetation Covers

The role of vegetation in controlling the development of flow landslides and, further, of modifying conditions such that solifluction or flow movements might occur was first stated by Capps (1919). As seen by Capps, the vegetation cover is capable of developing considerable strength due to its tenacious, feltlike properties. All other conditions being equal the vegetation cover either contains the thawed soil and sags with it developing solifluction lobes, or the cover ruptures and a flow of thawed soil spews out downslope carrying the overlying vegetation along. Similar arguments and observations of fluid flows of thawed soil spewing out from ruptured vegetation covers are made by Taber (1943) and Sigafoos and Hopkins (1952). Bird (1967) reports on a small flow some 20 m long that developed beneath thick tundra and flowed downslope leaving the overlying tundra intact, see Table 1.7.

Tundra vegetation covers are considered to be good insulators and Capps (1919) comments on the importance of moss covers in maintaining permafrost conditions in the underlying mineral soil. The importance of these insulative properties are graphically illustrated by Eakin (1919) who notes a frequent association of burned vegetation cover and initiated flow landslides, see Table 1.7. Heginbottom (1972) reports an increased frequency of flow landslides in conjunction with forest fire activity along south facing slopes of Boot Creek Valley, near Inuvik, N.W.T. The importance of forest fires in determining the distribution of flow landslides has also been discussed by Mackay and Mathews (1973).

Vegetation is also important in the stabilization of the artificial bi-modal flows that can result due to highway cuts and so forth in ice-rich soils. Lotspeich (1971) and Smith and Berg (1972) comment on the importance of draped-over insulative covers of moss in stabilizing the rapid melting headscarps of cuts.

(iii) Mechanisms Operative in Flow Landslides

In discussing the mechanisms operative in flow landslides it is first useful to focus attention on bi-modal flows and to consider the likelihood that different processes will be found seated in the steep headscarps compared with the process likely in the low angle tongues. Furthermore, it is evident that there may be a marked similarity between the processes at work in skin flows and in the tongues of bi-modal flows.

Many of the mechanisms of mass movement described in Sec 1.4.1 are felt to be as applicable to processes in these planar flow landslides as they are to solifluction. The similarity of many aspects of flows and solifluction was first suggested by Capps (1919) who considered that:

> "The origin and action of the slow soil flows are much the same as those of the sudden and violent flows."

In fact, the distinction in this thesis, between solifluction and flow landslides is, in part, a discrimination between slow and rapid flowage of thawed soil (for example: Capps, 1919; Taber, 1943; Sigafoos and Hopkins, 1952).

Although any of the mechanisms discussed in Sec 1.4.1 may be operative in flow landslides the importance of thaw-dominated mechanisms is evident. Eakin (1919), reporting on the effect of burned moss covers, described one skin flow that developed in the autumn as the result of spring burning and comments that these features are numerous wherever burning has occurred. Flow landslides are noted during periods of unseasonally high temperatures by Holmes and Lewis (1965) and Washburn (1947) comments that flow landslides are characterized by streamlets of mud derived from thawing till-like debris. Skin flows are broadly described as being limited to the zone of shallow annual thaw by Sigafoos and Hopkins (1952) who note that they begin as thin detachments of soil moving out over the permafrost table. From their descriptions it is evident that bi-modal flows may develop apparently because of increased thaw in the unprotected headscarp area. Similar forms of flow landslides are described by Capps (1919 and 1940) who comments on the importance of unseasonally high temperatures or the burning of vegetation covers. Bird (1967) documents a skin flow that moved outfrom beneath a thick vegetation cover that remained intact.

Along the Mackenzie River Valley, Hughes (1970) and Mackay and Mathews (1973) note that skin flows are seated in the active layer and that thaw promotes the detachment of a veneer of vegetation and soil. The role of thaw in promoting movement is also evident in the surface scours reported by Hardy and Morrison (1972) and is noted in a general manner by Isaacs and Code (1972).

The dominant role of thaw in governing the development of planar flows and, in particular, of the importance of thaw-consolidation can be summarized no more succinctly that it was by Taber (1943):

> "Rapid thawing and slow drainage are conducive to mudflows. Any shearing or settling of silts expanded by freezing results in compaction, and, if the silts are saturated, the water must escape immediately or carry part of the load. When water carries part of the load the mass behaves like a liquid, and this is important in most sudden soil flows."

The application of thaw consolidation theory is also generally supported by comments made by many authors on the importance of thaw-liberated water influencing the development of flow landslides (for example: Embleton and King, 1968; Capps, 1919 and 1940).

The effect of heavy precipitation has been considered by Taber (1943), Sigafoos and Hopkins (1952) and Mackay and Mathews (1973), who suggest that heavy rainfall aids skin flow development. The effect appears to be one of increased total stress increasing shear stress imbalance, increased pore pressures, as well as one of increased thaw rate due to the heat capacity effect of large amounts of relatively warm water.

Detailed descriptions of the nature of mass movements involved in the tongues of bi-modal flows are particularly scanty. Lamothe and St. Onge (1961) comment that the development of a low angle, 1^{o} to 2^{o}, tongue in a bi-modal flow is caused first by mudflows which carry the liquid-like mud and, secondly, by solifluction which removes the more viscous material. They note that a mud-stream that drains the headscarp hollow flows at rates of from 5 to 10 m/sec while the remainder of the tongue is estimate to move between 0.5 to 1 m/season. Mackay (1966) reports that the tongue of a large bi-modal flow, similar to the mudslumps reported by Kerfoot (1969) moved some 2 - 5 ft in 2 weeks in July 1963, but that it was otherwise quiescent. Mackay concludes that as the headscarp face retreated the broad tongue of the flow maintained an equilibrium gradient of about 3° but that there was no downslope removal of thawed soil and only an export of water out of the flow. On the other hand, a long narrow bi-modal flow (mudflow) reported by Kerfoot (1969) was observed to undergo a complex series of displacement with velocities over a 24 hour period ranging from 8.8 x 10^{-4}cm/s to 5.6 x 10^{-2}cm/s or higher.

Bi-modal flows reported by Lamothe and St. Onge (1961), Kerfoot (1969), Mackay (1966), Capps (1919), Eakin (1919), Holmes and Lewis (1965) and Hughes (1972) are caused by the exposure of massive ground ice or ice-rich soil by lacustrine stream or marine action. These flows have a bi-angular profile that is sustained as the headscarp retreats backwards as it is thawed. Lamothe and St. Onge suggest that the flow is initiated as stream action exposes ice-rich material at a meander bend. Similar action is inferred in flows described by Holmes and Lewis at a bend in the Kekiktuk River and must follow similar patterns in the flows which are being eroded by wave action in lacustrine or marine environments. Lamothe and St. Onge (1961) go on to suggest that a flow will then develop if a sufficient exposure of ice-rich soil can be maintained. They note that the steep backscarp can back-sap at rates of from 7 to 10 m/year depending on the aspect of the headscarp to incoming solar radiation. The steep back scarp is also sustained by the parallel development of a low-angle tongue which permits a continuous exposure of ice-rich soil. Lamothe and St. Onge also suggest that when the ground ice melts it produces mudflows that, in turn, further excavate the headscarp hollow. This view is disputed by Kerfoot (1969) who finds that the only functional role of all the tongues studied was the transportation of debris.

Mackay (1966) summarizes the main processes involved in the scarp retreat of bi-modal flows which are:- free fall or sliding of the active layer; erosion, both thermal and mechanical of the frozen scarp face; and slumping, partly rotational, of thawed debris blanketing the frozen scarp face.

It would, however, not be entirely correct to consider the mechanics of mass movement of bi-modal flows in an uncoupled fashion. For example, the absolute magnitude of the amount and rate of headscarp recession is governed by the equilibrium angle of the tongue and the rate at which colluvial debris can be removed from the base of the scarp and deposited elsewhere.

In turn, mass wasting of the head scarp can cause an undrained loading of the soil in the upper portions of the tongue area, a resultant increase in the excess pore pressures, which, in turn, will induce low angle instability. This process, whereby low angle movements can be induced in flow landslides by the loading of debris discharged from steeper slopes to the rear of the flow is not peculiar to periglacial areas and has been discussed by Hutchinson and Bhandari (1971).

Nevertheless, it can be seen that a consideration of the mechanisms operative in flow landslides must deal with two broad areas. The first is the description of mass movement on the low angle slopes, characteristics of skin flows and the tongues of bi-modal flows. The discussions of an earlier section on the importance of thaw-dominated mechanisms in relation to solifluction apply equally well to these planar flows. The second area concerns the mechanisms of movement in the steep headscarp areas of bi-modal flows. A review of the literature suggests that here the dominant process is thawing with a constant removal of the melt; properly called an ablation process.

Some discussion on the mechanisms of headscarp processes in the artificially induced bi-modal flows created in highway cuts is offered by Lotspeich (1971). He notes that if cuts are made with vertical faces rather than with the usual inclined face common in highway practice then stabilized slopes are more readily achieved as much less back-sapping occurs. This is due to the rapid initial sloughing of colluvial debris which falls on a relatively steep slope and is, in some cases, covered by the blanket of living moss derived from the original horizontal surface atop the cut. However, whether or not the colluvial debris now stable on angles from 30° to 45° will remain in th[illegible] condition over the life of the highway remains to be seen.

1.4.3 Slides and Falls

The remainder of the mass movement processes discussed in the literature can be considered under the heading of slides and falls. Bird (1967) discusses the occurrence of slides in northern regions but finds that there is nothing to suggest that any type of slide is peculiar to periglacial areas. If all slides occur through unfrozen or long-thawed soil or rock then it is reasonable to consider these movements within the framework of conventional practice. But, if mass movements occur through frozen soil Bird's comments are incorrect and this form of mass movement is of great interest.

Washburn (1947) reports on a slide at De Salis Bay that has occurred through frozen ground adjacent to a lake in the Canadian Arctic. This landslide has left a visible headscarp of frozen ice-rich soil some 100 feet long and 30 feet high. Washburn also attributes features in the vicinity of Mount Pelly to slides in frozen soil and although he notes that mass movements may have occurred in thawed soil which has then frozen he discounts the possibility for the slides reported.

Hughes (1970) describes deep-seated rotational failures in river banks in the Mackenzie River Valley where sands and gravels overlay glaciolacustrine silt and clay. Slides exhibiting translational and rotational movement accompanied by large scale gullying are also reported by Isaacs and Code (1972) who note that the mass movements must pass through frozen layers and suggest that these may be seated in unfrozen clays beneath overlying frozen zones.

Mass movements in glacial lake clays have been studied by Wahrhaftig and Black (1958) along the Alaska Railroad. Large deep-seated slides with some rotational movement are reported and permafrost has been documented in areas adjacent to recent activity. Movements are seated in extensive deposits of lake clays and well-developed vertical and horizontal ice veinlets are reported. The authors feel that movements occur only in thawed soil and comment that failure planes and contorted bedding found in certain excavations are the result of ancient stabilized landslides that have been frozen. They attribute the activity in their study area to the thermal disturbance resulting from the presence of the railroad. This is certainly true for some flow landslides noted. However, evidence in the form of old bent tree trunks and railroad construction records suggests that movement occurred before the railroad was built. Furthermore, they quote a unique case record in which a railroad roadmaster was lowered down the headscarp crack of a large slide. This individual reported that the crack extended through permafrost and that running water could be heard at the bottom. As no drilling has been undertaken in any of the major landslides in order to confirm ground temperature conditions the question of whether or not movements are occurring through frozen soil is not completely resolved.

A specific type of landslide called a "fall" is caused by bank erosion and is identified as a "thermal erosional niche" by Walker and Arnborg (1963) or as "caving blocks" by Frost (1960).

This form of mass movement found along the banks of rivers or large bodies of water is caused by the undermining action of warm water aided by the physical erosion and removal of thawed soil by river or wave action. This waterline erosion results in the formation of a large niche or undercut and the subsequent breaking off of large blocks of frozen material. The features reported by Frost (1960) are of considerable size and it is possible that the landslide reported by Washburn (1947) at De Salis Bay may be due to thermal erosion.

This process of bank recession caused by thermal and fluvial erosion of permafrost at the water line is reviewed by Gill (1972) who notes the importance of wave action in increasing erosion rates in the Mackenzie River delta. Gill notes that the greatest period of undercutting occurs in mid-July when water temperatures reach as high as 19°C. At this time of year high winds in conjunction with high water temperatures, may cause niche penetration of up to 3 to 5 m in less than 48 hours. Movements of approximately 180 m in 19 years are also noted along one shifting channel and are attributed to thermal-erosional processes. Similar rates of 10 m/year are also reported in the Colville River area by Walker and Arnborg (1963).

A particular form of periglacial mass movement is associated with features described as cambering and valley bulging, Higginbottom and Fookes (1970). Cambering involves the downward displacement of strata outcropping on sloping ground and is typically shown by the fracturing and tilting of relatively strong rock over relatively weak strata which can, in turn, be found to be strongly deformed and contorted. True cambering is characterized by dips of blocks or horizontal strata towards the valley bottom. Valley bulging can be defined as the upward displacement by anticlinal folding, faulting, or both in combination, of deformable strata in a valley floor, Higginbottom and Fookes (1970), and these authors comment that valley bulging is typically associated with cambering.

Observations of cambering and the associated valley bulging is summarized for sites in Britain by Higginbottom and Fookes (1970), for sites in Eastern Europe by Zaruba and Mencl (1969) and a case history is reported in Canada by Straw (1966). It is thought that cambering is associated either with the creep of frozen soils or alternatively with displacements in thawing soils aided by thaw-consolidation.

TABLE 1.1 COMPARISON OF SOLIFLUCTION TERMINOLOGY

Benedict (1970) (Alpine)	Washburn (1956) (Arctic)	Washburn (1947) (Arctic)	Capps (1919) and (1940) (Subarctic)	Sigafoos and Hopkins (1952) (Subarctic)
Turf banked terrace	Nonsorted steps	Solifluction sheets with lobate fronts	Terrace like ridges	Soil, solifluction or altiplanation terraces
Stone banked terrace	Sorted steps			
Turf banked lobe	Nonsorted step	Lobes	Lobate or mammillary flows	Soil or solifluction lobes
Stone banked lobe	Sorted step			
Non sorted sheet		Solifluction sheet		
	Sorted stripes			
Sorted stripes		Stripes and solifluction streams	Striped "high slopes".	Stripes
	Nonsorted stripes			

TABLE 1.2 PLEISTOCENE SOLIFLUCTION SLOPES

Author	Area	Soil Type	Angle Degrees	Residual Strength c'r (psi)	Ø'r (degrees)	Comments
Williams (1965)	South Devon	Unsorted "head" of sand, silt and angular blocks	1 to 6			
		Block streams overlying sandy silty head	6 to $12^{1}/2$ avg. 96 for 10 sites			Average movement 1500 ft
	South Central England; Wiltshire, Dorset	Sarsens overlying chalky solifluction debris, clayey in parts	1-1/2 to 2-3/4			Sarsens are a tertiary silcrete. Depth of movement 6 to 9 ft. Avg movement 6,000 to 13,000 ft.
	West Kent	Weald clay with sand and chert from the Hythe Beds	<1			Up to 21,000 ft movement.
Weeks (1969)	West Kent Sevenoaks By-pass	Solifluction lobes rubble in sandy silty clayey matrix	7			Lobes 10 to 13 ft thick. About 1200 ft movement.
	Trialpit Ch 317H	Soliflucted Weald Clay	4	0 to 0.2	15 to 15.6	
	Lower Street	Soliflucted Weald Clay	4	0.3	16	
	Quarry Hill	Wadhurst clay	7	0	12.4	
	Vauxhall Lane	Wadhurst clay	4	0	12.4	
	Ditton By-pass	Gault Clay	3	0	12.7	
	Boughton By-pass	Weathered London Clay	5	0	14	
	Tetsworth	Soliflucted Gault Clay	3-1/2	0	14	
Chandler (1970)	Welling-borough	Slip surface in between sandy clay and light blue clay.	6-3/4	0	23	
	Isham	Sandy clayey silt overlying clay	4	0	16	

TABLE 1.3 SOME REPORTED SOLIFLUCTION SLOPES

Author, Location	Site	Soil Type	Slope Angle (Degrees)	Rate of Movement (cm/year)	Comments
Rapp and Rudberg (1964)	Scandinavia	Tundra zone; fine grained Frost shatter zone; coarse grained.	General slopes: 3 to 5	3 to 5	In tundra zone rates 3 to 5 cm/year are 4 to 6 times rates in frost shatter zone.
Gradwell in Williams (1962)	New Zealand, Alpine		2 to 5 10	2 to 8 10 to 20	Movement of stone stripes.
Jahn (1960)	Spitzbergen	Wet clayey debris	7 to 15 3 to 4	5 to 12 1 to 3	
Budel, 1961 in Washburn (1967)	Spitzbergen		11	1.5 to 3.0	Notes rate dependent on grain size.
Rapp (1960) Sweden	Solifluction lobe S11 on line C1S	34% 0.06 mm	18	22 cm/year avg over 1955-59	Soil generally saturated. No noteworthy movements within 4 days after heavy rain in October 1959
	Solifluction slopes on lines C1S and C1N	Till: 10% 0.06 mm 40% 4 m	12 to 20	3 - 7	Lobes generally 1 m high and 5 - 10 m wide. Vegetated. No movements in summer on solifluction slopes.
	Talus slope on lines C1S and C1N	Coarse sandy rubble 7% 0.06 mm 55% 4 mm	35 Top of Scree 27 - 30 Base of Scree	3 - 5 0-1	
Smith (1960) South Atlantic	South Georgia	Till: fine sandy loam with boulders	21	2.5 - 5	Average for upper 0-25 cm layer of soil.
Washburn (1947) Canada	Mount Pelly, Victoria Island	Poorly sorted soil. Clay to pebbles	12	3 - 5	Solifluction lobe. Movement predominately in first 40 days after thaw.

TABLE 1.3 Some Reported Solifluction Slopes (continued)

Macar and Pissart (1964) France	Basses Alpes		8	0.6 - 4	Striped slope.
Bird (1967)	Northern Canada	High silt clay content	10	5 - 10	Continuous vegetation cover
			2 to 4	1	On slopes
			1	2 to 4	On lobes
Williams (1966) Canada	Schefferville, P.Q.	Silty soil	4 to 9	7 to 11	Average surface movements
		Silty soil	22	7	Surface movement
Williams (1959)	Norway	Till: with stones and boulders, clay and sand lenses in a silty-clay matrix.	22-1/2	Maximum 25 cm in spring season	Recorded 1956
Harris (1972) Northern Norway	Site A	Diamicton: Sand, gravel 76% Silt 15%	17	3.5	1969-70
		Clay 9% w_L 22.7% w_p 20.3%	5	1.75	1969-70
	Site B	Sand, gravel 75% Silt 14%	15	1.0	1969-70
		Clay [illegible] w_L 24.4% w_p 21.3%		0.5-2.7-5.1	1970-71
	Site C	Sand, gravel 84% Silt 12%	6	4	1969-70
		Clay 4%	11	6.0	1969-70
		w_L 20.7% w_p 17.8%	6 to 13	1.8-2.4-2.6	1970-71
Chandler (1972) Spitzbergen	Location 1		8.8 to 9.8		
	Location 2	Sand 10% Silt 70% Clay 20%	8 to 12, avg. 9.5	No movement	14 - 27 July 1971

TABLE 1.3 Some Reported Solifluction Slopes (continued)

Rudberg (1964) Sweden	Mountain Ridge	Stone stripe Frost Shattered material	15	0 - 0.1 - 1.0	1962-63
			9	0 - 0.1 - 0.5	Lower down ridge 1957-63
			10	0 - 0.1 - 0.5	Same ridge, shallow soil
			14	0 - 0.2 - 0.7	Same ridge 1957-63
				0 - 0.2 - 1.0	" " 1962-63
	Mt. Dalaine	Stone stripe	25	0 - 0.5 - 1.1	1955-63
				0 - 0.7 - 2.8	1955-57
				0 - 0.5 - 1.3	1962-63
	Mt. Dalaine	Stone stripes Fine soil in the surroundings	15	0.2 - 0.6 -1.7	1955-63
				0.9 - 1.6 - 3.0	1955-57
				0 - 0.7 - 1.7	1962-63
	Ridge	Wet Solifluction Soil	5	1.4 - 2.1 - 2.8	1955-63
				2.0 - 3.8 - 6.5	1955-56
				0 - 0.9 - 3.5	1956-57
				0.8 - 1.8 - 2.8	1957-60
				1.3 - 2.0 - 2.6	1957-62
				0 - 1.6 - 4.8	1962-63
	Mt. Dalaine	Solifluction lobe	20	0 - 3.5 - 4.3	1955-62: at base of high slope
	R. Dariesjokk Valley	Shallow solifluction soil	15	0 - 0.8 - 2.6	Lobate forms
			10	0 - 1.3 - 2.6	Area with lichens, grass: 1957-63
			15	0.5 - 1.7 - 3.7	1957-63
Benedict (1970) Colorado		Up to 47% fines	2 to 14	0.6 to 4.3	Average maximum rates
	Turf banked lobe 499	43% fines	13 overall 9.4 tread	0.1 - 1.7 - 4.2	Saturated in fall
	Sorted stripes Locality 2	22% fines	12.5	1.3 - 2.2 - 3.9	Saturated in fall. Rates are for fine soil which moves 2 times as fast as bordering coarse stripes.
	Turf banked Lobes 45	33% fines	6.5 overall 2 tread	0.1 - 1.0 - 2.3	Saturated in fall

TABLE 1.3 Some Reported Solifluction Slopes (continued)

Benedict (1970) Colorado	Lobe 45	33% fines	-	6.5 overall 2 tread	0.8 - 2.2 - 4.3	Down centerline of lobe
	Lobe 26 -	41% fines		14 overall 5 tread	-0.05 - 0.3 - 0.7	Dry in fall. Net retrograde movement at some locations
	Sorted stripes (Locality 1)			12	-0.1 - 0.03 - 0.6	Dry in fall
	Lobes 502 and 503	Blocky rubble over 47% fines		17 overall 12.5 tread	0.04 - 0.3 - 0.6	Elongated lobes move 3 times as fast as adjacent vegetated soil. Slope well drained, dry in fall.
Washburn (1967)	ES6 Slope	Diamicton: Avg. 57% fines, Range 20% to 79% w_L: avg. 35%, range 16% to 70%		2.5 to 3 (Avg. 2.5)	0.6 - 1.0 - 1.4	
		Jump 6.0, Gelifluction 1.4, Retrograde 3.6, September 0.5*				Accumulative mean readings over 5-year period.
	ES7 Slope	Diamicton: Avg. 45% fines, Range 22% to 90% w_L: avg. 18%, range 12% to 32%		10 to 14 (Avg. 10.5)	0.6 - 1.3 - 6.0	Slope divided into dry and wet sections. Avg. annual 1.3 cm/year exceeded by all wet stations.
		Jump 5.3, Gelifluction 2.0, Retrograde 1.8, September 0.5 Wet 10.8 Wet 6.4 Wet 0.7 Dry 4.2 Dry 1.1 Dry 2.0				Accumulative means given for all measurements
	ES8 Slope	Diamicton: Avg. 47% fines Range 18% to 89% w_L: avg. 18%, range 14% - 51%		11 to 14 (Avg. 11.5)	0.9 - 3.2 - 5.7	Slope divided into dry and wet sections. Avg. annual 3.2 cm/year exceeded by 64% of all wet sections. Distinction between wet and dry not as clear as in ES7.
		Jump 13.3 Gelifluction 4.3 Retrograde 2.6 September 0.3 Wet 15.1 Wet 4.6 Wet 2.0 Dry 12.2 Dry 4.1 Dry 2.9				Accumulative means given for all measurements.

* Due to different methods of calculation the average annual movement does not equal sum of J, G, R and S.

TABLE 1.3 Some Reported Solifluction Slopes (continued)

Washburn (1967)	ES15 Lobe	Diamicton: Avg. 50% fines Range 44% to 54%	Overall 4.5 Tread 3	Transverse 1.0 Axial 3.1	
	ES16 Slope	Diamicton: Avg. 7% fines with 40% gravel	25	1.1	Slope consists of loose grains with few fines and low moisture content.
	ES17 Lobe	Diamicton: Avg. 32% fines w_L: avg. 19%	Adjacent slope 15 to 23 Tread 12	Mean 7.6 Axial point 12.4	Slope wet and saturated all year. Front of lobe 3 m high at 45° angle.

TABLE 1.4 FROST HEAVE, POTENTIAL FROST CREEP AND RECORDED MOVEMENTS, NORTHERN NORWAY

Location	Slope Angle	Frost Heave (cm)		Potential Frost Creep (cm)		Total Observed Soil Movements (cm)	
		69-70	69-70	69-70	69-70	69-70	69-70
A	17°	3.5	9.2	1.06	2.57	3.5	
	5°	3.5	9.2	0.35	0.76	1.75	
B	15°	0.7	2.3	0.48	0.54	1.0	2.7
C	13°	0.65	-	0.18			2.4 (overall)
	11°					6.0	
	6°					4.0	

From data in Harris (1972)

TABLE 1.5 SLOPE ANGLE AND INDEX PROPERTIES, MESTERS VIG

Site	Slope Angle	% silt and clay	W_L% avg.
ES 6	2.6°	57%	35%
ES15	3.0°	54%	16%
ES 7	10.5°	45%	18%
ES 8	11.5°	48%	18%
ES17	12.0°	31%	19%
ES16	25.0°	8%	non plastic

From data in Washburn (1967)

TABLE 1.6 COMPARISON OF FAILED AND PREDICTED SOLIFLUCTION SLOPE ANGLES

Site	Strength ϕ'_r (c'_r=o) (Degrees)	Failed Angle (Degrees)	Predicted Angle (Degrees)	r_u* for failure	Reference
Sevenoaks	15	7	7.5	0.54	Weeks (1969)
Tonbridge	16	4	8.1	0.73	
Vauxhall	12.4	4	6.7	0.68	
Ditton	12.7	3	6.8	0.74	
Boughton	14.0	5	7.1	0.66	
Tetsworth	14.0	3.5	7.1	0.75	
Wellingborough	23	6.8	12.0	0.62	Chandler(1970)
Isham	16	4	8.8	0.70	
Northern Norway	29-33	5-17 5-10 6-13	15.5-18 15.5-18 15.5-18	0.86-0.51 0.86-0.72 0.81-0.68	Harris (1972)
Spitzbergen	36	6 8.5 12	20.0	0.84 0.78 0.72	Chandler (1972)

*ru based on $\gamma/\gamma = 0.5$

TABLE 1.7 SUMMARY OF FLOWS

Location, Author	Dimensions	Profile	Type	Comments
Southern Canadian Arctic Bird(1967)	Usually less than 100 m long.	Develope on 15° to 25° slope		General observation.
	20 m long.	Steep slope	Skin	Failed by flowage out from beneath tundra cover.
Canadian Arctic Lamothe and St. Onge (1961)	Headscarps 40 m in diameter	Headscarp steep, tongue 4°.	Bi-modal	Avg 7m/season backsapping of headscarp. Max to 10 m. Mud stream 5-10 m/sec. Soil in tongue 0.5 to 1 m/season
Canadian Arctic Robitaille (1951)		10° slope	Skin	Movement of 2.5 ft between start of thaw and 22 July. Soil flowing out over strandlines. Movement called solifluction.
Mackenzie River Delta Mackay (1966)	600 ft. wide 33 ft. scarp	Steep Head Scarp Low Tongue	Bi-modal	Tuktoyaktuk; 16 to 25 ft/season over 25 years. Aggravated by wave erosion.
	140 ft x 100 ft 8 ft. scarp	Scarp 45°-55° Tongue 3°	Bi-modal Aspect: S75°W	Kendal Island. Headscarp moved 12 ft. summer 1963. Avg. 6.5 ft 22 June - 2 Aug 63. Tongue moved 2.5 ft/2 weeks in July 1963
Mackenzie River Delta (Garry Island) Kerfoot (1969)	SITE A Similar to Site B	Steep scarp and low angle tongue	Bi-modal Aspect: S 30° W	Head Scarp Retreat: Year — Avg (ft) — Max Summer 64 — 5.5 — 10.4 Summer 65 — 5.2 — 9.6

TABLE 1.7 Summary of Flows (continued)

MacKenzie River Valley Hughes et al (1972)			Bi-modal	Retrogressive flows seated in ice rich glacial lake sediments.
			Skin	Detachment failures seated in active layer.
Mackenzie River Valley Mackay and Mathews (1973)			Skin	Active layer glides are movements of thawed soil along an inclined permafrost surface.
Cosna-Nawitna Region, Alaska Eakin (1919)	Thin cover of material	Flow on 10° slope. Final position at 8°.	Skin	Flow occurred suddenly in the autumn after a spring fire which removed part of the moss cover.
Nevana Coal Field, Alaska. Wahrhaftig and Birman (1954)	Semicircular headscarps	Many on slopes less than 10°. Frequent on 3° to 5°.	Skin and Bi-modal	Rates to several ft/min noted. Flows common in frozen claystones exposed to thaw.
North of Alaska Range Sigafoos and Hopkins (1952)	Headscarps niche 3 to 6 ft deep, 20 to 50 ft across and flow 50 to 100 ft overall.	Groups on 20° to 30° slopes. Random on 10° to 20°	Skin and Bi-modal	Rapid opening of fluid soil breaking restraining turf.
Fairbanks, Alaska. Taber (1943)	Headscarp 10 ft high	Low angle lobe	Bi-modal	
Alaska Capps (1919) and (1940)	100 to 500 ft long			Movements on planar surface to 3 - 4 ft overlying permafrost. Rapid movements noted breaking restraining turf.
Mount Chamberlin Area, Alaska Holmes and Lewis (1965)	Headscarp scar 5 to 10 ft deep, 50 to 100 ft across		Bi-modal	Till and colluvial deposits underlain by ground ice common in headscarps.
	Scar 6 to 8 ft deep	10° to 15° slope		Flow of 16 August 1958. Flow occurred after 2 days of warm weather in an unusually warm summer. Movement very rapid initially. Head scarp enlarged considerably in 7 days.

TABLE 1.7 Summary of Flows (continued)

	SITE B 120 m x 100 m Scarp 5 to 10 m Tongue 4-1/2° to 10° at toe		Bi-modal Aspect: N 50° E	Head Scarp Retreat Year — Avg (ft) — Max Summer 64 — 3.8 — 6.5 Summer 65 — 3.7 — 6.2 4 Jul 64 - 22 Aug 66 — 11.66 — 21.10 22 Aug 66 - 21 Aug 67 — 6.0 — 6.9
	Profile 1: 8 m high on 61° slope Profile 2: 5.5 m high on 53° slope			Profile I: 10 Jul - 15 Aug 64 7.8 cm/day 16 Aug - 5 Sept 64 5.3 cm/day Profile II: 28 Jul - 16 Aug 64 7.5 cm/day 16 Aug - 5 Sept 64 5.3 cm/day
	SITE C		Bi-modal Aspect: N 20° W	Summer 64 — 3.14 — 5.2 Summer 65 — 4.81 — 6.9
	SITE D Scarp 5.5 m Tongue 70m long	Tongue angles U 4° M 6° L 10°	Bi-Modal Aspect: S 60° W	Rates of tongue movement over 78 hrs.: .00088 cm/sec .00124 cm/sec .00353 cm/sec
	No details		Bi-modal	SITE E: Tongue velocities of 1.5 - 3.0 m/sec
Mackenzie River Valley Isaacs and Code (1972)	Tens of feet	15° to 35° slopes	Skin	Movement confined to active layer.
Inuvik Area Heginbottom (1972)		10° to 12° South facing slopes		South facing slopes. Boot Creek Valley Inuvik.
Mackenzie Valley Hardy and Morrison (1972)		Low angle slopes	Skin	Movements initiated by fire action on low angle slopes
Umiat Region, Alaska Anderson et al (1969)		Slope 5° to 30°	Debris flow (Bi-modal)	Flow in U-shaped channel 1-2 m deep and 8 - 10 m wide.

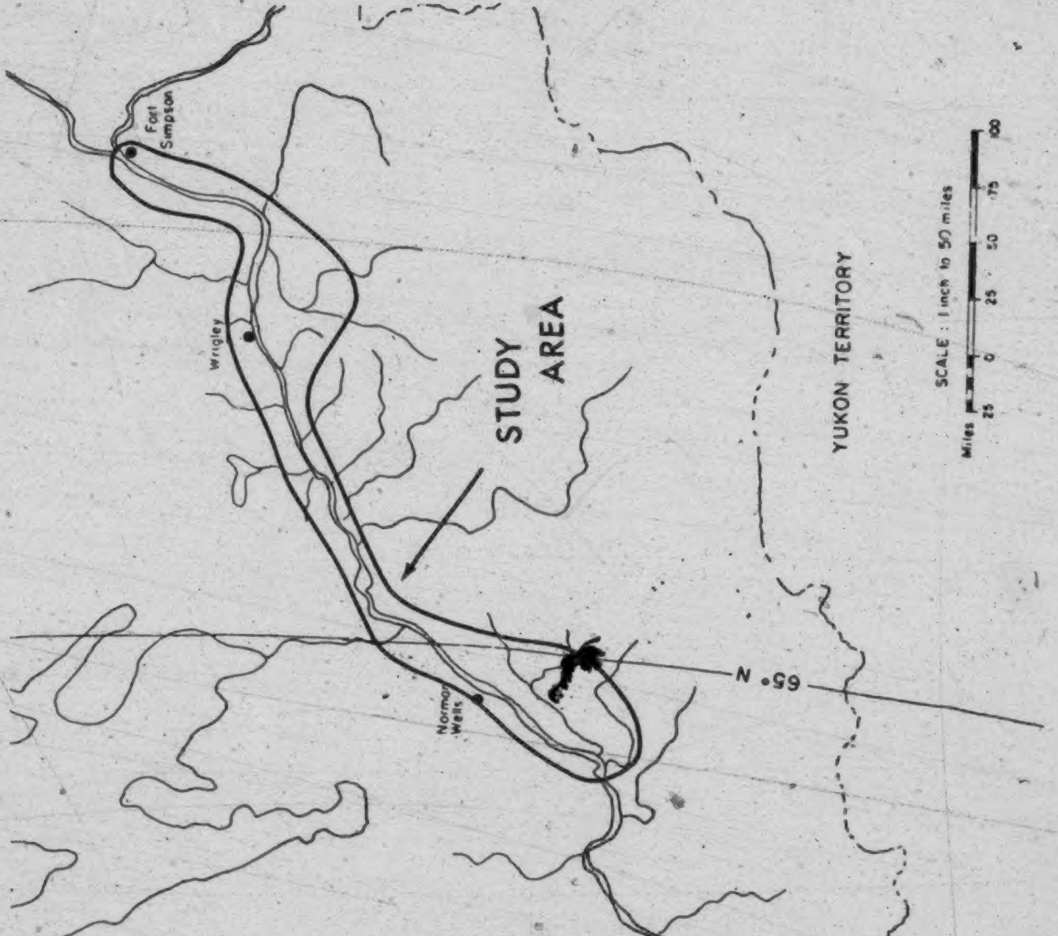
Fort Simpson
Wrigley
STUDY AREA
Norman Wells
65° N
YUKON TERRITORY
SCALE : 1 inch to 50 miles
Miles 25 0 25 50 75 100
Mackenzie River
NORTHWEST TERRITORIES
N
Inuvik

Fig 1.1 Location of the Study Area

CHAPTER II

THE LANDSLIDES AND THE ENGINEERING GEOLOGY OF THE STUDY AREA

2.1 Landslide Classification

2.1.1 Introduction

The classification of mass movement forms derived for use in the Mackenzie River Valley is presented in Fig 2.1. This classification concerns itself with landslides in soil and is not generally applicable to instability in bedrock. The observations made during the course of the field surveys and photographic interpretation of landslides is presented in Appendix A. It is intended that the description of the classification in the following section be read before a detailed consideration of Appendix A.

As the classification seeks to describe in a pictorial manner the types of mass movement encountered it is based primarily upon morphological evidence. The primary level of classification of flow, slide and fall is used in a descriptive sense with none of the mechanistic meanings often attributed to these implied. This descriptive approach is used in favour of a mechanistic or genetic classification as many of the landslides encountered have complex origins. And, as it is possible that some mass movement mechanisms have not yet been identified, it is desirable to avoid stressing one process at the expense of another.

The use of the terms flow, slide and fall as three distinct types of movement which have a characteristic morphologic appearance is the basis for classification systems established in geotechnical practice by Varnes (1957) and followed by Skempton and Hutchinson (1969).

The term flow has been chosen for a broad type of movement that exhibits the characteristics of a viscous fluid in its downslope motion. In many instances these movements resemble pure flow as there is no evidence that shear displacements have occurred along localized failure planes. In other landslides movements can be seen to have occurred partly along pronounced slip surfaces with the possibility of the remainder of the displacement distributed throughout the moving mass. Mobility is substantial and as it is largely distributed throughout the flow, pre-failure relief is rapidly destroyed. Flow movements generally continue until reduced gradients or obstacles are reached and many flows terminate in swiftly moving rivers. This definition parallels the description of flow landslide given by Varnes (1957) which is as follows:

> "In flows, the movement within the displaced mass is such that the form taken by the moving material or the apparent distribution of velocities and displacements resembles those of viscous fluids. Slip surfaces within the moving mass are usually not visible or are short-lived, and the boundary between moving and stationary material may be sharp or it may be a zone of plastic flow."

Conversely, landslides exhibiting more coherent displacements having a greater appearance of rigid body motion are called slides. Pre-failure relief remains substantially intact and although the total magnitude of movements may be great they appear to have accrued over a period of time.

Falls simply involve the direct and downward movement of detached blocks falling under the immediate influence of gravity and under conditions of no resistance to movement once movement is initiated.

It might also be pointed out that in the description and discussion that follow the terms landslide, mass-movement, slump and slip are used only as general terms and have no role within the proposed classification.

2.1.2 Flows

Those landslides considered under the general heading of flows can be sub-divided into the categories of skin, bi-modal and multiple retrogressive flows. This section consists of a general description of the three types of flow landslides identified in the study area and described in Appendix A. The term flow is also used for landslides outside the periglacial zone. In this thesis the term is used for those forms encountered within the permafrost zones and while a direct association with frozen conditions is not always stated it is implicit in the following discussion and in the description of Appendix A.

(i) Skin Flows

Skin flows involve the detachment of a thin veneer of vegetation and mineral soil and subsequent movement over a planar inclined surface. They are commonly active in long ribbon-like forms and may coalesce into broad sheets of instability. This category of flow is very shallow in comparison to its length. While skin flows can develop on steep slopes they are common on low angle, 6^{o} to 9^{o}, slopes. Skin flows are found throughout the study area and are particularly well-developed in burned-over areas. A summary of those flows that have been considered in any detail is presented in Table 2.1.

Shallow movements seated in GLB soils are common along the Hume and Hanna Rivers and slope angles from 7° to 11.5° have been measured at accessible sites. In this region skin flows occur frequently in burned-over areas. As the greater part of the field and aerial photographic observations in this and other areas were made along the river banks, skin flows have been observed predominantly in association with river and forest fire action However, skin flows can be found in burned-over scarps abutting long-abandoned ox-bow lakes and along the banks of small gullies and tributaries. Skin flows are then not necessarily or directly associated with river erosion. However, forest fires certainly encourage their development.

Skin flows along the Hanna and Hume Rivers appear partly to involve the re-initiation of movements or scarps that have, in the past, gone through similar cycles of instability and stabilization. Frequent note was made, during a brief reconnaissance of the Hume River, of broad sheets of instability on burned-over scarps at meander bends. Inspection of pre-burn aerial photography suggests that past instability was common and that the recent failures triggered by forest fires are seated in colluvial debris rather than undisturbed and intact GLB soils.

The exposure of burned scarps to incoming solar radiation also affects the occurrence of skin flows. Flows along the banks of a tributary of the Wrigley River were found on burned-over, south-facing slopes while north-facing slopes which had also been burned over remained stable, see Plate 2. However, the relative inclination of these slopes is also important as instability was noted on 14° to 18° slopes while the shallower, 9° to 10°, north-facing slopes remained stable. Many skin flows were noted in a recently burned-over area on the south bank of the Great Bear River during the 1971 aerial reconnaissance.

Large ribbon-like skin flows were observed on the steep 23° to 33° north-facing slopes of the Camsell Range near the Root River. At one location some 10 flows have occurred and they appear to be seated in colluvium derived from in situ weathering of shales. A cross-section through a typical flow has a steep section along which movement was initiated and a more shallow run-off section ending at a pile of debris. Common with skin flows in other areas, marked stripes in the form of changes in vegetation cover the slopes in this area and are witness to past movements of the same type.

(ii) Bi-Modal Flows

The term bi-modal flow is used to describe a form of mass movement that has a bi-angular profile and is also intended to signify that two distinctly different modes of mass movement can be seen within the confines of the flow. Well-developed bi-modal flows have a low angle tongue and a steep headscarp. A single flow can be divided into three main parts. The flow begins at a roughly semi-circular headscarp which serves as the source area for the colluvial material in the lobe or tongue, which leads out from the source area. This shallow, elongated, lobate tongue in turn ends at the third portion of the bi-modal flow, the terminal area.

The headscarp region can be described as an expanded spatulate-like bowl (Capps, 1940), as a semi-circular hollow (Bird, 1967), as an amphitheatre (Kerfoot, 1969) or as having a characteristic horseshoe shape (Washburn, 1947). These headscarps often have a smooth but steeply dipping face with inclinations of up to 40°. The planar scarps are bare of rooted vegetation although moss overhangs are common. Ground ice can usually be found beneath the moss curtains and in very active flows frozen soil is directly exposed to the atmosphere. Thin veneers of soils in these rapidly melting headscarps flow in pulses down to the break in slope where the lobe begins. On the headscarp, soils undercut by melting can collect in pools, and when a certain critical height is reached, this aggradation of colluvium then flows downscarp carrying clods of intact soil and other debris. Within the same scarp, less wet soils can be subject to desiccation and large blocks of dried soil may move by gravity fall. In some instances, headscarps appear to have failed by the detachment and subsequent flow of a significant depth of soil that has thawed in-situ before moving downscarp. The form of movement at the headscarp is, therefore, both flow and fall and in only one case has a slide movement been noted in an otherwise bi-modal flow.

The lobes of bi-modal flows can develop on angles as low as 3°, and have been found up to 14°. In small bi-modal flows the surface of the lobe is often grooved by irregularities in the overhanging moss covers as the lobe moves out from beneath the headscarp. Active flows have tongues devoid of living vegetation and colluvial debris covers a chaotic mass of partly buried vegetation derived from the top of the headscarp. Smaller lobate features may be formed superimposed on the main lobe and small melt-water streams with branching tributaries can also be contained within the flow. Although the tongues usually lead out at right angles from the source area in the headscarp, curved lobes have been noted. The soil contained in the active lobes has little or no bearing capacity and large clods of drier soil barely float in the moving flow. In some flows the surfaces can be found covered with clods of soil intermixed with vegetation which, although appearing firm, only cover a very liquid-like soil slurry. Often, the lobes can be constrained to flow between drier areas or over steeper gradients and in doing so develop crevassefeatures and tension gashes reminiscent of ice glaciers. Other lobe areas are firmer and while movements appear to be slower, evidence of movement can still be found. The lobe areas may be either long and narrow or more short and wide in relation to the size of the headscarp hollow.

Bi-modal flows often terminate in a pile of colluvial material and transported debris which is thrust out into a stream or river causing it to detour sharply around the toe. In other cases, bi-modal flows can be found perched on top of more resistant till or bedrock and here the toe of the flow spills out and over the steep frontal scarp. In less active bi-modal flows the frontal terminus is eroded away.

Bi-modal flows usually occur as single features but they can be found along a broad front.

Small bi-modal flows of approximate average dimension, of 50 ft long by 20 ft wide, and with lobe angles of from 4° to 10° and headscarps of from 5 to 20 ft high are ubiquitous features within the study area. They can be found in isolated locations, or with increased frequency they have been noted along the bank of the MacKenzie River and many tributaries and they can be found superimposed with larger, different types of landslides. Vegetation overhangs, which will be discussed later, are common in these smaller flows. In headscarps less than about 10 ft high they usually drape over the entire scarp. When cut away, the moss overhangs reveal high ice content soils and thick (up to 6 inch) ice lenses can be found in almost any headscarp. Movements within the lobes are noticeable with evidence in the way of grooved soil moving out from beneath vegetation overhangs and sheared-off branches caught in the lobe but attached to firm ground. Access to the headscarp is difficult as lobe conditions are very wet and soft. Probing in smaller lobes suggests that flow occurs in a thickened active layer overlying frozen soil. No samples were taken of frozen soil beneath the lobes but a metal rod driven into hard, resistant soil developed a resistance to torque confirming the presence of frozen soil. Depths to permafrost of from 3 to 4 feet are common.

The larger bi-modal flows studied during the course of the survey are summarized in Table 2.2 and are discussed in Appendix A. Typical bi-modal flows are shown in Plates 6, 8 and Figs A.15, A.16, A.18 and A.21. Larger bi-modal flows are also shown in Plates 3, 4 and 5 and Figs A.11 and A.12.

(iii) Multiple Retrogressive (MR) Flows.

This sub-classification is required to describe a certain form of mass movement which adapts an overall flow form of movement but, unlike skin or bi-modal flows, these MR flows retain some portion of their pre-failure relief. Contained within the landslide bowl are a series of arcuate, concave downslope, ridges derived from the headscarp as it receded backwards by a series of failures. Although the overall profile of these landslides is bi-angular their form suggests that a series of retrogressive failures have occurred at the headscarp. These headscarps exhibit, in some locations, flow-dominated processes but in others rotational slides can be found. It might be argued that this form of landslide, for example, the Fort Simpson MR flow, Mile 226, should be classified as "complex". Some salient features of MR flows are shown on Plate 1 and on Figs A.2 and A.3 and MR flows classified in the study area are summarized in Table 2.3

2.1.3 Slides

Those landslides considered under the general heading of slides can be sub-divided into the categories of block, multiple retrogressive, and rotational slides. The following part of this section consists of a general description of the three types of landslides identified in the study area and described in Appendix A.

(i) Block Slides

Block slides involve the movement of a large single block that has moved out and down with varying degrees of backtilting. The moving mass remains intact and the surface of the block supports upright, living vegetation which is similar to that found upslope beyond the slide area.

Well-developed gullying is associated with block slides. Steep-sided, V-notched gullies first develop at right angles to the river but do not extend much behind the slide area. Frequent extensions to the gullies occur at right angles to the perpendicular gullies and run parallel with the river behind the slide block.

A summary of the block slides studied is presented in Table 2.4,and Plate 7 presents a typical example.

(ii) Multiple Retrogressive (MR) Slides

MR slides are characterized by a series of arcuate, concave towards the toe, blocks that step backwards higher and higher towards the headscarp. There can be a degree of backtilting or rotational failure of the components but this is usually observed only on blocks that have fallen too near the toe. Intense gullying can be found in association with MR slides in some areas.

A summary of the MR slides studied is given in Table 2.5 and a typical MR slide is shown on Plate 9.

(iii) Rotational Slides

Small rotational slumps are frequently found in the thawed or unfrozen fluvial deposits of small rivers and they can also be noted in the headscarps of MR flows in the southern region of the study area. These rotational failures are entirely similar to the classical circular type of failure common in soft clays in more temperate regions. This sub-category is useful in both describing landslides that exist by themselves as well as describing certain components of mass movement within larger landslides

2.1.4 Falls

Fall landslides occur in areas where river erosion undercuts frozen banks resulting in a frozen block of soil cantilevered out over a thermal-erosion niche, see Sec 1.4. The undermined blocks fail in tension and often with an outward or backward movement before falling into the river.

Falls have been observed along the Hume, Hanna and Mountain Rivers. They have been noted primarily in recent fluvial deposits but indicators of fall movement such as forward-toppled trees have been seen in GLB soils. Falls have also been noted in isolated instances along the Mackenzie River where fluvial islands are being actively eroded. A typical example is shown on Plate 10.

2.1.5 Conclusions

(i) Comments on the Classification

The classification presented seeks to describe any given landslide type at the moment of observation. However, as the descriptive classification is based only on two main categories, slide and flow, distinctions as to type may be difficult and it is useful to amplify the proposed classification by considering areas of possible overlap.

Some difficulties arise in discriminating between skin and bi-modal flows. For example, the Hanna River Flow, Fig A.21, is classified as being a bi-modal flow but as the difference between the headscarp angle and the lobe is minor this landslide might well be called a skin flow. Furthermore, it has been observed that movements can be re-initiated in the tongues of stabilized bi-modal flows. At the moment of initiation these movements would properly be called skin flows. However, movements may, in time, sap backwards to the headscarp of the old bi-modal flow and at that instant a bi-modal flow may be re-initiated.

It is also possible that bi-modal flows may recede headwards until, by a process of continuous back-sapping, the tongue of the flow reaches the upland behind the landslide. When this occurs a given bi-modal flow would not have a bi-angular profile. But, as the sequence of events leading to its mature form can be re-created from the geometry of the flow in relation to its surroundings, it is possible to classify the landslide as having been a bi-modal flow. Furthermore, the flow described above would not fit well into the skin flow classification as movements would not appear to have developed as the detachment of a veneer of material over a planar surface. An example of this type of flow can be found at Hume River, Site HU1, Fig A.22. The mature flow resembles a skin flow, Plate 11, but, when viewed in its active stage on older aerial photographs a distinct, steep, headscarp is visible.

Problems have also arisen in assigning certain landslides into either the MR flow or MR slide category. Although the retrogressive aspect of these landslides is evident it is often difficult to decide on the overall primary category. For example, the Fort Simpson Landslide, Mile 226, is classified as being an MR flow. The multiple retrogressive aspect of this landslide can be seen in the series of arcuate ridges contained within the landslide and which, on close inspection, can be seen to be due, in part at least, to a series of rotational slides in thawed soil at the headscarp. However, the overall appearance of this landslide is one of flow-dominated movements and there is evidence to suggest that the arcuate ridges are also partly derived from flow processes. Similar difficulties also arise in classifying the Mile 265, MR flow, Table 2.3 and the MR slides at Miles 293, 300 and 621, Table 2.5. These landslides have been classified based upon which form of movement, slide or flow, appears to dominate.

While it might appear that duplication exists within the slide category of movements by the use of block and MR slides in addition to rotational slides, this distinction is useful. In some block and MR slides rotational components of movement of slumped material may sometimes, but not always, be observed while in others the slump block may move down as much as 150 to 200 feet with no apparent rotational movements. In contrast, those landslides classified as rotational slides always exhibit a considerable rotational component of movement. Anticipating later conclusions, it can also be pointed out that while block or MR slides are associated with large movements occurring in part through frozen soil, rotational slides are used to describe smaller scale mass movements apparently seated in unfrozen or thawed ground. The rotational slide sub-category is also useful in helping to describe mass movement types contained within other landslides as at the Fort Simpson Landslide, Mile 226.

Such landslides as the ones at Big Smith Creek, Mile 471, and Old Fort Point, Mile 480, require close inspection before they are classified. These landslides have a marked bi-angular profile, Figs A.11 and A.12, Plates 3 and 4, and while they resemble a block slide they lack all the typical features. These landslides are classified as bi-modal flows for reasons described in detail in Appendix A. It is possible that the initial failure of such landslides involved slide movements. However, the ongoing degradation of these landslides resembles a bi-modal flow and the more mature bank profiles in the vicinity have a marked low angle tongue and a steep headscarp area.

(ii) Comparisons with Reported Phenomenon

Solifluction as discussed in Sec 1.4 has not been studied at all in the study area and the landslides considered under the headings of skin and bi-modal flows are not solifluction movements. However, within the proposed classification of Fig 2.1 solifluction could enter the classification as the fourth type under the flow category. As solifluction is, perhaps, the most commonly discussed periglacial mass movement form it is useful at this time to make certain distinctions between the flows studied and solifluction.

A fundamental difference between solifluction and the other forms of flow landslides is the marked difference in the rate at which movements develop. Solifluction involves the slow downslope movement of mineral soil and the overlying vegetation mat which is stretched, contorted and then re-grows in harmony with downslope motion. On the other hand, skin and bi-modal flows are characterized by a violent tearing of the vegetation mat and catastrophic movements which result in an entirely different appearance.

Another, more subtle, difference is that solifluction can be considered to be the characteristic deformation mode ofmany naturally occurring active layers. By specifying naturally occurring active layers one seeks to exclude the effects of catastrophic events such as forest fires or heavy rains and high temperatures which increase the rate and depth of thaw. That is,a natural depth of active layer is conceived as being the mean depth under seasonally average conditions. If this average slope regime is violently disturbed, solifluction either becomes more intense or skin and bi-modal flows can be generated. Considered in this fashion, solifluction can be suggested to be the equilibrium condition of many slopes and other forms of flow landslides evolve from this base condition.

Landslides identical to skin flows observed in the study area have been reported by others both in periglacial areas and in the Mackenzie Valley. These landslides have been summarized in Table 1.7 and discussed in Sec 1.4. It can be noted that the classification of this form of landslide as a flow-dominated movement is, however, opposed to the classification presented by Mackay and Mathews (1973) who, following Varnes (1958), classify them as active layer glides or slide movements. This difference is one of opinion.

Bi-modal flows appear to be as common outside the study area as they are within it. They have been observed (on aerial photography) by the author in the upper reaches of the Hume, Arctic Red, Peel and Bonnett Plume Rivers and along the Rat River in the Richardson Mountains. They have been noted along Stony Creek, near Fort Macpherson, and in gravel pits and highway cuts on the Dempster Highway (Strang, 1972). Bi-modal flows have been observed in the Canadian Arctic, in the Beaufort Sea and the Mackenzie Delta area , as well as in certain areas of Alaska, Table 1.7

Kerfoot (1969) distinguishes between two types of bi-modal flows, that is, mudslumps and mudflows, and in doing so focuses attention on a difference also noted in some bi-modal flows in the study area. The processes at work in the headscarp of both mudslumps and mudflows are essentially similar and create the characteristic bi-angular profile. However, in mudslumps there is little export of soil particles away from the ablating scarp and the hollow excavated by the landslide might be called a thermokarst or subsidence feature. It might also be argued that, if there is a net export of soil out of the system, this movement is as much mass transport by running water as it is mass movement due to landslide processes. Mudflows, however, partake of considerable mass movement in the tongue portions. While it has been recognized that both varients of bi-modal flow might occur within the study area, the author has not been able to make the detailed observations required to discriminate as to sub-type. In fact, most bi-modal flows observed have well-developed toes thrust out into fast-moving rivers indicating that considerable mass movements are involved.

Bi-modal flows are also called retrogressive-thaw flow slides by Hughes et al (1972).

The fall landslides observed in the study area appear to be similar to the forms noted by others and considered in Sec 1.4. On the other hand, shear movements in frozen soil have not been generally noted in periglacial regions and, in fact, Bird (1967) appears to suggest that such movements would not be found.

2.2 Quaternary Geology

(i) Glacial History

The landslides described in the preceeding chapter are almost wholly seated in the glacial lake basin, GLB, sediments found along the Mackenzie Valley. As the distribution of landslides is, therefore, partly controlled by the distribution of these quaternary sediments it is of interest to consider their history.

During the latter stages of the Pleistocene era, it appears that Laurentide glacial ice advanced from the north-east against the east flanks of the Mackenzie Mountains in the area north of Fort Good Hope (Hughes, 1970; and Hughes et al, 1972). When the ice lay against the mountain front, large glacial lakes were impounded and extensive quantities of coarse and fine-grained soils were laid down in these glacial lake basins.

The Mackenzie River and many, if not all, of its tributaries probably occupy the same relative positions today as they did during the onset of the Pleistocene era. Today, many of these tributaries and predominantly the west bank rivers draining the Mackenzie Mountains are important suppliers of coarse and fine sediments into the Mackenzie River. It is reasonable to argue, therefore, that during the period beginning with the retreat of the ice sheets large quantities of material were available for deposition. Continental ice has advanced across the Mackenzie River Valley and against the mountains more than once during the last glaciation.

North of the study area, Hughes (1970) finds ice-marginal features such as moraines, ice-marginal channels, and kame terraces along the east flank of the Mackenzie Mountains to elevations as high as 4,000 ft. Glacial erratics are also found at elevations up to 5,000 ft and indicate an older and more extensive Laurentide advance. Moraines marking significant late Wisconsin re-advances of the Laurentide ice sheet are also found in the area to the north-west of Fort Good Hope (Hughes et al, 1972).

Within the northern part of the study area ice moved northwesterly from the Great Bear Lake region. One stream of ice moved northward down the Mackenzie River from the Fort Norman region, through Norman Wells, stopping near the Hanna River, while another advanced northward along the east flank of the Franklin Mountains, swinging westward at Fort Good Hope (Mackay and Mathews, 1973). Within the southern portion of the study area around Fort Simpson, Rutter and Minning (1972) find evidence for two advances of continental ice with flow towards the west and north-west. Erratics are found up to at least 5,100 ft in the Mackenzie Mountains and it is suggested that Laurentide ice advanced over and across these mountains.

At some time contemporary with, or after glaciation of the Mackenzie valley, the ice dams north of the study area caused the impounding of the river system and the creation of large proglacial lakes. Large lakes may also have been formed in crustally-depressed basins peripheral to the retreating ice sheet and it may be speculated that the lake basin in the Sans Sault Rapids - Fort Good Hope area was partly due to damming behind bedrock highs since breached along the Lower Ramparts of the Mackenzie River.

Evidence for some form of dammed lake exists in the Fort Good Hope area and an extensive spill-way system can be found to the west of the present, lowland, lake basin (Hughes, 1970; Mackay and Mathews, 1973). These spill-ways apparently drained the glacial lake and are found at elevations from 800 to 300 ft above sea level. In the middle of the study area Hughes (1970) reports strandlines at elevation 550 ft near Mile 460 on the west flank of the McConnell Range and strandlines have been noted by the author at 550 ft on both sides of the valley near Mile 310. Rutter and Minning (1972) note that glacial Lake McConnel constructed a prominent beach at about 850 ft and others at lower elevations in the area around Fort Simpson. It is not known if the glacial lakes formed along the Mackenzie River were interconnected, if they were an extension of glacial Lake McConnell, or if they resulted at different times upstream from local ice advances.

Irrespective of their exact origins, glacial lake basin sediments have been documented in the study area in three major areas. Extensive deposits of GLB silts and clays laid down in the impounded lakes are found in the Fort Simpson to Willowlake River area, from Keele River to Fort Norman and from Sans Sault Rapids to Fort Good Hope. Major rivers such as the Liard, North Nahanni, Redstone, Keele and Mountain discharged vast amounts of fine sediments into these lakes and today extensive deposits of GLB silts and clays overlain by sands occupy huge areas along the Mackenzie River in the above three areas and especially along the lower reaches of the Hume, Hanna, Mountain, Little Bear and Great Bear Rivers (Hughes, 1970). When the glacial lakes that sustained the growth of these sedimentary sequences were finally drained many of the lake deposits were eroded (Rutter and Minning, 1972).

GLB sediments occur in two topographic settings (Hughes, 1970). The first area is along the large plains bordering the Mackenzie River and the lower regions of major tributaries as noted above. In these deposits silt and clay is typically mantled by sand. This sequence has been the subject of field study and is considered in detail in a later section. The second topographic setting has not been considered in any detail within the study area and consists of GLB deposits found on the sloping shoulders and locally along valley floors of valleys within or near the Mackenzie Mountains.

The typical sedimentary sequence of the GLB soils encountered in the study area consists of coarser-grained soils grading into clay at depth. The relative proportions of coarse-grained sands and gravels over silts and clays change from area to area and in some cases rapid changes are apparent. The type sequence of sands and gravels over clayey silts over silty clays and variations in the relative proportions has many implications with regard to the type and distribution of landslides. There are no detailed explanations for the exact sequence of events leading to the observed present-day conditions.

(ii) Landslide Occurrence

The forms of mass movement noted in the Mackenzie River Valley are almost entirely seated in GLB sediments or in colluvial slopes derived from GLB sediments. Areas of active flow or slide movements in the study area usually coincide with terrain units that have been mapped as glacial lake basin, GLB, soils by the Geologic Survey of Canada. However, this coincidence is, in part, negated by the fact that landslide activity is one of the indicators used in mapping GLB soils. As the properties of these GLB soils will be considered in later sections, this section will dwell on the occurrence of landslides in other materials which will not be considered in any further detail.

Continental till is the dominant surficial till in the southern portion of the study area (Rutter and Minning, 1972). Landslides have been noted in till on the north bank of the Mackenzie near Fort Simpson and two large failures can be found at Miles 340 and 345, Fig A.5. These failures can be classified as MR slides. Further north, till is common along both banks of the Mackenzie from Wrigley and to the confluence of the Redstone and the Mackenzie Rivers at Mile 440. In this reach the Mackenzie River flows in a single channel of fairly regular width with little sign of bank instability. Till and rock outcrops are common and the only instability noted was a series of inactive MR slides seated in till immediately opposite the Johnston River, Mile 394. Below Mile 440, instability increases along the banks and by Mile 455 and to Mile 470 massive instability is associated with GLB sediments underlain by till. Till complicates any understanding of the morphology of landslides in this reach. Till has also been noted in the area around Mile 500 and in isolated outcrops near Mile 625. These areas have not been considered in any detail and no landslides appear to be associated with them. Skin flows have been found in what appears to be till or till-derived colluvium in a recently burned area near the Wrigley River, Table 2.1.

Falls and rotational slides can be found in recent fluvial deposits and they have been studied primarily along the Mountain, Hume and Hanna Rivers. Falls are found where frozen fluvial sediments are being thermally and physically eroded. They are particularly active in the lower reaches of the Mountain River. It is reasonable to suggest that similar processes might be encountered in the banks of other highly-braided gravel-bed rivers such as the Keele, Redstone, Dahadinni, Root and North Nahanni Rivers. Falls have also been noted in the frozen sands found in some sections of the recent fluvial deposits of the Hanna and Hume Rivers, but in other reaches small rotational slides are common. These slides are seated in unfrozen silts and clayey silts and have been described elsewhere. They have only been observed in passing but they are often to be associated with finer-grained flood plain soils laid down in old ox-bow lakes.

Instability forms in Cretaceous and Devonian sediments have been observed in some parts of the study area. Particularly interesting landslides are seated in Cretaceous sediments adjacent to the Mountain River between Virgin and Campsite Creeks, Fig A.17. None of the bedrock landslides have been studied or commented on in this thesis.

Well-developed skin flows can be found in weathered Devonian Shales along the steep mountain slopes bordering the Root River, Fig A.5.

2.3 Permafrost Conditions

2.3.1 General Observations

The definitions and usage of permafrost terminology followed in this thesis follow that established by Brown (1967) and will not be considered in any detail.

The study area is located entirely within the widespread permafrost region of the discontinuous zone as mapped by Brown (1970). Permafrost conditions inferred from the presence of ground ice have been noted in all sections of the study area. Apart from the Hume and Mountain River sites, discussed in detail elsewhere and in which permafrost is approximately 160 and 155 ft thick, information on the depth of permafrost is scanty. Near Fort Simpson, permafrost can be at least 70 ft thick as an almost vertical exposure of frozen ground was found in the Fort Simpson Landslide, Mile 226. Permafrost thicknesses of 150 - 200 ft are measured in the Norman Wells area (Brown, 1970) and data provided by Scott (1972) suggests some 150 ft in the GLB sediments of the Sans Sault Rapids area. North of the study area Brown (1970) notes permafrost thicknesses to greater than 300 ft in the Inuvik area.

Many distinctive features occur on the ground surface in the permafrost region which are characteristic of underlying conditions. The best developed features noted within the study area which attest to both frozen ground conditions and high ice content soils are associated with the thawing of permafrost. Such indicators of frozen ground conditions as pingos, polygonal ground, circles, mounds and steps (see Brown, 1970), caused by freezing or freeze-thaw processes have not been observed within the study area.

The most prominent feature associated with the thawing of permafrost soils within the study area are the thaw lakes or thermokarst topography found on top of the glacial lake basin plains. Thermokarst is a term used for uneven land subsidence caused by the melting of ground ice (Brown, 1970) and resulting in the formation of irregularly-shaped and variably-sized thaw lakes which pit the surface of ice-rich soil. These lakes are common within the study area and where they have been drained by the encroaching bank erosion of streams incised into the GLB plains, the lakes appear as hollow depressions of relatively uniform width but shallow depth. It is generally accepted that permafrost is absent under the larger thermokarst lakes.

Flow landslides are also indicators of frozen ground conditions and a definite association has been noted, during the survey, of ice-rich soils in conjunction with bi-modal and MR flows. Comments by Hughes et al (1972) on mass movements in the same general region also suggest that the development of detachment slides followed by retrogressive-thaw flow slides are associated with frozen ground conditions and high ice content soils.

Permafrost conditions are also indicated in some areas by the surficial drainage patterns that can develop. All surface water derived from rain or melt must flow overland in a thin surface zone. On the gentle slopes, above the tree line or in areas of scrub brush and stunted spruce, one can frequently observe the development of a striped terrain unit. These stripes are alternating units of different types of vegetation with the thicker and more prominent growth apparently established where run-off flow is concentrated and where the active layer is consequently greater. In areas around Norman Wells one can find single lines of spruce established in small drainage-ways with the slightly raised highland either side devoid of larger vegetation.

2.3.2 Ground Ice Conditions

Ground ice has been found in association with active landslides in all parts of the study area. Its presence has been confirmed by visual sightings and, in some instances, by reasonable inference.

Before proceeding to a description of the ground ice forms encountered and which are detailed in Appendix A, it is useful to consider some aspects of the problems involved in classifying ground ice. There is no standard, international terminology for the varieties of subsurface ice and no descriptive or geometric classifications have been accepted universally. A number of genetic classifications have been proposed but, as the genesis of certain forms of ground ice are still open to question, these classifications are, in part, premature.

The classification used in describing the ground ice forms encountered follows from one given by Mackay (1972). Ground ice in the thermal contraction, tension rupture and segregated ice categories have been noted. The use of the term segregated ice requires some clarification with respect to the sense in which it is used in describing the ground ice encountered. Mackay (1972) uses the terms segregated ice and injection ice in a genetic classification to discriminate between two different origins for ground ice. Segregation ice results from in-situ freezing of water attracted to a freezing front while injection ice is caused by the intrusion of water under pressure and results in the formation of sill ice and pingo ice (Mackay, 1972). Sill ice grows when water is intruded and freezes into a tabular mass while pingo ice is water intruded and which, on freezing, forms a dome or hydrolaccolith. On the other hand, segregational ice can also cause the formation of thin, tabular, lenses of ice of varying thickness. The well-known closely-spaced rhymthmically-banded ice often referred to as ice gneiss or sirloin ice, the massive ice lenses noted in the Mackenzie Delta, and the latticed, renticular ice structures observed in this study, all may be attributed to segregational processes. There can be, however, gradual transitions from injection ice to segregational ice. Shumskii (1964, p. 228) and Mackay (1971 and 1972) observe that it is often difficult or impossible to determine whether a particular body of ice grew in response to ice injection or segregation processes.

In order to describe certain ground ice features encountered in the field a segregation ice category will be used, but in a descriptive sense only. Ice wedges have been found in chance exposures from Mile 473 north, seated in both recent fluvial sediments in the flood plains of tributary rivers and along the Mackenzie River. Ice wedges have also been found in the sandy top member of the GLB sequence. They have not been studied in any detail and were noted primarily as indicators of permafrost conditions. A summary of their observed occurrence is given in Table 2.6.

Segregated ice has been found in GLB soils in all parts of the study area. Thick ice lenses are usually associated with the more silty facies of the GLB sequence and ice lenses of at least 10 inches in thickness have been found. The silty-clay or clay soils usually contain thinner lenses and are, characteristically, laced with a three-dimensional lattice of predominantly sub-horizontal and sub-vertical ice veinlets which will be called lattice ice.

The detailed description of the types of ground ice encountered is given in Appendix A for the general observations made during the 1972 survey and during the 1973 winter drilling programme.

2.3.3 Permafrost Conditions at Block and MR Slides

Both block and MR slides are found in GLB soils and, while isolated MR slides have been noted in till, they have not been investigated. Block slides are common where glacial-lake deltaic fine sands, silts and gravels are found overlying GLB silty clays in areas such as near Camsell Bend, around Fort Norman and below Sans Sault Rapids. The dominant stratigraphy is sand and interbedded clayey silts and sands overlying a silty clay. The stratigraphy in MR slides is similar although the interbedded silts are less noticeable. A highly plastic silty clay has always been found at or near river level in the vicinity of all block and MR slides. All members of this sequence have been found in a frozen condition and the various observations made on ground ice conditions in conjunction are detailed in Appendix A.

Within the study area, permafrost depths are variable but a figure of up to 160 ft is characteristic of the terrain type found in association with slide movements. Now, as slide movements are found in banks ranging in height from 120 to 240 ft and as permafrost will extend well towards the river bank (see Mackay and Mathews, 1973) permafrost will be found in a significant portion of a bank cross-section. Therefore, the possibility exists that if a deep-seated failure extending well back into the GLB upland is found that this failure has occurred through frozen soil. If the bank heights are low, say at the minimum of around 100 ft and permafrost is thick to around 160 ft, then relatively more failure is associated with frozen ground than for high, 240 ft, banks with only 120 ft of permafrost. For higher banks and thinner permafrost, failure will then be seated in frozen sands and silts bottoming out in unfrozen clay or silts depending on the relative proportions of the soil stratigraphy. However, for lower banks with clay at river level, the assumption of failure through frozen sands over unfrozen clay is also reasonable due to a combination of circumstances. Near river level permafrost temperatures will be approaching $0^{\circ}C$ and the clay will contain large quantities of unfrozen water. For these conditions it might be speculated that the pore water phase is continuous and that modified effective stress parameters might govern shear strength so that from a strength point of view the clay will react as if it is unfrozen. Thus, for most combinations of bank heights , soil stratigraphy and permafrost conditions, block and MR slides can be characterized as involving failure through frozen sands and silts underlain by unfrozen clays.

As there is no evidence in the way of instrumented borings that confirms that the slide masses found in block and MR slides are frozen, it is useful to summarize the circumstantial evidence. The remnants of a large block slide near Mile 655 which had moved to near river level revealed large ice wedges and frozen sand in recently exposed river cuts and indicates that at least the top portion of the block was frozen. Permafrost depths in this reach are not known but some 15 miles inland, drilling at the Hume River revealed at least 160 ft of permafrost although the soil stratigraphy was different. As the bank heights at Mile 655 are around 200 ft it is expected that a significant proportion of the pre-failure bank cross-section was frozen. At the Mountain River MR slide, drilling about 400 ft behind the headscarp found some 155 ft of permafrost in a bank 220 ft high. Visual sightings of massive ground ice along the toe area of the Mountain River slide were made in recently cut sections of a slide mass which had come down from an indeterminate height confirm that some portions of the blocks are frozen.

Other corroberative evidence is summarized in Appendix A and it can be noted that the bi-modal flows that develop along the toes of some MR slides and the rapid changes of dip of generally flat-lying varves along the faces of some block slides suggest the presence of melting ground ice and thus to permafrost conditions.

A strong argument for frozen conditions in the slide mass can also be made by considering the vegetation patterns in and adjacent to slide areas. As pointed out by Mackay and Mathews (1973), permafrost can be considered to begin beneath the upland vegetation of spruce found bordering the top of most high and unstable river banks in the study area. The permafrost table may be bent slightly inwards underneath the bank in response to thermal disturbance along the pre-failure bank face. Now, it can be observed that the failure of block and MR slides extend backwards up to 500 - 700 ft behind the tree line as inspection of slide masses indicates that they are covered over with spruce covers in all respects identical to the stands in undisturbed terrain. While it is necessary to infer the presence of permafrost beneath this undisturbed terrain, in some regions the results of the winter drilling programme supplemented by observation by Scott (1972) confirms that permafrost appears to be generally present. For example, at the Mountain River site 155 ft of permafrost was found behind the slide area. At this site the slide masses are covered over with spruce, either similar to or denser than the upland cover and the inference that the slide masses are partly frozen has been confirmed by visual sightings of ground ice along the toe portion of the slides.

The thermal influence of the river and the degree of thermal disturbance along the bank will determine the amount of inward bending of the 0°C isotherm from a pivot point at the tree line, Fig 2.3. This problem can be considered by way of a simple steady state model. The mean annual temperature of the Mackenzie River calculation from data in Gill (1971) is +4°C in the delta region and Mackay and Mathews (1973) also suggest a value of +4°C. Along the upland beneath the spruce cover the mean annual soil surface temperature (MASST) can be deduced from the extrapolation of the in-situ ground temperatures below the level of zero annual change until they reach ground surface. Using data obtained by Scott (1972) in the Sans Sault Rapids area MASST values of from -2.3 to -2.5°C are obtained and these compare favourable with MASST values of -3.0°C assumed by Mackay and Mathews (1973). Thus, for steady state conditions the 0°C isotherm will be found more or less equidistant from these two surfaces until it bottoms out at whatever the permafrost depth is commensurate with the MASST and geothermal gradient away from the thermally disturbed area (see also Mackay and Mathews, 1973, Fig 8). It might also be pointed out that a more detailed analysis of this problem is not warranted because of the uncertainties involved in knowing MASST values for the sloping bank which might be expected to range from at least -2 to +2°C.

2.4 Geotechnical Considerations

(i) Index Properties

As the exploration of the study area progressed it became evident that the majority of the landslide forms encountered were seated in a silty clay soil either in natural or colluvial deposits. Samples of silty clay collected from all areas during the summer survey are presented in Table B.1, Appendix B, and are coded according to the place names as shown. The relatively high percentage of illite and the low percentage of montmorillonite in the clay fraction is noteworthy.

Samples were also obtained during the winter drilling programme and borehole logs are given in Figs B.1 to B.4. Samples taken during the drilling programme are coded according to hole number and depth, such as HU1-2-55.0, where the 55.0 refers to the depth below ground surface.

Field water contents and ice contents expressed as a water content are given in Table B.2 in borehole logs, Figs B.1 to B.4, and plotted against depth and compared to the plastic and liquid limits for the Mountain and Hume River sites in Figs B.5 to B.8.

The relative position of the various samples are shown on a plasticity chart, Fig B.9 and the figure showing the relationship between plasticity index and % clay is given in Fig B.10. Information on grain size distribution is given in Figs B.11 to B.13, and in Table B.3.

(ii) Geotechnical Testing

As the predominant clay mineral of the Mackenzie Valley clays encountered is illite, it can be expected that the effective stress residual strength parameters (c'_r, ϕ'_r) will be high. A series of direct shear tests on normally consolidated remoulded Mountain River Blue Clay indicated the peak parameters to be $c' = 1$ psi, $\phi' = 26.5^o$, and the residual parameters to be $c'_r = 0$, $\phi'_r = 23^o$ for samples tested at normal effective stresses from 8.0 to 40.0 psi (Roggensack, 1972)*. The residual value of $\phi'_r = 23^o$ is in good agreement with published values for illite.

Void ratio versus effective stress and void ratio versus permeability relationship were obtained for a sample of clayey, silty sand taken from beneath the permafrost at the Mountain River site and are presented in Fig B.14.

---

*Personal communication

Strength tests were also conducted on frozen samples but the results of this testing are presented elsewhere.

(iii) Piezometric Observations

During the survey a series of field tests were made at selected sites using 2 types of portable piezometers. The first was designed for use in the survey and consisted of a pressure transducer mounted in a tapered, self-sealing housing. The second used an open standpipe attached to a porous tip.

The piezometers were designed to be gently pushed into position and to be withdrawn on the completion of the test. As the absolute magnitudes of the pore pressures measured were small and as the sites were easily disturbed special care was required to ensure that little disturbance was caused before and during the tests. Since the purpose of the tests was to investigate the total pore water pressure above a thaw interface and to investigate the relative proportion of hydrostatic to excess pore pressure it was necessary to know the position of the water table. Although surface conditions were very wet in the two sites where measurements were made, tests were conducted in those areas where small surface pools of water could be found in order to accurately define all boundary conditions. The results of all field tests are presented in Fig 2.2.

The first series of tests were conducted in a silt run at the Fort Norman Landslide, Fig A.15. Tests P1 and P3 were made using the transducer piezometer beneath free-standing water collected in two small ponds in the middle of the silt run while test P2 was made at the edge of the silt run. Tests P1, P2 and P3 were made on June 17, 1972, and further tests, P4 and G1, were conducted on June 23, 1972. The results of the piezometer measurements are presented in Fig 2.2. It can be seen that excess pore pressures were measured in tests P1, P3, P4 and G4. Hydrostatic conditions for the water contents measured, Table B.2, should result in r_u values of about 0.51 where

$$r_u = \frac{Pw}{\gamma z}$$

where Pw is the total pore pressure, and

γz is the total stress

The r_u values measured, or inferred, for the geonor open tip test where a minimum value was measured, are considerably in excess of the hydrostatic condition of $r_u = 0.51$.

Placement of the piezometer was exceptionally easy in tests P1, P3, P4 and G1 and a slight upwards force was required to ensure slow placement as the assembled piezometer and attached rods sank easily under their own weight. On the other hand, considerable thrust was required to place test P2 and the relatively firmer soil conditions are indicated by the lower r_u measurement. The higher pore pressures measured in the initial stages of test P2 are likely caused by disturbance due to the placement operation. Tests P1 and P3 were extended to one and two hours duration in order to confirm that equilibrium conditions had been established.

After each test permafrost conditions were checked by probing in the hole vacated by the piezometer. In all instances, frozen soil was encountered and the depth of the active layer in the silt run varied from 1.65 to 3.1 ft. In holes P1 and P4, the soil stratigraphy was inspected by the simply expedient of hand probing. On probing the low effective stress conditions were apparent and little resistance to penetration was met over the entire depth although large chunks of hard soil could be felt contained within a matrix of softer soil. At the end of the probe a remarkably flat, smooth surface, the thaw interface, was reached. This surface was hard and cold and although no samples were obtained it was quite definitely the base of the active layer within the silt run.

One test, H1, was made in a bi-modal flow along the Hanna River, Fig A.21, and the significant details of the test are given in Fig 2.2. This test was also made beneath free water in a small surface depression. After the test, hand probing confirmed that the piezometer tip had been placed above the thaw interface.

Pore pressures were also measured in the lobe of a bi-modal flow at Mile 462. Pore pressure conditions in this lobe were near hydrostatic as an r_u value of 0.61 measured is not greatly different from a hydrostatic value of 0.54 based on measured water contents, Table B.2.

2.5 Observations on Terrain Disturbance

2.5.1 River Action

As the landslide survey concerned itself with mass movements associated with the Mackenzie River and its tributary waters and as the greater portion of field work was conducted by a river-based operation it is only natural that considerable note should be made of the importance of river action in promoting landslide activity. However, unlike landslide activity associated with river action in more temperate climates the importance of river action may be as much one of thermal influence as physical erosion.

A primary cause of instability in some reaches of the Mackenzie stems, in part, from the presence of highly-braided gravel-bed tributaries that drain the east flanks of the Mackenzie Mountains and flow into the Mackenzie River. Rivers such as the Liard, North Nahanni, Root, Redstone, Dahadinni, Keele and Mountain appear to be important suppliers of coarse and fine sediment to the Mackenzie River. The importance of these rivers, historically, in partly determining the location of GLB basins has been discussed in the preceding section

Today, these rivers, flowing on generally steep, longitudinal slopes, dump large amounts of sediment into the Mackenzie which is unable to transport the imposed bedload. The Mackenzie River, in turn, deposits these imposed bedloads in the form of islands around which it must pass. This form of river morphology is particularly evident downstream from the North Nahanni and the Root; the Dahadinni, Redstone and the Keele; and the Mountain Rivers where the Mackenzie is characterized by sinuous channels and many islands formed from recent fluvial deposits. There is channel splitting around sand bars and wooded islands and where the river is actively eroding GLB deposits landslides occur.

It also appears, however, that the formation of islands and their influence on lateral channel shifting while being a necessary is not sufficient condition for instability. For example, from Wrigley at Mile 355 to the Dahadinni River at Mile 417, the Mackenzie River flows in a single channel of fairly regular width with little sign of lateral shifting or bank instability. There are few islands and a well-defined trim line appears to demarcate the average annual flood level. Below the Dahadinni and to the Redstone River at Mile 433, the Mackenzie also flows in a relatively straight reach with little landslide activity along river banks although there are frequent sand bars and small islands. It can be seen that conditions downstream from the Dahadinni River should favour landslide activity as it is a braided gravel-bed stream and many islands are contained in the Mackenzie River downstream from this confluence. The banks, however, are seated in tills and bedrock with the result that instability is generally absent as it is from Wrigley to the Dahadinni where banks appear to be either till or bedrock. Downstream from the Redstone and particularly below the Keele River there is a marked increase in landslide activity along the east bank where the Mackenzie is actively eroding GLB deposits. Therefore, the widening of the river channel below the Keele River is as much a consequence of bank stratigraphy as it is of river action and the deposition of fluvial islands.

However, it is generally true that there is a marked association with landslide activity and channel splitting downstream from braided gravel-bed tributaries of the Mackenzie River.

An interesting phenomenon is also observed along the Mackenzie River below the confluence with the Keele River. As can be seen in Fig A.8, the Mackenzie River increases its width from one mile to about 5 to 6 miles in this reach and massive instability is found along the east bank, Figs A.9 and A.10. However, instability is completely absent along the low-lying west banks seated in apparently easily erodible, recent, fluvial sediments. It might be suggested that the Mackenzie River is being caused to erode against the east bank by active orogeny in the Mackenzie Mountains tilting the river towards the east.

The consequences of active river erosion on the distribution of flow landslides is particularly evident along the Hanna and Hume Rivers. Both the Hanna and the Hume flow in a U-shaped channel meandering in a flood plain entrenched some 50 to 75 ft into a glacial lake basin. As the rivers meander in their entrenched channels the bends of the river come in contact with, and erode, GLB scarps. The greater percentage of active bends abut this upland while the straighter reaches are cut through recent fluvial deposits. Skin and bi-modal flows can be found seated in the GLB soils at active bends and recent flows cause the rivers to detour around the toes or terminal portions of the flows. This rapid change in direction results in active erosion of the fluvial deposits always found opposite flows in the GLB upland and this erosion results in the development of falls and rotational slides in the fluvial soils. It can also be noted that rotational slides can also be found in the straighter reaches between bends and these likely occur in response to rapid drawdown conditions caused by changing levels in the Mackenzie River. Their proximity to the river and evident rotational aspect suggests that these slides are not associated with frozen ground.

2.5.2 Knobby Terrain

Old GLB scarps, long-abandoned by shifting river channels or by further entrenchment of the river system, can in some areas develop a characteristic knobby appearance. This feature has been noted in banks opposite the Ochre River, along the Great Bear River and the Mountain River and near Mile 653. It is not clear if the knobby terrain along these banks results from erosional features, shallow mass movements or if it is the modified remnants of old MR slides.

2.5.3 Boulder Pavements

Along many reaches of the Mackenzie River well-developed boulder concentrations pave the banks up to the trim line. These boulder pavements apparently result from some form of ice shove mechanism and it is considered unlikely that they could have been formed by water action alone. Although the boulder pavements are commonly found along till banks which appear to be inherently more stable by themselves no landslides have been found in boulder-paved reaches. It is possible, therefore, that they may have a "rip-rap" or stabilizing effect on river banks.

2.5.4 The Influence of Vegetation and Forest Fires

The frequency and extent of flow landslides in areas recently burned-over by forest fires is striking. The role of the forest fire in promoting landslide activity has been noted along the Hume and Hanna Rivers, along the south bank of the Great Bear River, on an unidentified tributary to the Wrigley River and in frequent locations along the Mackenzie River. Evidently an important aspect of forest fires is their influence on the energy budget and it is generally known that one effect of forest fires or artificial removal of surface cover is a thickening of this active layer. As no direct observations have been made of this effect further discussion will be left until a later chapter. Another role of forest fires is to drastically alter certain critical mechanical properties of the organic surface covers found throughout the study area.

Vegetation cover plays an important role in the development of bi-modal flows. In bi-modal flows that have developed in unburnt areas an organic vegetation cover is frequently found draped over the head and side scarps. These curtains have never been noted over about 10 ft in depth of hang and under these covers of moss, lichen and roots one usually can find a void filled with dank, musty air. Upon cutting into these overhanging covers frozen ice-rich soils are always found. Under these insulative configurations the vegetation covers may significantly retard the melting and, therefore, the headward movement of an active bi-modal flow. However, as natural covers apparently cannot exceed about a 10 ft depth, this process is only effective in slowing or stopping shallower bi-modal flows. Or, it will stop a bigger flow only when the headscarp approaches a height of 10 ft, all else being equal.

One influence of forest fires is the possible effect on this natural stabilizing process. It has been observed that forest fires cause a desiccation of the surface mat which becomes brittle upon partial burning. For example, frequent cracks were seen in the burned moss covers above the headscarp of the Hanna Island Landslide, Fig A.18, and in the burned-over terrain along the Hanna River. When the surface covers lose their natural resilience on being burnt and desiccated, moss curtains cannot develop. In fact, no vegetation curtains have been observed in any flows with extensively burned up-scarp conditions. It is suggested, therefore, that small bi-modal flows may more easily progress into larger flows if fire has destroyed the efficiency of a natural stabilizing mechanism.

2.5.5 Gully Formation

Frequent note has been made of the strong association between gully formation and landslides seated in GLB sediments. Although it is far from clear if gullying has any influence on landslide occurrence certain features may be noted.

Gullying is marked in association with the block slides at Fort Norman, Miles 513 to 515 and below Sans Sault Rapids, at Miles 648 to 654. It appears that post-slide conditions enhance gully action as easily erodible thawed sands and silts are exposed in the slide mass and adjacent to it. It is possible that gully action picks out the initial geometry of failure. A detailed description of the gullying near Fort Norman is given in Appendix A. In these block slides, silty clay was found close to river level and other exposures along this reach suggest that the sand-silt varve sequence extends close to river level. The gullying in this reach is incised almost to river level and they are likely seated in the silty clay found at river level. Therefore, deep-seated gullying is a possible indicator of thick sand and silty sand sequences within a GLB sequence.

Support for this conclusion exists in the bi-modal flows found downstream from the Keele River. For example, at the Old Fort Point Landslide, the clayey-silt member of the GLB sequence extends to within 40 ft of the top of a 250 ft high bank and this stratigraphy is common in this reach. Although gullies are common in this area none are deep-seated and the more recent ones generally appear to perch on top of the finer-grained soils. A small gully can be seen on the downstream side of the Old Fort Point Landslide, Plate 4, and it extends behind this landslide at a level approximately equivalent with the base of the sand.

A different form of gullying of the type outlined above is common in the Keele River area and has also been noted between Fort Simpson and Camsell Bend. As already observed, these gullies are never deep-seated but are actually perched in relation to the landslide movements adjacent to them. Consider the gully visible on the downstream side of the Old Fort Point Landslide, Plate 4, and considered schematically in Fig 2.4. The bottom of this gully is higher than the top of the bowl of the Old Fort Point Landslide and is separated from it by a thin ridge of apparently stable soil. Similar gullies can also be seen in the aerial photographs of this reach. A somewhat similar gully can be found adjacent to the west scarp of the Fort Simpson Landslide, Fig A.3. Although the gully is seated at a slightly lower elevation than the bowl of the landslide it is separated from the bowl by a high ridge of stable soil. Identical gullies to that found at the Fort Simpson Site also are found either side of the Cameron Point Landslide, Mile 265. A comparison of the 1961 aerial photography which shows this MR flow with the 1944 coverage with no landslides, indicates that failure occurred between but not including the two gullies.

This form of gullying, as outlined in Fig 2.4, is found in conjunction with either bi-modal or MR flows. We have established that these landslides are associated with the rapid melting of ice-rich soil. However, it appears that the formation of a gully results in the slow thaw and stabilization of the permafrost beneath and adjacent to the gully. The gully forms before the landslide develops and forms a plug of thawed, stabilized soil which is not affected by the latter, adjacent flow landslide.

It does not appear that the gullies actively encourage flow landslides but their presence points out the stabilizing effect of the slow thaw of permafrost in contrast to the catastrophic effects of adjacent rapid melting.

2.5.6 Climatic Change

The possible importance of climatic change and its influence on ground thermal regime should be considered briefly as long term changes in ground temperatures and permafrost depths could influence landslide occurrence. Judge (1973) has reviewed the evidence of climatic change in both Canada and Alaska and notes that an average warming of 2 to 4°C has occurred in some parts of Alaska over the last 100 years. He also notes that some 2.2°C warming of the ground may have occurred at Fort Providence, N.W.T., over the last 75 years although this may be due to artificial causes. Judge also notes that a general warming trend has occurred over the past few hundred years since the Little Ice Age of the seventeenth century. These changes in temperature could prove to have significant effects as it is evident that a long-term change of 1°C in the mean annual surface temperature would result in a change of the depth of permafrost of at least 50 - 75 ft.

TABLE 2.1 SKIN FLOW PROFILES

Location	Angle (degrees)	Comments
Hanna River	11.5	
	6	
	8.6	Flow 3 ft below adjacent burned-over surface
Hume River	9 to 10	Some lobes at 6^{o}
Root River	23 to 33	Flows in weathered shale. Dimensions in the order of 1000 ft long by 75 ft by 3 ft deep. Angle estimated from topographic map.
Wrigley River	14 to 18	Flows in till (?). Both banks burned, instability restricted to north banks. South banks 9^{o} to 10^{o}. Angle estimated from topographic map.

TABLE 2.2 BI-MODAL FLOW PROFILES

Name, Location	Lobe Angle (degrees)	Headscarp Angles	Length (feet)	Area (Square Feet)	Comments & Aerial Photographs
Mile 207 to 219	7 to 10	steep			Frequent flows along the south bank in silty clay.
Mile 218	7				Rotational failure of headscarp in sandy loam over silty clay
Wrigley Flow, Mile 350	3	steep	3500	10^8	Lobe angles measured at 4, 4-1/2 degrees. A17496-64.
Big Smith Creek, Mile 471	9	31	600		Bank 190 ft. 50 ft sand over clayey silt to silty-clay at river level. A17496-189.
Ice Buttress, Mile 473	9	steep			Massive cantilevered block of frozen sand, 25 ft deep with a 20 ft extension exposed at the top of the headscarp.
Old Fort Point, Mile 480	14	38	600		Bank 250 ft. 40 ft sand over clayey-silt to silty-clay at river level. A17496-185.
Fort Norman, Mile 517	3	36	800	4×10^5	Bank 130 ft. 20 ft sand over silty-clay. A17496-174.
Little Norman, Mile 518	6	40	300	9×10^4	Bank 80 ft. 70 ft sand over silty-clay at river level. A17496-173.
Mile 550	7 to 8	steep			Lobes begin at trim line. A17496-165.
Hanna Island, Mile 635	6 to 7	40	400	4×10^4	Bank 63 ft. Veneer of sand over silty-clay.
Hanna River	6	12	200	4×10^4	
	5.5	steep			
	6	17			
Mile 642	13	28			Small flows at 6.5 to 7.5 degrees within tongue of flow.
Mountain River	5	steep	3500	10^8	Dimension estimated off aerial photography. Flow perched on bedrock. A12607-133

TABLE 2.3 MULTIPLE RETROGRESSIVE FLOW PROFILES

Name, Location	Lobe Angle (Degrees)	Head Scarp Angle	Length (Feet)	Comments and Aerial Photographs
Mile 221	4.5	Steep	2300	Adjacent bank at 10.2 degrees. Bank 180 ft. A11028-351.
Mile 225	4.7	Steep	2200	Adjacent bank at 30 degrees. Bank 180 ft. A22913-110 to 113.
Fort Simpson Mile 226	5	20°	1700	Pre-flow bank at 18 to 23 degrees. Bank 187 ft. A22913-109.
Cameron Point Mile 265	6.5	Steep	1100	Bank at 125 ft. A17504-50.

TABLE 2.4 BLOCK SLIDES

Name, Location	Bank Height (feet)	Angle Overall (degrees)	Comments and Aerial Photo Number
Camsell Bend, Mile 275	120	15	Typical profile, A17496-6
Fort Norman, Mile 513 to Mile 515	130	13	Typical profile, A17496-175
Mile 641 to 653	125 to 175 (some to 200 ft)	-	Typical profile, A19947-65. No maps, bank height estimated.

TABLE 2.5 MULTIPLE RETROGRESSIVE SLIDE PROFILES

Name, Location	Bank Height (feet)	Angle Overall (degrees)	Comments and Aerial Photo Number
Mile 293	120	13.6	Re-activated slide:A17496-16
Mile 300	170	13.6	A17496-19
Mile 350	260	-	Small bi-modal flows seated in toe:A17496-67
Mile 475	225	10.0	Large toe upthrust in river channel: A17496-125
Mile 484	240	14.0	A17496-126
Mile 621 Axel Island	185 to 235	9.5 to 14	Adjacent banks at 23 degrees: A19947-45
Mountain River	220	12 to 13	Series of failures: A19947-49
Hume River	100 to 125	-	A8331-88: No maps, bank heights estimated

TABLE 2.6 SUMMARY OF ICE WEDGE OBSERVATIONS

Site	Location	Comments
Ice Buttress landslide	Mile 473	Occasional thin ice wedges in the sand member of GLB sequence.
North Bank Mackenzie River	Near 507	Top of 6 in thick ice wedge exposed about 2 ft in fluvial deposits over Tertiary sediments.
Fort Norman landslide	Mile 517	Possible indication of ice wedges in melt features along the headscarp seated in sand member of GLB sequence.
Hanna River		Ice wedges found in recent cut bank in fluvial sediments. Wedges irregular sized, an average 2 - 4 in thick, exposed about 3 to 4 ft.
Mountain River		Ice wedges exposed by fall landslides. Wedges seated in fluvial deposits.
Block Slide	Mile 653	Ice wedges exposed in a block slumped to river level. Wedges seated in sand member of GLB sequence.

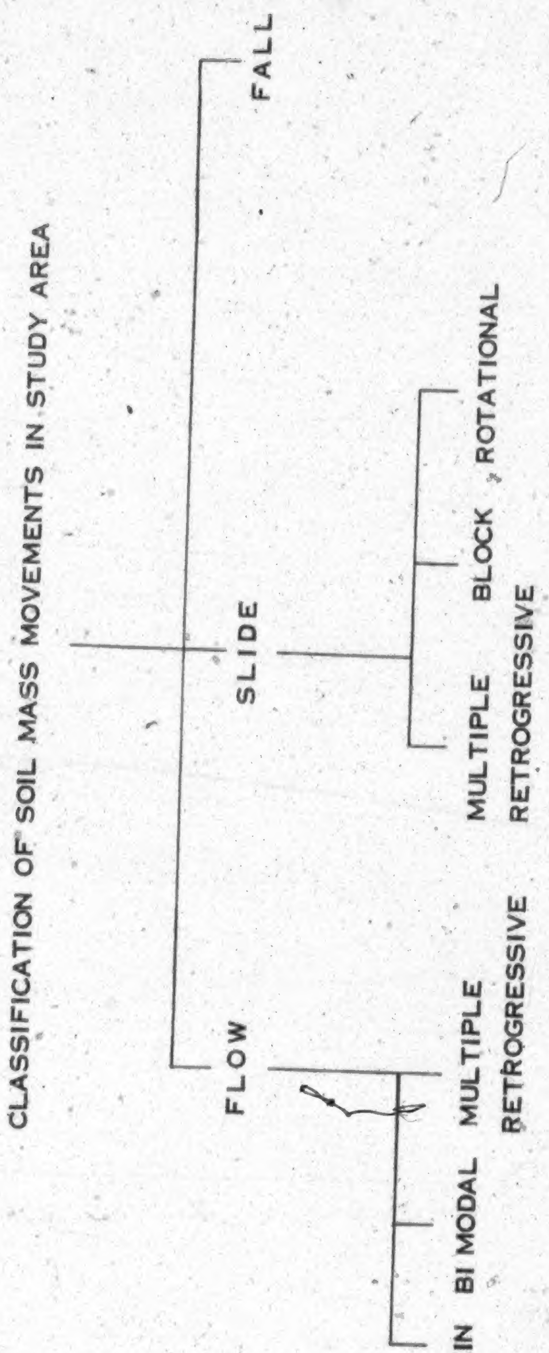
CLASSIFICATION OF SOIL MASS MOVEMENTS IN STUDY AREA
FLOW
SLIDE
FALL
SKIN
BI MODAL
MULTIPLE RETROGRESSIVE
MULTIPLE RETROGRESSIVE
BLOCK
ROTATIONAL

Fig 2.1 Landslide Classification

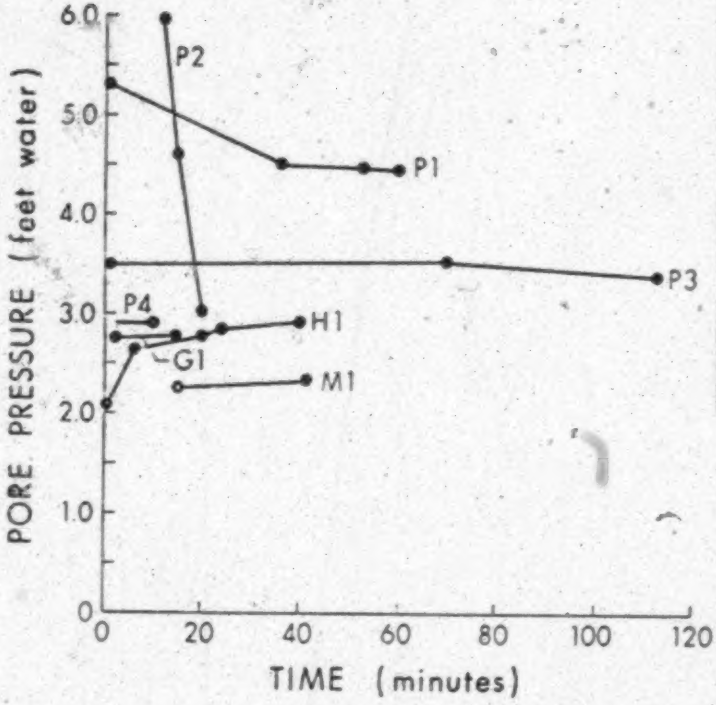

CODE	P1	P2	P3	P4	G1	H1	M1
Site	FORT NORMAN					Hanna River	Mile 642
Depth of Tip	2.1	3.1	1.9	1.65	1.87 average	1.5	2.05
Equalized Pore Pressure	4.45	3.0	3.4	2.85	2.77[4]	2.9	2.3
Ratio of Pore Pressure to Depth	2.1	0.97	1.79	1.73	1.48	1.93	1.12
r_u	1.08[1]	0.50[1]	0.91[1]	0.88[1]	>0.78[1]	[3]	0.61[2]
Piezometer Type	T[5]	T	T	T	G[6]	T	T

Notes

(1) Based on water content = 30.5%, G_s = 2.76

(2) Based on water content = 40%, G_s = 2.76

(3) Water content not taken

(4) Pore pressure not equalized, minimum reading recorded

(5) Transducer mounted in U of A Probe Piezometer

(6) Geonor open stand pipe tip, Intake length 1.17 feet

Fig 2.2 Results of Field Piezometer Tests

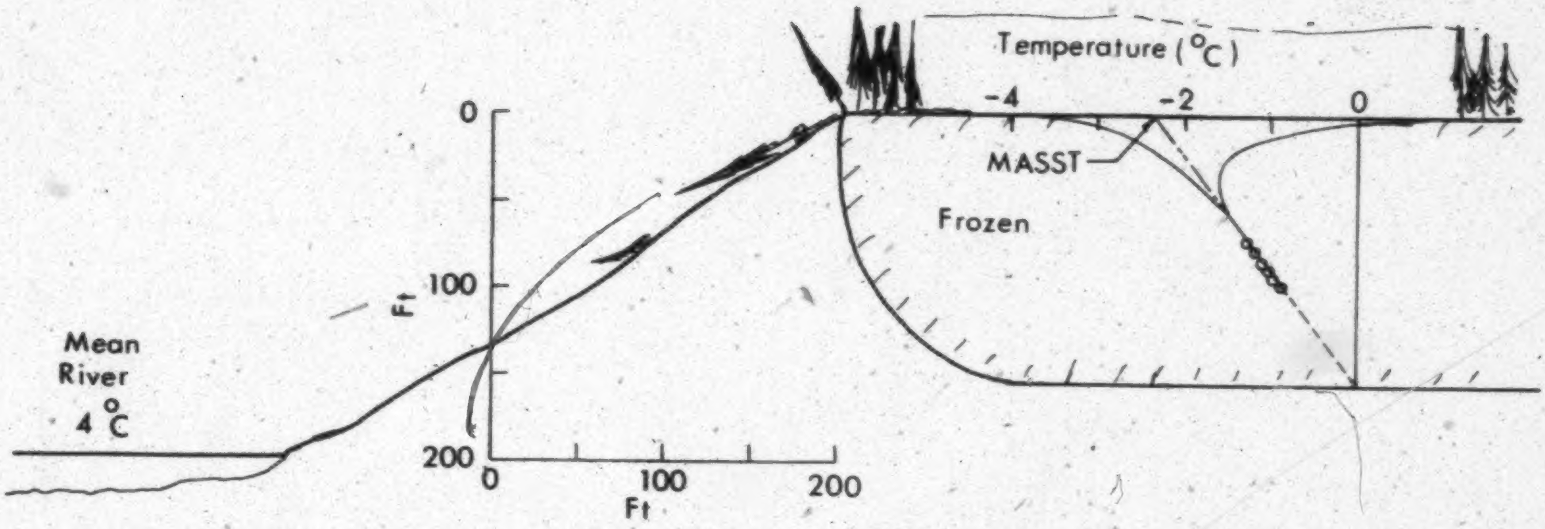
Temperature (°C)
-4
-2
0
MASST
Frozen
Mean
River
4 °C
0
100
200
Ft
0
100
200
Ft

Fig 2.3 Permafrost distribution adjacent to a high river bank

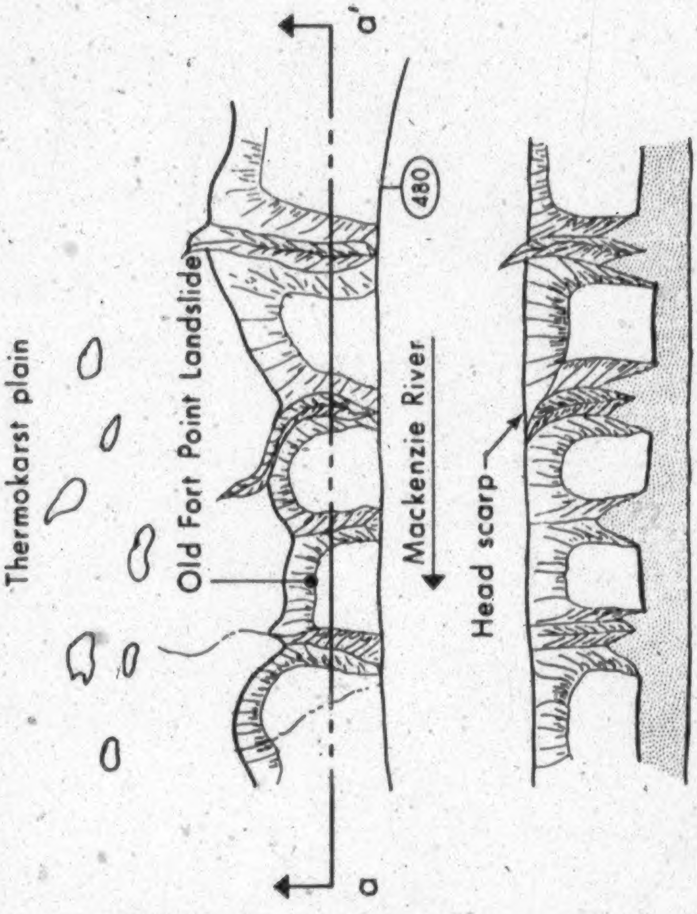
Thermokarst plain
Old Fort Point Landslide
Mackenzie River
480
a
a'
Head scarp

Cross Section along a-a' indicating depth of gullies in relation to head scarp and adjacent landslides

Sketched from aerial photo A11975-209
Horizontal scale 1" = 800"

Fig 2.4 Typical gully formation adjacent to flow landslides

CHAPTER III

THAW - DOMINATED MASS MOVEMENTS

3.1 Introduction

This chapter investigates mass movement mechanisms in thawing soils and, where possible, introduces these models into simple one-dimensional stability analyses and compares them with actual slope failures. The results of a field study in the Mackenzie Valley coupled with a review of the periglacial mass movement literature emphasises the role of thaw in a wide range of landslide types. There is overwhelming evidence to suggest that the slope stability of such forms as solifluction lobes, skin flows and the tongues of bi-modal flows is partly controlled by the rate of advance of a thaw interface as it penetrates into the underlying permafrost. The geotechnical implications of thaw under these conditions can be quantified and the characteristic shape of these slopes makes them amenable to analysis in one dimension. Thaw is also of fundamental importance in the headscarps of bi-modal flows but, in many cases, melting occurs in a different manner than for solifluction, etc. Often ice or ice-rich soil is exposed directly to the atmosphere and the melt is constantly removed, a thaw process called ablation.

Therefore, in order to undertake an orderly consideration of thaw dominated failure mechanisms it is evident that an appreciation of the factors influencing thaw must first be gained. The problem will be considered briefly with the greater part of this chapter devoted to geotechnical consideration.

3.2 Some Aspects of the Thaw of Soils

3.2.1 The Energy Balance

The micro-climate of a particular site is governed by a host of complex and interrelated factors. These factors have been summarized by Geiger (1965) and to whom the reader is referred for a detailed explanation of any of the terms or concepts used in the following section. The climate near the ground in turn determines the net flux that is transmitted into the ground and in a coupled manner the temperature and temperature gradients in the ground.

The energy balance at the interface between the atmosphere and the ground can be expressed in the following manner;

$$R_n = LE + H + G \qquad 3.1$$

$$\text{or} \quad 1 = LE/R_n + H/R_n + G/R_n \qquad 3.2$$

where R_n is the net radiation, LE is the latent heat of evapotranspiration, H is the convective heat flux and G is the soil heat flux. In turn, R_n is expressed as

$$R_n = (Q)\ (1 - a) + I \qquad 3.3$$

where Q is the incoming solar or shortwave radiation, a is the albedo and I is the net longwave radiation (Stefan Boltzsmann radiation). Thus we can solve for G the ground heat flux as

$$G = Q(1 - a) + I + LE + H \qquad 3.4$$

and knowing the absolute magnitudes and daily variation of Q, a, I, LE, and H it would be theoretically possible to predict the depth and rate of advance of a thaw interface.

However, the prediction of the above variables for a given site and surface cover under varying cloud covers, wind velocities, relative humidity, surface temperature, air temperature, and so forth is another matter indeed. While the solution may be indicated in a symbolically straightforward manner all variables are inter-related to different degrees and a detailed consideration of their interaction is beyond the scope of this thesis. We shall consider some typical values of the major components of Eq 3.1 and 3.3 as it is found in later sections that an understanding of these components aids us in understanding mass movement processes.

Typical values for albedo are given in Table 3.1. The amount of incident solar radiation absorbed by a given surface increases as the surface becomes darker. Albedo is also affected by water content as wet surfaces appear darker than dry surfaces. Typical values of the ratios in Eq 3.2 are presented in Table 3.2 and where possible all three ratios are deduced using Eq 3.2. All case records presented are for either high alpine or sub-arctic sites and it is noteworthy that for a range of sites, with the exception of the Chitistone Pass site, that the ratio G/R_n is 0.195 with a range (0.09 to 0.26). Some values for the Q and I components of Eq 3.2 are given in Table 3.3 for some of the sites already noted in Table 3.2.

Let us now briefly consider some of the implications of Eq 3.1 and 3.3 in terms of the relative magnitudes of the components as shown in Tables 3.1 to 3.3. Firstly, the amount of thaw over a season will be governed by the amount of soil heat flux, G, that can penetrate into the soil. The importance of the LE and H components in reducing the available flux is evident. The ratio G/R_n is, in part, governed by the wetness of the surface as can be seen for the Barrow site, Table 3.2, where the ratio gradually increased during the thaw season as the tundra surface became drier. As the albedo appears to be constant for a tundra surface over the season (Haag, 1972) it appears that the ground heat flux increased in relation to net radiation once the surface became drier and the evaporation barrier lessened.

The amount of thaw will also be affected by cloudy days during which the ratio G/R_n will increase as relative humidities are high and little evaporation will occur. However, the absolute magnitude of G might be significantly lower because cloud cover would decrease incoming solar radiation, and thus R_n, by Eq 3.3.

Changing the surface cover will also affect the thaw depth for a variety of reasons. Changes in vegetation cover from living to burned, or cleared, will decrease the albedo and increase the amount of R_n and thus of G. A comparative study reported by Linell (1973) has shown for one site in which the spruce and brush cover was removed 4.5 m of permafrost was thawed in 26 years while an adjacent site stripped of all vegetation underwent 6.7 m thaw in the same time. The control site covered with spruce, brush, moss and grass maintained an active layer depth of about 1 m and it is suggested that the primary control in the disturbed sites was exerted by albedo. Alternatively, covering a dark wet soil with a light sand will increase albedo and have the opposite effect on R_n and G. A thick covering of sand would, however, tend at the same time to increase the ratio G/R_n as there might now be less water available to reduce G by evaporation. On the other hand, the effect of forest fires is, in part, the reduction of evapotranspiration as both living canopies are destroyed and surface runoff is rapid. Thus, in burned areas thaw is accelerated because lessened LE results in increased G.

In conclusion, we can follow Gold and Lachenbruch (1973) in noting that

> "Although attempts are being made to determine the time dependence of the surface temperature by measuring the components of the surface head exchange, the greatest benefit of these measurements has been to provide a general qualitative to semi-quantitative appreciation of the influence of relief and surface factors .... on the relationships between ground temperature and weather."

Thus, in order to gain quantitative information on the thawing of soils it is necessary to proceed to a consideration of problems that can be described using a temperature, rather than a flux boundary condition.

3.2.2 Mathematical Models in Thawing Soils

Many aspects of the thawing of frozen soils can be considered with ease using temperature boundary conditions although specific problems such as ablation melting require the specification of a flux boundary condition. A wide range of available solutions have been discussed by Nixon and McRoberts (1973) who focus attention on both solutions for and factors influencing the rate of thaw. This parameter is of considerable interest in geotechnical problems and we will concentrate on its role in defining the mechanical response of a thawing soil in a later section. We shall now consider certain analytic solutions for thaw in frozen soils, factors influencing the prediction of thaw rates, typical rates of thaw for likely boundary conditions and finally compare mathematical models with field studies.

If a uniform homogeneous frozen soil is subjected to a step increase in temperature from T_g in the ground, to T_s at the surface, a thaw interface is caused to move through the frozen soil as given by

$$X = \alpha \sqrt{t} \qquad 3.5$$

where X is the depth of thaw, t is the elapsed time since T_s was applied and α is the rate of thaw, a constant which must be determined. This problem was first solved by Neumann (see Nixon and McRoberts). Written functionally

$$\alpha = f\,(T_s, T_g, L, k_u, k_f, c_u, c_f) \qquad 3.6$$

where L is the volumetric latent heat of the soil, c_u and c_f are the volumetric heat capacities of unfrozen and frozen soil and k_u and k_f are the thermal conductivities of unfrozen and frozen soil. A graphical solution to Eq 3.6 is given by Nixon and McRoberts.

If the Neumann problem is simplified by assuming that $T_g = 0$ and that temperatune gradients in the thawed zone are linear then the so-called Stefan problem is formulated as

$$X = \sqrt{\frac{2k_uT_s}{L}} \cdot \sqrt{t} \qquad 3.7$$

Nixon and McRoberts consider the importance of the variables of Eq 3.6 on the magnitude of α and find that in problems involving thaw the dominant variables are ground surface temperature, the thermal properties of the thawed soil and the total quantity of water that changes state. They consider the importance of unfrozen water content and suggest that L be defined as

$$L = \gamma_d \, (1 - W_u) \, w \, L^1 \qquad 3.8$$

where L^1 is the latent heat of ice, γ_d is dry density, w is the water content, and W_u is the unfrozen water content expressed as (g water/g(ice + water)) at the T_g of interest. If L is then lumped at 0°C the path-dependent nature of W_u can be accounted for with ease for all practical purposes.

As the variables (T_g, k_f, c_f) can be shown to be of lesser importance in thaw problems, α determined from Eq 3.6 can be estimated to a reasonable degree of accuracy by Eq 3.7. A detailed consideration of the error involved has been presented by Nixon and McRoberts (1973) where other variations of the solution to the thaw problem with a step increase in surface temperature are also considered.

Step temperature increases are considered to be a reasonable temperature boundary condition for a wide range of thawing slopes. For natural environments where snow covers are not artificially cleared winter snows can remain for some time and it is argued that by the time that snow covers melt air temperatures have reached summer highs. As spring is a somewhat transient event in northern regions, the air temperature available for the thawing of the active layer reasonably approximates a step temperature. Surface temperatures deduced from measured gradients in the Mesters Vig are shown in Fig 3.1 and it can be seen that a step temperature is a reasonably approximation for the variation in surface temperature. It might be argued, however, that for certain sites that step temperatures are not reasonable and that a time-dependent surface temperature must be used. A useful analytical model for this case is to make the surface temperature follow a sinusoidal variation. If we define an equivalent step temperature, T_e, as the thaw index in degree days (the area under the sine curve) divided by the length of the thaw season, as is usual practice, in thaw calculations, it can be shown that

$$T_e = \frac{2\ T\ max}{\Pi} \qquad 3.9$$

where T max is the peak temperature of the sine variation. A typical example is shown on Fig 3.2 and we observe some justification for the use of an equivalent step temperature in calculating the depth of thaw penetration. Furthermore, Nixon (1973) has shown that the maximum excess pore pressures set up in a homogeneous medium by a sinusoidal surface temperature actually slightly exceeds the pore pressures generated using a step temperature defined by Eq 3.9.

Before proceeding to a consideration of case records it is useful to first investigate the possible range of the rate of thaw α. Solving Eq 3.6 for a range of T_s from 2.0 to 20.0°C and for water (ice) contents ranging from 5.0 to 70.0% the maximum range of α that can be expected for this wide variety of conditions is from 0.01 to 0.10 cm/s$^{1/2}$, Fig 3.3. For more reasonable ranges of T_s for field problems from 5.0 to 15.0°C and water contents between 30.0 and 60.0% the range can be shown to be about from 0.025 to 0.05 cm/s$^{1/2}$

Let us now investigate the applicability of the analytic solutions considered and in particular if thaw can proceed under natural conditions in accordance with Eq 3.5. A summary of 15 case histories available in the literature are presented in Table 3.4 and the progression of thaw with the square root of time for these studies is plotted in Fig 3.4. For most sites there is a noticeable linear relationship between X and $t^{1/2}$ in accordance with Eq 3.5. Measured α values are compared with predicted on Fig 3.5. Step temperatures are either averaged from measured surface temperatures or deduced from air temperature records as noted on Table 3.4. Keeping in mind that no corrections have been made to allow for unfrozen water content, that ice contents are in some cases crudely averaged, that a variety of methods have been used to deduce T_s, and that in some sites an organic layer covered mineral soil, the agreement between measured and predicted α values is quite good. It can also be observed that the range of α values observed for a range of sites is well within the predicted range of Fig 3.3.

In many field situations the assumption of uniform conditions with depth in the Neumann problem is unrealistic due to the presence of a surficial layer of organic soil or peat having different thermal properties. For such profiles the depth of thaw will no longer be governed by Eq 3.5 for the entire thaw season. In order to solve this problem a simple extension to the Stefan problem to allow for a two-layer problem has been given by Nixon and McRoberts (1973) as follows. Consider a surficial layer of height H with thermal properties k_1, L_1, overlying an infinite depth of soil with properties k_2, L_2 with an applied T_s. From Eq 3.7 the time required to thaw H is

$$t_o = \frac{H^2 L_1}{2k_1 T_s} \qquad 3.10$$

where the depth of thaw in the surficial layer is governed by Eq 3.5. For the under-lying soil the depth of thaw, X, measured from the surface of the top layer is

$$X = \sqrt{\left(\frac{k_2}{k_1} H\right)^2 + \frac{2k_2 T_s}{L_2}(t - t_o)} - \left(\frac{k_2}{k_1} - 1\right)H \qquad 3.11$$

Two case histories have been considered using Eq 3.11 and are presented in Fig 3.6. As the case histories are not completely documented it was necessary to first obtain a ratio k_1/L_1 from Eq 3.10 knowing (t_o, H, T_s) from measured field data. Then obtaining L_1 for a high water content peat it was possible to obtain k_1 for use in Eq 3.11 and to then solve for the depth of thaw in the underlying soil knowing (k_2, L_2 and T_s). The comparisons between predicted and measured are quite reasonable and again point out that step temperatures are a useful approximation to the temperature boundary condition for thaw problems.

In the above comparisons of predicted and measured depths of thaw Kersten's (1949) data for a silt-clay soil was used for conductivity, k_u. While there is little experimental confirmation of Kersten's work (see Nixon and McRoberts) recent laboratory measurements of the α value agree well with predicted values using Kersten's data (Smith, 1972; Nixon, 1973).

Further work on the thawing of soils by Nixon (1973) also concludes that the effects of thaw strain and water migration or convection in one-dimensional problems are negligible and substantiates the assumption, implicit in our treatment of the thawing of soils, that conduction is the principal mode of heat transfer.

Many of the headscarps of bi-modal flows reported in the literature and observed in the study area expose ice or highly ice-rich soils directly to the atmosphere. As such, their surface temperature is necessarily $0^{o}C$ and it is impossible to quantify the thermal solution to this class of problem by using a temperature boundary condition. This is an ablation problem and requires the specification of a flux boundary condition such as that presented by Carslaw and Jaeger (1947) which results in the following solution

$$V = \frac{F}{L + c_1 T_g} \qquad 3.12$$

where V is the steady state velocity (cm/day) of the ablation surface, F is the steady state flux ($cal/cm^2 day$) impinging on the ablating surface, L is the latent heat per unit volume of frozen soil (cal/cm^3), c_1 is the volumetric heat capacity ($cal/cm^{3\,o}C$) and T_g is the ground temperature (^{o}C). As the heat involved in warming up frozen ground at the in-situ temperatures of interest is very small compared to the values of L in soil exposures susceptible to this form of mass wasting we may write

$$V = \frac{F}{L} \qquad 3.13$$

We shall consider the application of this model in a later section.

This section has summarized the analytical solutions to thawing problems that are required in the following discussion of mass movement mechanisms, as well as having introduced, in a quantitative sense, certain factors concerning the energy balance at the earth's surface. For additional information on this subject the reader is referred to a recent review by Gold and Lachenbruch (1973). We have seen that the use of step temperature boundary conditions serves in many respects as a reasonable approximation to actual field behaviour and we have reviewed the dominant variables influencing the rate of thaw, α. It should be noted that we have never explicitly defined where, or indeed what, the boundary is between the atmosphere and the underlying soil. Under conditions in which a flat mineral soil surface is directly exposed to the atmosphere the boundary is more readily visualized than it is for a site with a hummocky peat covered interface and where the interface may well be a zone of finite depth. Furthermore, while we have reviewed some case studies where the depth of thaw may be predicted by assuming that air temperatures are uniquely equivalent to soil surface temperatures this is not necessarily true for all cases. However, we are not concerned here with accurate predictions but rather that the models used are applicable to field situations and it has been shown that this is indeed the case.

3.3 Instability Mechanisms in Thawing Soils

3.3.1 Thaw Consolidation Model

(i) Derivations

Shallow landslides such as solifluction, skin flows and the tongues of bi-modal flows have certain mechanistic similarities that can be considered under the heading of thaw consolidation. As noted in Sec 1.4 there is a dilemma that exists in the slope stability analysis of these low angle thaw slopes that will now be detailed.

The dilemma involves the inability of conventional limit equilibrium analysis to predict mass movements on low angle slopes. A wealth of geotechnical experience in temperate regions suggests that it is entirely appropriate to consider the stability of long shallow slopes using an infinite slope analysis. It is well known in this case that by applying a simple statical balance of forces that the factor of safety F_s becomes (for example: Weeks, 1969)

$$F_s = \frac{\gamma'}{\gamma} \frac{\tan \phi'}{\tan \theta} \qquad 3.14$$

where γ'/γ is the ratio of effective to total unit weight and is usually 1/2, ϕ' is the angle of shearing resistance in terms of effective stress ($c' = 0$) and θ is the slope angle, Fig 3.7. Eq 3.14 has been derived for the pore water condition of steady state seepage parallel to the slope, Fig 3.7, with the ground water level at the slope surface.

Assuming that it is appropriate to introduce a residual value for the strength parameter ϕ'_r then slopes should be stable at an angle given by

$$\tan \theta = \frac{\tan \phi'_r}{2} \qquad 3.15$$

Illitic clays with $\phi'_r = 23^\circ$ are common in the study area. As these clays are found either by themselves or as part of a colluvial deposit, an angle of $\phi'_r = 23^\circ$ in Eq 3.15 represents a lower bound for possible slope behaviour. Thus from Eq 3.15 all slopes should be stable below 12.5°. But many slopes in the study area (see Tables 2.1, 2.2) are actively slipping on angles from 3° to 9° and these movements cannot be explained in terms of the model described above. Furthermore, we have seen that many of the solifluction slopes described in the literature (Sec 1.4) also cannot be predicted by Eq 3.15 (see Table 1.6).

These low angle movements can be explained within the framework of a limit equilibrium model if the presence of excess pore water pressures are invoked. This point of view has already been suggested by Weeks (1969) and Chandler (1970) although as we shall see later their proposed mechanisms for the generation of these pressures are not consistent with the salient features of solifluction movements.

It is contended that excess pore water pressures can be set up in thawing soils and that they are consequent upon what has come to be called thaw consolidation. Morgenstern and Nixon (1971) have solved a one-dimensional thaw consolidation problem by coupling the traditional Terzaghi consolidation theory with a moving thaw boundary defined by the Neumann solution, Eq 3.5. The solution is formulated in terms of a ratio, R, the thaw consolidation ratio: where

$$R = \frac{\alpha}{2\sqrt{c_v}} \qquad 3.16$$

where α is defined by Eq 3.5 and c_v is the coefficient of consolidation. This ratio expresses the relative influence of the rate at which water is produced by thaw and the rate at which it may be squeezed out of the thawed soil overlying the moving thaw interface. For an infinite soil mass thaw-consolidating under self weight conditions the excess pore pressure has been found to be

$$u = \left(1 + \frac{1}{2R^2}\right) \gamma' d \qquad 3.17$$

where $\gamma' d$ is the effective stress after complete dissipation of excess pore pressures.

Considering a slope, Fig 3.7, where a thaw front has penetrated to a depth d the effective stress on a plane aa', after the dissipation of excess pore pressures, would be $\gamma' d \cos \theta$. It is, therefore, assumed, analogous to Eq 3.17, that a measure of the excess pore pressure, u, on aa' is

$$u = \gamma' d \cos \theta \left(\frac{1}{1 + \frac{1}{2R^2}} \right) \qquad 3.18$$

and applying a statical balance of forces the factor of safety becomes

$$F_s = \frac{\gamma'}{\gamma} \left(1 - \frac{1}{1 + \frac{1}{2R^2}} \right) \frac{\tan \phi'}{\tan \theta} \qquad 3.19$$

It can be seen that if no thaw occurs or if no excess pore pressures are set up Eq. 3.19 reduces to Eq 3.14. Eq 3.19 can then be solved in terms of R and water content, Fig 3.8.

The solution to Eq 3.19 can be extended if α is defined as in Eq 3.7 and by assuming that all the water in a unit volume of soil is frozen. Using conductivity k_u defined as a function of water content and L by Eq 3.8 (with $W_u = 0.0$) both k_u and L are then uniquely defined by a given water content. A solution to the infinite thaw slope can then be presented (Fig 3.9) by plotting the slope angle required for limit equilibrium ($F_s = 1.0$) against water (ice) content. As the solution for α is more or less independent of frozen ground temperature it is possible, therefore, to isolate the relative effects of step temperature and c_v in reducing equilibrium slope angles.

When R values are low in a thawing soil no excess pore pressures are generated, while if R is high effective stress levels approach zero. Considering the parameters contained in R it is reasonable to conclude that the degree of uncertainty in obtaining a value for the thermal parameter α is much less than the uncertainty in estimating or measuring c_v. The complete range in α values for expected field conditions is from 0.025 to 0.07 cm/s$^{1/2}$ and we have seen that the thermal parameter can be estimated with reasonable accuracy, Fig 3.5. The value c_v, on the other hand, may easily range from 10^{-1} cm^2/s for sandy soils to 10^{-5} cm^2/s for fine-grained clayey soils and while c_v enters the R value under the square root its potential variation and the factors affecting it make the degree of uncertainity associated with obtaining the correct c_v value much higher. Therefore, we can conclude that the analysis of thaw slope stability resolves itself into a requirement for a detailed knowledge of geotechnical properties of thawing soils such as c_v and the effective stress parameters (c', ϕ'). It is less dependent on a detailed knowledge of the thermal solution.

(ii) Extensions to the Linear Theory

It is useful to first consider certain extensions to the theory of consolidation for thawing soils before proceeding to a discussion of the thaw slope model. These extensions (No. 1 to 4 below) have been presented by Nixon (1973) in order to amplify the basic thaw-consolidation model incorporating linear Terzaghi consolidation theory with a Neumann thaw problem.

1. When a frozen soil thaws under undrained conditions it is entirely possible that there is an initial effective stress in the soil skeleton before any drainage or volume change occurs. This initial effective stress is called the residual stress and may reasonably be put equal to zero for ice-rich or high void ratio soils in the thawed, undrained state. For soils with lower void ratios, high dry densities or no visible ice the residual stress may be high. Thus, if the residual stress in a thawed soil is of significant magnitude the excess pore pressure predictions of Eq 3.17 are too high and substantial strength can be mobilized before drainage occurs.

2. The linear Terzaghi consolidation model assumes a linear relationship between void ratio and effective stress. Nixon (1973) has shown that while this assumption has been shown experimentally

to be justified at low void ratios or at high effective stresses it is unrealistic for some soils at high void ratios or low stress levels. High void ratio soils are, in fact, markedly non-linear and the soil skeleton of an ice-rich soil must expel considerable quantities of water to gain only small corresponding increases in effective stress. For these soils, the residual stresses are also low and the net effect is that the simple linear thaw-consolidation model underestimates the magnitude of the excess pore pressures set up at the thaw interface.

3. The pore pressures generated by a sinusoidal variation in surface temperature have also been compared to the pore pressures associated with an equivalent increase in step temperature. It has been demonstrated that the excess pore pressures under the sine variation slightly exceed the pressures obtained under the equivalent step temperature over a certain range in depth.

4. If an actively penetrating thaw interface in a thaw-consolidating soil suddenly encounters a thick ice lense the pore water pressure regime in the soil now changes depending upon certain variables. Nixon (1973) has presented an analytic solution for this problem and shows that for shallow thick lenses the excess pore pressures increase with time depending upon the discharge capacity of the soil and the rate of melting of the ice. Under certain conditions, zero effective stress levels may be reached and maintained.

3.3.2 Some Aspects of the Model

(i) Laboratory Testing

Thaw consolidation theory has been shown to be capable of accurately predicting the mechanical response of thawing soils for a variety of laboratory experiments and for a field study. Laboratory experiments by Smith (1972) have confirmed the applicability of the linear theory for low void ratio remoulded soils and tests by Nixon (1973) on ice-poor natural soils show similiar agreement. Further tests on ice-rich natural soils by Nixon have shown that departures from linear theory are required to interpret these soils and that their behaviour upon thaw can be successfully predicted. Laboratory experiments by Nixon have also proved the existence of residual stresses in both remoulded and natural soils. Furthermore, thaw consolidation theory has also been shown to be capable of accurately predicting the thaw response of silty-clay soil beneath a hot oil pipeline (see Nixon, 1973).

(ii) The Fort Norman Landslide

Excess pore water pressures were measured in the field during the 1972 summer programme and the results of the testing have already been presented in Fig 2.3 and discussed in Sec 2.4. Most of these tests were made in the clayey, sandy silt of a colluvial deposit at the Fort Norman Landslide, Appendix A. The thawed Fort Norman silt has an in-situ water content of 31% (Table B.2). Frozen void ratios are not known. Relationships for e versus log ∇', k and c_v are given in Fig 3.10.

The measured excess pore pressures expressed in terms of the ratio r_u, Eq 1.4, ranged from 0.88 to 1.09 where $r_u = 0.52$ for hydrostatic conditions. It is of interest to see if these values can be predicted.

Let us first consider the simple linear thaw-consolidation model. As field temperature records are not available α must be approximated. If we assume the following reasonable parameters:

$T_s = 10^oC$, $k_u = 0.0032$ cal/cm^{o}Cs, L = 36 cal/cm^3 based on W = 31%, $W_u = 0.0$ then from Eq 3.7, $\alpha = 0.042$ cm/s$^{1/2}$. At a void ratio of e = 0.85, $c_v = 1.5 \times 10^{-3}$ cm^2/s from Fig 3.10 and by Eq 3.16, R = 0.54. For R = 0.54 and under self weight loading conditions the excess pore pressure, calculated from Morgenstern and Nixon (1971) and expressed as $r_u = 0.70$, is somewhat less than measured. A non-linear model may explain the measured pore pressures but as the frozen void ratio is not known such a model cannot be explored in detail.

However, it is felt that the geostatic pore pressure conditions measured may be due to thawing over an ice lense. Assuming the same thermal parameters as used above and a $k = 1.05 \times 10^{-6}$ cm/s from Fig 3.10, Nixon's method can be used to show that full geostatic conditions can be reached if an ice lense is encountered at a depth of 2 ft. Furthermore, it can be shown that, assuming $c_v = 1.5 \times 10^{-3}$ cm^2/s, Fig 3.10, that the ice lense need be only 0.33 cm in thickness in order to achieve an $r_u = 1.0$. This method is sensitive to both the values of k and c_v selected for the thawed soil overlying the ice lense. In particular, the field value may be influenced by macro-structure and, whereas, there is good agreement between different laboratory tests, a representative field k may be significantly less than 1×10^{-6} cm/s.

(iii) Slopes in the Vestspitsbergen

Excess pore pressures have also been measured in the field by Chandler (1972) during a study of thawing slopes in Vestspitsbergen. A probe piezometer similiar to the one used in the Mackenzie Valley was used. According to Chandler some tests were conducted with the tip pushed to refusal at the base of the active layer while other tests were made at intermediate depths. Excess pore pressures measured ranged from r_u values of 0.65 to 0.84 and for which a $r_u = 0.50$ corresponds to hydrostatic conditions. The soil in which tests were conducted was a clayey, sandy silt similiar to the Fort Norman Silt. As clay contents are as high as 20% it is expected that the slope deposits will have a substantial c_v value. Chandler presents data that shows that the thaw interface has moved some 12 cm in 10 days although the α value cannot be estimated. Thus for this site it is suggested that the excess pressures measured are due to thaw-consolidation processes. It is to be noted that this mechanism is not considered by Chandler who suggests that the pore pressures are due to a blocked drainage mechanism. He suggests that internal erosion has formed subsurface channels of higher permeability which, when filled with water and covered by finer-grained soils, cause excess pore pressures. However, it is felt that this process would more likely contribute to reduced pressures due to the improved drainage conditions. He also suggests that possible overnight freezing may cause a similiar situation; we shall consider this point in Chapter V.

3.3.3 The Sedimentation of Thawing Soils

(i) Theory.

While we have assumed in the preceding section that a frozen soil will consolidate upon thaw it has by no means been proven that soil-like conditions are always immediately realized once the ice phase of a frozen soil is melted. Although thaw-consolidation theory is capable of predicting conditions under which the effective stresses in a soil can approach the quick condition, the theory does so from the point of view that a soil, defined by certain mechanical parameters, already exists.

Conversely, it can be speculated that if the void ratio of a thawed soil is high enough the released mineral grains find themselves entirely separated from on another with no particle to particle contact and, therefore, under conditions of zero effective stress. In this environment a soil does not exist and a finite passage of time is required in order to achieve a soil-like state as the dispersed particles settle into a state of grain to grain contact and begin to transmit effective stresses.

Although we are primarily interested in formulating mechanisms for mass movements in thawing slopes we must first consider the basic aspects of sedimentation theory. This is made necessary because it appears that the processes and implications of sedimentation have been, hitherto, completely overlooked in geotechnical practice. It can be noted here that in addition to its importance in periglacial environments the theory is also of fundamental importance in many other fields of engineering.

The development of a theory of sedimentation for a dispersion, or suspension, of solids in a fluid is presented in detail in Appendix C. Appendix C also considers experimental verification of the theory and extends the basic theory into sedimentation-consolidation theory as well as presenting some aspects of thaw-sedimentation.

If we prepare and place a dispersion of uniform and sufficiently low concentration in a container it is possible to observe the following behaviour, Fig 3.11. After some small initial time a sharp interface will form and the top of the dispersion will settle with a constant velocity m_2. Concomitant with the fall of the top interface a less distinct interface may, under some conditions, be observed to rise from the base of the cylinder with velocity m_1. At some time t_f the two interfaces will intersect and the dispersion will have vanished. This behaviour of the dispersion during the time up to t_f is governed by the theory of hindered settling. This theory was first presented by Kynch (1952) and is based on the single main assumption that the velocity of fall of particles at any given point in a dispersion depends only on the local concentration of particles. This concept in turn leads to the idea of particle flux which is defined as the product of velocity of fall times particle concentration. Kynch's work is considered, and extended, in Appendix C and to which the reader is referred for both the theoretical proof and experimental verification of the linear settling modes discussed above.

If the dispersion had been made up of rigid particles such as sand it would be noted that after t_f no further settlement of the interface would occur. However, if a finer-grained dispersion is sedimented, further displacement will occur and the continuing settlement will be governed by conventional consolidation theory.

Furthermore, if we monitor the pore water pressure at the base of the cylinder we will also note the following behaviour. Irrespective of the type of dispersion, an initial pore water pressure equal to the total stress of the column of the dispersion will be measured. If the dispersion is made up of exceedingly clayey particles a zero effective stress condition will be maintained at the base of the column up to time t_f, Fig 3.11, after which pore pressures will dissipate according to consolidation theory. For the majority of finer-grained dispersions in which linear settling modes are observed some dissipation of pore pressures will occur before time t_f. For coarse-grained particles it is expected that the pore pressures at the base of the cylinder will rapidly dissipate as shown on Fig 3.11.

Up to t_f the sediment formed will be governed by conventional consolidation theory although the process is complicated by the moving boundary formed by continuing sedimentation. This problem is referred to as sedimentation-consolidation and is considered in Appendix C. After t_f the top surface does not aggrade and the subsequent consolidation and dissipation of pore pressure is governed by conventional theory.

We are now in a position to consider certain aspects of thaw sedimentation by making various simplifying assumptions. Firstly, it is assumed that thaw is governed by the Neumann solution. Secondly, it is assumed that the flux plot relating particle flux and concentration is linear (see Fig C.23). If we now thaw a homogenous soil of initial concentration, c_i, less than c_m, it is possible to derive an expression predicting the depth, X_F, at which soil-like conditions are first reached as (Eq C.47)

$$X_F = \frac{\alpha^2}{2} \frac{(c_m - c_i)}{S_m} \qquad 3.20$$

where S_m is the particle flux at c_m.

The results of sedimentation tests on a series of soils is summarized in Table 3.5. The flux plots for these soils are given in Fig C.12 to C.14 and it can be seen that the assumption of a linear relation between S and c is reasonable at the higher range of concentrations. It is apparent that if the in-situ frozen water contents of the Fort Norman or Devon Silts are less than about 90% then the soil will already have established grain to grain contact and will not undergo a sedimentation mode.

The solution to Eq 3.6 for Fort Norman Silt and for Devon Silt and Devon Sand is given in Table 3.6. Here Eq 3.6 has been solved for a $T_s = 10^{\circ}C$. The results indicate that for initial uniform concentrations corresponding to water contents of from 100 to 150% thawed Fort Norman Silt will remain in a dispersion from depths of 0.4 to 1.3 cm and Devon Silt from 9.9 to 32.1 cm. It is interesting to note that while S_m for Devon Sand is much lower than for Fort Norman Silt the X_f values are almost equivalent due to the increased rate of thaw for the sandy soil.

The estimation of the depth X_f is inversely related to the flux, S_m, which must be measured experimentally for a given soil. The determination of S_m is quite sensitive to the precision of the technique used to observe sedimentation modes and it is felt that if experiments of a higher order of accuracy were conducted the measured S_m would be even lower. Therefore, the prediction of Table 3.6 may underestimate the depth to which a dispersion may be sustained during thaw-sedimentation.

(ii) Implications

It has been shown theoretically that when an ice-rich soil begins to thaw-sediment that it is entirely possible to maintain a dispersion to some critical depth. Thus critical depth is dependent upon certain mechanical parameters which can be determined from a simple test and is also a function of the rate of thaw. During the time interval in which the dispersion exists a soil does not even exist. Under these conditions the only shear strength that can be mobilized is due to the viscous resistance of the dispersion.

If conditions favoured the existence of a thaw-sedimentation environment on a slope the following conditions would be expected. As the soil thawed, thin sheets of dispersion would be created. These layers of dispersion would then flow downslope governed by the slope inclination and the inherent rheologic properties of the thaw-induced dispersion. The displacements caused by this process would be gross and cannot be readily estimated.

3.3.4 Conclusions

There is, therefore, evidence to suggest that thaw-consolidation theory is capable of predicting the behaviour of thawing slopes. The importance of thaw in controlling solifluction and flow movements has been reviewed in Chapter 1 and the theory presented in this section quantitatively describes the qualitative theories of certain early investigators such as Taber (1943), Paterson (1940) and Washburn (1947). We have seen that the thaw consolidation model is capable of predicting low angle slope failures in terms of certain thermal and geotechnical parameters. While the simple linear model may not be entirely adequate for the high void ratio soils characteristic of shallow thawing slopes we have briefly reviewed extensions to the theory. In particular, we have noted the importance of thaw over an ice lense for shallow depths. This extension is of major importance in a consideration of thaw slope stability as Mackay (1972) has observed the frequency of high ice content soils immediately beneath the active layer in many parts of the Mackenzie Valley. It is possible that the depth and thickness of ice lenses is as much a controlling factor in the stability of skin flows as is thaw-consolidation itself.

It is also suggested that thaw consolidation theory can, in part, predict the low angle movements found in the tongues of some bi-modal flows.

Mass movements in the tongues of some bi-modal flows also partake of what can be called viscous flowage and the theories of sedimentation and thaw-sedimentation discussed in this section give insight into this process. It has been shown that under suitable circumstances of soil composition, void ratio and rate of thaw that zero effective stress conditions can be maintained for significant times or depths in a thaw-sedimenting soil. During this interval the thawed deposits can only mobilize shear strengths due to their inherent rheologic properties and thus would exhibit viscous flowage.

The theory of sedimentation might also be applied to the thawed deposits that can be found collecting in pools beneath the headscarps of actively ablating bi-modal flows. It can be speculated that under optimum circumstances it is possible to collect and maintain a reservoir of thawed dispersion, which never quite completely sediments. Once a critical depth or height is reached this dispersion then breaches the reservoir area spewing out a viscous slurry which flows downslope along the tongue.

Both thaw-sedimentation and thaw-consolidation theories predict conditions under which zero effective stress conditions are maintained or can be approached during the thaw of ice-rich soils. Under these conditions a frictionally dependent shear strength cannot be mobilized and if any strength is to be realized it must stem from the rheologic properties of the soil-water system. Once the void ratio of a thawed deposit is reduced to such an extent that grain to grain contact is achieved, effective stresses are developed and a frictional strength can be mobilized. However, there is no reason to suppose that immediately upon achieving grain to grain contact that a soil suddenly can develop frictional shear strengths alone. For example, drained tests on remoulded, normally consolidated, samples of English clays reported by Bishop and Henkel (1957) indicate an increase in shear strength for more rapid times to failure. This increase amounted to a 7% increase in deviator stress at failure for a 10-fold decrease in times to failure and suggests that even at low void ratios soils can exhibit a strain rate dependent, or viscous, shear strength component. Therefore, if a deposit at a zero effective stress condition can mobilize only a viscous resistance and if low void ratio soils exhibit a degree of viscous resistance it can be concluded that the relative components of friction and viscous resistance will vary, in some as yet to be determined manner, between these two limits. This point of view was taken by Morgenstern (1967) who added a viscous resistance component to the shear strength of a high void ratio marine sediment in order to obtain a more realistic shear strength model. However, the possibility of a substantial viscous component of shear strength, especially in high void ratio soils, is generally overlooked in geotechnical practice and a detailed consideration of the problem is beyond the scope of this thesis.

For this reason, therefore, the mass-movement model considered in this section has been formulated with the implicit assumption that the shear strength of a thawed soil can be adequately predicted using effective stress strength parameters in conjunction with known or predicted effective stresses. Thus while it is a relatively straightforward matter to discuss qualitatively, conditions under which flow landslides continue to deform and to even formulate realistic mass movement models (see Morgenstern, 1967; Johnson, 1970) any further consideration of the problem is handicapped by a lack of appropriate constitutive relationships for a "frictional-viscous" soil.

However, the frictional strength model derived in this section is considered to be an entirely reasonable means of forecasting the onset of limit equilibrium and, therefore, of predicting conditions under which thawing slopes will be stable.

Mass movements may be initiated by thaw-consolidation or thaw-sedimentation processes. Once initiated, these movements generally partake of some form of flow and further increases in thaw rate or thaw depth only aggravates the rate or amount of movement by either process. From a geotechnical point of view the models presented are adequate and we are generally more interested in avoiding unstable conditions than in predicting the gross movements involved in slope failure deformation.

It can also be pointed out that while the control exerted by vegetation may play a signigicant role in the overall stability of thawing slopes, we shall not consider it in detail. It can be observed that the effect of forest fires alters the thermal regime at a site and increases the depth and rate of thaw (see Heginbottom, 1973). Increasing the rate of thaw will decrease the stable slope angle due to thaw consolidation response and increased depth of thaw can result in instability due to thawing of ice lenses otherwise protected from seasonal thaw. The strength of the vegetal mat will also affect slope stability as the mat can sustain considerable deformations and mobilize finite strengths. The observation made by Bird (1967) of a skin flow that spewed soil out from beneath a moss cover, Table 1.7, provides evidence of the strengths that can be mobilized.

3.4 The Ablation Problem

3.4.1 The Solution of the Ablation Problem

The headscarps of many bi-modal flows undergo a melting process properly called ablation. In many flows ice-rich soil is directly exposed to the atmosphere and the thawed soil and water continuously sloughs off and down the steep slope The surface of the frozen soil is, therefore, always at the melting temperature, 0°C, as the melt is removed this thawing process is called ablation. The simple mathematical treatment for this problem has already been presented in Sec 3.3.2.

Because the ice-rich soils are directly exposed to their surroundings and are not protected by a covering of thawed soil or vegetation rapid melting rates are possible. Table 3.7 summarizes the rates of back sapping for headscarps observed in the study area and for others noted in detail in Table 1.7. In some cases rates of movement have been averaged over 28 years while in others movements have been measured over portions of the thaw season. If we now estimate the? ice contents of the frozen headscarps as being equivalent to a latent heat L of between 40 to 60 cal/cm^3 it is possible to present a graphical solution to Eq 3.13 as in Fig 3.12.

For example, the Fort Simpson Landslide, Table 3.7, back-sapped with an observed velocity of 7.2 cm/day into soil with a latent heat of about 55 cal/cm^3. From Fig 3.12 it is evident that the average flux required to cause this average velocity was 400 cal/cm^2 day. For the remainder of the velocities observed, ranging from 3.5 to 12.5 cm/day, the inferred flux is, therefore, from about

200 to 650 cal/cm^2 day.

These flux values are much higher than the magnitudes of ground heat flux G usually encountered in thawing active layers beneath typical surface covers. For instance, in Barrow, Alaska, Table 3.3, the net radiation, R_n, at a tundra site ranged from 340 to 155 cal/cm^2 day over the thaw season and the maximum measured ratio of G/R_n was about 0.23. Thus G varied from between 36 to 78 cal/cm^2 day. Furthermore, it is evident for the possible range of R_n and G/R_n given in Tables 3.2, 3.3, that ground heat flux seldom exceeds a value of about 100 cal/cm^2 day for natural, vegetation covered sites. Certainly, if the ground heat fluxes inferred above for bi-modal flows were generally available for melting in active layer problems then typical active layer depths would be substantially increased. Inspecting the energy balance, Eq 3.1, and re-writing as

$$G = R_n - LE - H \qquad 3.21$$

it is argued that some combination of the components occurs in such a manner as to significantly increase G for ablation problems. It is instructive to briefly consider some aspects of the energy balance and its role in increasing G. The concave, parabolic shape of many active bi-modal flows may tend to concentrate or focus radiation and thus increase R_n. The R_n impinging on the typical scarp face may also be higher compared to the values in Table 3.3 because the scarp face is inclined to a horizontal surface whereas the R_n values quoted were measured on horizontal surfaces.

As the noon angle of the sun at 65° North latitude is about 45° during the summer season, the mean daily angle will be considerably lower. Thus, a considerable increase in R_n might be expected for a steep surface inclined more nearly perpendicular to the sun's rays. Furthermore as the albedo of the dark wet surface typical of ablating headscarps will be lower than the albedo of a natural vegetated site (see Table 3.1), R_n will also be increased as predicted by Eq 3.3.

The LE, or evapotranspiration, component of Eq 3.2 usually accounts for a considerable proportion of the energy budget, see Table 3.2, and substantially reduces the R_n available for thaw. However, along the headscarps melt water is rapidly removed away from the system. Thus, while there is high potential for evaporation it may be argued that the ratio LE/R_n is small along the headscarps. If this is the case then G will be increased compared with the usual situation and as evaporation can typically account for 150 to 200 cal/cm^2 day the effect may be highly significant.

Circumstances under which the third component, H, may also change so that G is increased can also be envisioned. The magnitude of H is dependent upon the wind velocity which influences the rate of heat extraction out of the system. As bi-modal flows are always found set into or depressed into the surrounding terrain the ablating scarps will be sheltered from the wind and the flux available for ablating may be greater. It can also be noted that while H usually enters Eq 3.1 under the negative sign the sign may be reversed for the headscarp region. As the soil surface near the headscarp is maintained at 0^oC the air immediately adjacent will also tend to 0^oC. However, this air being more dense than the surrounding air, some air will sink creating a density current. This current could then bring warm air from out of the system and by entering Eq 3.21 as a positive term increase rather than decrease the ablation flux.

3.4.2 Implications

Field exploration at site HU1-1 (see Appendix A) on the Hume River has confirmed certain aspects of the conditions felt to be applicable in the headscarps of bi-modal flows. Drilling in the GLB soils adjacent to an inactive flow has revealed a clay with water (ice) contents in the upper 20 to 30 ft of the deposit of from 1-1/2 to 3 times the liquid limit which is about 48%, in a soil with average clay content of 45%. The high ground-ice contents in conjunction with a thawed soil at average water contents well above the liquid limit could permit an ablation mechanism to sustain itself once the process is initiated.

While it might be expected that bi-modal flow activity would be favoured on slopes with a southerly view this is not always the case. For example, Kerfoot (1969) describing bi-modal flows on Garry Island found that more than 80% of the observed recessions occurred during July and August and active flows were reported with aspects on all points of the compass. Kerfoot also observes that while:

> "it may seem easy to conclude that slope aspect is a dominant factor influencing scarp retreat .... (however)....... comparisons made between stakes located around the same mudslumps revealed that the maximum retreat did not always occur on the slopes with the most southerly aspect."

This effect may be partly caused by the fact that the sun will not set during these summer months and solar radiation, especially on steep slopes, will be received on all slopes.

Both Kerfoot (1969) and Mackay (1966) also note that a certain portion of the measured recession rates of the headscarps results from erosion by running water which causes the formation of so-called badland topography. This feature has not been observed in the study area. However, if it causes a significant amount of erosion the magnitude of the flux predicted by Eq 3.13 would have to be reduced accordingly.

The magnitude of the movements produced by active bi-modal flows are catastrophic. For example, a flow initiated in a 30-ft high bank ablating at a rate of 25 ft/yr would, if it produces a 3^{o} angle tongue, back-sap some 550 ft over a 22 yr period. The geotechnical implications of these movements are self-evident and point out the possible hazards involved in artificial cuts in ice-rich soil.

3.5 Other Processes in Thawing Slopes

Rotational slides, Fig 2.1, can be found in association with thawing permafrost soils under certain specialized conditions. Rotational failures can be found in the headscarp areas of MR flows if the headscarps are made up of frozen sands or silty sands. For example, at the Fort Simpson Landslide, Appendix A, a section of the headscarp has failed in a rotational manner and two auger holes both advanced to a depth of 12 ft confirm that a thawed silty sand was involved in the movement. It appears at this site that a thaw interface has advanced well into the sand before failure has occurred. As the sand will likely be ice-poor it will be thaw-stable and furthermore it will not ablate. As a typical exposure will be covered over by the intact upslope vegetation mat thaw can only proceed in from the face of the exposure which, in turn, will be stable at angles approximately equal to the drained condition. As the thaw proceeds further into the bank the seepage paths become longer and pore pressures start to back up in the slope and failure finally occurs. It is interesting to note that this process is one of the few circumstances in which rotational failures can be caused in sand.

Rotational failures can also be found in the fluvial deposits found adjacent to rivers in the study area. These failures appear to be associated with already thawed soil and will be discussed in Chapter VI.

Mass movements in the tongues of bi-modal flows may also be aided by undrained loading, a process which has been discussed in detail by Hutchinson and Bhandari (1971) for flow landslides in temperate regions. When masses of colluvial debris are detached from the headscarps of bi-modal flows they come to rest at the base of the scarp. The weight of this falling debris acts as a total stress increment and sets up an increment of excess pore pressure equal to the increase in total stress. If the underlying soil is relatively impermeable this excess pore pressure is not immediately dissipated and thus aids in sustaining low angle movements.

It can be noted that while it might be argued that undrained loading is responsible for the excess pore pressures measured at the Fort Norman Landslide (see Sec 3.3) it is not considered likely. When visited, the headscarp of this landslide was not actively ablating and a skin of desiccated soil covered the underlying frozen clay which was found at a depth of 18 inches horizontally into the headscarp. As the site was visited early on in the thaw season, in the latter part of June, it is unlikely that any failure could have occurred which would account for the measured pore pressures.

Furthermore, the surface of the silt-run in which measurements were made was very smooth and there was no evidence of recent colluvial debris which could have caused undrained loading.

TABLE 3.1 ALBEDO OF VARIOUS SURFACES

Surface	Albedo (%)	Source
Light sand	30 - 60	Geiger (1965)
Sandy soil	15 - 40	"
Fields	12 - 30	"
Woods	5 - 20	"
Dark soil	7 - 10	"
Water Surfaces	3 - 10	"
Tundra surfaces:		
1. Shrub	16 - 17	Haag (1972)
2. Wet sedge	18 - 25	"
3. Winter road	7 - 11	"
4. Burn	10	"
Borel Forest:		
1. Forest	14	"
2. Seismic line	13	"
Seeding Experiment on Winter Road:		
Control	15	"
Spring after use	8	"
1st growing season	11.5	"
2nd growing season	13.2	"
3rd growing season	14.0	"

TABLE 3.2 RATIOS OF COMPONENTS OF THE ENERGY BALANCE

Cover	Period of Observation	$\frac{G}{R_n}$	$\frac{LE}{R_n}$	$\frac{H}{R_n}$	Comments	Source
Alpine Tundra	Mid-July noon	0.15	0.62	0.22	California Mtns	Terjung et al (1969)
Lichen	Daily avg 5 days in July	0.10	0.56	0.34	Sub-arctic site near James Bay, Ont.	Rouse and Kershaw (1971)
Old Burned Lichen	Daily avg 4 days in July	0.15	0.50	0.36		
Tundra	1 June	0.20	0.50	0.3	Tuktoyaktuk, 2-week averages. Albedo constant at 0.15	Haag (1972)
	15 June	0.20	0.43	0.37		
	1 July	0.15	0.50	0.45		
	15 July	0.20	0.50	0.3		
	1 Aug	0.23	0.78	0.0		
	15 Aug	0.20	0.65	0.15		
Winter Road	1 June	0.09	0.77	0.14	Norman Wells, 2-week averages. Albedo at 0.10.	
	15 June	0.26	0.42	0.32		
	1 July	0.18	0.30	0.52		
	15 July	0.20	0.46	0.34		
	1 Aug	0.26	0.60	0.14		
	15 Aug	0.26	0.56	0.18		
Tundra	20-22 July	0.04	0.29	0.66	Chitistone Pass, Alaska	Brazel (1970)
	9-11 Aug	0.02	0.96	0.02		
Spruce	July to Aug.	0.27			Mackenzie Delta. Measurement at base of spruce canopy.	Gill (1971)
Tundra	27 June	0.17			Barrow, Alaska. Tundra surface became drier in August.	Mather and Thornthwaite (1958)
	5 July	0.13				
	15 July	0.14				
	25 July	0.15				
	5 Aug	0.17				
	15 Aug	0.23				
	25 Aug	0.23				

TABLE 3.3 SOME VALUES OF NET RADIATION AND INCOMING SOLAR RADIATION

Cover	Period of Observation	Radiation cal/cm^2 day		Comments	Source
		Net	Incoming Solar		
Alpine Tundra	Mid-July noon*	2304	2880	California Mountains	Terjung et al (1969)
Lichen	July 19 noon*	921		Sub-arctic site near James Bay	Rouse and Kershaw (1971)
Old Burned Lichen	July 17 noon*	864			
Tundra	20-22 July avg.	241		Chitistone Pass, Alaska	Brazel (1970)
	9-11 Aug avg.	171			
Unvegetated	15 July		520	Incoming solar from statistical equation. Net radiation from range of daily readings.	Gill (1971)
	15 Aug		320		
Beneath spruce canopy	15 July	25-75	43		
	15 Aug	20-40	26		
Equisetum	15 July	200-350			
	15 Aug	100-200			
Tundra	5 July, 10 day avg	335	430	Barrow, Alaska. Tundra surface became drier in Aug.	Mather and Thornthwaite (1958)
	15 July	315	415		
	25 July	255	330		
	4 Aug	192	270		
	14 Aug	155	270		
	24 Aug	97	165		

* Reading for a period at noon expressed in ly/day.

TABLE 3.4 CASE HISTORIES FOR RATE OF THAW

Code	Measured α cm/s$^{1/2}$	Code	Step Temperature	Soil Profile	Predicted α cm/s$^{1/2}$	Comments
1	0.024	T	8.3 avg[1]	Avg w/c 35%	0.036	Salix Alnus Gill (1971)
2	0.027	P				
3	0.030	P	8.6 avg[1]	Avg w/c 23%	0.042	Salix Equisetum Gill (1971)
4	0.040	P	9.3 avg[1]	Avg w/c 20%	0.044	Equisetum Gill (1971)
5	0.025	T	7.8 avg[1]	Organics and silty clay Avg w/c 35%	0.035	Picea, Gill (1971)
6	0.030	P				
7	0.030	T	At 3 in depth mean 4°C estimated surface 5.0°C	Tundra soil Avg w/c 60%	0.021	Drew (1958)
8	0.041	P	Mean, measured surface temp 6°C.	Estimated w/c 35%	0.030	Kelley and Weaver (1969)
9	0.033	T	Thaw index-thaw season = 5.8°C from air temp.	Avg w/c 35% in silt and clayey sand	0.029	18 cm organic soil at surface. Aitken (1965)
10	0.059	T	Thaw index - thaw season = 10.5°C from air temp.	6 cm peat w/c 56% over silty clay, avg w/c overall 30%	0.043	Aitken (1964).
11	0.053	T	Avg soil surface temp 7.5°C.[2]	Diamicton: sand, silt, clay. Avg w/c 20%	0.052	Site ES6, TCS 6B No organic cover Washburn (1967)
12	0.058	T	Avg soil surface temp 11°C.[2]	Diamicton. Avg. w/c 17%	0.053	TCS 7B No organic cover. Washburn (1967)
13	0.067	T	Avg soil surface temp 15°C[2]	Diamicton: Avg. ice tentents 22%	0.060	TCS 7A. No organic cover Washburn (1967)
14	0.025	T,P	Monthly mean surface: 10°C	Silty clay. Avg w/c 30%	0.041	Sparse vegetation Powell (1961)
15	0.044	T,P	Monthly mean surface: 11°C	Sand with clay lenses avg w/c 20%	0.054	Sparse vegetion. Data is an average for 2 stations Powell (1961)

1. T_s deduced from average of thaw index, mean of maximum and minimum measured surface temperature and surface temperature extrapolated from temperature gradients.

2. Average soil surface temp from extrapolation of measured gradients
Code T = depth of thaw from temp. profiles Code P: depth of thaw from probing.

TABLE 3.5 SUMMARY OF SEDIMENTATION TESTS

Soil	c_m (gm/cm^3)	Max Water Content (%)	S_m (gm/cm^{2}s)
Fort Norman Silt	0.792	89.6	4.3×10^{-5}
Devon Silt	0.795	88.0	1.75×10^{-6}
Devon Sand	1.23	43.4	3.81×10^{-4}
Glass Beads (13 micron)	1.44	26.4	1.44×10^{-4}
Emery (12 micron)	1.93	25.4	4.05×10^{-4}
Glass Beads (67 micron)	1.52	25.0	2.96×10^{-3}
Grit (#40 - #200 sieve)	1.36	47.0	1.10×10^{-2}

TABLE 3.6 SUMMARY OF CRITICAL DEPTHS FOR THAW-SEDIMENTATION

Boundary Conditions	Initial Concentration c_i (gm/cm^3)	Initial Water Content W/C %	α cm/s$^{1/2}$	Depth X_f cm
	FORT NORMAN SILT			
$T_s = 10^{\circ}C$	0.734	100	.023	0.4
$c_m = 0.792$ gm/cm^3(W/C = 90%)	0.642	120	.022	0.9
$S_m = 4.28 \times 10^{-5}$ gm/cm^{2}s	0.549	150	.021	1.3
	DEVON SILT			
$T_s = 10^{\circ}C$	0.730	100	.023	9.9
$c_m = 0.795$ gm/cm^3 (W/C = 88%)	0.635	120	.022	22.1
$S_m = 1.75 \times 10^{-6}$ gm/cm^{2}s	0.540	150	.021	32.1
	DEVON SAND			
$T_s = 10^{\circ}C$	1.14	50	.035	0.14
$c_m = 1.23$ gm/cm^3 (W/C = 43%)	1.02	60	.031	0.26
$S_m = 3.81 \times 10^{-4}$ gm/cm^{2}s				

TABLE 3.7 SUMMARY OF THE RATE OF MOVEMENT OF HEADSCARPS IN BI-MODAL FLOWS

Flow	Movement	Rate cm/day	Comments
Hume River (HU1)	70 ft in 6 years	3.6*	Aerial Photography
Hume River (HU2)	250 ft in 6 years	12.7*	Aerial Photography
	500 ft in 28 years	5.4*	
Fort Simpson Landslide	10 ft in 6 weeks	7.3	Field Observation
Fort Norman Landslide	120 ft in 11 years	3.3*	Aerial Photography
Arctic Red River gravel pit	12 meters spring thaw to 2 Aug 1972.	20.0	Strang (1972). Assumed 60 days thaw.
Isachsen	23 to 33 ft/summer	7.0 to 10.0*	Lamothe and St. Onge (1961)
Kendall Island	Avg 6.5 ft in 41 days	4.8	Mackay (1966)
Garry Island (Site B)	10 July to 15 August	7.8	Kerfoot (1969)
	16 August to 5 September	5.3	See also Table 1.7

*Assumed thaw season = 100 days

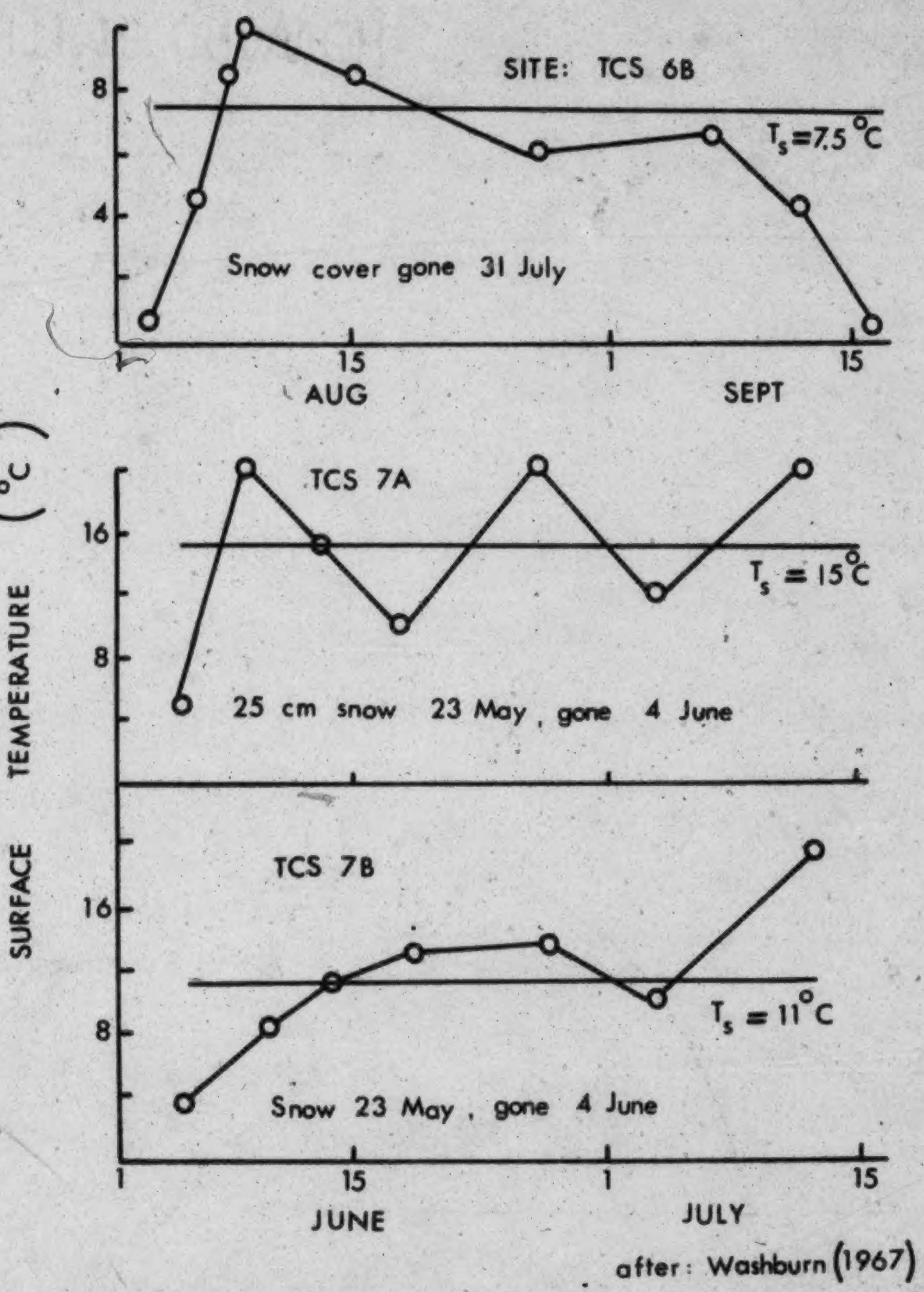

after: Washburn (1967)

Fig 3.1 Ground surface temperatures in the Mesters Vig

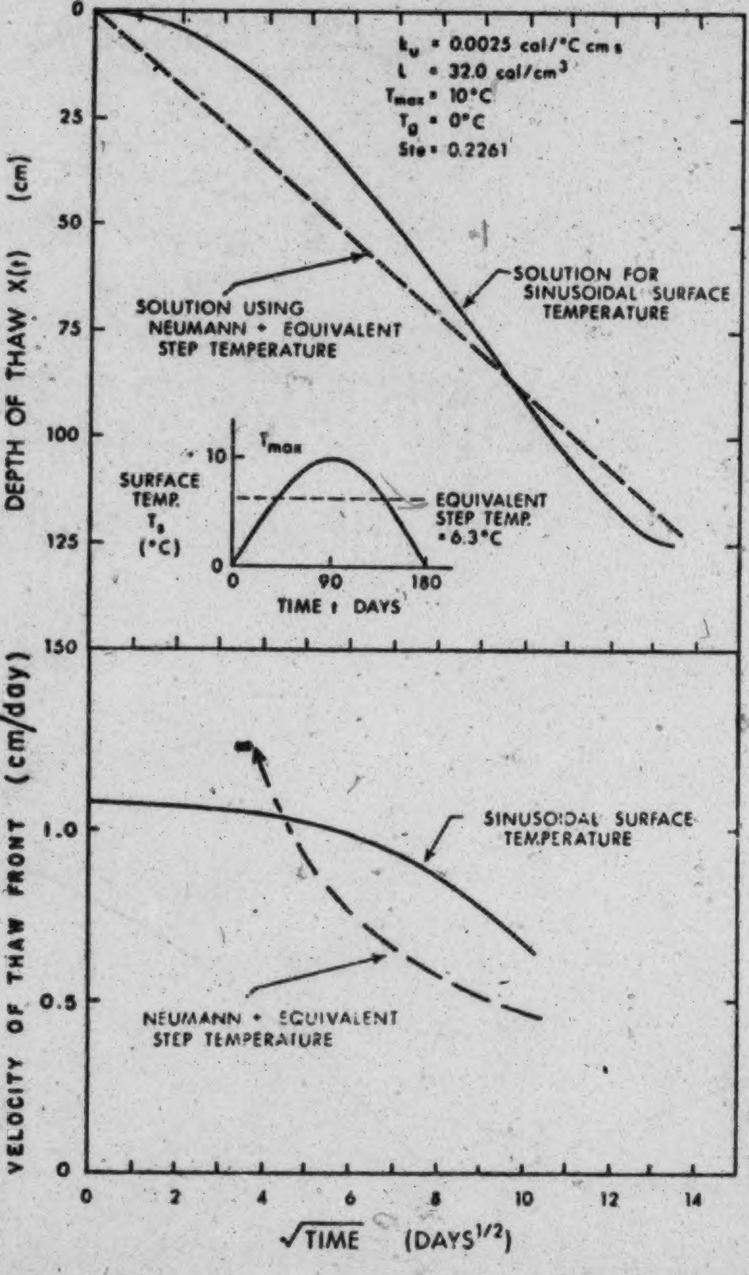

After Nixon (1973)

Fig 3.2 Rate of thaw for sinusoidal surface temperature

Fig 3.3 Effect of T_s on rate of thaw

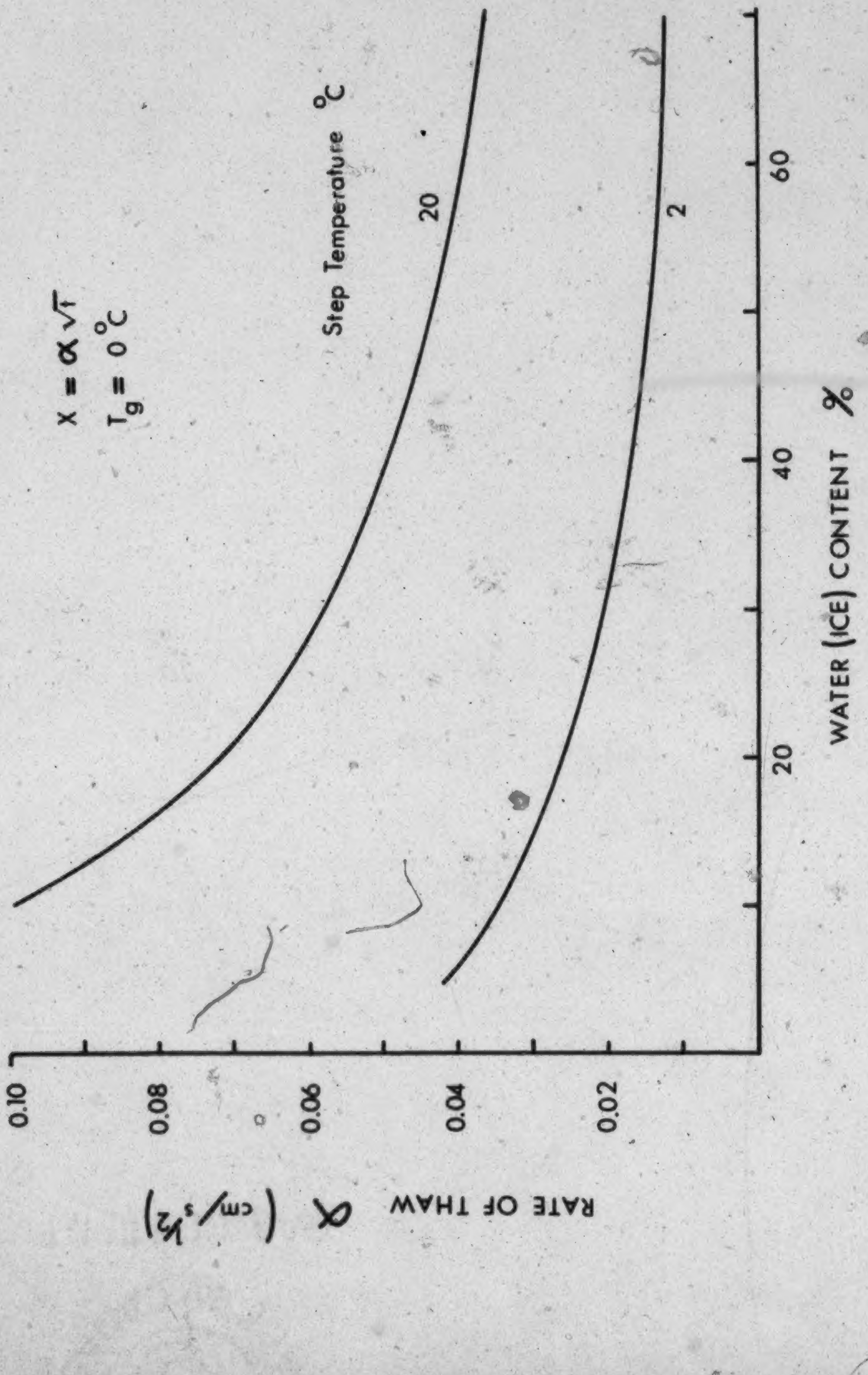

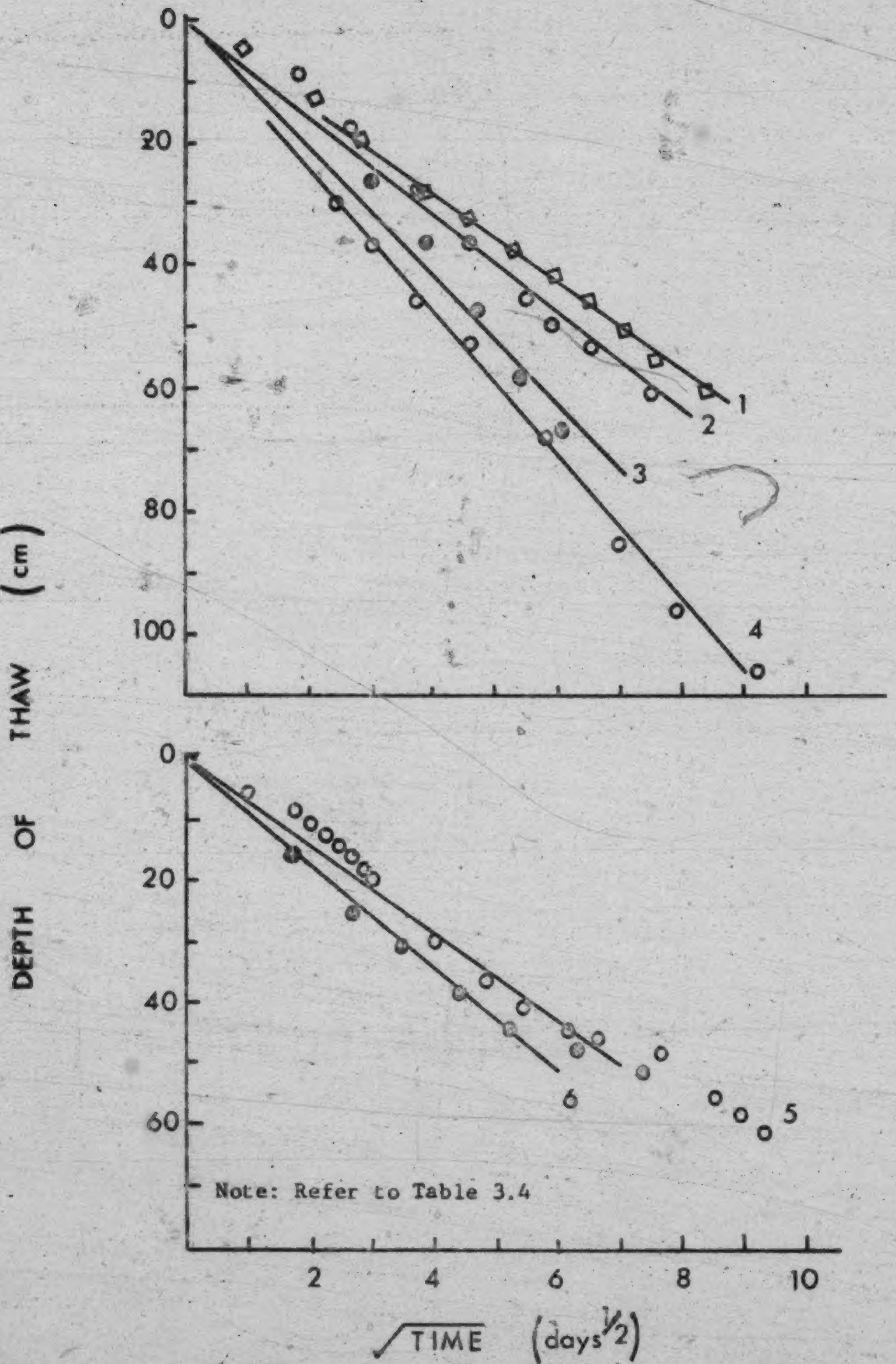

Fig 3.4 Measured rates of thaw

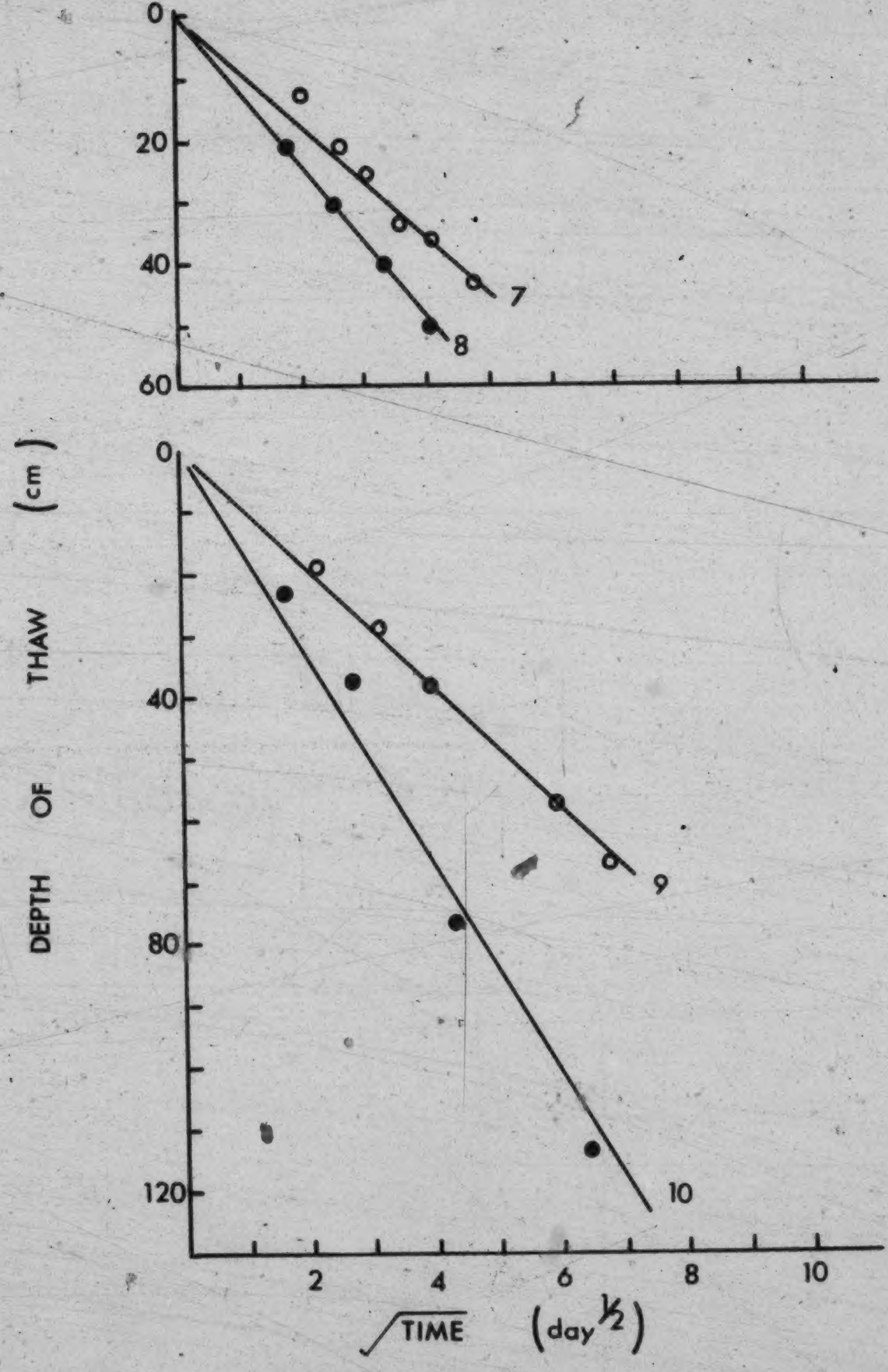

Fig 3.4 (continued)

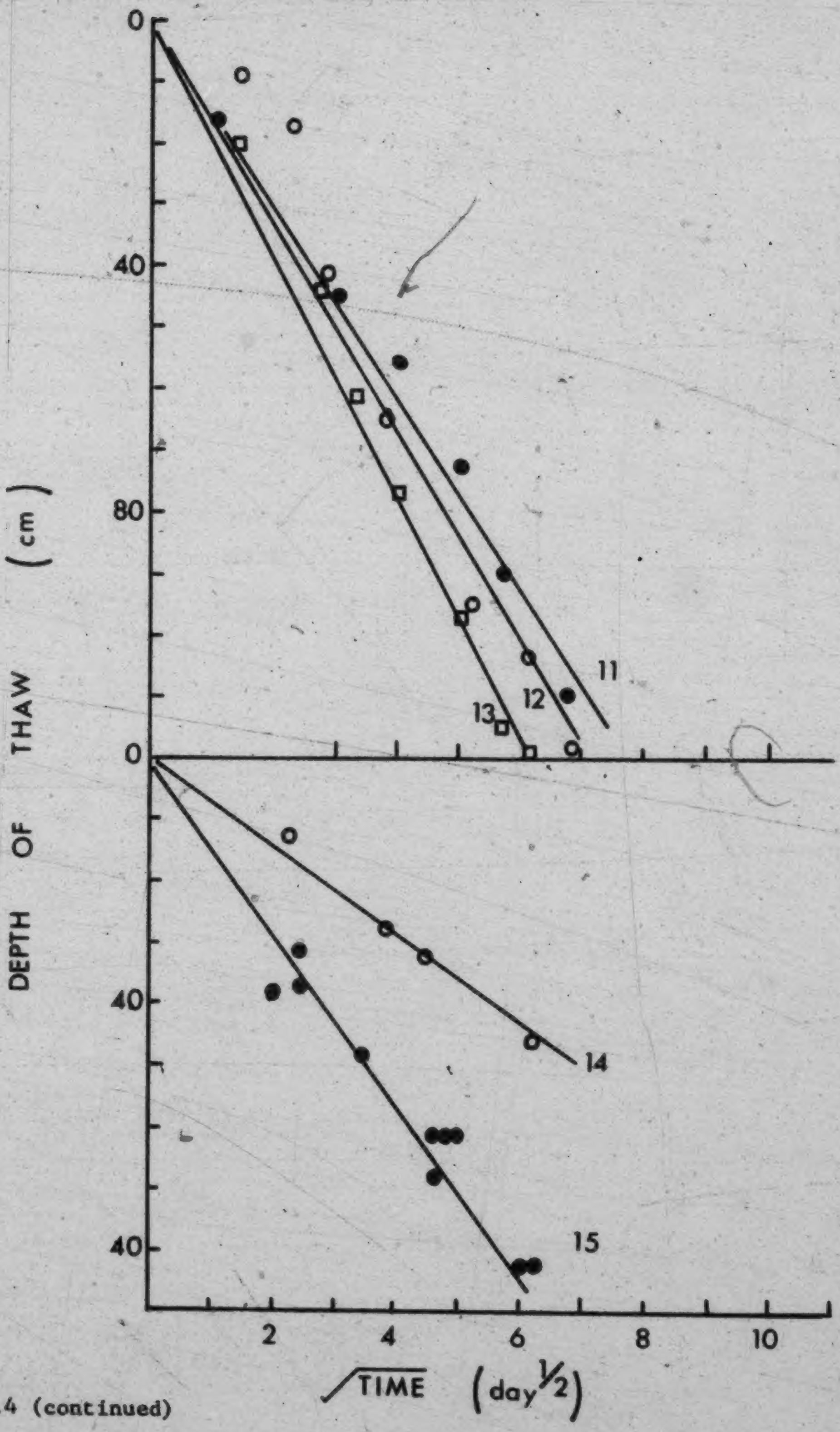

Fig 3.4 (continued)

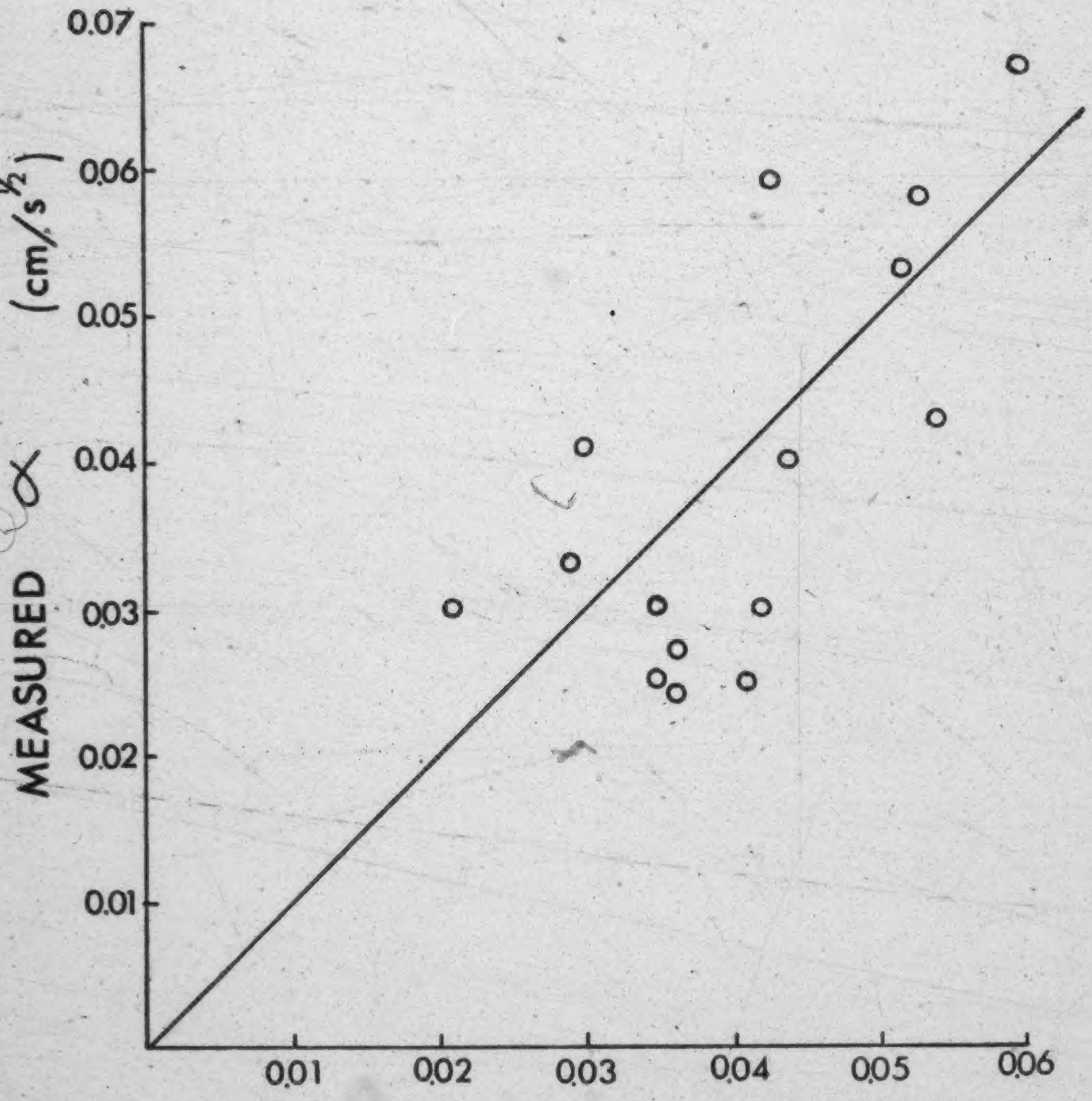

Fig 3.5 Comparison of measured and predicted rates of thaw

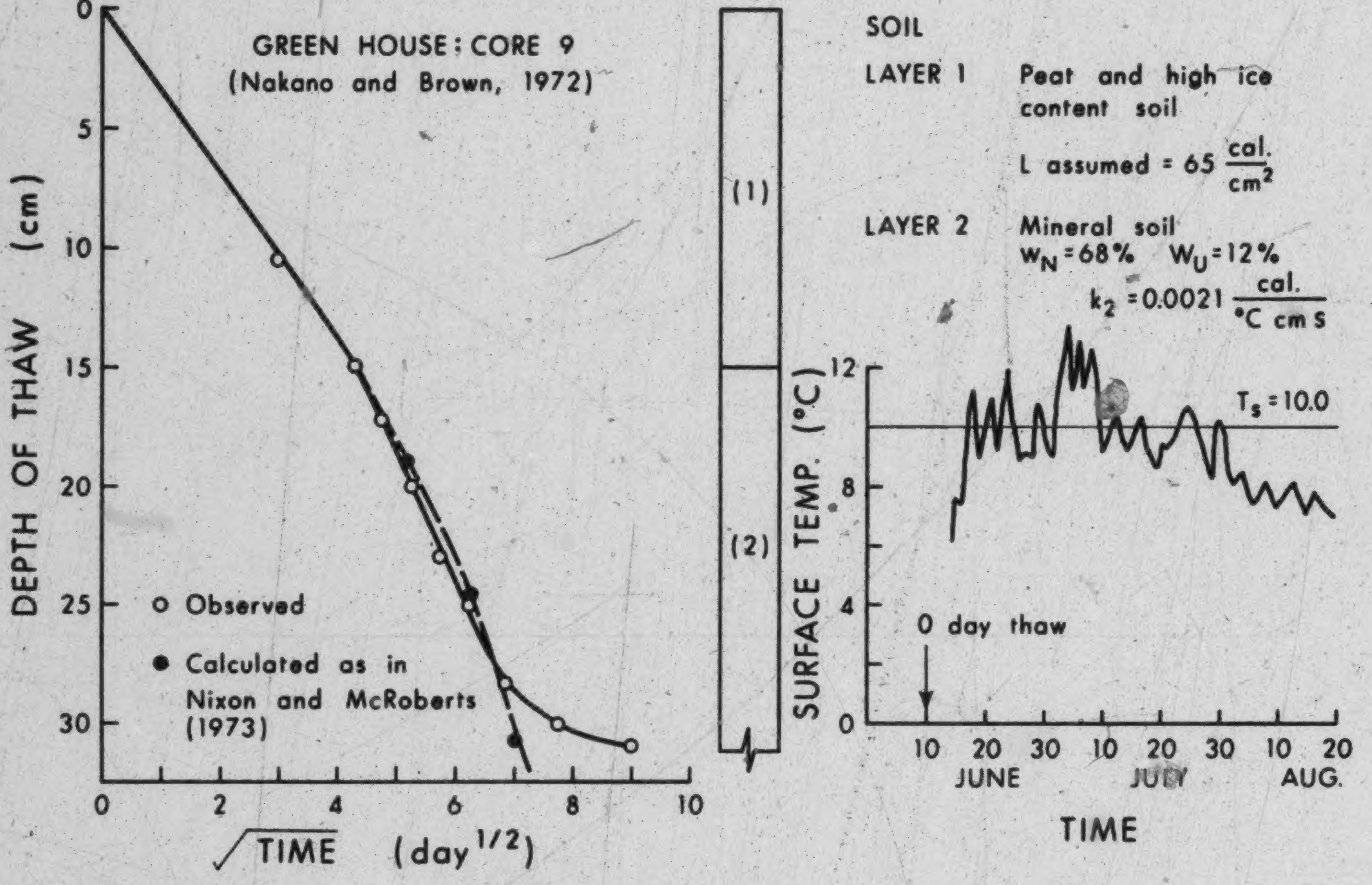

Fig 3.6 Depth of thaw under organic covers

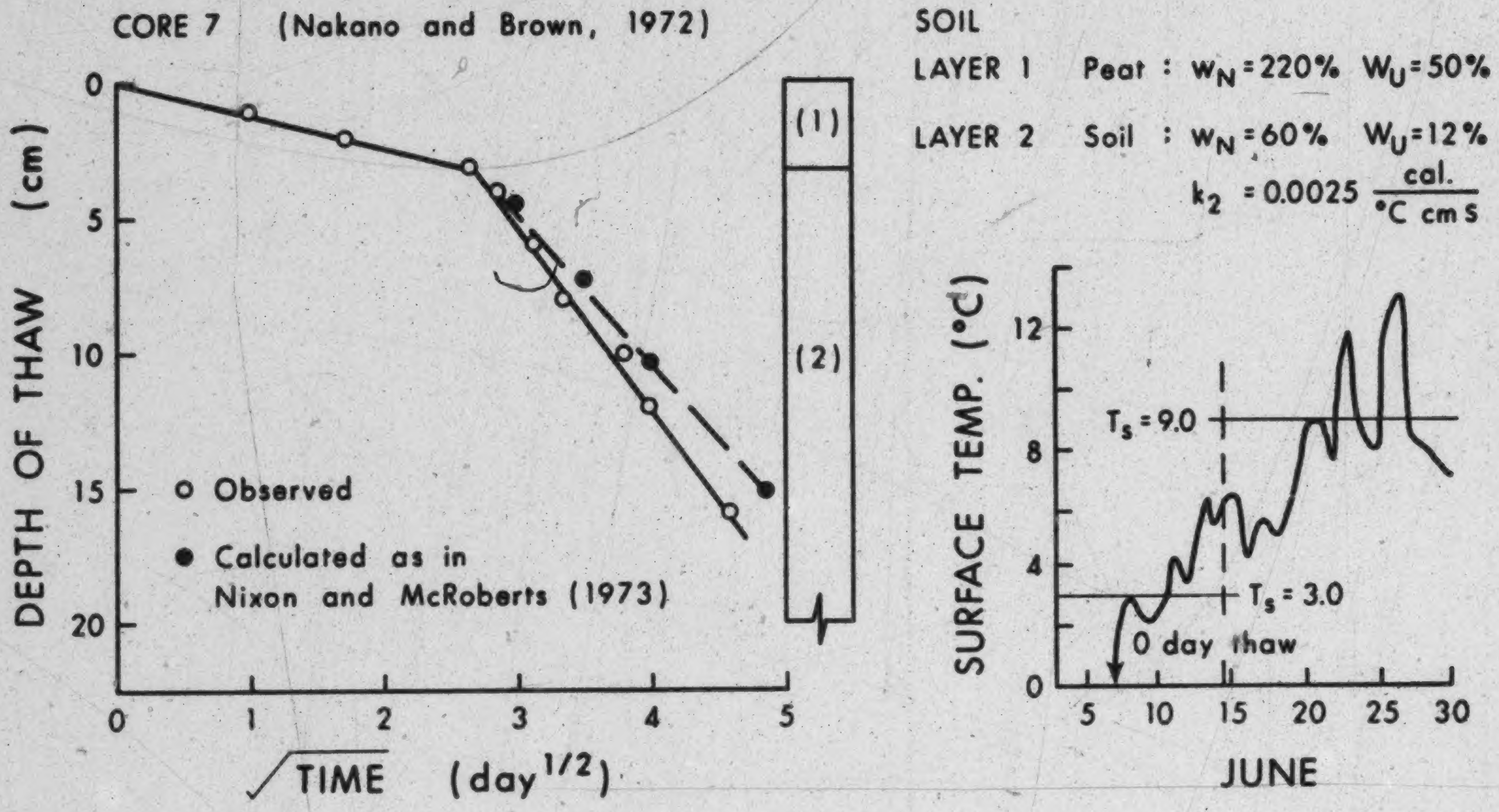

Fig 3.6 (continued)

CASE 1 SEEPAGE SLOPE

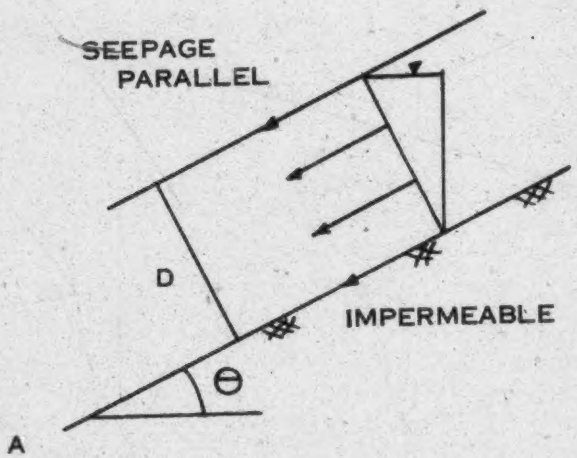
SEEPAGE
PARALLEL
A
D
IMPERMEABLE
Θ
A

ON PLANE AA

PORE PRESSURE = $\gamma_w D \cos\theta$

TOTAL STRESS $\gamma D \cos\theta$

EFFECTIVE STRESS $= (\gamma - \gamma_w) D \cos\theta$
$= \gamma' D \cos\theta$

$$F_s = \frac{\gamma' \tan\phi'}{\gamma \tan\theta}$$

CASE 2 THAW SLOPE

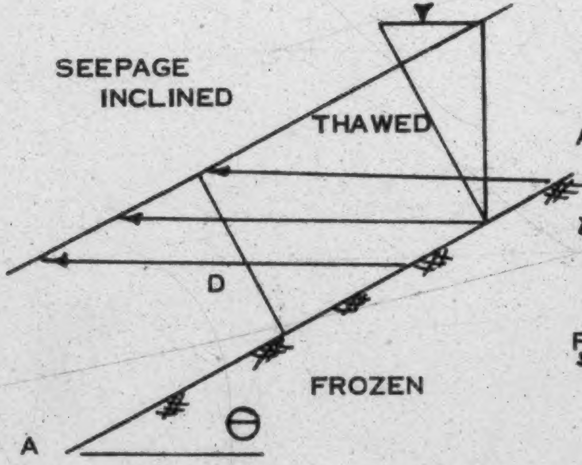
SEEPAGE
INCLINED
THAWED
A
D
FROZEN
Θ
A

ON PLANE AA

PORE PRESSURE $= \gamma_w D \cos\theta + \gamma' D \cos\theta \left(\frac{1}{1 + \frac{1}{2R^2}}\right)$

EFFECTIVE STRESS =
$\gamma D \cos\theta - \gamma_w D \cos\theta - \gamma' D \cos\theta \left(\frac{1}{1 + \frac{1}{2R^2}}\right)$

$$F_s = \frac{\gamma'}{\gamma}\left(1 - \frac{1}{1 - \frac{1}{2R^2}}\right)\frac{\tan\phi'}{\tan\theta}$$

WHERE $R = \frac{\alpha}{2\sqrt{C_V}}$

Fig 3.7 Infinite slope analysis formulation

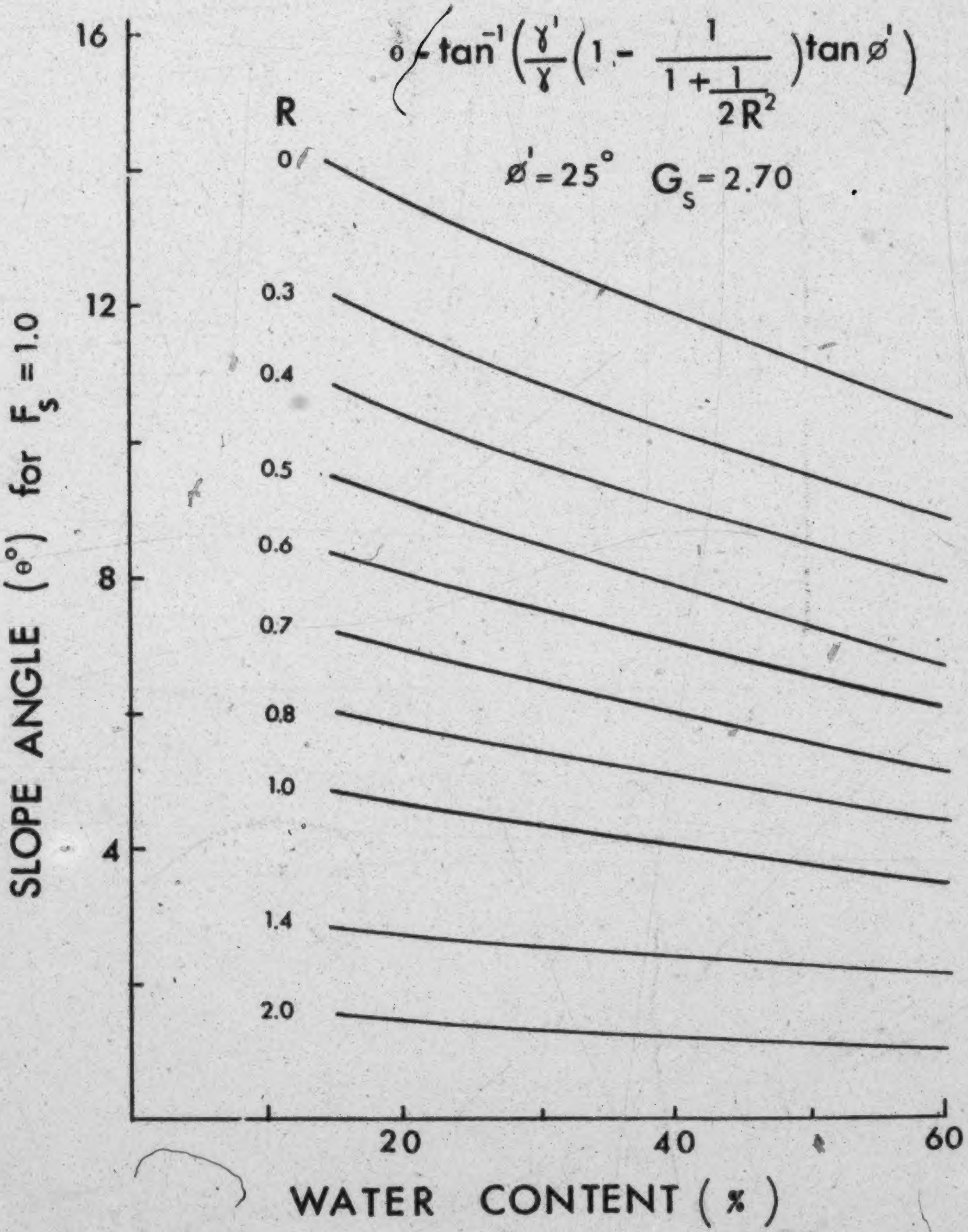

Fig 3.8 Solution to the infinite slope analysis in terms of the ratio R

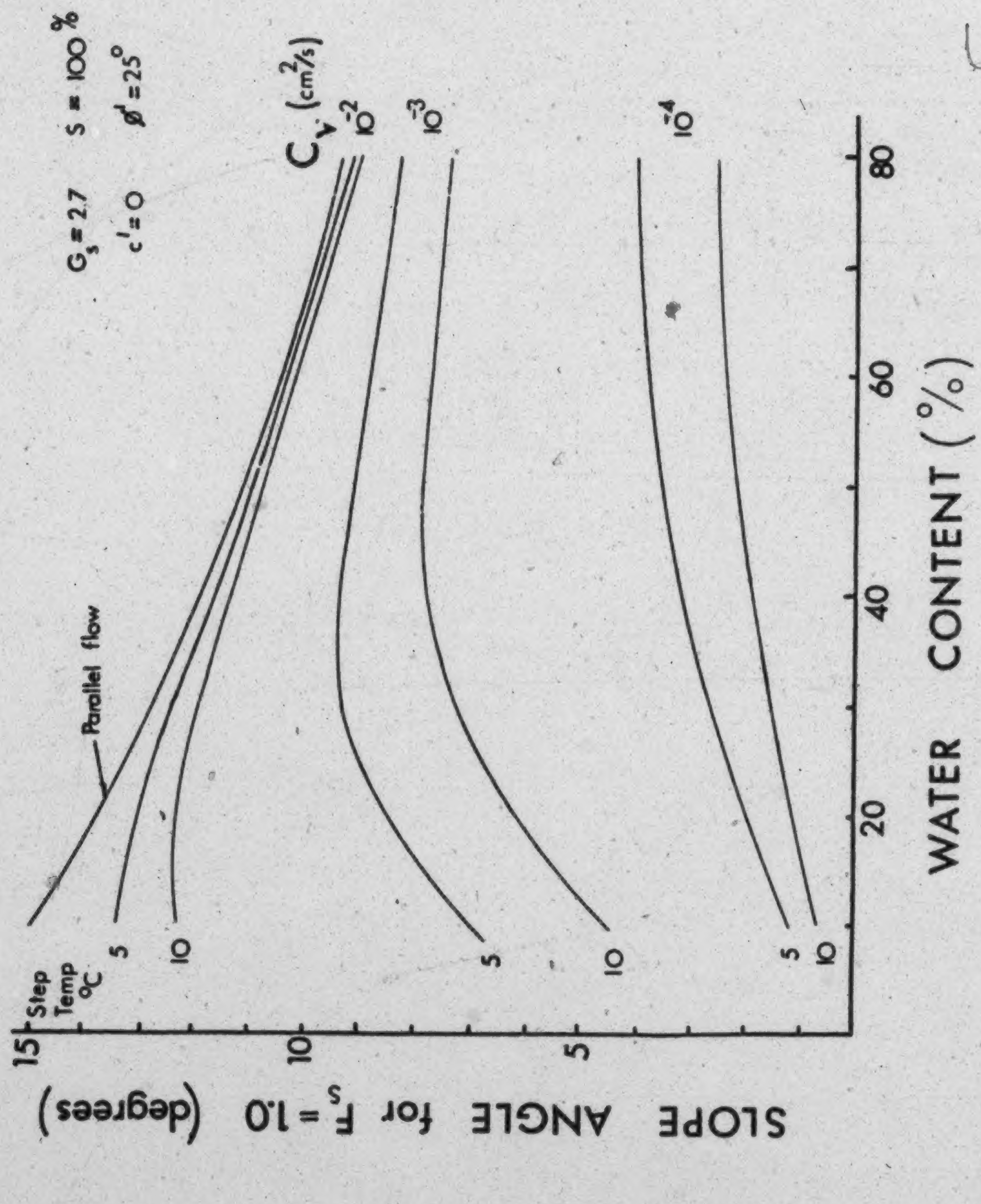

Fig 3.9 Solution to the infinite slope analysis in terms of T_s and c_v

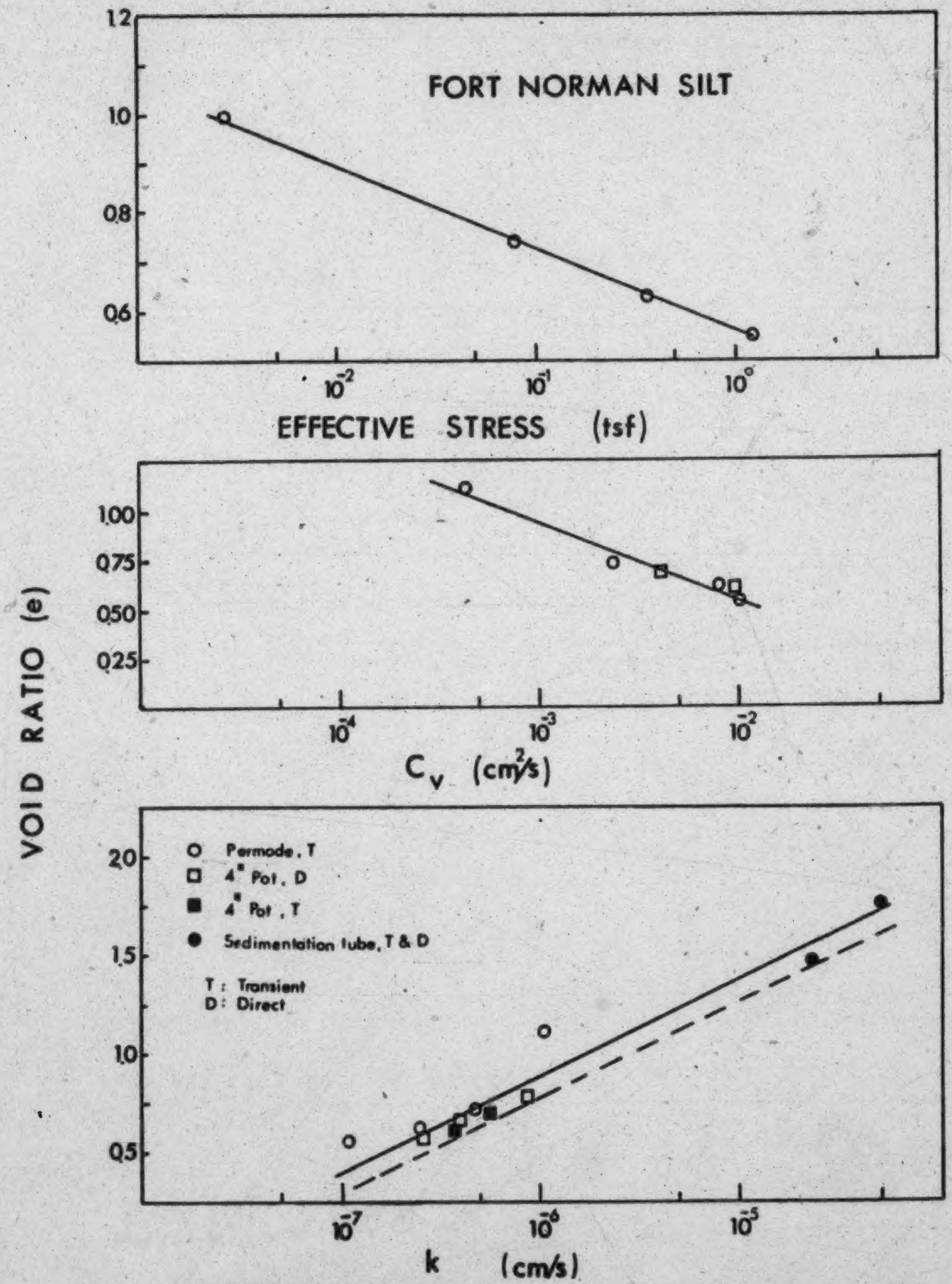

Fig 3.10 Void Ratio versus effective stress, permeability and coefficient of consolidation for Fort Norman Silt

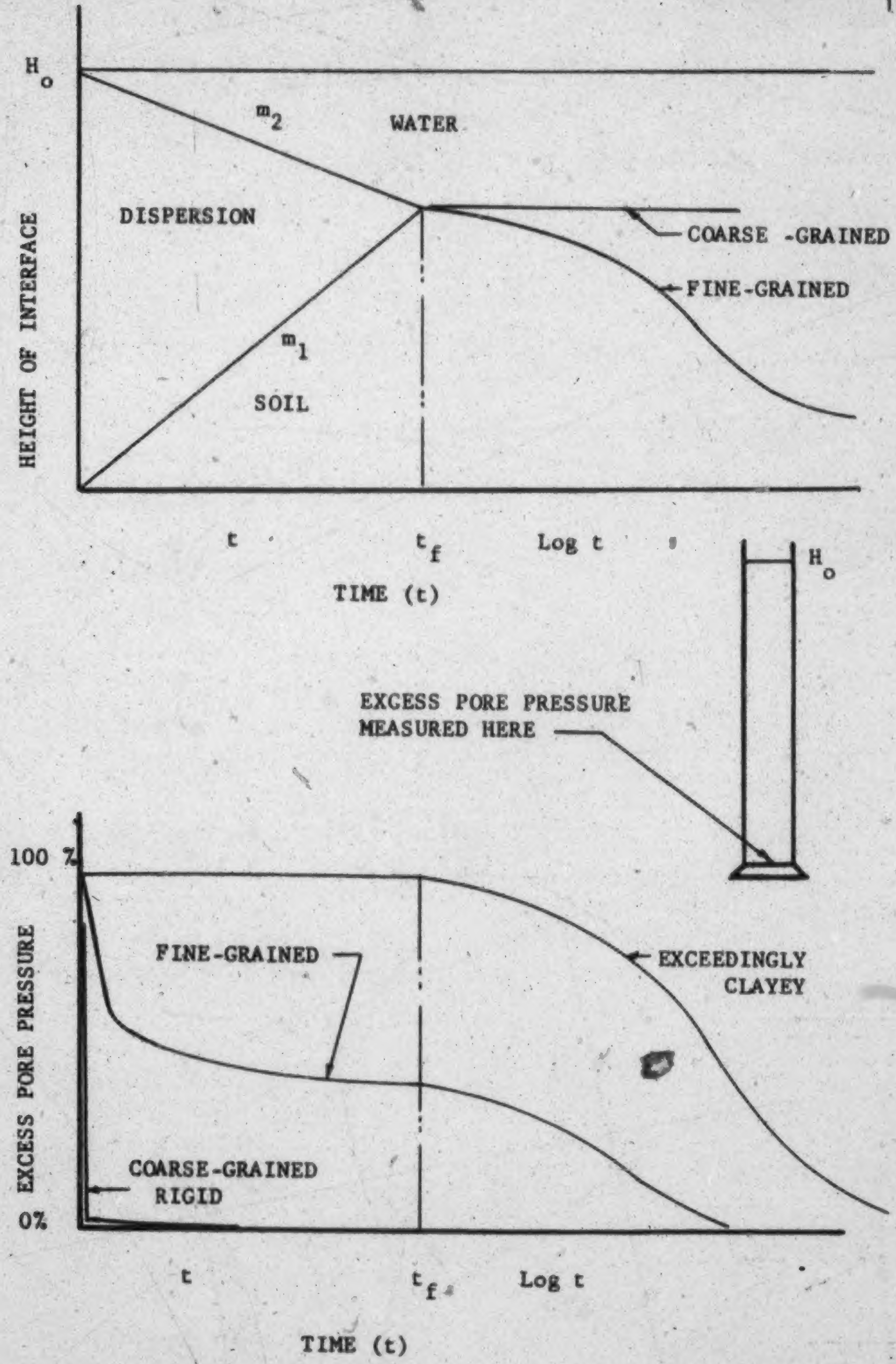
H
o
m
2
WATER
DISPERSION
COARSE -GRAINED
FINE-GRAINED
m
1
SOIL
HEIGHT OF INTERFACE
t
t
f
Log t
TIME (t)
H
o
EXCESS PORE PRESSURE
MEASURED HERE
100 %
FINE-GRAINED
EXCEEDINGLY
CLAYEY
EXCESS PORE PRESSURE
COARSE-GRAINED
RIGID
0%
t
t
f
Log t
TIME (t)

Fig 3.11 Characteristic hindered settling and post-sedimentation settlement behaviour

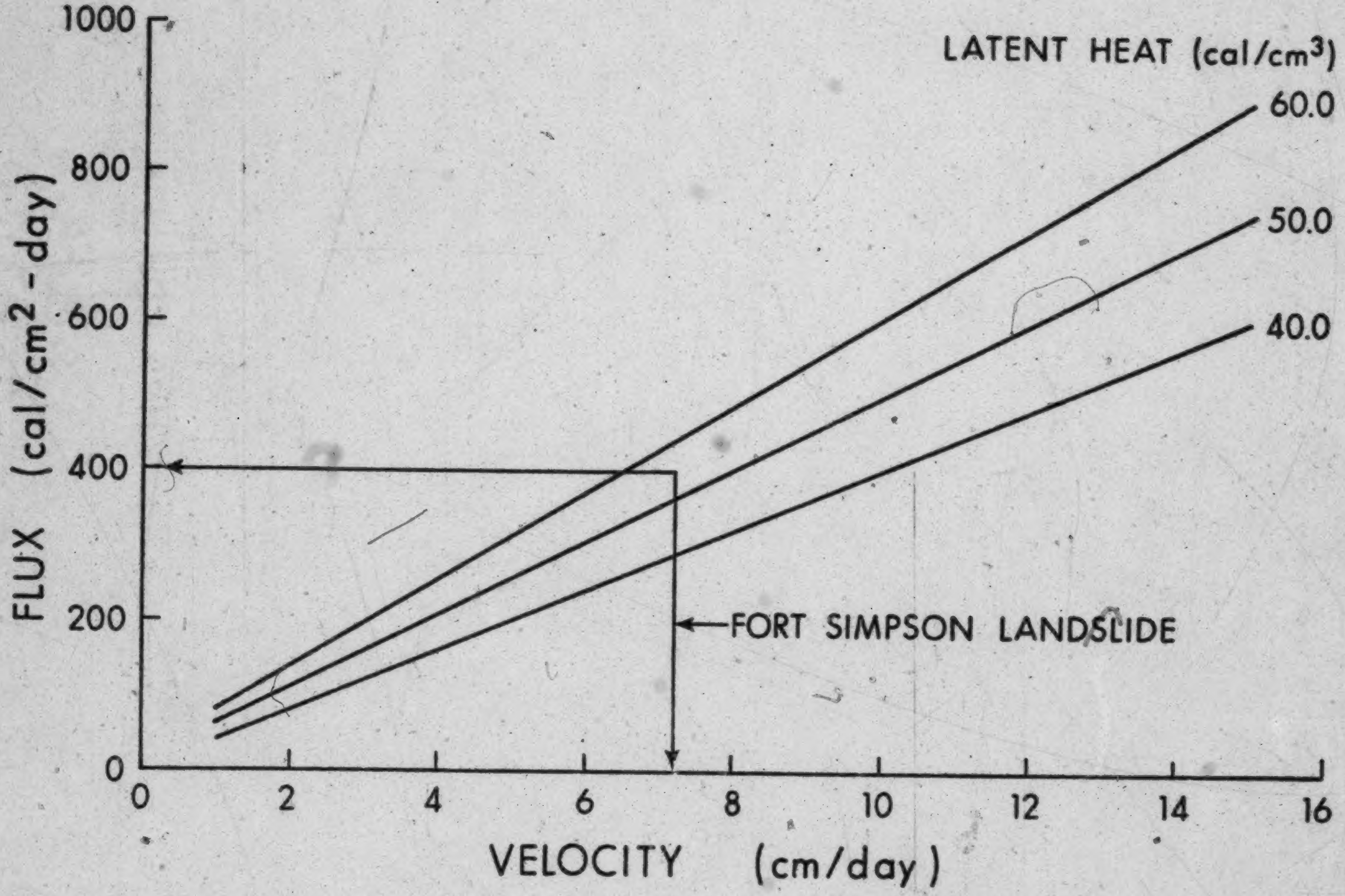

Fig 3.12 Graphical solution to the ablation problem

CHAPTER IV

INSTABILITY IN FREEZING SOILS

4.1 The Phenomenon of Pore Water Expulsion in Freezing Soils

When an ice-water interface advances through a freezing saturated soil it can be observed that under certain conditions of soil type and stress level that water is expelled away from the ice interface. While it is widely known that water is attracted or migrates towards a freezing front, it has not hitherto generally been recognized that an opposite or expulsion process can also exist in freezing soils. Furthermore, it can be shown experimentally that those soils which usually are considered to be frost susceptible, that is, they attract water, can be rendered non-frost susceptible and be made to expel water under certain conditions of stress level and freezing rate.

The geotechnical implications of this expulsion phenomena can be severe. When water is expelled by an advancing freezing front positive, excess, pore pressures can be set up in both open and closed systems. These high pore pressures may contribute to a wide range of instability problems.

The phenomenon of pore water expulsion is widely discussed in the literature. Taber (1930) was apparently the first to note that

> "some soils, when kept saturated with water, freeze with no uplift of the surface ..... some of the water must be pushed downwards by the growing ice crystals and expelled from the soil."

Beskow (1935) reports on a series of freezing tests on a till broken up into a range of samples of different grain sizes. He finds that coarser-grained saturated samples underwent a loss in weight during open system freezing tests while finer-grained samples gained weight. Although Beskow attributes this loss in weight to sublimation of ice during the progress of the test his data is not inconsistent with the concept of pore water expulsion. In a translation of his earlier work it is evident that Shumskii (1964) is clearly aware of the existence of pore water expulsion in coarse-grained soil. Shumskii comments that large pore water pressures can result from blocked drainage of expelled pore water and that the phenomenon also accounts for certain natural ground ice types. Khakimov (1957), citing the results of earlier laboratory testing by Sumgin, states that

> "part of the water is squeezed out during the freezing of saturated sand, i.e. the moisture of the sand decreases as a result of the expansion of the water during its transformation into ice."

Khakimov also reports on certain field observations made during the freezing of an annular shaft in saturated sand and comments that the rise of water in an adjacent borehole is due to the expulsion of water.

Balduzzi (1959), freezing saturated silts in an open system, also observed the expulsion of pore water. Wissa and Martin (1968) find that when saturated Ottawa sand was frozen in a closed system with free axial expansion allowed, heave and a positive pore pressure was recorded. When an identical sample was frozen in an open system water was expelled from the sand during the freezing process. Expulsion of water during the freezing of sand is also reported by Castro (1969) and Chamberlin et al (1972) note that excess positive pressures can be set up in sand samples being frozen for testing purposes if drainage is not allowed during freezing.

It is generally accepted that the cause of water expulsion on freezing stems from the fact that when water freezes into ice its volume expands by some 9%. When the pore water in soil freezes it also undergoes this change of state volume change. This process is best seen by considering two models in a freezing soil, Fig 4.1. The first, a closed system, is created when a sample in a container freezes from the top and no drainage of pore water is allowed at the base of the container. Conversely, an open system results when a free flow of water is allowed either into or out of the container. Now, if a saturated incompressible soil is placed in a rigid container with smooth sides and frozen from the top in a closed system a volume expansion ΔV of

$$\Delta V = 0.09nV \qquad 4.1$$

where n = porosity

V = total soils volume

0.09 = percentage increase in change of state volume

will result, see Fig 4.1. However, if the same soil is frozen under an open system a volume of water predicted by Eq 4.1 will be expelled from the soil with the result that no heave or volume expansion of the soil will be observed.

Wissa and Martin (1968) present results of freezing tests on saturated Ottawa sand for both open and closed systems. Their data, Table 4.1, indicates an excellent agreement between predicted heave or volume expulsion and measured values. Castro (1969) applies Eq 4.1 to saturated sand samples in order to calculate the initial porosity of samples before freezing.

It has not, however, been widely recognized that finer-grained soils may also expel water under certain conditions. It is known that fine-grained silts and clays attract water towards a freezing front and that the application of a suitable surcharge can inhibit this migration. However, once the tendency to heave has been depressed, pore water can be expelled away from an ice-water interface.

It is generally accepted that frost susceptibility is characterized by an attraction of water, manifested by heave or heave pressures, and the growth of ice lenses. The traditional method of discrimination between frost and non-frost susceptible soil has been made solely on the basis of grain size characteristics, and Townsend and Csathy (1963) conclude that the pore size distribution is the soil property which has the fundamental and primary influence on frost action. That is, fine-grained soils heave and develop ice lenses while coarse-grained soils do not. However, as it can be shown that frost susceptible soils can be rendered non-frost susceptible in that water is expelled away from an ice-water interface, it is evident that a distinction based solely on grain size is unsatisfactory.

This conclusion that grain size is of fundamental and primary influence was reached in spite of considerable evidence to the contrary that suggests that stress level is important. Beskow (1935) was apparently the first to observe that increased pressure causes a decrease in heaving rate in a silty soil. Beskow manipulated the stress levels by changing either the surface load, the pore water pressure or combinations of both and found that the heaving rate was identical for identical combinations. The larger the pressure differential across the sample the slower the heaving rate. As pointed out by Wissa and Martin (1968) this is nothing more than a straightforward application of Terzaghi's effective stress principle.

Similar observations were made by Vialov (1965) who changed both effective stress levels and drainage conditions in freezing samples of silty loam and clay in order to prepare artificially a range of samples for creep testing. As summarized in Table 4.2, Vialov found that at higher effective stress levels both the silt and the clay soils lost their tendency to attract water and underwent no volume increase for free swell and open system boundary conditions.

It is well known in highway practice that ice lensing may be stopped by applying a large enough overburden pressure. It is also appreciated that if a suction is applied to the pore water in the still unfrozen soil below a freezing front that ice lensing and heave may be stopped. This stress-dependent nature of frost susceptibility has, therefore, been understood for many years and stress levels have been manipulated in practice to control frost susceptibility.

The contention that fine-grained soils could be made to expel water has been investigated experimentally. Saturated Devon silt was frozen uniaxially under an applied total stress and under conditions of no axial restraint. Tests* were conducted by freezing from the top in a closed system and measuring pore water pressures at the base of the sample or by freezing in an open system and observing flow direction in a burette. At low total stress negative pore pressures were noted while at high total stresses positive pore pressures were measured. When the freezing system was expelling water no heave of the soil surface was monitered. For Devon silt overconsolidated to 7 kg/cm^2 the stress level K at which zero pore pressures or no flow occurred was 0.3 kg/cm^2, Table 4.3. That is, at a total applied stress of 0.3 kg/cm^2 no flow occurred in either direction and as the pore pressures were zero the value K expresses the effective stress level at which a freezing Devon silt changes

---

(*Unpublished tests conducted by E.C. McRoberts & J.F. Nixon, 1971) behaviour from attraction to expulsion of water.

Once a freezing test is underway, it is important to confirm that a condition of no axial restraint is developed between the side of the sample container and the frozen soil overlying the yet unfrozen soil because if substantial friction was developed the total stress applied to the sample would be unknown. In order to inspect this condition the following test was made during the freezing process. Under a closed system, an increment of total stress was applied and the resultant change in pore pressure measured. That little friction was developed was demonstrated by the observation that the immediate change in pore pressure equaled the total stress increment.

Similar tests were performed by Arvidson (1973) and are summarized in Table 4.3. It is noteworthy that the pressure at which expulsion began is slightly different depending on the technique used to measure it. Furthermore, the test results suggest that the critical stress level at which migration of water changes sign is also dependent upon the rate of heat extraction.

The test data presented suggests that the following equation may be written to describe the experimental results; that is,

$$\sigma - u = K \qquad 4.2$$

where σ = total stress
u = pore water pressure
K = a constant to be derived experimentally

Eq 4.2 is simply the statement that when the effective stress immediately beneath a freezing front in a soil reaches a certain critical level K that attraction of water towards the freezing front is no longer possible.

Considerable insight into the prediction of the expulsion phenomenon may be gained by a consideration of the capillary effects model as summarized by Williams (1967). The capillary model suggests that the ice-water interfaces seated in the pores of a soil are curved. A pressure difference exists across this interface due to the interfacial energy of the interface and this pressure difference established on freezing is given by

$$\nabla_i - u = C \qquad 4.3$$

where ∇_i = stress in the ice

and u = pore water pressure

and where C is a constant for a given soil

$$C = 2\frac{\nabla_{iw}}{r} \qquad C.4$$

where ∇_{iw} = surface tension ice-water

r = equivalent pore radius of the soil

Two conditions are predicted by Eq 4.3. If the stress level established on freezing is less than C, water migration occurs towards the interface and an ice lense grows. If the stress level C is exceeded, ice propagates through the pores of the soil.

Except for the case in which a thick ice lense has established itself there is no reason to suppose that the stress in the ice ∇i is exactly equivalent to the total stress ∇ at that level. For example, if we imagine a soil under a hydrostatic state of stress about half of the total stress is carried in the soil skeleton. When ice forms in the pores of the soil it can be argued that some portion of the total stress may still be carried by the soil skeleton and, therefore, ∇i is not equal to ∇. However, assuming, as does Williams (1967), that ($\nabla i = \nabla$) then the capillary effects model predicts that

$$\nabla - u = C \qquad 4.5$$

which is analgous to Eq 4.2 if (C = K). Thus, the capillary model can be interpreted to suggest that in a given soil, water migration due to the freezing process can be caused to change direction. Furthermore, the critical stress level predicted by Eq 4.4 by Williams (1967) and which is from 0.15 to 0.5 kg/cm^2 is of the same order of magnitude for the silty soils reported in Table 4.3.

The test data presented in Table 4.3 confirms experimentally that pore water can be expelled from a fine-grained soil. While there is some theoretical justification for Eq 4.2 in the predictions of Eq 4.5, it must be emphasized that there may be other variables influencing the phenomenon of water expulsion which are not embraced in either equation. Firstly, the rate of heat extraction could easily affect the efficiency of the process and the influence of step temperature, Table 4.3, suggests that such an effect cannot be ignored. The tests performed by Arvidson (1973) also suggest that stress history affects the response of the soil on freezing. It was observed, Table 4.3, that for tests conducted under the same step temperature, that overconsolidating the soil reduced the critical stress level. Furthermore, this observation is contrary to what would be predicted by the capillary effects model. Eq 4.4 suggests that as the soil becomes progressively more overconsolidated the critical stress level should increase rather than decrease because one would expect a decrease in the radius r with decreasing void ratio.

4.2 Mathematical Models

(i) One-Dimensional Models

In formulating the following models it is assumed that when a freezing front advances through a saturated soil, water is expelled in accordance with Eq 4.1 at all effective stress levels; that is, $K = 0$. In order to keep the development as general as possible, a relationship of the form

$$\Delta V = EV \qquad 4.6$$

where $E \leq 0.09n \qquad 4.7$

is assumed to allow for those cases in which less than the complete change of state volume is expelled. Thus, Eq 4.6 allows for fine-grained soils with high unfrozen water contents or for freezing rates at which Eq 4.1 is not applicable. It is further assumed that the still unfrozen soil beneath the freezing front reacts is an incompressible medium.

When freezing in a closed system, large positive pore pressures will result due to the increase in change of state volume. If a soil is frozen uniaxially, under conditions of nominally free axial restraint, and is expelling water, a positive pressure equal to the overburden pressure plus any mobilized frictional restraint will be developed. If a saturated soil is frozen in a closed system and is expelling water under conditons of no volume change then very large positive pressures will, theoretically develop. Within the assumptions made, the solution for the pore water pressure in the free heave closed system is trivial. As the soil beneath the freezing front is saturated the expelled water cannot be forced into the soil and the pore water pressure is instantaneously made equal to the overburden pressure. The water expelled will either freeze in the pores, form ice lenses, or cause hydraulic cracking and be extruded to the surface. Cracking, surface icings, as well as ice lenses were observed by Castro (1969) who froze sand samples in closed systems. By quickly immersing saturated sand samples in a glycol and dry ice bath at -50°C a closed system test configuration was effectively reached after a few seconds. Due to the destructive nature of this freezing on his samples, Castro changed to open system freezing.

As these closed system forms of freezing are not felt to be as important in geotechnical application as open systems they will not be considered further.

Let us consider an ice-water interface advancing at a rate dy/dt through a saturated soil expelling water according to Eq 4.6. In a time dt a volume of soil dy will be frozen expelling a volume of water dv where

$$dv = E\, dy \qquad 4.8$$

and the flow F expelled in a time dt is

$$F = \frac{dv}{dt} = E \frac{dy}{dt} \qquad 4.9$$

When the flow F is expelled on freezing and if, as commonly observed, there is no heave of the frozen soil surface in an open system then the expelled water must be made to flow through the still thawed soil. This flow is assumed to be governed by Darcy's law

$$F = k\, i \qquad 4.10$$

where k = soil permeability
i = hydraulic gradient

A gradient i must, therefore, be established at any time t such that the imposed flow F can be discharged through the still unfrozen soil. The maximum excess pore water pressure that must be set up to cause flow will occur at the ice-water interface. Thus positive excess pore pressures are generated in response to the flow boundary condition and they result from the impeded drainage in the still unfrozen soil.

Consider a sample of a saturated soil of length L freezing and expelling water one dimensionally through an open system against an external head L maintained in the pore water at the base of the sample. If at a depth ($y = Y$) measured from the top of the sample the advance of the ice interface ($dy/dt = 0$) or if ($E = 0$) then the flow F will be identically equal to zero. On the other hand, if (dy/dt, $E > 0$) then

$$F = E \frac{dy}{dt} = ki \qquad 4.11$$

Expressing the head H as the excess head required to cause a flow F to be discharged then

$$i = \frac{H}{L-y} \qquad 4.12$$

and it follows that

$$H = \frac{E\,(L-y)}{k} \frac{dy}{dt} \qquad 4.13$$

The pore pressure at the ice water interface at ($y = Y$) is then (γ_w ($Y + H$) where γ_w is the unit weight of water. Clearly the pore pressure cannot exceed the total stress at depth Y. It follows, therefore, that the effective stress level in the still unfrozen soil below the ice-water interface can rapidly approach zero depending upon the relative magnitude of E, dy/dt, and k.

This model is based on the assumption, stated earlier, that the critical stress level K is equal to zero. This is a reasonable assumption for coarse-grained sandy soils. For finer-grained soils, the effective stress level would tend to approach a magnitude K as predicted by Eq 4.2, instead of becoming zero. It is argued that as the effective stress level is reduced, by impeded drainage, to the critical stress level the pore pressures cannot exceed a value ($u < \sigma - C$) as attraction rather than expulsion would now occur.

But with the onset of attraction of pore water the pore pressure will be reduced as there is now no expulsion flow to build up pressure. However, as there will be a concomitant increase in effective stress Eq 4.2 now governs the freezing process and expulsion re-occurs. Thus, it is suggested that for a soil with a non-zero K value the effective stresses tend to the critical stress level rather than zero.

(ii) Two-Dimensional Model

Fig 4.2 outlines a more general model in which a flow F is applied to a region bounded by two impervious boundaries. At any time t it is assumed that the region of still unfrozen soil is contained in the region $(0 < x < L, 0 < y < B)$ and that an open system is created by allowing free drainage along $(x = L, 0 < y < B)$. It is required to find the head H that will cause all the water created by the applied flow F to discharge through the region of permeability k.

Assuming that the soil is a rigid incompressible medium, the Laplace equation

$$k\ (\nabla^2 \phi) = 0 \qquad 4.14$$

governs flow where ϕ is the velocity potential and H is the excess head or excess pore pressure causing flow and which are related by

$$\phi = -k\ H \qquad 4.15$$

A solution can then be obtained using a separation of variables technique and the details of the solution are given in Appendix D.

The solution derived in Appendix D can be expressed in terms of three-dimensionless variables as

$$\frac{H\,(x,B)}{\frac{FL}{k}} = f\left(\frac{x}{L}, \frac{B}{L}\right) \qquad 4.16$$

and is presented graphically in Fig 4.3.

A solution for the excess pore pressure consequent upon expulsion in a two-dimensional open system can now be obtained by solving Eq 4.9 for the flow F and by then introducing the value obtained in Eq D.25 or in Fig 4.3.

Both the open system models studied have assumed that the still unfrozen soil reacts as a rigid incompressible medium or that there are no transient or time effects to be considered in the solution. The solutions predict that if a flow F is applied at the interface,a head H is instantaneously required to satisfy the condition of no heave. As the rate of advance of the freezing front changes, so the flow F and thus the head H changes. For soils with a non-zero critical stress level it has also been argued that the effective stress level approaches the K value rather than zero if the drainage is severely impeded. This conclusion is based on quantitative arguments alone, and it is to be noted that as the freezing process in soils has not yet been completely understood this conclusion is still somewhat tentative.

The analytical solutions presented pertain to rather simple geometric boundaries. Given the power of the various numerical techniques available today it is evident that complex geometric regions, with varying flow boundary conditions resulting from varying magnitudes of E and of freezing rate, can be easily modeled. For example, a finite element technique was used to solve the problem shown on Fig 4.4 and the close agreement with the analytical solution is evident.

The prediction of the rate of movement of an ice-water interface, dy/dt, involves the solution of the thermal boundary condition of the freezing problem. A review of some useful analytic solutions are presented by Nixon and McRoberts(1973).

4.3 Some Consequences of Pore Water Expulsion

(i) Mass Movements

When the expulsion of water away from an advancing freezing front results in excess pore pressures due to impeded drainage the effective stresses in the underlying soil are also reduced. As reduced effective stresses result in decreased soil shear strengths it is possible that unsafe conditions may be created beneath a wide range of engineering structures and one might cite problems involved with chilled pipelines and artificial offshore islands. It can be noted that this mechanism may also play a role in the movement of glaciers which advance over sediments, freezing them, and causing expulsion conditions.

Let us now inspect an example problem, Fig 4.5, and consider the conditions that will result at Point A if water is expelled on freezing. Under a constant step temperature, the thermal solution follows from the Neumann problem (see Chapter 3) and the rate of advance dy/dt of the ice interface is

$$\frac{dy}{dt} = \frac{\alpha}{2\sqrt{t}} \qquad 4.17$$

and from Eq 4.9

$$F(y) = \frac{E\alpha^2}{2y} \qquad 4.18$$

At the surface Eq 4.18 predicts that F is infinite. This is an inherent characteristic of the Neumann problem and although a time-dependent temperature condition could be considered the example would be needlessly complicated. Let us consider the problem after the freezing front has advanced into the soil.

The solution for α for reasonable thermal properties is α = 0.07 cm/s$^{1/2}$ and assuming E = 0.09n (and with n=0.40) then

$$F(y) = \frac{8.83 \times 10^{-5}}{y} \quad \frac{cm^3}{cm^2 s} \qquad 4.19$$

A solution to the flow-specified problem for point A(y) can then be obtained from Fig 4.3 using (x/L = 0). As it is assumed that the water table in the gravel remains at the insulated surface, the maximum excess pore pressure that can be set up at A(y) equals the effective stress at that depth. That is, we are assuming that the critical stress K is zero. The solution on Fig 4.5 is presented in terms of minimum permeability required to cause zero effective stress conditions at A(y). It should be noted that in this problem that a finite rate of advance of the freezing front is predicted at a depth of 100 cm so that the effective stresses will always approach zero along the impervious boundary regardless of soil permeability.

The range of permeability predicted for zero effective stress is in the range of K values for sand and silty-sand which should expel water under the stress levels implicit in the problem. Thus the possibility of low effective stress on pore water expulsion is entirely likely for field conditions with similar boundary conditions.

There are no case histories of slope failures or foundation problems available to the author to suggest that the mechanism considered above may be applicable to any observed instability phenomenon. Furthermore, any possible failure surface, in a situation in which pore pressure expulsion was causing reduced effective stress, would pass partly through frozen ground. For this overall configuration, and considering the rate and temperature dependence of frozen strength, significant shear strengths would be set up in the frozen soil thus contributing to stability.

(iii) Ground Ice Forms

Various forms of ground ice have been attributed to expulsion phenomena. Shumskii (1964) clearly states that

> "the formation of injection ice is associated with the expulsion of water from coarse-grained soils and often with the expulsion of supersaturated fluid (quicksand-like) masses in soils which freeze as closed systems. Ice is intruded under the pressure of water expelled along the planes of weakness in freezing soil."

and comments further on the role of expulsion in the formation of pingos and in other ice lense forms.

In a recent paper (Mackay (1973) has presented a definitive study of the role of expulsion phenomena in nourishing the growth of pingos. Mackay argues that while injected ice may form in the early growth stage, the main role of expulsion is to first provide a source of water for pingo growth and, secondly, to lower effective stress conditions beneath the juvenile pingo. This combination of available water and low effective stress then favours the growth of segregation ice. Mackay also cites evidence confirming that expulsion in a closed system freezing environment can create artesian conditions beneath an advancing freezing front.

(iii) Frost Susceptibility

The consequences of pore water expulsion and the influence of stress level in determining the direction of water movement have a direct bearing on the frost susceptible nature of freezing soils. A discussion of this problem is beyond the scope of this thesis and some aspects of the problem are considered by Arvidson (1973).

4.4 The Importance of Freezing in Solifluction

A mechanism, called ice-blocked drainage, has been proposed by various authors (Siple, 1952; Chandler, 1970 and 1972) to account for instability in solifluction slopes. It is reasoned that when a freezing front advances into a slope it forms a blanket of impermeable frozen soil overlying the talik in the still unfrozen active layer. This blanket can then block or back up the water flow and thus set up excess pore pressures. While this mechanism is possible it is not considered likely.

In Sec 1.4 we have seen that solifluction slopes consist of fine-grained silty or clayey soils. For the usual depths of active layers, say up to 6 ft, the stress levels in the slope are such that water will always be attracted to an advancing freezing front. Then, when a freezing front advances into a soil, pore water sub-pressure would be more reasonably expected. That this is the case is witnessed by the frequent observations made of ice lenses in solifluction slopes (see Sec 1.4). The ice lenses formed appear to be of the segregational ice variety and it is suggested that their common occurrence in solifluction slopes supports the view that during freezing excess pore pressures are unlikely.

The condition of ice-blocked drainage may tend to nourish the growth of ice lenses and in this manner contribute to solifluction. The formation of ice lenses and the bulking of solifluction slopes during the freezing cycle is a vital element in the cycle of events that leads to instability due to thaw consolidation processes. It has been shown that the freezing of saturated clayey soils in a closed system leads to the generation of excess pore pressures on thaw (Smith, 1972; Nixon, 1973) and it is argued that the freeze-thaw cycling in an open system characteristic of solifluction slopes is of fundamental importance in the mechanics of solifluction movements.

The process of bulking during freezing is also a vital part of the frost creep mechanism in solifluction soils (see Sec 1.4) and while it is felt that the importance of frost creep is over-emphasized by many authors it cannot be discounted.

Yet another role of the freezing process in solifluction slopes is the creation of conditions which favour the downslope creep of ice and ice-rich soil. It will be shown, in the following chapter, that significant deformations can accumulate due to the rheologic creep of frozen soils. The bulking of solifluction soils during freeze back and the creation of ice lenses will aid this movement mechanism.

While it is relatively straight-forward to suggest ways in which freezing contributes to solifluction movements it is another matter entirely to resolve the different degrees of importance of the various mechanisms. However, it is felt that the dominant mechanism in solifluction movements is the freeze-bulking, thaw-consolidation cycle. This argument is supported not only by the quantitative observations of many investigators (see Sec 1.4) but also by the thaw consolidation model presented in Sec 3.3.

TABLE 4.1 FREEZING DATA ON OTTAWA SAND

Test Data	Open System Test	Closed System Test*
Porosity	0.359	0.354
Volume Soil	2190 cm^3	2190 cm^3
Water Expelled	73 cm^3	-
Heave	+	73 cm^3
Predicted	70.7 cm^3	69.7 cm^3
Ratio:		
Predicted to Measured	0.97	0.95

Data from Wissa and Martin (1968)

* The average of two tests

+ The test was conducted under constant volume conditions but a small negative or upwards load was required to maintain this condition. Thus a slight contraction would have been measured under free axial restraint.

TABLE 4.2 FREE SWELL FREEZING TESTS ON RUSSIAN SOILS

Drainage	Soil	Total Stress Level (kg/cm^2)	Water Content Initial (%)	Water Content Final (%)	Soil Texture
Open System No back pressure	Silty, sandy loam	0	33.0	39.0	Laminar *
		0	29.0	36.5	"
		0	25.0	32.5	"
		0.25	30.0	29.7	Massive +
		0.5	29.0	28.6	"
		5.0	25.0	25.0	"
"	Clay	0	21.4	34.0	Laminar
		1.0	21.0	23.6	"
		10.0	19.0	20.0	Thinly laminar
		50.0	19.0	19.0	Massive
Open System Back pressure = 10 kg/cm^2	Silty, sandy loam	15.0	25.0	25.0	"
Open System Back pressure = 24 kg/cm^2	Clay	50.0	19.0	19.0	"

After Vialov (1965)

* Laminar soil texture is a term used to describe segregation ice lenses

+ Massive soil texture is a term used to describe the presence of ice cement-ice crystals only distributed in the soil with no noticeable disruption of the homogeneity.

TABLE 4.3 EXPULSION/ATTRACTION TESTS IN DEVON SILT

Soil	Stress History (units kg/cm^2)	Step Temperature (0^oC)	K (kg/cm^2)	Test Code	Source
DS	$P_c^* = 7.0$	-10	0.3	A	This study
DS	$P_c = 7.7$	-5	0.55	A	Arvidson (1973)
DS	n/c+	-5	1.4	A	"
DS	n/c	-5	1.28	B	"
DS	$P_c = 4.88$	-5	0.86	B	"
DS	$P_c = 7.7$	-5	0.70	B	"
DS	$P_c = 8.8$	-5	0.75	B	"
DS	$P_c = 7.7$	-10	0.57	B	"
MDS	$P_c = 7.7$	-5	2.3	B	"

DS: Devon Silt MDS: Modified Devon Silt (Finer Grained)

TEST CODE A: K deduced from pore pressure measurements
B: K deduced from pore water migration

*P_c = preconsolidation pressure
+n/c= normally consolidated

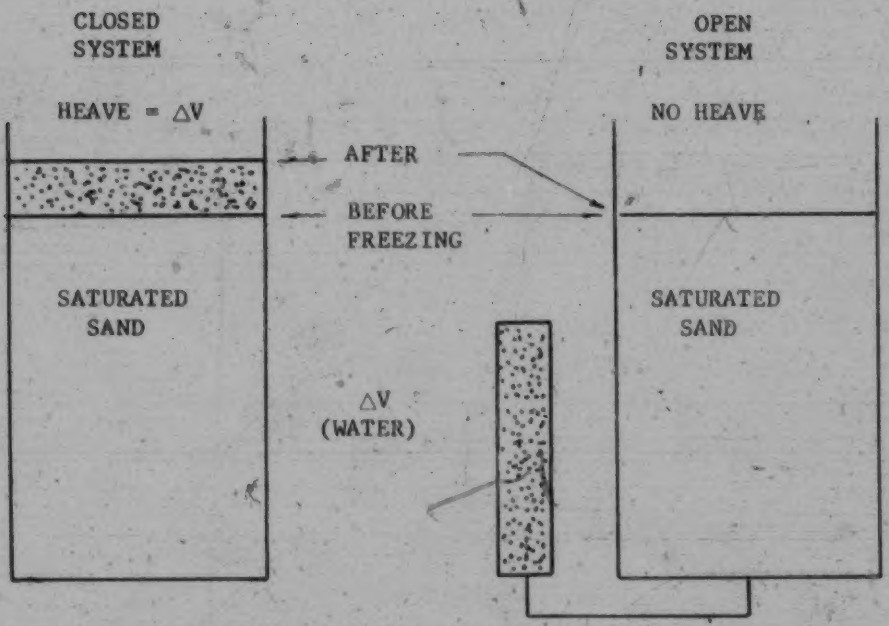
CLOSED SYSTEM
HEAVE = ΔV
OPEN SYSTEM
NO HEAVE
AFTER
BEFORE FREEZING
SATURATED SAND
SATURATED SAND
ΔV (WATER)

TOTAL SOIL VOLUME = V
POROSITY = n
CHANGE IN VOLUME ON FREEZING = ΔV

$$\Delta V = 0.09nV$$

Fig 4.1 Closed and open system freezing tests

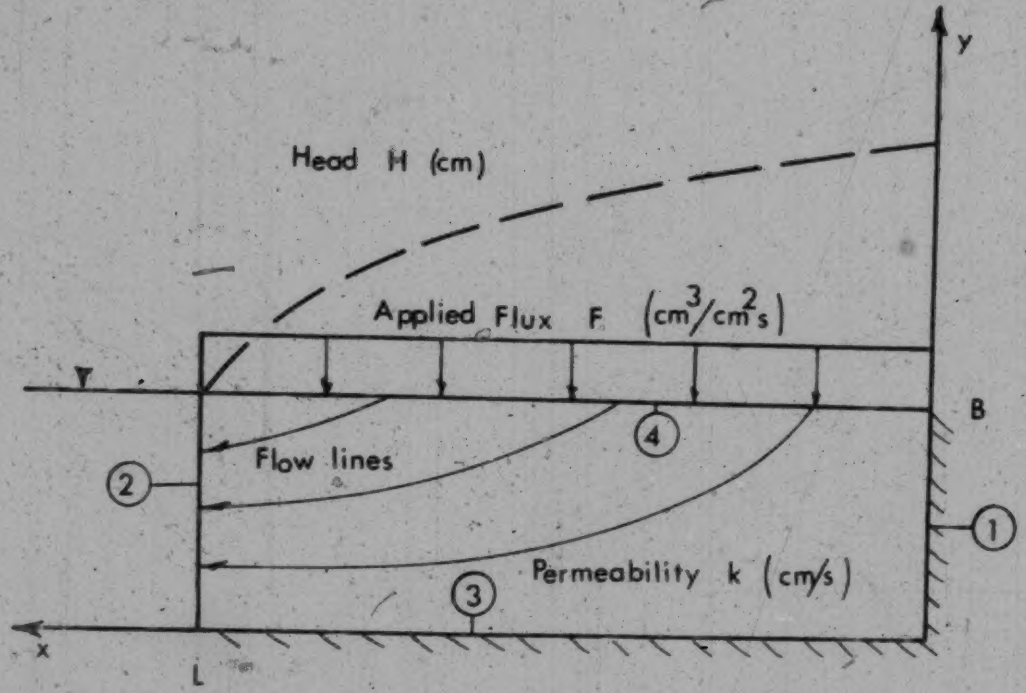
Head H (cm)
Applied Flux F $(cm^3/cm^2 s)$
Flow lines
Permeability k (cm/s)
y
x
B
L
①
②
③
④

Fig 4.2 Two dimensional freezing problem

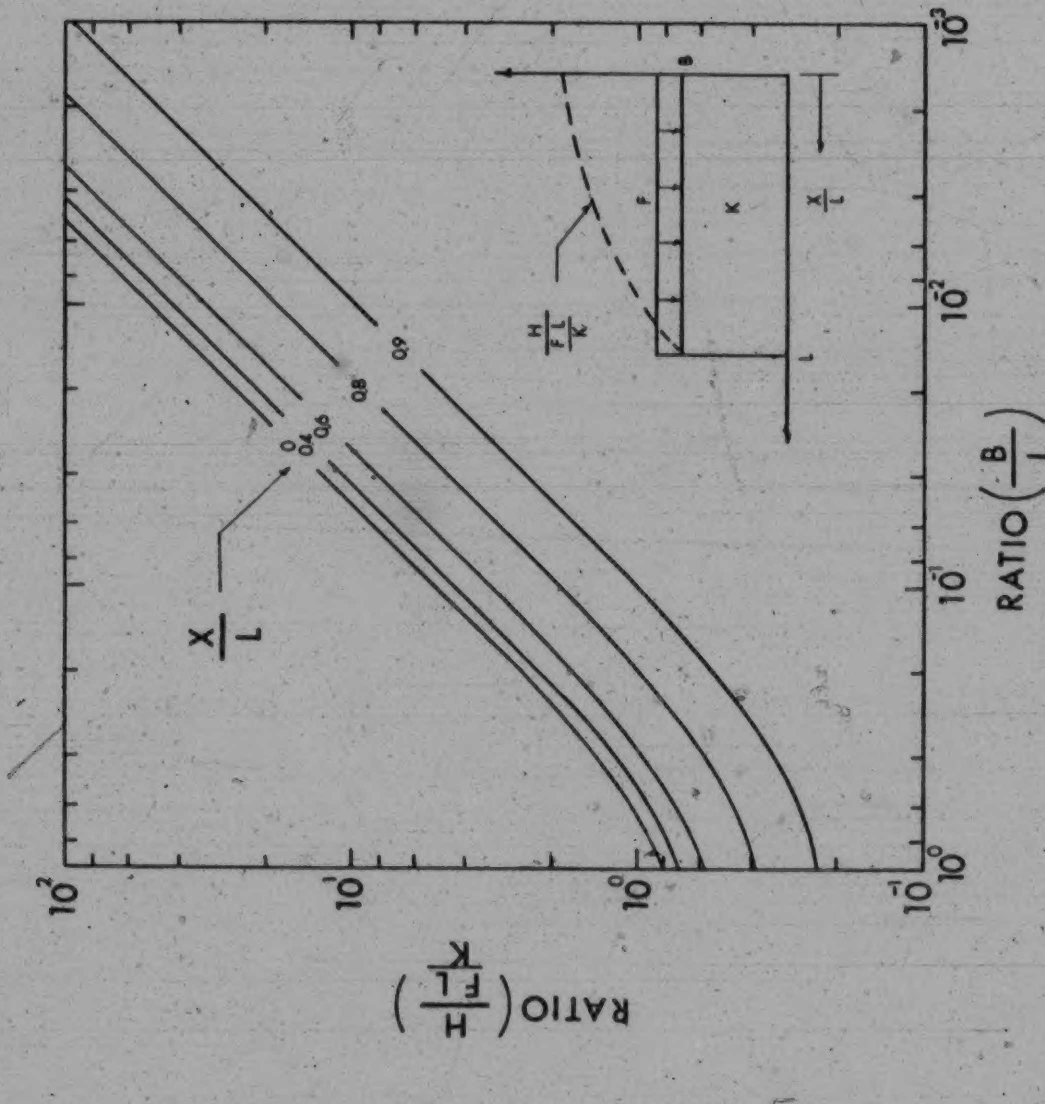

Fig 4.3 Solution to the flow specified problem

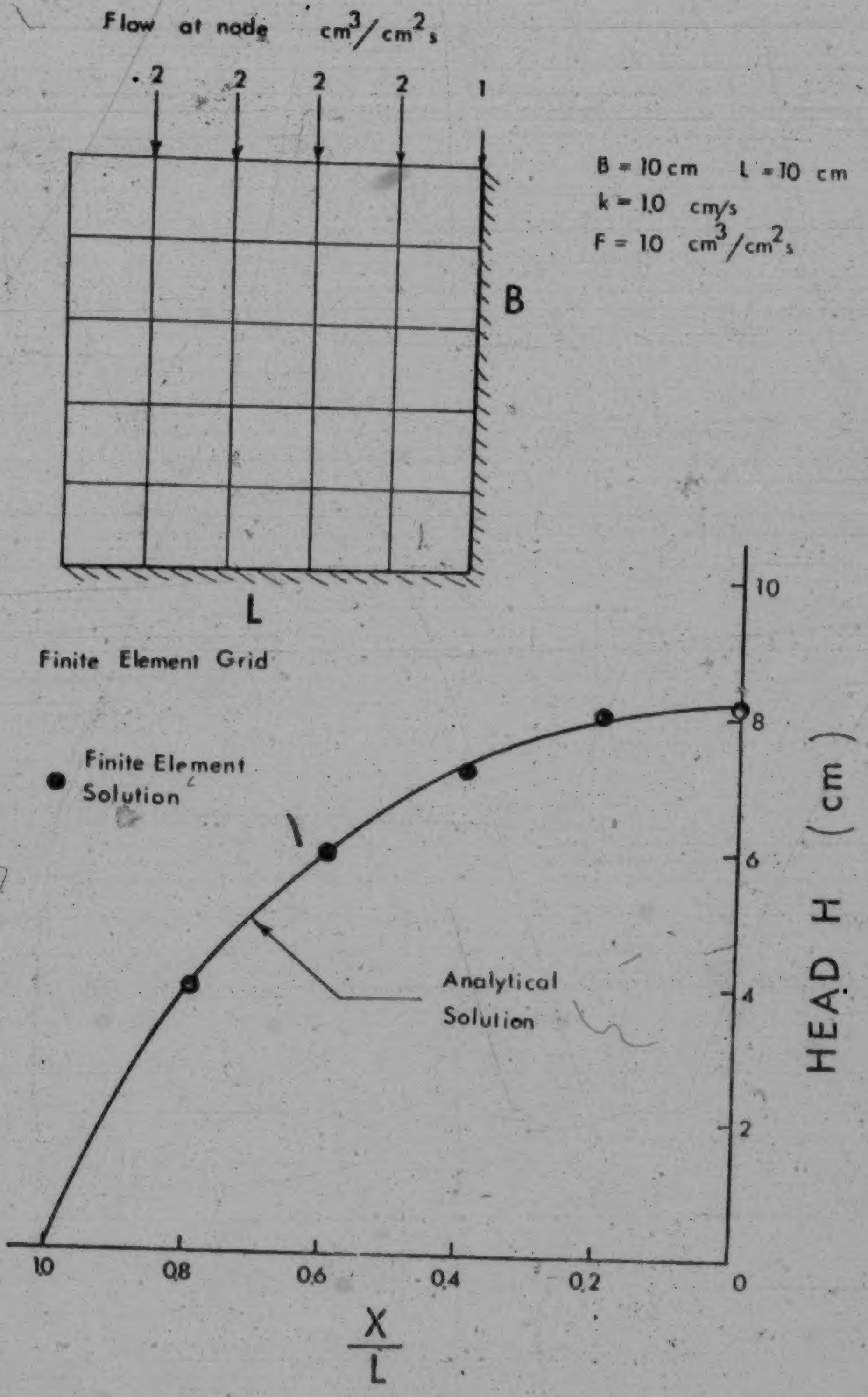

Fig 4.4 Comparison with a finite element solution

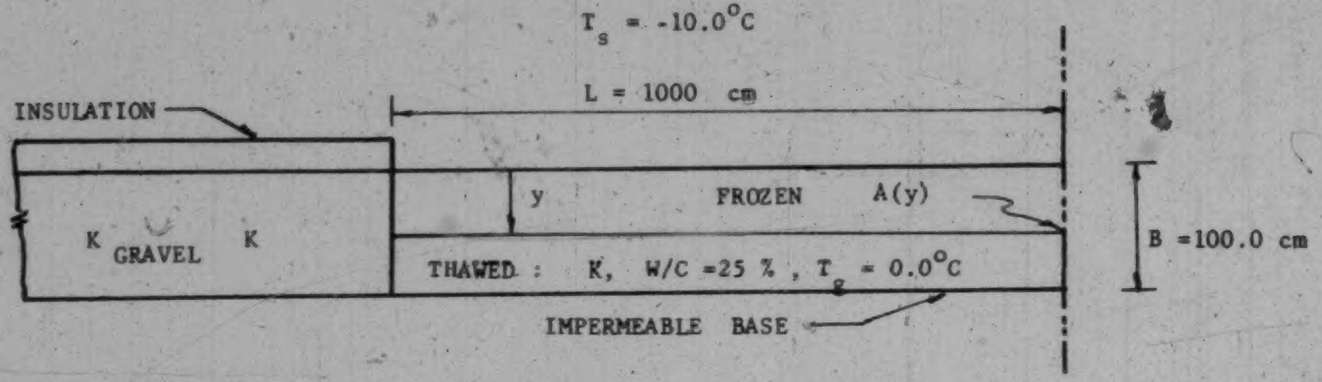
T_s = -10.0°C
L = 1000 cm
INSULATION
y
FROZEN
A(y)
B = 100.0 cm
K GRAVEL K
THAWED : K, W/C = 25 %, T_g = 0.0°C
IMPERMEABLE BASE

DEPTH	F $\left(\frac{cm^3}{cm^2\ s}\right)$	B/L	$\frac{H}{FL/K}$	HK(cm^2/s)	$H^{=}_{max}$(cm)	K^{*}(cm/s)
25	0.00000353	0.075	6.6	0.0233	25	0.00093
50	0.00000176	0.050	10.0	0.0176	50	0.00035
75	0.00000118	0.25	20.0	0.0236	75	0.00031

= BASED ON γ = 2.0
* PERMEABILITY AT WHICH EFFECTIVE STRESS AT A(y) = 0.0 , OR K = HK/H_{max}

Fig 4.5 Solution to a typical freezing problem

CHAPTER V

MASS - MOVEMENTS IN FROZEN SOILS

5.1 Introduction

Inspecting the range of landslide forms possible in periglacial regions it is evident that a variety of failures are associated with the deformation of frozen soils or ice. Mass-movements such as the falls initiated by thermal erosion and the large block and MR slides found along parts of the Mackenzie River Valley are, in part, the result of shear failure through permafrost soils. On the other hand, we have seen in Sec 1.4 that it is possible that some of the downslope movement attributed to solifluction may be due to the creep of frozen soil.

In order to appreciate the range of mass-movements possible in frozen soil it is necessary to give attention to certain special features of the geotechnical properties of frozen soils. It is known, in a general way, that the load-deformation characteristics of frozen soils are dependent on the magnitude of the applied stress, the rate of deformation and the temperature.

As noted by Anderson and Morgenstern (1973) it is convenient to sub-divide this load-deformation response into three areas: elastic behaviour, creep behaviour and strength. When a slope is formed by either natural or artificial means it will undergo an immediate, initial deformation; but, as these deformations will likely be small compared with subsequent movements they will not be considered here. Slope movements can then be associated either with creep deformations or gross displacements due to shear failure.

It is well-known that frozen soils exhibit time-dependent deformations under the action of a constant load and that, in general, creep curves for frozen soils correspond to the classical creep curves which may be divided into several sections. The generalized creep behaviour model of permafrost soils under constant deviatoric stress (see Vialov, 1965; Sayles, 1968; Ladanyi, 1972) suggests that the deformations of a loaded mass of frozen soil accumulate in the following manner. Immediately after the application of the deviatoric stress there is an instantaneous deformation. At low stress levels these deformations enter a primary stage characterized by decreasing strain rates which, finally, reach some steady state value which, if maintained, describe a secondary creep mode. With time, this constant deformation rate stage passes into a final or tertiary stage of creep which terminate in creep rupture. It is further suggested that this behaviour is dependent on stress level. For high stresses the transition is directly from primary to tertiary creep while for low stresses the primary mode ends with ever decreasing or zero strain rates. At intermediate stress levels the secondary creep stage exists for longer periods of time and it is often inferred that for certain stress intensities creep deformations can continue at a constant rate more or less indefinitely (see Sayles and Thompson, 1972).

The strength of frozen soil is a response of the technique used to measure it. It is known that the strength of frozen soil is time dependent (Vialov, 1965; Sayles, 1968) with the mobilized strength decreasing with increasing time to failure. It is also suggested that for a range of frozen soils that an ultimate or long-term strength exists and which is defined by Sayles (1968) as being

> "The maximum stress that the frozen soil can withstand indefinitely and exhibit either a zero or continuously decreasing strain rate with time."

The division of load-deformation behaviour into creep and strength is, however, arbitrary as the two concepts are closely interrelated. Vialov (1965) relates creep and strength via his definition of damped and undamped creep. He considers that if

> "the stress does not exceed a certain limit referred to as the limiting long-term strength then the deformation is damped (damped creep); if the stress does exceed the above-mentioned limit, then undamped creep develops. Limiting long-term strength is also referred to as ultimate strength, threshold of creep, etc."

He also points out that

> "it should be noted, that such a division of the deformation processes into damped and undamped creep, the separation of the various stages (primary, secondary, tertiary) and the concept of a limiting long-term strength are arbitrary since such a division will depend to a significant degree upon the duration of the experiments .... Those deformations, considered in this book as stabilized, could continue to grow if observed for longer periods. Those deformations, considered as flow with a

> constant rate (secondary creep), could become slowly damped if observed for longer periods of time, or on the contrary, they could develop at increasing rates."

Furthermore, the discrimination between creep and strength is very much a function of the ice content of the soil. The concept of long-term strength is generally accepted as being inappropriate for ice as it creeps under extremely small stresses and Vialov (1965) has pointed out that the concept of long-term strength does not apply for what he calls "ice-saturated frozen soils". He does suggest that the concept can be applied to "structured soils". For structured soils it would appear that Vialov suggests that creep deformations either terminate in a tertiary stage at stress levels above the long-term strength (in the undamped mode) or deccelerate with time at stress levels below the threshold stress level (i.e. the damped mode). For structured soils the long-term strength and the threshold stress level are identical. More recent work by Sayles (1973) on frozen Ottawa Sand suggests that the long-term ultimate creep strength of structured soils is basically a function of the strength of intergranular contacts governed by the angle of internal friction.

On the other hand, it appears that ice will not exhibit a damped creep mode and load-deformation response either terminates in creep rupture or continues in a secondary stage more or less indefinitely. That is, the long-term strength or threshold creep level is approximately zero. By inference, it is then likely that ice-rich soils will exhibit a wide range of behaviour between the above extremes. Furthermore, we shall see that under certain circumstances, admixtures of soil grains in ice serve to significantly reduce the strength of ice itself.

In order to model slope deformation behaviour for permafrost soils it is then necessary to first formulate a series of models of load deformation response. For practical purposes, two simple models that seem to be justified are a secondary creep model and a long-term strength model. These models are justified in that they have been observed to some degree in actual experiments. The intent of this chapter is, therefore, to investigate a range of natural slope processes in frozen soils within the framework of certain models. It is far from clear if these models are in all regards adequate but they are valuable in that they help bound possible slope deformation behaviour.

5.2 Secondary Creep Model

5.2.1 The Model

It is entirely possible that some downslope movements of permafrost slopes may be caused by the creep deformation of frozen soils. Although the subject is complex, experiments on the creep of ice and ice-rich soils suggests that significant deformations may accumulate in permafrost soils under sustained stresses. While it is possible to formulate simple models to simulate slope deformation processes there is a lack of both experimental data from which relevant constitutive relationships may be derived and of field observations to confirm or modify the mass movement models used. While there have been various field studies conducted concerning the deformation profiles of permafrost slopes (see Carson and Kirkby, 1972) these studies have been confined to the active layer where mass-movement processes other than creep likely dominate. However, other studies considered in detail in Chapter 1 suggest that the magnitude of deformations that can accrue in the active layer during the winter season may be most reasonably explained by creep deformations.

Laboratory creep studies are difficult to undertake and tests of long duration are required in order to isolate whether one is in primary or secondary creep or if a test will terminate in the tertiary mode. The mode of creep deformation observed depends upon stress level, time and temperature and most creep tests reported on frozen soils have been done at high stress levels, low temperatures, and over relatively short time intervals. Investigation of creep deformation in natural slopes requires test data from long duration tests at low stress levels and at temperatures near the melting point. Furthermore, a significant percentage of the available creep data has been conducted on either frozen remoulded soils or soils with low ice contents and little information is available for ice-rich soils.

As we are concerned here with the creep deformations of natural permafrost slopes of a geologic age we can likely exclude the possibility of creep rupture since these slopes would have long since failed. Theoretically, therefore, it would be necessary to attempt to discriminate between slopes on which secondary creep still continues unabated with the passing of time and slopes on which deformations have stopped or are decreasing. However, we shall limit our attention to a simple secondary creep model which will serve as an upper bound on possible slope deformation behaviour.

In order to predict creep deformations using the results of various laboratory and field experiments it is necessary to relate shear stresses and shear strain rates. As the experimentally derived constitutive relationships governing the creep, or flow, of ice or ice-rich soils can, generally, depart from the linear, or

Newtonian, viscous flow law, it is necessary to seek a more general relationship. Following Meier (1960) it can be assumed that the strain rate is a function of the deviator stress or generally

$$\dot{\varepsilon}_{ij} = f(\sigma'_{ij}) \qquad 5.1$$

and the magnitude of the deviator stress is, in turn, measured by the octahedral shear stress

$$\tau_o = \frac{1}{3}\sqrt{(\sigma_1-\sigma_2)^2 + (\sigma_2-\sigma_3)^2 + (\sigma_3-\sigma_1)^2} \qquad 5.2$$

where (σ_1, σ_2, σ_3) are the principal stresses.

Similarly, an octahedral shear strain rate ε_o is defined as

$$\dot{\varepsilon}_o = \frac{1}{3}\sqrt{(\dot{\varepsilon}_1-\dot{\varepsilon}_2)^2 + (\dot{\varepsilon}_2-\dot{\varepsilon}_3)^2 + (\dot{\varepsilon}_3-\dot{\varepsilon}_1)^2} \qquad 5.3$$

where ($\dot{\varepsilon}_1$, $\dot{\varepsilon}_2$ and $\dot{\varepsilon}_3$) are the principal strain rates.

The creep constitutive relationship can then be expressed as

$$\dot{\varepsilon}_o = f'(\tau_o) \qquad 5.4$$

and it will be shown that a general expression for both ice and frozen soils of this functional relationship takes the form

$$\dot{\varepsilon}_o = A\tau_o^m + B\tau_o^n \qquad 5.5$$

where A, B, m and n parameters that must be derived experimentally. It can be noted that by specializing with ($m = 1$, $B = 0$) the linear, Newtonian, flow law is recovered and that for ($A=0$) the form of the flow law for ice given by Glen (1955) is obtained.

In order to predict creep displacements on an inclined surface one must then measure the parameters of Eq 5.5 and insert the constitutive relationship into suitable slope deformation model.

A simple assumption that can be made about the state of creep deformation of an infinite slope of frozen ice or soil is that deformation occurs as simple shear in a direction parallel to the slope surface. It is assumed that the slope is made up of a dense fluid and that the only shear stress components are those which produce the simple shear flow. For an infinite slope of incompressible fluid of unit weight γ inclined at an angle θ to the horizontal, the shear stress at any depth is

$$\tau = \gamma z \sin \theta \qquad 5.6$$

and the normal or hydrostatic stress is

$$\sigma = \gamma z \cos \theta \qquad 5.7$$

where z is measured normal to the surface.

As the principal stresses are ($\sigma + \tau$, σ, $\sigma - \tau$) the octahedral shear stress becomes

$$\tau_o = \sqrt{\frac{2}{3}}\, \gamma z \sin \theta \qquad 5.8$$

As the velocity at any depth V_x has been assumed to be parallel to the slope and is independent of the downslope co-ordinate, x, the engineering shear strain rate $\dot{\gamma}$ can be written as

$$\dot{\gamma} = \frac{\partial V_x}{\partial z} \qquad 5.9$$

where x is taken parallel to the slope. As the principal strain rates are $(\frac{\dot{\gamma}}{2}, 0, -\frac{\dot{\gamma}}{2})$ the equivalent octahedral shearing strain rate becomes

$$\dot{\varepsilon}_o = \sqrt{\frac{1}{6}} \quad \frac{\partial V_x}{\partial z} \qquad 5.10$$

The above development for ε_o and τ_o can be found in Meir (1960).

It is now assumed that the viscous fluid governed by Eq 5.5 overlies a parallel, rigid surface at depth, H, along which no slip occurs. Substituting Eq 5.8 and 5.10 into Eq 5.5 and integrating results in

$$V_x(z) = \frac{\sqrt{6}\,A(\sqrt{\frac{2}{3}}\,\gamma \sin \theta)^m (H^{m+1} - z^{m+1})}{m+1} + \frac{\sqrt{6}\,B(\sqrt{\frac{2}{3}}\,\gamma \sin \theta)^n (H^{n+1} - z^{n+1})}{n+1}$$

5.11

for the depths $(0 \leq z \leq H)$ and the velocity at the surface can then be determined for z=0 with all other parameters specified.

5.5.2. Constitutive Relationships

In order to estimate the creep deformation rates expected in permafrost slopes using Eq 5.11 it is necessary to determine experimentally the parameters in Eq 5.5 for the stress range, temperature and soil types of interest. For natural slopes one, therefore, requires information at stress levels from as low as 0.03 kg/cm^2 to as high as at least 6.0 kg/cm^2 and at temperatures from the melting point to say -5.0°C. It is evident that one is more interested in soils with high ice contents than in those soils with water contents below or near the plastic limit. There are few studies that satisfy these requirements.

Since ice forms a significant part of many permafrost soils a study of the creep behaviour of ice serves as a reasonable guide to the creep behaviour of frozen soils. Recent studies by Mellor and Testa (1969) are noteworthy because the stress levels and temperature ranges used are of engineering interest and because the study is, in part, a critique of the test procedures used in the past to define secondary creep rates in ice. As a result of creep tests conducted at stress levels from 0.1 to 0.44 kg/cm^2 the authors point out that stress laboratory studies in which secondary creep was assumed to have developed in a few days are doubtful. On the other hand, shorter duration tests at higher stress levels yield creep rates generally coincident with longer duration tests at the same stress level. For example, the flow law deduced by Glenn (1955) for tests of 2 to 6 days duration and embodied in the data presented by Meier (1960) agree well with longer duration tests, see Fig 5.1.

Meier (1960) has summarized the early testing of Glenn (1955) and the results of borehole and tunnel deformation analysis in temperate glaciers in Europe and North America. He finds that the best fit relationship between τ_o and $\dot{\varepsilon}_o$ takes the form

$$\dot{\varepsilon}_o = 0.018\,\tau_o^{1.0} + 0.13\,\tau_o^{4.5} \qquad 5.12$$

where $\dot{\varepsilon}_o$ is in %/year and τ_o is in bars. This plot has been extended to include more recent studies as shown in Fig 5.1 and for which a reasonable relationship is

$$\dot{\varepsilon}_o = 0.04\,\tau_o^{1.1} + 0.08\,\tau_o^{4.5} \qquad 5.13$$

The role of ice temperature in influencing the flow law for ice appears to be negligible for test temperatures between -1 to -4°C and for the borehole and ice tunnel deformation data for temperate glaciers at their pressure melting points. Testing by Steinmann (1958) at -1.9°C and -4.8°C suggests some dependence on test temperature. However, this variation is generally masked in Fig 5.1 by other variables such as ice type and test configuration. Stress level appears to be the dominant factor in determining strain rate.

Recent work by Colbeck and Evans (1973) reports that the flow law for temperate glacier ice takes the form

$$\dot{\varepsilon}_o = 0.14\,\tau_o + 0.02\,\tau_o^{3} + 0.0018\,\tau_o^{5} \qquad 5.14$$

which yields strain rates approximately an order of magnitude faster than either Eq 5.12 or 5.13 at the same stress level. Colbeck and Evans suggest that these faster rates result from testing at the pressure melting point. However, as the data summarized by Meier (Eq 5.12) is partly from borehole and tunnel deformation in temperate glaciers and is slower than Eq 5.14 which, in turn, is based on creep tests of less than 200 hours duration then the results may be questioned. However, it should be noted that if the flow law derived by Colbeck and Evans were used it would give faster deformation when substituted in Eq 5.11 than would the other flow laws noted above. If the flow law of Eq 5.13 is substituted in Eq 5.11 and solved for a series of infinite slopes then the solution is as given in Fig 5.2. The apparent linearity of the solution is due to the fact that the second term of Eq 5.5 does not begin to influence the velocity unless slopes are steep or thicker than 100 ft. This dependence on the lower stress range part of the equation points out the need for creep testing in soils at low stress levels. It should be noted also that the flow law for ice derived in Fig 5.1 has been determined using test data from unconfirmed compression tests only and has not been generalized for more complex loading states except for the borehole and tunnel deformation data from Meier (1960). Triaxial tests on ice reported by Chamberlain(1969) and Sayles (1973) indicate that the shear strength of ice is dependent upon confining pressure. These tests suggest that the implicit assumption of the cohesive nature of the load-deformation response of ice made by many is, perhaps, an unwarranted simplification. However, as the possible effect of confining pressures would be to depress the strain rate at a given stress level the flow law of Fig 5.1 serves as an upper bound on load-deformation behaviour.

While it might be assumed that a study of creep rates in ice would provide an upper bound to the creep rate possible in frozen soils there is some indication that the presence of some soil in an ice matrix can increase the creep rate of ice alone. Swinzow (1962) observed closure rates in an ice tunnel and noted that ice with a low concentration of soil crept faster than ice alone, while very dirty ice crept faster than adjacent clear ice. Recent studies by Hooke et al (1972) have found that when ice samples are salted with a dispersion of fine sand the creep rate was increased to about 150% that of ice. The authors found that a soil volume fraction greater than about 0.1 always depressed the creep rate and that by the time a volume fraction of around 0.35 was reached the creep rate was reduced by an order of magnitude.

There is, however, a lack of useful creep-rate testing in frozen soils. Much of the available work which has been summarized by Anderson and Morgenstern (1973) can be criticized in terms of the requirements suggested by Mellor and Testa (1969) as being of too short a test duration although at higher stress levels this requirement might be relaxed. The results of some work reported by Sanger and Kaplar (1963), Vialov (1965), Sayles (1968) and Thompson and Sayles (1972) is shown in Fig 5.3 and compared to the best fit line for the creep of pore ice in Eq 5.13.

Perhaps the best study of creep-rate in frozen soils and one that also provides additional evidence that ice-rich soil can creep faster than ice is the recent description of the behaviour and analysis of the in-situ creep of a tunnel reported by Thompson and Sayles (1972). This tunnel, excavated beneath some 20 m of ice-rich Fairbanks silt, was found to creep over a one-year period. It was found that the best model that could predict observed in-situ deformations was a secondary creep model of the form of Eq 5.5 with one term only. Uniaxial creep tests were also made on the natural silt soil at the stress range and temperatures relevant and a secondary creep mode of deformation resulted. It was found that the ice-rich silt deformed some 3.3 times faster in the field than in the laboratory and, furthermore, this rate appears to be faster than is characteristic of pure ice alone, see Fig 5.3. It can be noted that if the flow law derived from this data was put into the one-dimensional creep model discussed earlier significantly faster creep velocity would result than those shown in Fig 5.2.

Before proceeding to a discussion of the implications of the mass movement model being studied in this section it must be noted that the form of the constitutive relationship or the flow law derived above is in itself a model. As already noted the so-called secondary creep mode of creep deformation is a generalization of the creep behaviour of frozen soil. In fact, there are few studies that confirm that true steady-state creep does, in fact, exist for any significant time period.

For example, Sayles (1968) presents a series of deformation-time curves for Ottawa sand at various temperatures. At stress levels which did not result in creep rupture after periods up to 100 days it is possible to fit an approximate straight line to a secondary creep region resulting in the points given in Fig 5.3. However, a detailed inspection of the data suggests that the deformation rate is slowly decreasing with time. More recent testing, Sayles (1973), at various confining pressures confirms this conclusion.

On the other hand, close inspection of a typical creep curve for undisturbed Fairbanks silt (Thompson and Sayles: 1972, Fig 7) suggests that the sample has undergone primary, secondary and has entered the tertiary creep phase. While it may be a reasonable approximation to say that the secondary creep rate was so much over the 8-day creep test it does not follow that this test applies to the 1-year in-situ deformation of the tunnel. The fact that the field observation fits a secondary creep rate some 3.3 times faster than the laboratory tests suggests that the in-situ movements may have been partly due to creep rupture deformations. Finally, it can be noted that Vialov (1965) finds that for frozen silts only a primary mode exists at lower stress levels and, therefore, for a stress condition less than some critical or threshold level the creep rate will always tend to zero.

5.2.3 Application of Creep Model

The solution of the infinite slope model coupled with the best fit constitutive relationship for ice, Fig 5.2, suggests that creep velocities of from 0.2 to 2.0 cm/yr are possible in slopes from 2 to 10 ft thick on inclinations of from 5^{o} to 30^{o}. When compared with the winter deformations obtained in some solifluction slopes (see Chapter 1) and which might be explained by creep deformations the above range of velocities appears to be reasonable.

Any natural slope can be expected to have a complex structure of ice lenses and frozen soil the solution embodied in Fig 5.2 can, of course, be objected to as it assumes that any given slope consists of uniform ice overlying a rigid base.

There are no case records available for natural or artificial slopes with which to compare the predictions of Fig 5.2. However, it is possible to apply the flow law of Eq 5.13 to the measured deformations of two rock glaciers reported by Wahrhaftig and Cox (1959). In order to bound the likely cross-sections of flow for these glaciers it is necessary to consider both an infinitely wide slope and flow in a semi-circular channel. Following Meier (1960) it is possible to extend the infinite slope model already considered by modifying the solution in terms of a shape factor R/d so that

$$\tau_o = \sqrt{\frac{2}{3}} \quad \frac{R}{d} \gamma z \sin \theta \qquad 5.15$$

where R is the hydraulic radius and d is the depth of flow. For a semi-circular channel R/d reduces to 1/2. The first rock glacier reported by Wahrhaftig and Cox is approximately 35 m high, and flows, on a slope of 14°, with an average measured velocity of 0.7 m/year. Assuming a unit weight of 1.8 gm/cm^3 Eq 5.11 predicts a velocity of 5 m/year and when modified by Eq 5.15, about 1.0 m/year. The second glacier is some 25 m high, standing on a 20° slope and flows with a measured velocity of 1.6 m/year. The calculated velocities are 0.8 m/year for the semi-circular channel and 3.7 m/year for an infinite slope. Considering the many assumptions embodied in the model this agreement is encouraging.

In this study we have assumed that the generalized creep behaviour discussed earlier serves as a useful engineering approximation for the description of creep and that, in particular, the secondary creep mode is a good model for creep in permafrost slopes significantly below creep rupture stress levels. Although there is certain evidence that may contradict this view it is evident that approximations are required in order to gain any insight whatsoever into the process of creep deformation on natural slopes. In conclusion, it appears that while the model is not justified for structured soils it may be reasonable for ice-rich soils.

5.3 Mass-Movements due to Shear Displacements

5.3.1 Introduction

Landslide movements that display shear displacements along well-defined slip surfaces have been found in permafrost soils in certain parts of the study area. These landslides, classified as block and MR slides, have been discussed in

Chapter II and described in detail in Appendix A. A common feature of this type of mass movement is that shear failure has occurred through frozen ground. This form of mass movement is rather novel and it is of considerable geotechnical interest to analyze these landslides quantitatively with a view towards predicting their occurrence. The following features are characteristic of block and MR slides observed in the study area.

(1) Slide movements are associated with banks significantly higher than about 150 ft and in which the sand and silt member of the GLB sequence make up the greater portion of the bank profile. The relatively greater percentage of sands and silts can be observed in most reaches and is also witnessed by the deep-seated gullying that is found cohabiting with these slides. All block and MR slides have been found in conjunction with a blue-grey silty-clay at river level.

(2) Various observations made, suggest that failure occurs through frozen sands and silts bottoming out in either unfrozen or partly frozen clay. Since this clay may have a similiar strength response whether it is thawed, or partly frozen near 0°C, a useful mass movement model for frozen soil overlying unfrozen silty clay.

This section will then consider slide movements in conjunction with the concept of long-term strength of frozen ground.

5.3.2 Shear Strength of the Unfrozen Component

The shear strength of the unfrozen soil beneath the capping of permafrost in block and MR slides can be predicted using conventional geotechnical practice. For clayey, fine-grained soils slightly below 0°C a considerable proportion of the water phase of the soil remains unfrozen. As the temperature gradients near the bottom of the permafrost are in the order of 1°C/80 ft a considerable portion of the soil nominally below 0°C may be considered unfrozen. It is speculated, therefore, that the boundary between what is a frozen soil, with regard to shear strength considerations, and what can be considered an unfrozen soil is not necessarily the 0°C isotherm and while the effective stress parameters for the frozen and unfrozen soils might not be identical it is expected that the pore water phase is continuous.

The shear strength of the unfrozen component may be formulated in terms of effective stresses and the strength parameters (c' ϕ'). Departures from conventional practice for the analysis of these landslides involve the role of permafrost and its effect on pore water pressures.

The first departure from the conventional conditions expected in more temperate areas can be seen from a consideration of steady state seepage conditions. The terrain behind all block and MR slide areas is pitted with thermokarst lakes. These lakes represent holes in the permafrost and the pore water pressure regime in the soil beneath these lakes will be transmitted beneath the permafrost and out to the valley walls. If a lake is close to the valley wall it is expected that the pore water pressures will be higher beneath the permafrost than they would be in the same soil for the same conditions if permafrost were absent.

Pore water pressures may also be influenced by thaw-consolidation effects as the permafrost thaws from below in response to the thermal disturbance associated with previous instability or in response to climatic changes. Although the rate of thaw will be low, drainage paths are long and permeabilities are low. Therefore, the possibility exists that excess pore pressures may be generated. The situation is, however, far from simple and while no detailed studies have been made it is useful to review, qualitatively, the factors influencing this type of thaw.

The temperature gradients near the base of the permafrost are low with the result that, say, the first 40 ft of soil above the base of the permafrost defined by the 0°C isotherm changes in temperature from 0°C to -0.5°C. This soil may have a high percentage of unfrozen water and when thawed the decrease in volume due to ice-water transformation, of what ice does exist may cause a pore water deficiency. Put another way, the residual stress, Nixon (1973),may be high and the soil may swell upon thaw. But GLB silty clays while having high unfrozen water contents in the soil contained between ice lenses do have substantial ice lenses even at depths up to 150 ft. (See Figs B.2 to B.4) Thus, if a large enough volume of soil is considered the total water content may well be close to the original water content in equilibrium with the effective stresses at a given depth before freezing. The result of a cycle of freeze and thaw may then be, overall, to cause a net volume decrease with excess water produced upon thaw. Although the rates of thaw may be low and the residual stresses high, drainage paths will be long and the possibility exists that the shear strengths may be reduced upon thaw due to increased or excess pore water pressures.

High pore pressures may also be set up beneath the capping of permafrost during the winter months when a skin of seasonally-frozen soil is formed along the slope profile. As the ground water seepage will be cut off it is possible that pore water pressures may increase.

5.3.3. Strength of the Frozen Component

Anderson and Morgenstern (1973) have noted that the nature of the strength of frozen soil can be attributed to the presence of unfrozen water and the various responses of ice to loading which can range from pressure melting to brittle fracture. A detailed discussion of the nature of the interaction of the soil, water and ice phases of a frozen soil and their influence on shear strength is beyond the scope of this thesis. Rather, this section will review certain aspects of experimental testing which yield quantitative information useful in slope stability calculations

The classic method by which the time dependence of shear strength may be empirically correlated was presented by Vialov (1965) and involves plotting the reciprocal of the creep stress measured in an unconfined test versus the log of time to failure. This relationship has been shown to be linear for test durations in the order of from 0.1 to 100 hours and if extrapolated gives a measure of the long-term strength taken at, say, 50 or 100 years.

There is, however, a lack of useful experimental data. Vialov's original work was conducted on heavily overconsolidated Jurassic soils the water contents of which, and the test temperatures, are too low to be of use in the study area. However, one test series is noted on Table 5.1.

The results of tests on frozen sand by Sayles (1968) are summarized in Table 5.1 and are interpreted using Vialov's construction based on tests of up to 200 hours duration. Vialov's method may also be applied to strength data presented for frozen clayey soils by Akili (1971) and Neuber and Wolters (1970), Figs 5.4 and 5.5. It is of interest to note that there is a linear relationship between long-term strength and test temperature. The results of these tests are also summarized in Table 5.1.

Unconfined, constant rate of strain, tests were conducted on undisturbed samples obtained from 3-inch diameter Shelby tubes taken at the Mountain River Site, M1, Fig A.19. These tests, Fig 5.6, were conducted at different times to failure and an estimate of the long-term, 100-year, strength was made graphically, see Fig 5.7. Tests were made using a conventional load press in a cold room and jacketed samples were failed in a parafin bath maintained at -1.0°C. Some difficulties were experienced in keeping the samples at -1.0°C for the longer duration tests and the resultant uncertainty in predicted stress at failure is indicated on Fig 5.7. A summary of the properties for each test is given in Table 5.2. The grain size curves, Fig B.13, were calculated based on a sample taken from the whole sample after it had been thawed and mixed.

There is evidence to suggest that Vialov's concept of long-term strength is not entirely adequate and that the long-term strength of frozen soil is frictional. The frictional nature of unfrozen soils is well-known and recent work, reported by Chamberlain (1969) and Sayles (1973), finds that polycrystalline ice exhibits a frictional response in that mobilized shear strengths are increased by confining pressures. Recent work by Sayles (1973) suggests that the long-term strength of saturated frozen sand is frictional with angles of 31° and 29° being deduced from constant load and constant strain rate tests respectively. Sayles concludes that

> "the long-term ultimate creep strength of saturated frozen (Ottawa) sand with porosity of 37% or less is a function of the angle of internal friction which could be determined through triaxial tests on unfrozen sand, freely drained."

The extensive series of tests undertaken by Neuber and Wolters (1970) may also be recast, Fig 5.8, to indicate that for a sandy and for a silty soil there is a marked frictional response for short-term tests of from 0.5 to 5.0 hours duration. The similarity between the drained angle of unfrozen soil and the apparent angle is striking. If the long-term strength is frictional then there should be little change in the deviator stress at failure for longer duration tests. This was found to be the case for the silty soil for tests at the same confining pressure. A plot of the reciprocal of the deviator stress at failure against log time showed only the slightest decrease in strength from tests of about 2 to 5 hours duration to tests of about 20 to 30 hours duration. When extrapolated to 100 years these tests predicted an angle $\phi_f = 25^o$, Fig 5.9. An estimate of the lower range of the frictional angle can also be made by extrapolating the shorter term tests and an angle $\phi_f = 16.5^o$ is predicted, Fig 5.9. Thus, Neuber and Wolters data can be interpreted to show that the long-term strength of a silt is frictional and that a reasonable estimate of this frictional response can be deduced from a drained test on unfrozen soil.

But, if the long-term strength of frozen soil is frictional then the strength predictions, of Table 5.1, should tend to zero becuase these tests were all conducted at zero confining pressure. It would appear that the prediction of a finite unconfined shear strength results because tests of sufficient duration have not been considered. There is, however, some experimental data that supports the view that the long-term unconfined strength is indeed zero. Tests by Vialov (1955) apparently conducted using a spherical indenter, show a marked drop-off in strength for longer duration tests, Fig 5.10. If we reconsider the test data presented by Sayles (1968) for Ottawa sand at 31^oF, Fig 5.10, it can be seen that the best fit of the data suggests greater lowering of the long-term strength than reported in Table 5.1. Furthermore, this interpretation agrees with the latter conclusions of Sayles (1973).

One is lead to conclude, therefore, that Vialov's concept of long-term strength for structured soils is inadequate. Vialov's approach will overestimate the long-term available strength of frozen soils at low confining pressures and, conversely, underestimate the strength at higher pressures.

5.3.4 Slope Stability of the Mountain River MR Slides

The slope stability of the MR slides at the Mountain River site can now be considered in relation to the shear strength models discussed in the preceeding section. As no block or MR slides have been observed in pre-failure attitudes it is necessary to approximate the pre-failure geometry. Furthermore, as no detailed survey has been made of post-failure geometry, air photographs and maps must be used to assemble a reasonable cross-section for analysis. Fig 5.11 outlines the cross-section considered at the Mountain River site and which is typical of MR slides in general. The bank height, measured using a helicopter altimeter was 220 ft, and this value agrees with topographic maps. The overall length of the landslide blocks can be measured on aerial photographs to be from 200 to 500 ft with an average extent of 300 ft. The failed blocks have overall angles of from 12° to 20° from the toe to the headscarp. Based on these measurements a reasonable pre-failure profile can be assembled as shown on Fig 5.11. It is then assumed that any potential failure surface begins at a point 300 ft back from the headscarp and ends at the toe of the slope. The stability analyses conducted assumed that permafrost 155 ft in depth forms a cap over unfrozen soil. It is also assumed that the bulk density of all soils is 2.00 gm/cm^3. A detailed description of the Mountain River site is given in Appendix A, a representative cross-section in Fig A.20 and the borehole log in Fig B.1.

Slope stability calculations were made on a non-circular slip surface using the method established by Morgenstern and Price (1965). The slip surface was varied about a pivot point at the top of the landslide by a series of surfaces at angles of from 25° to 70° as shown on Fig 5.11. This pivot point was established from measurements made on aerial photographs. The shear strength parameters of the unfrozen soil were fixed at ($c' = 140$ psf, $\phi' = 26^{\circ}$) based on remoulded samples, see Sec 2.4, and r_u values (see Eq 1.4) of 0.25, 0.5, and 0.75 used in the thawed soil. Computer runs to calculate the factor of safety F_s were then made at each r_u value by varying both the undrained strength that could be mobilized in the frozen soil and the failure surface as given by the angle θ. At each r_u value the maximum undrained strength c_u required in order to achieve $F_s = 1.0$ was noted. This c_u was then plotted against r_u, Fig 5.12, and the slope angle θ_c on which the highest c_u was mobilized is also given. Thus Fig 5.12 gives a prediction of the long-term shear strength that was mobilized in the frozen part of the slide at failure.

An additional stability calculation was made using a circular arc (see Bishop, 1955). Using the same parameters for the thawed soil and ($c_u = 3{,}200$ psf , $r_u = 0.50$) for the frozen soil a $F_s = 0.98$ was calculated.

In order to proceed with the analysis it is necessary to have some indication of the r_u value for the underlying unfrozen soil. Unfortunately the piezometer installed in boring M 1, Fig A.19, was indicating negative pressures immediately upon installation and it has not been possible to return to the field. However, the pore pressure regime may be inferred from the following. As the unfrozen zone beneath the permafrost was penetrated the drill stem fell some 7 ft under its own weight and with the drill stem brake partially engaged . Large quantities of wet sandy silt were pumped up from below 155 ft and the hole could not be kept open below the permafrost table as it immediately filled in with flowing soil. The water content of the thawed soil brought to the surface by the air-return was found to be 31% (void ratio 0.85), although this water content may have been artificially increased by the pumping operations. However, it can be seen in Fig B.14 that even if the void ratio was significantly decreased to allow for a possible increase due to pumping that low effective stress conditions would be predicted based on the e versus log σ' curve for the remoulded silt. Furthermore, frozen samples with similiar grain size curves (i.e.: compare Fig B.13 with M1-170.0, Fig B.12) have water (ice) contents in the range 20% to 25%, or void ratios of 0.54 to 0.68. As the effective stress for hydrostatic conditions at 155 ft is about 5.0 tons/ft^2 the void ratio corresponding to an $r_u = 0.5$ is about 0.48, Fig B.14. Therefore, it can be argued that if a layer of soil is caused to thaw at the base of the permafrost some consolidation would have to occur in order for the thawed soil to reach a void ratio in equilibrium with a hydrostatic condition. However, as seepage paths are long this condition would not be reached instantaneously and excess pore pressures would be set up. Thus, for the above reasons, it is felt that low effective stress conditions exist beneath the permafrost and that the r_u value for the unfrozen soil is high.

The predicted long-term shear strength based on samples taken from the lower portion of the permafrost is given in Fig 5.7. These tests were conducted at an average temperature of -1.0°C which compares favourably with the expected average temperature of the permafrost at the slide. A direct comparison of the test data with Fig 5.12 would suggest that rather low r_u values existed at failure. Referring to Fig 5.9 it can be seen that the unconfined tests of Fig 5.9 would underestimate the average c_u which should be increased to allow for the effect of confining pressure. If the predicted c_u from test data is arbitrarily increased to allow for a confining pressure equivalent to, on average, 75 ft of permafrost then the c_u value required in Fig 5.12 is consistent with the high pore pressures inferred in the unfrozen soil.

It may be aruged for the reason noted in the preceeding section, that any agreement whatsoever between the predicted shear strengths of Fig 5.12 and 5.7 is fortuitous. It is of interest, then, to inspect the stability of the cross-section of Fig 5.11 assuming that a frictional strength is developed in the frozen soil. This can be done with ease using the circular arc shown on Fig 5.11 which represents a reasonably average failure surface. If it is assumed that the thawed soil is governed by ($c' = 140$ psf, $\phi' = 26^{\circ}$, $r_u = 0.50$) the mobilized friction angle in the frozen soil can be varied in order to achieve $F_s = 1.0$ overall. In order to calculate the mobilized friction angle ϕ_f in the frozen sand the effective stress level in the sand must be assumed. If the grain to grain contacts in the sand-ice system carry all the load; that is the total equals the effective stress, then $r_u = 0.0$. For this condition, the required frictional response for limit equilibrium is calculated to be ($c_f = 0$, $\phi_f = 29^{\circ}$). If it is assumed that not all the total stress is carried in the frozen soil skeleton, say $r_u = 0.25$, then the required response is ($c_f = 0$, $\phi_f = 36^{\circ}$). These friction angles are quite reasonable and if a r_u value higher than 0.50 is assumed in the underlying thawed soil the value ϕ_f for limit equilibrium will be correspondingly higher.

It is noteworthy that a reasonable agreement between observed and predicted behaviour for failure in an MR slide has been achieved using both the unconfined long-term strength model and the frictional model for shear strength in frozen soil. Noting the many assumptions required in order to arrive at a bank profile and the uncertainty as to the actual failure surface as well as to the in-situ strength parameters and the pore pressures beneath the permafrost, the agreement is encouraging. It suggests that the stability of the large block and MR slides encountered in the study area may be considered using conventional geotechnical practice but points out the need for considerable research on the fundamental aspects of strength in frozen soil.

TABLE 5.1 SUMMARY OF LONG TERM SHEAR STRENGTHS (100 YRS)

Soil	Temperature	Strength (psi)	Source
Bat Baioss Clay	-1°C	79.0*	Vialov (1965)
Ottawa Sand	31°F	73	Sayles (1968)
Manchester Fine Sand	31°F	65	Sayles (1968)
Sault Ste Marie Clay	-1°C	14	Akili (1971)
Fat Clay	-1°C	35 to 41*	Neuber and Walters (1970)
Mountain River clayey-sandy silt	-1°C	21	This study

* Strength extrapolated to -1.0°C.

TABLE 5.2 SUMMARY OF SHEAR STRENGTH TEST DATA FOR FROZEN MOUNTAIN RIVER SOILS

SOIL PROPERTIES

Test	Depth	W_n%	γ_B	W_L%	W_P%
M1-1	126.0	20.0	1.96	25.4	15.5
M1-2	126.4	25.1	1.95	non-plastic	
M1-3	133.4	21.0	1.94	24.6	15.6
M1-4	125. 0	21.0	2.01	24.5	15.7
M1-5	132.6	25.3	1.92	non-plastic	

TEST DETAILS

Test	Measured Rate of Def "/min	H_o	H/D	Time to failure (hrs)	Strain at Failure %	Axial Stress at Failure (psi)	Temperature °C.
M1-1	0.045	5.00	1.80	0.23	12.0	183	-1.05
M1-2	0.045	6.00	2.10	0.36	16.6	242	-0.95
M1-3	0.0041	5.54	2.01	4.2	18.7	69	-1.05
M1-4	0.00044	5.23	1.90	17.0	8.6	76	-1.00 [1]
M1-5	0.00044	5.33	1.94	26.0	13.0	93	-1.05 [2]

[1] Temperature to -1.8°C at 7% strain, sample partly unloaded.

[2] Temperature to -1.2°C after 9.5% strain.

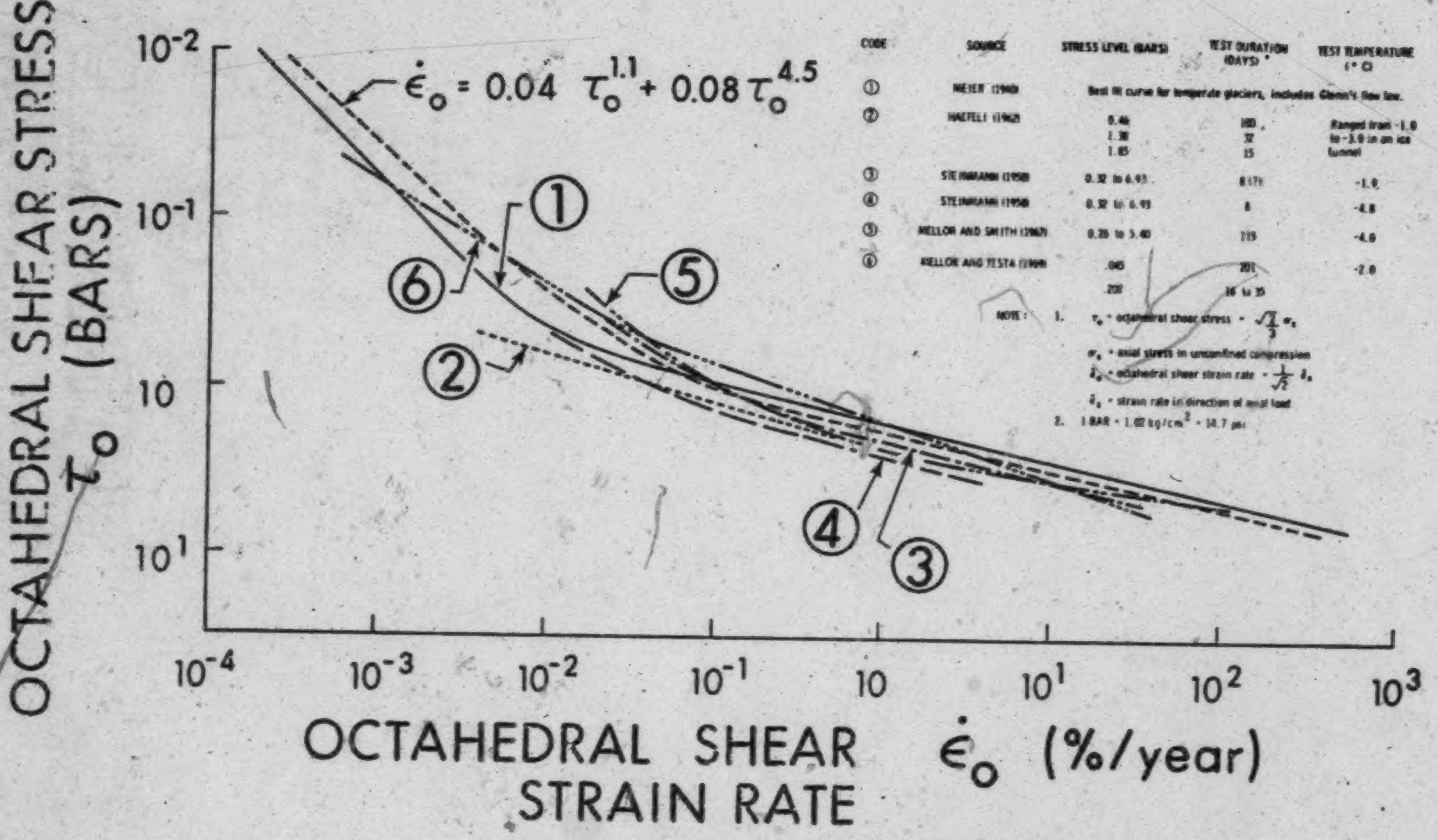

CODE	SOURCE	STRESS LEVEL (BARS)	TEST DURATION (DAYS) *	TEST TEMPERATURE (° C)
①	MEIER (1960)	Best fit curve for temperate glaciers, includes Glenn's flow law.		
②	HAEFELI (1962)	0.46 1.38 1.85	180 32 15	Ranged from -1.0 to -3.0 in an ice tunnel
③	STEINEMANN (1958)	0.32 to 6.93	8 (7)	-1.9
④	STEINEMANN (1958)	0.32 to 6.93	8	-4.8
⑤	MELLOR AND SMITH (1967)	0.28 to 5.40	115	-4.0
⑥	MELLOR AND TESTA (1969)	.045 .200	201 16 to 35	-2.0

NOTE: 1. τ_o = octahedral shear stress = $\sqrt{\frac{2}{3}}\,\sigma_1$

σ_1 = axial stress in unconfined compression

$\dot{\epsilon}_o$ = octahedral shear strain rate = $\frac{1}{\sqrt{2}}\,\dot{\epsilon}_1$

$\dot{\epsilon}_1$ = strain rate in direction of axial load

2. 1 BAR = 1.02 kg/cm^2 = 14.7 psi

Fig 5.1 The Flow Law for Ice

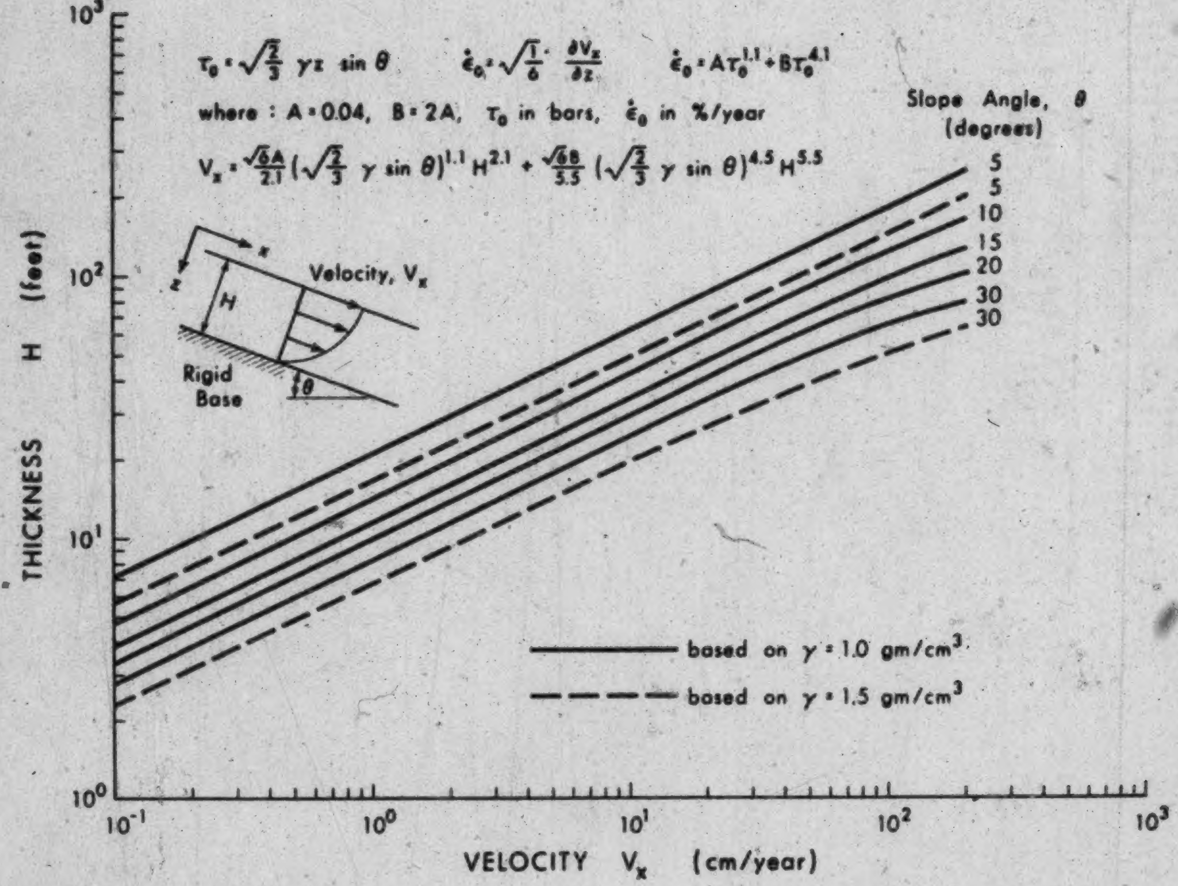

Fig 5.2 Solution to the infinite slope creep problem

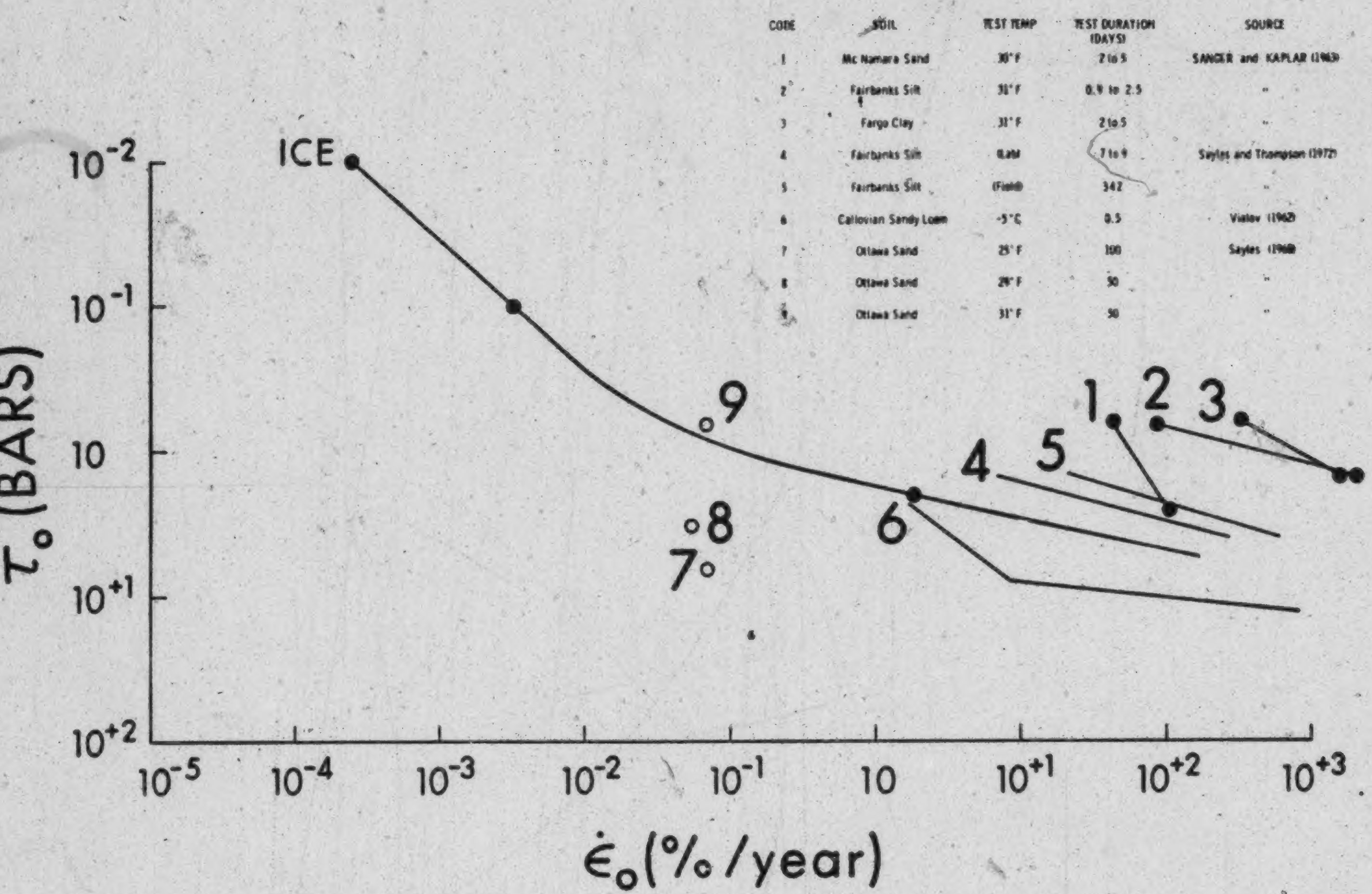

CODE	SOIL	TEST TEMP	TEST DURATION (DAYS)	SOURCE
1	Mc Namara Sand	30°F	2 to 5	SANGER and KAPLAR (1963)
2	Fairbanks Silt	31°F	0.9 to 2.5	"
3	Fargo Clay	31°F	2 to 5	"
4	Fairbanks Silt	(Lab)	7 to 9	Sayles and Thompson (1972)
5	Fairbanks Silt	(Field)	342	"
6	Callovian Sandy Loam	-5°C	0.5	Vialov (1962)
7	Ottawa Sand	25°F	100	Sayles (1968)
8	Ottawa Sand	29°F	50	"
9	Ottawa Sand	31°F	50	"

Fig 5.3 The flow law for ice compared with secondary creep rates in soil

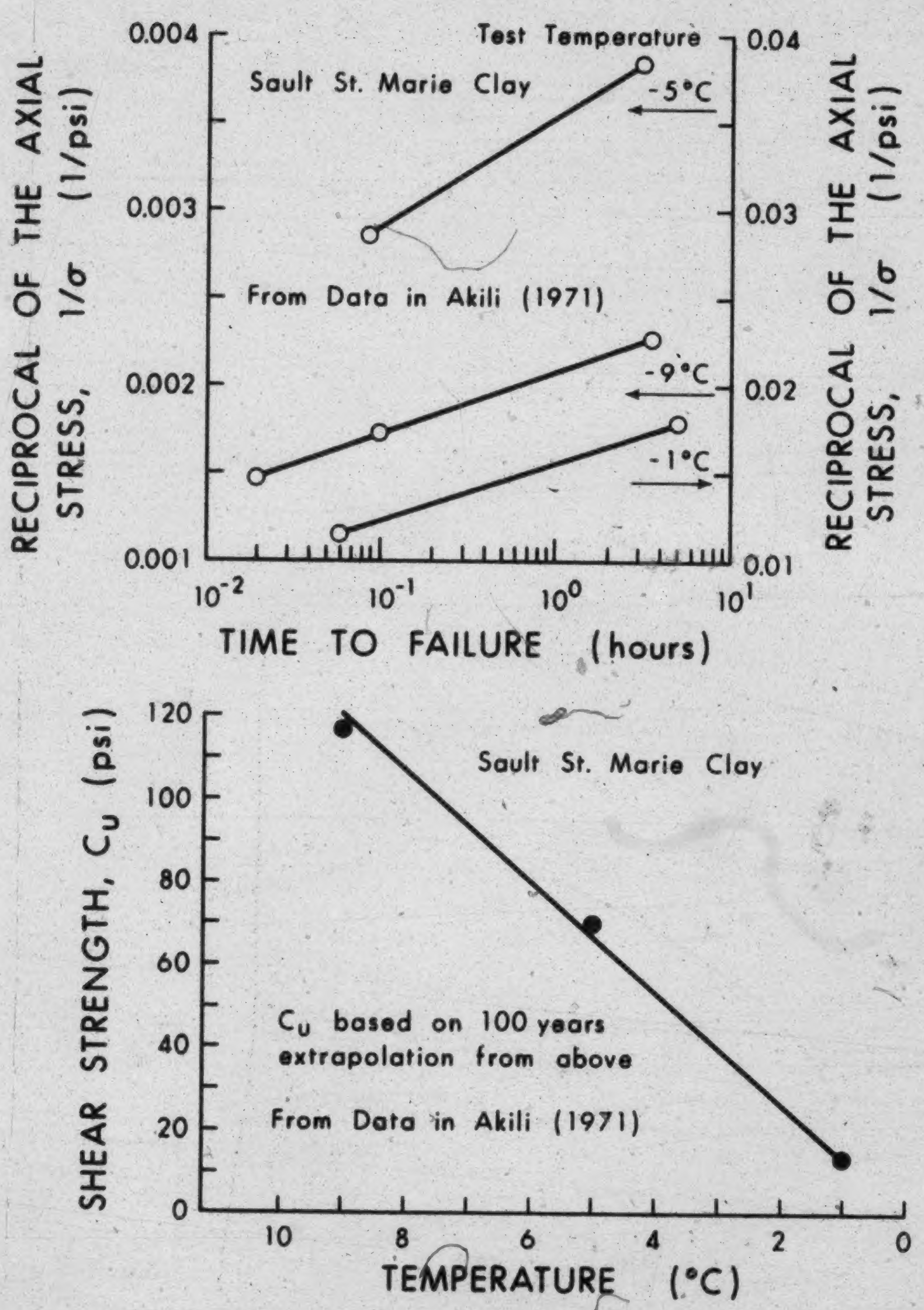

Fig 5.4 Unconfined long-term strength data for Sault Ste Marie Clay

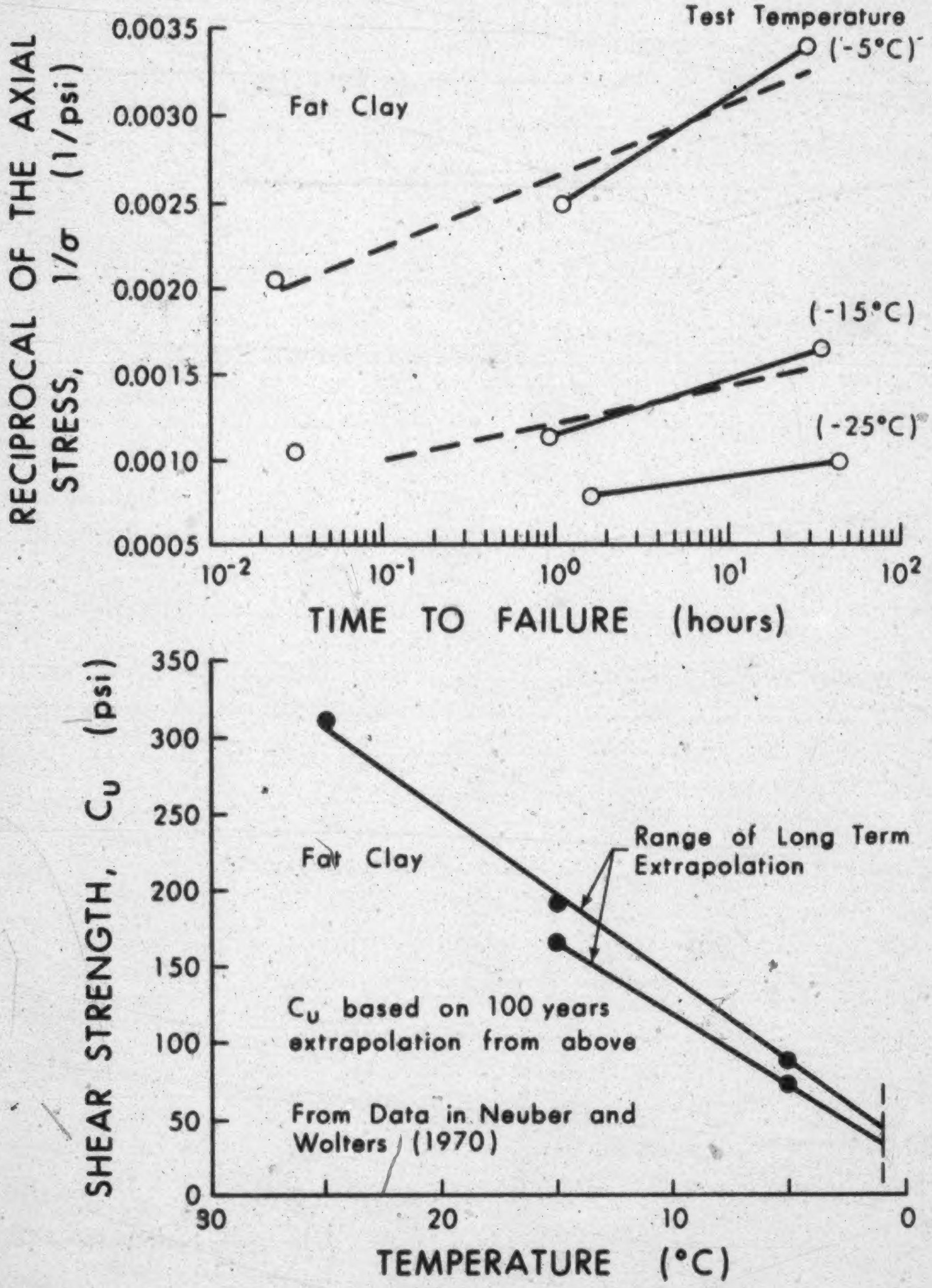

Fig 5.5 Unconfined long-term strength data for a Fat Clay

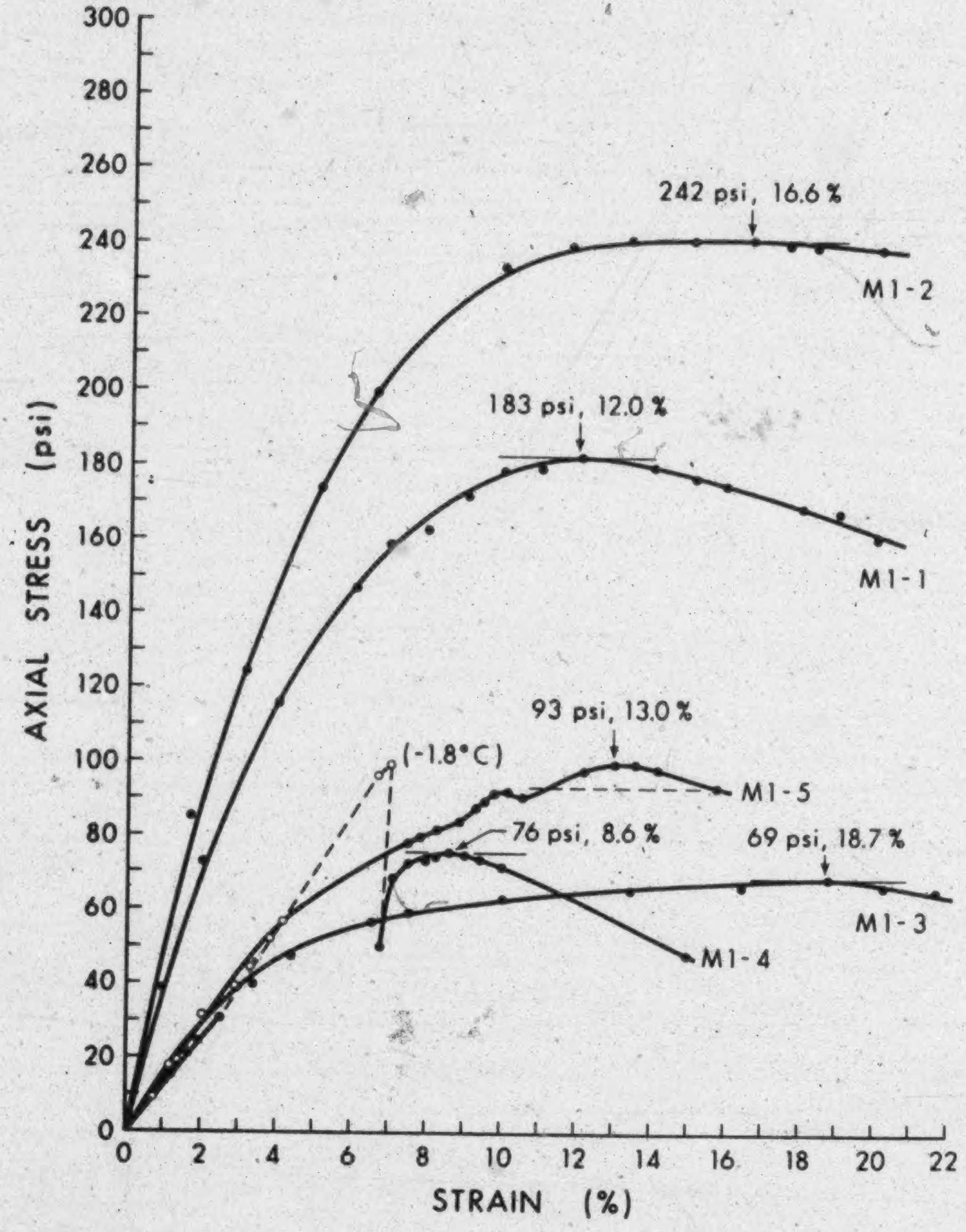

Fig 5.6 Stress-strain relationships for frozen Mountain River Silts

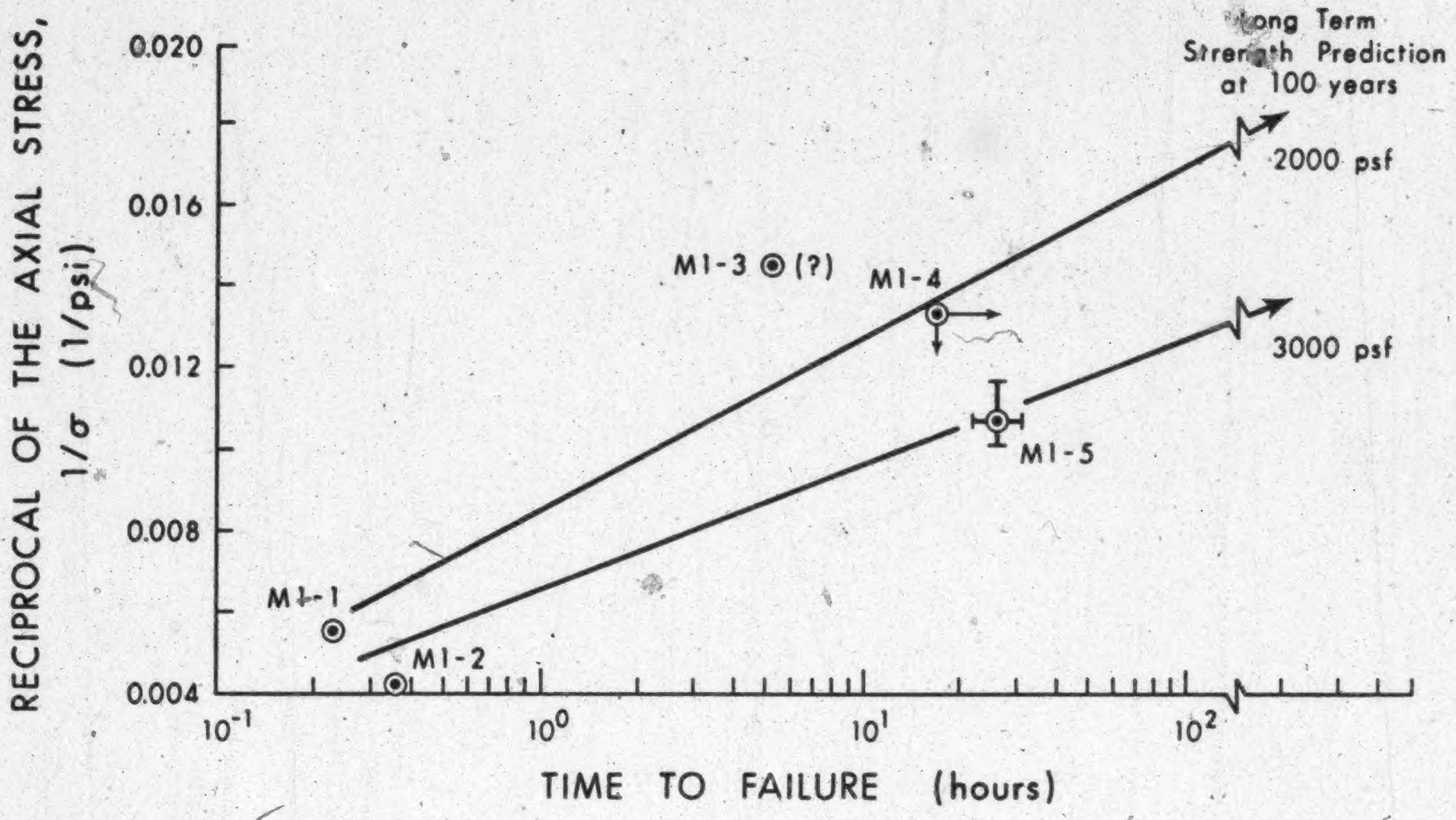

Fig 5.7 Long-term strength for Mountain River Silt

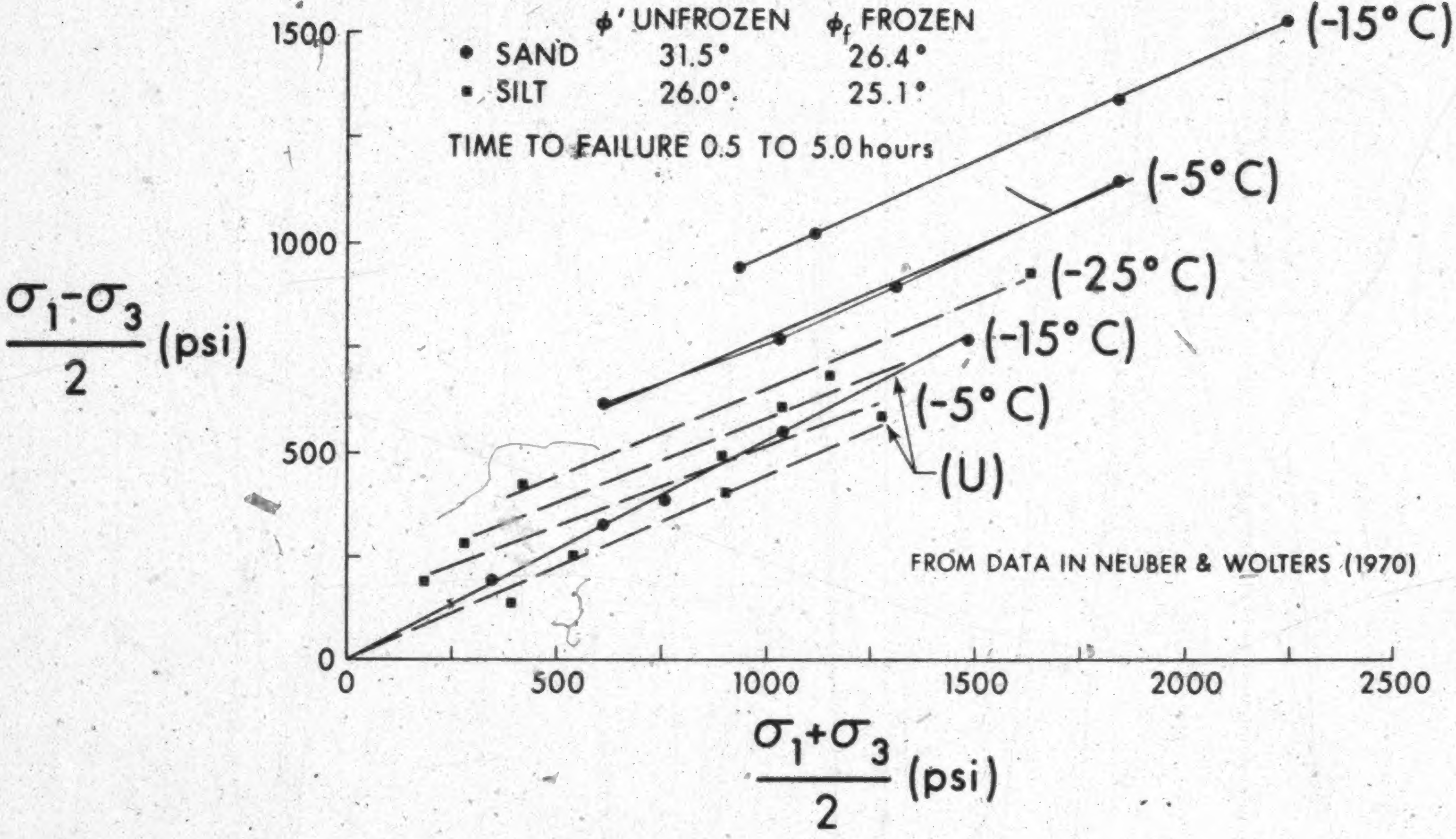

FROM DATA IN NEUBER & WOLTERS (1970)

Fig 5.8 Frictional Response of Frozen Soil

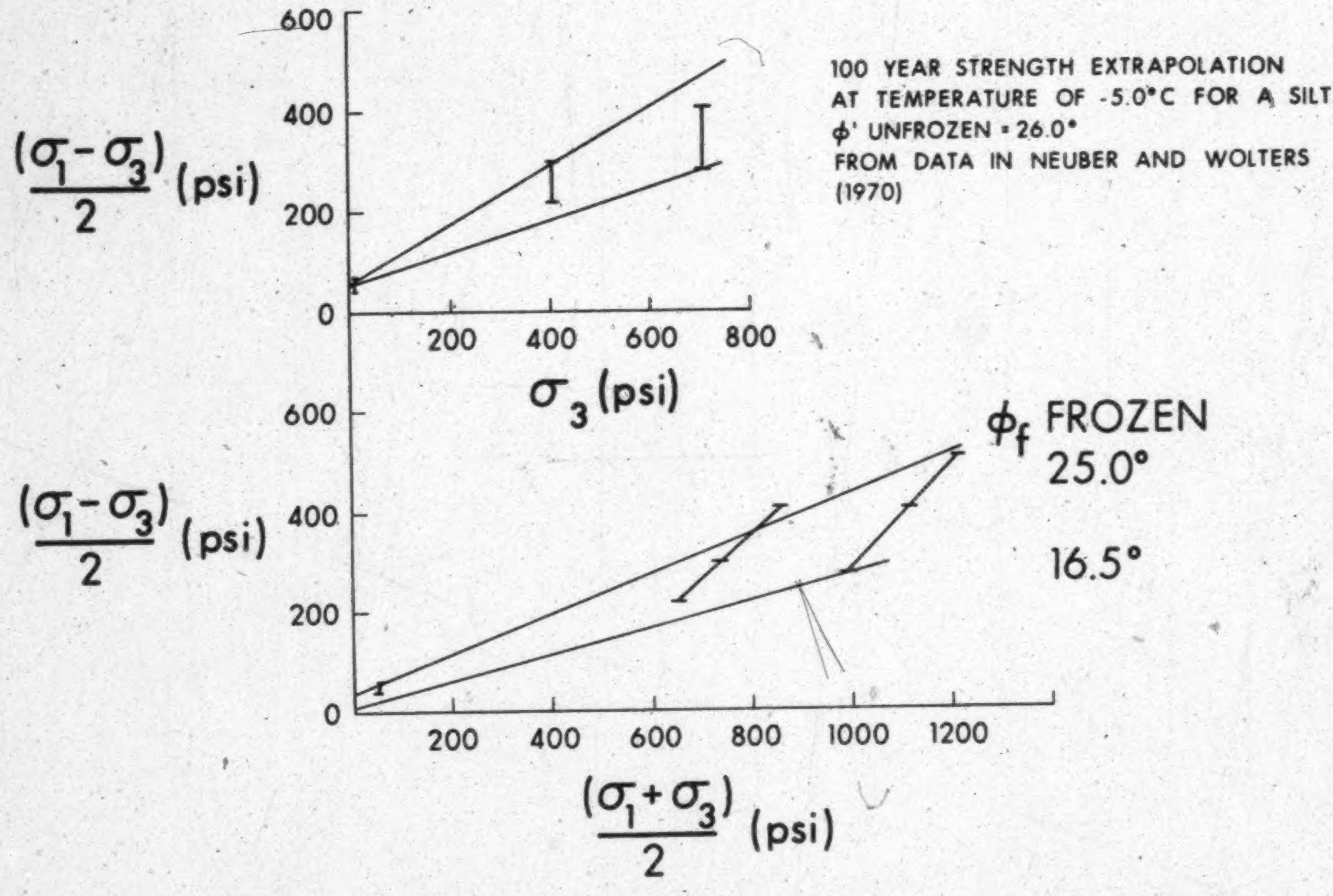

Fig 5.9 Long-term frictional response

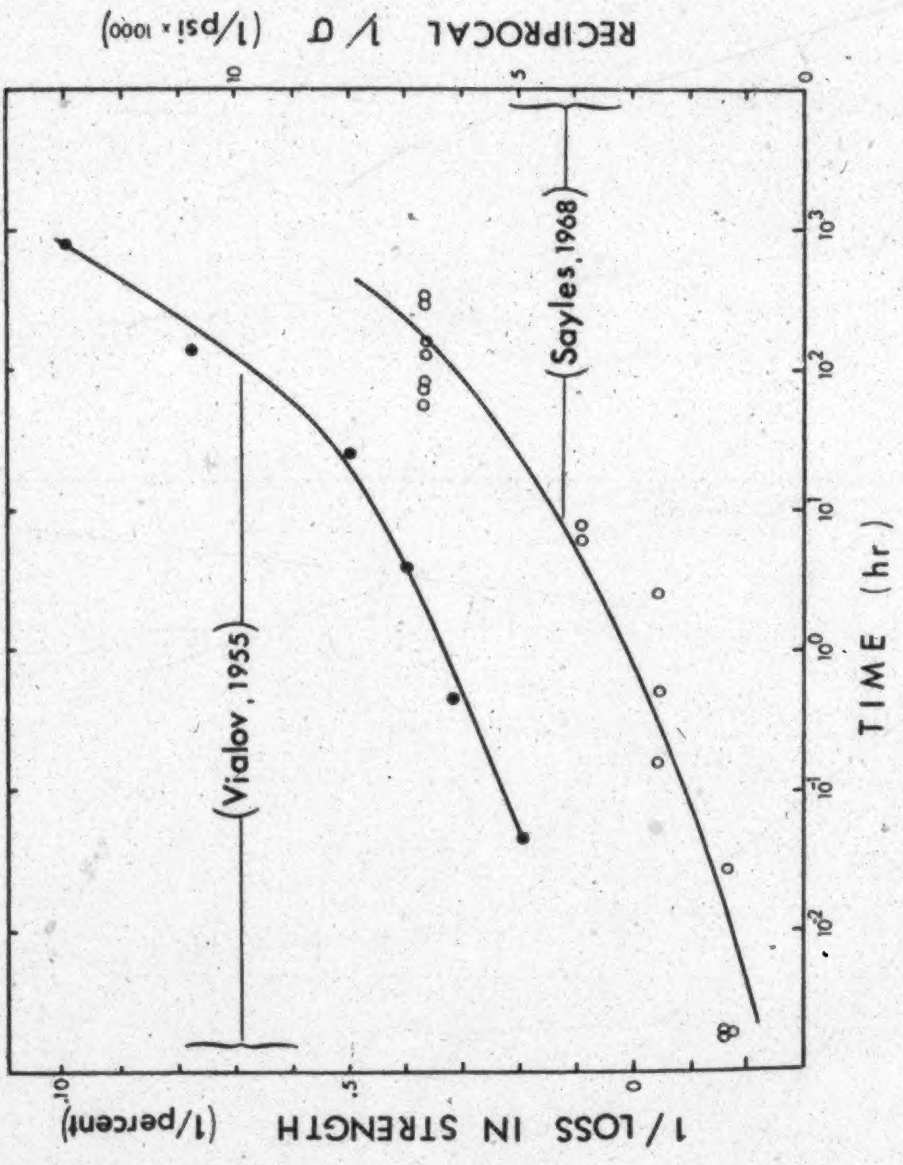

Fig 5.10 Unconfined long-term strength tests

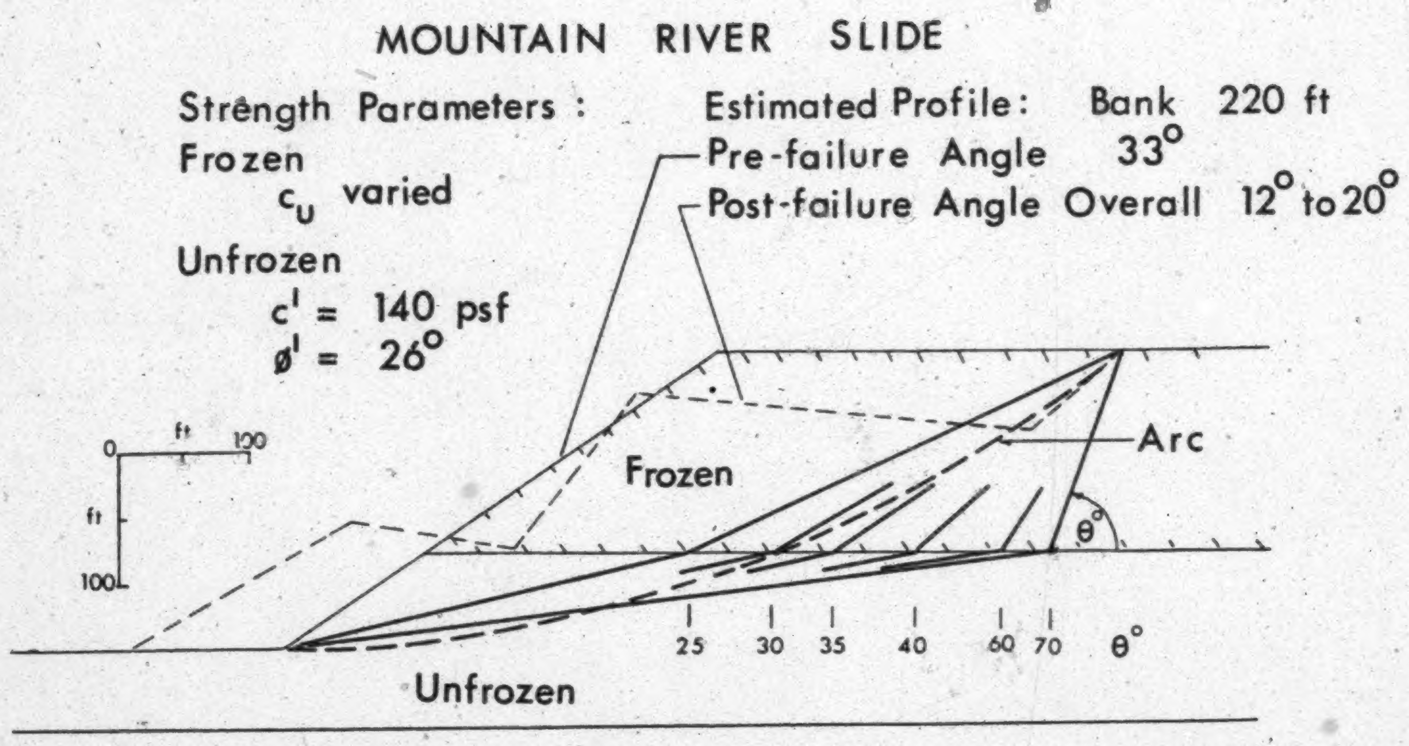
MOUNTAIN RIVER SLIDE
Strength Parameters :
Frozen
c_u varied
Unfrozen
$c' =$ 140 psf
$\phi' =$ 26°
Estimated Profile: Bank 220 ft
Pre-failure Angle 33°
Post-failure Angle Overall 12° to 20°
Arc
Frozen
Unfrozen
θ°
25
30
35
40
60
70
θ°
0
ft
100
ft
100

Fig 5.11 Mountain River slide cross-section

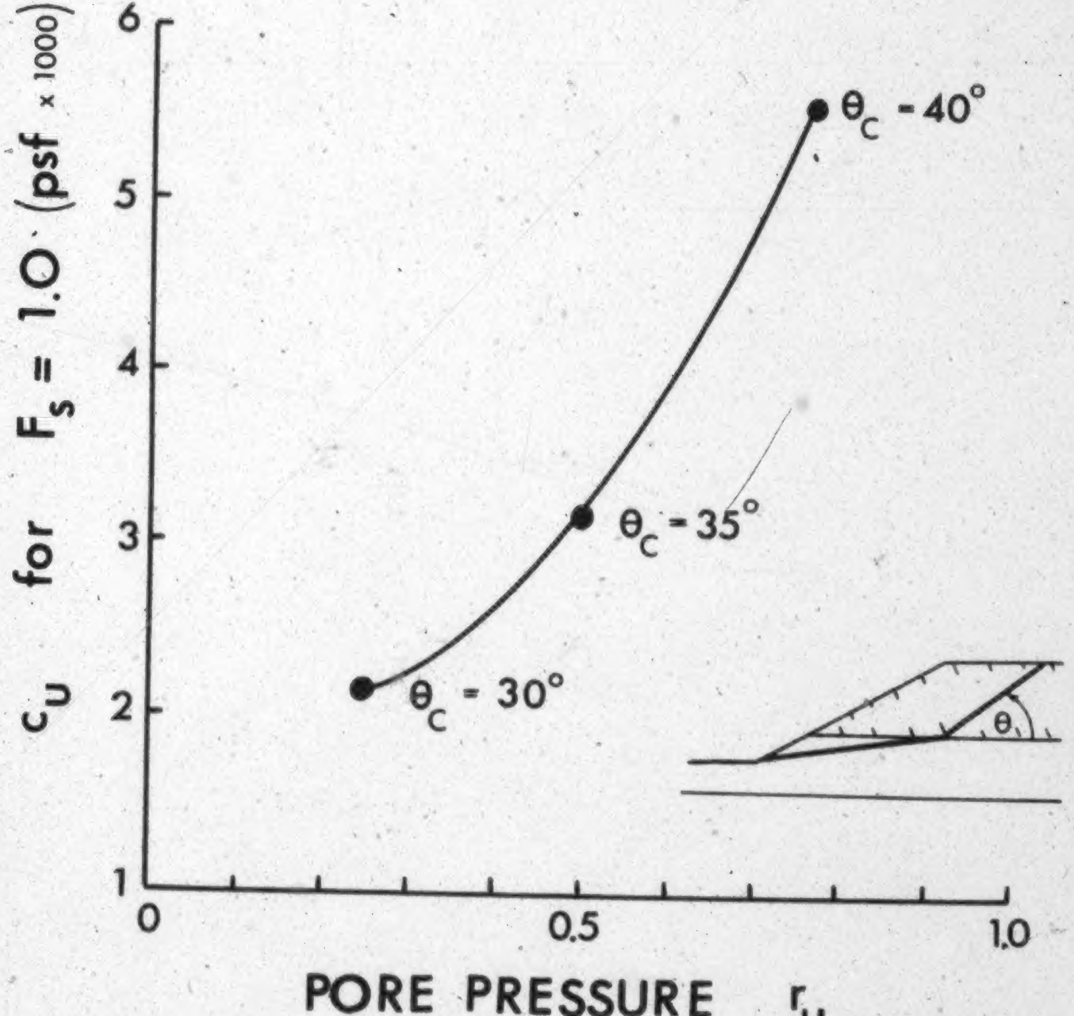

Fig 5.12 Results of slope stability calculations: Mountain River Slides

CHAPTER VI

SOME ENGINEERING CONSIDERATIONS OF LANDSLIDES IN THE MACKENZIE RIVER VALLEY

6.1 The Initiation of Landslides

6.1.1 Stress Imbalance

The onset of shear failure in soils is due to a net imbalance between the forces tending to cause downslope movement and the shear strength that can be mobilized along a potential failure surface. The initiation of some of the landslides observed in the study area can be simply explained by the consequences of this stress imbalance and without recourse to any mechanism peculiar to a periglacial environment.

One fundamental cause of this stress imbalance is the oversteepening, erosive, action of rivers. It has been observed throughout the study area that landslide activity is, generally, restricted to areas of active bank erosion. In some reaches of the Mackenzie terrain units, such as GLB soils which are prolific producers of a wide range of instability, immediately become stable when the eroded scarps are abandoned by the river. Scarps may be abandoned by down-cutting of the river bed into more stable soils or by the deposition of fluvial soils along the toe of the bank and although exceptions can be noted these banks are usually stable and will remain so unless re-eroded or artificially disturbed. In most instances, fall landslides are the direct consequence of river action. Frozen sediments, when undermined by intense river action at meander bends become undercut and fail in tension. Some rotational slides appear to be the result of rapid drawdown conditions caused by flooding and the subsequent rapid drop in river levels. This process may occur either due to flooding caused by ice jams or by heavy rains in the upper reaches of the Mackenzie drainage system. Ice jams are common along the Mackenzie and affect both the main rivers and the smaller tributaries. The rapid rise and fall of river elevation of up to 20 ft in a few days in response to ice jams appears to be of fairly frequent occurrence with lesser flood crests being caused by heavy rainfalls especially in the upper reaches of the Liard River.

Heavy rainfall may also initiate skin flows by increasing the total shear stress due to saturation of the soil and organic cover. Accompanying this increasing in shear stress is a parallel decrease in shear strength due to reduced effective stresses. The presence of an active layer at shallow depth contributes to the maintenance of saturated conditions and while, as we have seen the presence of frozen soil may aid other instability mechanisms, it is suggested that skin flows can be initiated under conditions in most respects similar to shallow landslides in temperate regions. Mackay and Mathews (1973) have emphasized the importance of heavy rainfall in initiating skin flows in the Mackenzie River Valley and Savel'yev (1972) notes that the stability of the active layer on slopes formed of silty sands and sandy loams is usually disrupted during prolonged rains.

6.1.2 Initiation of Skin and Bi-Modal Flows

It was noted, in the preceding section, that skin flows could be started by heavy rainfall creating a stress imbalance. Rainfall might also encourage the occurrence of skin flows by increasing the rate of thaw, thus contributing to instability by thaw-consolidation effects. It can be seen that the rate of thaw would be increased not only by the effect of the presence of warm water but also by the increase in thawed conductivity of the organic and mineral soil cover upon saturation.

Vegetation also exerts considerable control on the stability of thawing active layers. One of the characteristic indicators of solifluction activity is the bulbous, solifluction lobes formed when thawed soil is restrained by the overlying organic cover. When the organic cover is disturbed or destroyed this restraining influence is lost and skin flows can develop. Firstly, it can be noted that fire action destroys the natural resilient nature of the organic cover making it more brittle. Another effect is that the rate and depth of thaw beneath the vegetation cover may be increased not only because the mat is now less thick, but the albedo of the surface will have increased thereby increasing the heat flux into the ground. It can also be noted that any artificial disturbance such as line-cutting and overland vehicular traffic will have a similar effect.

Skin flows may also be initiated by the cumulative action of many cycles of freeze and thaw which tend to concentrate finer-grained soils at depth. These finer soils bulk and form ice lenses during the freezing cycle and become thaw unstable. Thus, while the rate of thaw may be more or less constant with depth the R value, Eq 3.16, increases with depth as c_v decreases with increasing fines. The effective stress strength parameters will also decrease with depth as the more silty-clayey soils become concentrated. The freeze cycle will tend to reduce the strength even more on thaw by leaving the soil grains in an exceedingly loose state thus decreasing the effective angle ϕ'. On the other hand, freeze-thaw cycles may tend to stabilize a slope as a macrostructure is imparted to the soil significantly increasing the permeability and, therefore, the rate at which excess pore pressures may be dissipated.

The first stage in the development of a bi-modal flow is some process or combination of processes that removes insulating covers of vegetation and thawed soil exposing thaw-susceptible or ice-rich soil in such a manner than an ablation mechanism can be started and sustained. Any of the mechanisms discussed above which cause the initiation of skin flows can lead, ultimately to the development of a bi-modal flow. In fact, bi-modal flows are initiated by some other form of mass movement.

Small rotational slides, in turn initiated by rapid draw-down conditions, may start a bi-modal flow, Fig 6.1. When a flood crest rises, possibly increasing the rate of melting, and then rapidly recedes causing a slump in thawed soil, ice-rich soil, if exposed, may now ablate. This process would be favoured at locations where the erosive action of the river was high so that the initial and subsequent colluvial debris could be quickly removed.

Skin flows that occur near the bends of swiftly flowing rivers also encourage the development of bi-modal flows because the colluvial debris usually found at the base of a skin flow may be easily removed. Furthermore, it may be suggested that river action at the toe may first initiate the skin flow, Fig 6.1.

Fall landslides may also be initiated by intense erosive attack at the bend, Fig 6.1. The subsequent failure in tension of a block of frozen soil and its rapid removal by the river action responsible for its formation would then form a potent mechanism for the initiation of a bi-modal flow.

Factors influencing a bi-modal flow were investigated in detail at Site HU-1 on the Hume River. A series of bi-modal flows, found at a bend in the Hume River, have been described in detail in Appendix A. The drilling programme established that conditions in an undisturbed bank immediately downstream from the most recently active flow would sustain an ablation mechanism as it was found that in-situ ice contents were up to 1.5 to 3.0 times the liquid limit of a silty clay soil, see Figs B.2 to B.4. Permafrost was found in all borings and as shown on Fig A.23 it is likely that frozen soil extends up to the trim line. Evidence of fall landslides or skin flow activity is suggested by the instability of a row of large spruce bordering the trim line, Plates 11 and 12. These spruce are rooted in soil some 27 ft above low water level, taken as the top of the ice cover. This abrupt change in vegetation from spruce to sparse willow suggests that flooding to this elevation is possible. Along the 27 ft elevation line frequent note was made of small thermal erosion niches and the forward-toppled trees are common in this reach of the river.

It is thought that the most likely mechanism of initiation of the flow landslides at this bend is as follows. In the past, when the present flow landslide at Site HU-1 (which is now almost stabilized) was initiated a large tongue extended out into the river. This tongue caused the Hume to actively erode the opposite fluvial bank and to be deflected away from the spruce covered GLB bank down-river from the active flow. This situation was then maintained as the flow ablated backwards into the GLB upland. But as the bi-modal flow is now becoming inactive the tongue in the river is being eroded away, and the river will soon regain its former regime in a straight channel. Once this occurs the now-unprotected GLB bank will be actively eroded and a bi-modal flow will be initiated once a suitable set of circumstances combine to expose the ice-rich soil found beneath the spruce cover.

During the course of the field exploration, frequent note was made of the importance of forest fire action in increasing the frequency of flow landslides. It has been observed, in small bi-modal flows, that a vegetation curtain drapes the entire headscarp reducing the melting rate of the headscarp. Furthermore, in its undisturbed state, this curtain can be found up to maximum heights of about 10 ft. However, when burned the vegetation mat becomes brittle and cannot bend over and mould itself against the headscarp. Therefore, while a natural stabilizing process would tend to offset the initiation mechanisms of Fig 6.1 this process is not effective in burned-over regions. Thus, a small mass-movement, which would normally be healed in undisturbed terrain, would quickly grow in a burned-over or otherwise disturbed river bank.

The preceding mechanisms, outlined in Fig 6.1, all are associated with toe erosion. This follows from the frequent occurrence of instability with rivers and with bends in particular. On the other hand, many bi-modal flows can be observed perched well above the trim line or in areas with no toe erosion. These flows are likely caused by the direction action of forest fire activity or other unseasonal processes such as heavy rains or high temperatures which initiate skin flows.

6.1.3 Other Initiation Mechanisms

Many of the larger forms of mass-movement such as block slides and MR slides and flows are seated in banks undergoing a continuous state of degradation. No block or MR slides have been found in the study area for which before and after aerial photographs are available. However, two MR flows, the Fort Simpson Landslide and the Cameron Point Landslide, Table 2.3, have occurred recently and comparative aerial photography is available. These landslides, described in detail in Appendix A, appear to have been initiated by the failure, in shear, of the frontal portion of the present colluvial mass. The toe area of both of these MR flows consists of a slightly more intact and massive segment which is felt to be the relic of the initiating movement. Once this movement occurred ice-rich silty clay was exposed beneath a capping of silty sand and a series of bi-modal flows in the clay and rotational slides in the sand were initiated and resulted in the rapid growth of the landslide mass.

There is no direct proof to support the view that the initial movements at these two MR flows were seated partly in frozen soil. However, frozen ice-rich soil is found all along the east flank of the Fort Simpson Landslide right down to the river's edge and it is supposed that the same conditions would have been found along the pre-failure bank. Inspection of pre-failure photography indicates that the spruce cover is identical in both areas.

Furthermore, as the pre-failure spruce cover is at least 120 years old some permafrost could be expected under such a mature cover. It is suggested that the initial movement occurred through frozen soil and likely bottomed-out in unfrozen soil beneath the permafrost.

This combination of shear movements through frozen and then unfrozen soil also appears to be the most reasonable failure mode for the block and MR slides encountered in the study area and has been discussed in earlier chapters.

found in the study area for which before and after aerial photographs are available. However, two MR flows, the Fort Simpson Landslide and the Cameron Point Landslide, Table 2.3, have occurred recently and comparative aerial photography is available. These landslides, described in detail in Appendix A, appear to have been initiated by the failure, in shear, of the frontal portion of the present colluvial mass. The toe area of both of these MR flows consists of a slightly more intact and massive segment which is felt to be the relic of the initiating movement. Once this movement occurred ice-rich silty clay was exposed beneath a capping of silty sand and a series of bi-modal flows in the clay and rotational slides in the sand were initiated and resulted in the rapid growth of the landslide mass.

There is no direct proof to support the view that the initial movements at these two MR flows were seated partly in frozen soil. However, frozen ice-rich soil is found all along the east flank of the Fort Simpson Landslide right down to the river's edge and it is supposed that the same conditions would have been found along the pre-failure bank. Inspection of pre-failure photography indicates that the spruce cover is identical in both areas.

Furthermore, as the pre-failure spruce cover is at least 120 years old some permafrost could be expected under such a mature cover. It is suggested that the initial movement occurred through frozen soil and likely bottomed-out in unfrozen soil beneath the permafrost.

This combination of shear movements through frozen and then unfrozen soil also appears to be the most reasonable failure mode for the block and MR slides encountered in the study area and has been discussed in earlier chapters.

The combination of circumstances by which these shear movements are initiated is open to speculation. Certainly, the existence of erosive attack by river action is of considerable importance. This can be no more clearly seen that at Sans Sault Rapids area where the Mountain and the Carcajou Rivers flow into the Mackenzie, Fig A.17. At the Mountain River site, M1, large MR slides are seated in GLB soils and clay outcrops at river level. However, at site C1 on the Carcajou only 3-1/2 miles away the same GLB soils are found perched on bedrock above river level and the only landslide form observed was bi-modal flows. Thus, it is argued that as the Carcajou site is protected from direct attack slides cannot develop.

Block and MR slides have not been found in banks less than about 100 ft high in the study area. As river banks in the study area less than 100 ft high will, characteristically, be frozen to below river level this observation suggests that block or MR slides cannot be initiated in banks that consist primarily of frozen soils. On the other hand, the presence of permafrost seems to be a requisite condition for shear failure in the higher banks. For example, at Mile 556 near Norman Wells, a section of river bank made up of sands and silts overlying blue-silty clay is found in a headland being actively eroded by the river. The river channel must be deep in front of the bank as the navigation channel is routed to within 100 ft of the bank. However, no landslides occur in this reach, whereas banks 150 ft high in other sections of the Mackenzie, with similar composition, are active. The only apparent difference between this and other banks is that an old terrace is perched above this section of the bank. Therefore, it would appear that either there is no permafrost at this site, or that the ground ice conditions have been modified in such a way as to lessen the susceptibility towards slide movements.

It is also thought that the recent warming of the climate in northern regions as a result of climatic change since the Little Ice Age (see Chapter II) may have, in the past 100 years or so, resulted in an increased frequency of slide movements. For example, an increase of mean soil surface temperature by 2°C would result in the degradation of about 100 - 150 ft of permafrost. This would have the effect of rendering banks from 200 to 250 ft high, with say 300 ft of permafrost, unstable, as they are today, with only 150 ft of permafrost.

Long-term warming due to climatic change, forest fire activity, or artificial disturbance would also reduce the strength of the frozen component. We have seen that the long-term strength of frozen soil is sensitive to increased temperatures and mass-movements may be initiated by any warming cycle that reduces long-term strength or increases creep rates.

6.2 The Continuing Degradation of Frozen Slopes

Once initiated, bi-modal flows can be observed to ablate backwards at catastrophic rates. A necessary condition for the sustained growth of these flows is that the headscarp must consist of ice or ice-rich soils. However, in order to start the flow when its exists as a small notch, a second condition requires that moss overhangs or curtains cannot develop and that ablated debris is removed. Once the ablating scarp grows to a vertical height of about 10 ft the flow will proceed at a fast rate irrespective of the condition of the vegetative cover. All other conditions being equal, a bi-modal flow will not develop in a sandy soil. Firstly, a frozen sandy soil will not ablate and when thawed will remain stable on quite steep slopes. Furthermore, as the albedo of a light, sandy scarp is relatively high compared to the wet dark surface of a ice-rich soil the heat flux available for melting will be less. Secondly, a sandy soil will not flow downslope in a low-angle tongue and so that there will be little backward retrogression of an exposed sand scarp. For example, Kerfoot (1969) has reported high, steep bluffs of frozen sands and gravels being actively eroded by the sea. His observations point out that the bluffs fail by steep, skin flows which occur towards the end of the thaw season and involve a detachment of some 2 to 3 ft of soil equal to the active layer depth. Similar processes have also been observed in cut banks in frozen fluvial sands along the Hanna River.

Within the study area, typical banks consist of a variable thickness of sand overlying an ice-rich silty clay. If a given bank is made up primarily of finer-grained soil, a bi-modal flow will ablate backwards until the low angle tongue penetrates the highland behind the slope. This process is particularly active if the flow is seated in the first 20 to 30 ft of the GLB clays which are ice-rich. A good example of this form of bi-modal flow is found at site HU1, Fig A.22. The retrogressive movement of these flows can only be arrested if the ablating scarp is effectively insulated. Once a flow survives its juvenile stage it can be naturally stopped by a combination of insulative processes. If the bank is made up of ice, or ice-rich soils alone, the flow will proceed backwards until the headscarp becomes less than 10 ft in height and vegetative covers form. Another insulative mechanism may occur if a fall landslide is initiated in the headscarp. It is possible, on higher scarps to find a top curtain of moss that causes a differential melting ~~and an~~ undermining of the headscarp. When thaw proceeds far enough, a block may fail in tension and rotate down covering the scarp. As this block is covered by intact vegetation it may tend to heal the headscarp. A third process is effective if the bank has a sand capping. When the flow is initiated it may be seated entirely in clayey soils. But as backsapping proceeds, the headscarp begins to gain a capping of sand. This sand can slough down over the clay changing the albedo and reducing the ablation rate. Furthermore, the sand will mix with the clay and the colluvial deposits in the tongue will gradually become more stable as a continuing admixture of sand reduces the effectiveness of thaw-consolidation processes in the tongue and increases the shear strength of the colluvium.

The fundamental importance of soil stratigraphy can be seen by comparing the Fort Norman Landslide, Fig A.15 which has a thin cap of sand with the Little Norman Landslide, Fig A.16, with only a thin deposit of clay at the base. It can be seen that the Little Norman Landslide has not developed as extensively as the adjacent bi-modal flow apparently as a direct consequence of the soil stratigraphy.

Soil stratigraphy also exerts a fundamental control in influencing the types of larger landslides that can develop on the higher banks in the study area. We have seen that block and MR slides which are associated with deep-seated gullying are usually restricted to banks in which the sand-silt member of the GLB sequence is thick. On the other hand, active landslides such as the Old Fort Point, Fig A.12 and the Big Smith Creek, Fig A.11, landslides, which can be considered to be bi-modal flows, are found in banks with only a thin veneer of sand and silt overlying silty-clay. While it can be argued that these landslides are associated with slide movements during their initiation, evidence has been presented, Appendix A, to suggest that the continuing degradation of the headscarps at these landslides proceeds by a process of mass wasting on the exposed scarp and transport down the lower angle tongue. Unlike ice-rich headscarps which ablate, these scarps fail by the development of skin flows in an active layer formed along and down the headscarp. Thus, in banks where more thaw-susceptible soil is exposed bi-modal flow development can be sustained while more sandy banks are restricted to instability mechanisms involving shear displacements.

The development of the tongue of the bi-modal flow also aids in this natural evolution of landslide forms. It might be expected that the finer-grained frozen soils would be more susceptible to shear failure than more sandy soils by virtue of their lower strength at the same temperature and rate of loading. However, the formation of an extensive tongue protects the headscarp from active toe erosion and, in fact, acting as a stabilizing element tends to suppress high shear stress and the possibility of shear displacements.

The rate of loading also plays a role in the continuing degradation of higher banks. In bi-modal flows which continually retreat, the shear strengths mobilized are higher than in block or MR slides which are loaded at a much slower rate. The importance of rate of loading may also be a factor in the landslides that develop along the Mackenzie from Mile 470 to 488, Fig A.10 Here MR slides are found at the only two sections of the reach where the erosive attack of the Mackenzie is somewhat abated. For example, at Mile 475 an active MR slide is found just around a bend from a reach where flow landslides have been mapped. There was no visible evidence of changes in stratigraphy and it is felt that a slide has developed as a result of mild erosive attack over a long period of time. Conversely, where there is substantial erosive attach bi-modal flows have been initiated and shear movements have not occurred because the higher rates of loading make this form of mass movement impossible.

6.3 Stabilization of Landslides

As toe erosion is a significant factor in the initiation of a wide range of landslide types in the study area the prevention of toe erosion will tend to stabilize potential landslide areas. For example, fall landslides can be easily prevented by the provision of adequate armour along susceptible reaches. Many block and MR slides appear to be in a state of quasi-equilibrium with a factor of safety near unity and the cessation of active toe erosion will likely stabilize further gross displacements in these slides. This can be seen in certain reaches of the river where GLB banks, abandoned from direct erosive attack, appear to be stable.

Once initiated, bi-modal flows can only be stabilized by the provision of adequate insulation along the thawing headscarp. For large scarps, a suitable design will also have to allow for significant creep displacements in the frozen soil, as well as for the possibility of an ultimate long-term shear failure. The amount of insulation required in order to prevent thaw can be designed using Eq 3.13 and the velocity rates of Table 3.7 to give an upper bound on the heat flux available for thaw. Toe armour will not stabilize bi-modal flows, and it is thought that the judicious use of erosion protection will be of considerable importance in preventing the initiation of bi-modal flows adjacent to engineering works.

A common technique used in landslide stabilization in temperate regions is the reduction of shear stress in the landslide mass by benching. This technique would be completely unsuitable for most landslides in the study area as many surficial failures would be caused in the exposed permafrost soils. On the other hand, large surcharges along the toes of slides would, in conjunction with toe-armour, provide a suitable method of stabilization in certain cases.

Another common technique in landslide stabilization is the reduction of pore water pressures. This technique may be possible in the larger slides and we have seen in Chapter V that high pore pressures might be expected beneath the permafrost capping in block and MR slides. Although the high pore pressures are consequent upon thaw-consolidation are of vital importance in the initiation of skin flows and solifluction it may not be possible to provide suitable drainage in order to stabilize such slopes. Whereas counterfort drains are a useful technique in the stabilization of shallow slopes in temperate regions they would not be suitable for a thawing active layer and, furthermore, the surficial disturbance associated with their installation would likely aggravate the situation.

Some landslides may be stabilized by various artificially induced freezing processes which would attempt to increase the mobilized shear strength by reducing the average soil temperature. This technique would only be useful in slide or creep movements as the rate and amount of thaw, which controls flow landslides processes, is not significantly dependent upon frozen ground temperature. Furthermore, freezing soils at depth may cause pore water expulsion and thus contribute to instability processes rather than serving as a stabilizing force.

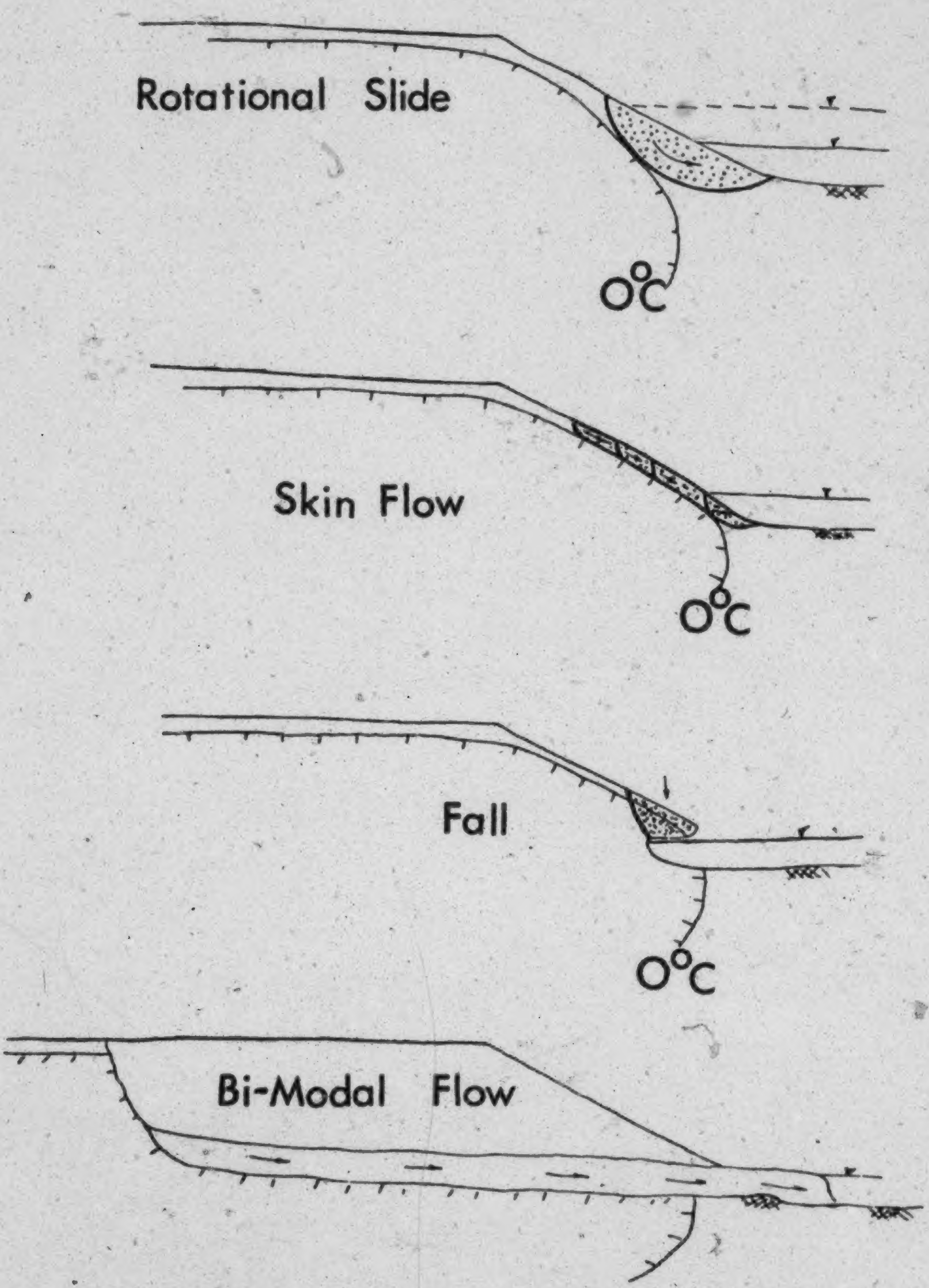
Rotational Slide
0°C
Skin Flow
0°C
Fall
0°C
Bi-Modal Flow

Fig 6.1 Methods of initiation of Bi-Modal flows

CHAPTER VII

CONCLUDING REMARKS

The landslide classification presented in Fig 2.1 has been derived for use in the Mackenzie Valley and is restricted to mass-movements in soil. The classification was conceived using a morphological or descriptive framework and any mechanistic or genetic overtones were avoided. As most of the landslide forms studied in the field and reported in the literature have multiple mechanistic origins it can be concluded that a classification based on a mechanistic framework would be unworkable. The classification presented is somewhat dominated by field experience in the Mackenzie Valley. In order to extend the classification for general use in periglacial areas field study should be undertaken of mass-movement forms in soil above the tree line, in the high arctic and in regions with a different Pleistocene history. If solifluction is placed in the classification under flow movements, it is felt that the classification of Fig 2.1 will be complete for all mass-movements in soil in periglacial areas. It is thought that landslides in rock can be most readily included in a general classification by splitting the classification into soil and rock sub-sections at the highest level, leaving the soil classification as above, and by developing a parallel classification for movements in rock. The components of the rock classification would be a function of the rock structure

This study has concentrated upon identifying possible mass-movement mechanisms for landslides in periglacial areas and a wide range of possibilities in thawing, frozen and freezing soils have been considered. It was anticipated, at the outset, that there would be a lack of factual case records which could be used to test proposed mechanisms. Although this shortage has, in some respects, been met as a result of the field programmes undertaken, it is evident that there is scope for a wide range of future field investigations.

Many aspects of mass-movement in thawing soils can be predicted using thaw-consolidation theory. The thaw-consolidation ratio R controls the maintenance of excess pore pressures in the soil and we have seen that the thermal solution required for the theory can be readily estimated using simple analytical methods. It has been shown that a step temperature boundary condition often represents a useful approximation for naturally induced thaw and that the actual magnitude of the range of the rate of thaw is small. On the other hand, the ratio R is also controlled by the permeability and compressibility of soil and little is known concerning the in-situ magnitude of these parameters and the role of cycles of freeze and thaw in effecting these parameters by changing the macrostructure of the soil. Instability on natural slopes may also be encouraged by thaw over an ice lense and the excess pore pressures set up on thaw are very sensitive to the magnitude of the permeability of the overlying thawed soil. The shortage of well-documented field case records of thaw-induced instability is obvious and research into the in-situ properties of a thawing slope coupled with measured excess pore pressures will certainly be of great value. This is especially true of field information on the role of cryogenic structure in influencing the mechanical response of soil on thaw. During the field and drilling programmes frequent observations were made of a lattice type of ground ice which is found in a three-dimensional structure around silty clay soils. While considerable insight into the role of this and other freeze-thaw induced macrostructures may be gained from laboratory tests it is thought that field tests will be required in order to adequately inspect the behaviour of a representatively large volume of soil.

It is possible that other aspects of mass-movement in thawing soils may be predicted by thaw-sedimentation theory. However, as sedimentation theory has not, hitherto, been recognized in geotechnical practice its application to periglacial processes is still speculative. A more significant contribution of sedimentation theory in its present development is that it confirms that a soil at very high void ratios is governed by consolidation theory. Sedimentation theory also provides the means by which to assess the void ratio at which consolidation processes begin to govern a soil mass.

The term bi-modal flow has been suggested for use in describing a form of mass-movement found within and without the study area. A simple solution for the rate of ablation of the headscarps of ice-rich bi-modal flows has been presented and this solution can be used to estimate the heat flux available for melting. In turn, this calculated flux can be used in designing artificial cuts in frozen soils. While there are a few case records available which yield the rate of melting of the headscarp there have been no measurements reported of the magnitude of the net radiation impinging on the ablating surface. Field measurements of the actual flux available would yield valuable insight into an important mass-movement form.

The only mechanism considered in freezing soils is the expulsion of pore water. It has been shown that it is possible to generate low effective stress conditions when expelled water is backed up due to impeded drainage. While this mechanism may not be a significant factor in the stability of shallow slopes it may influence deeper slopes.

Mass-movement mechanisms in frozen soils have been considered using creep and long-term strength models for the load-deformation response of permafrost soils. As there is a dearth of any useful creep data for frozen soils a representative flow law for ice was assembled. This flow law interprets the load-deformation response of ice using a secondary creep model. While it might be surmised that a study of ice deformation would serve as an upper bound on the behaviour of soil it has been shown that this need not be so. The flow law for ice was then used to predict the rate of deformation of an infinite slope of ice flowing as a laminar fluid and the velocities computed suggest that creep may be a problem in ice-rich permafrost. Whether or not permafrost soils will creep with the velocities deduced can only be resolved by long-term creep testing of ice-rich soils and by field observations.

Slide movements involving shear displacement through frozen soils have been studied using a long-term strength model for frozen soil for a slide at the Mountain River. Within this class two possibilities have been considered. The first approach was to use an empirical relationship suggested by Vialov (1965) in order to predict the long-term unconfined strength of frozen soil. An estimate of the long-term strength of the frozen component of the Mountain River slide was made and compared with the cohesive strength required for limit equilibrium. Although reasonable agreement was found, the predicted strength using Vialov's method was somewhat less than required in the slope stability analysis. As Vialov's method was based on unconfined samples this difference suggests that the long-term frozen strength may be frictional. The alternative approach using a frictional model was then investigated and it was found that a reasonable frictional response of the frozen soil was required for limit equilibrium.

The mass-movement models studied in frozen soils point out the acute lack of knowledge concerning the fundamental nature of the load-deformation response of frozen soils. Nevertheless the models considered are encouraging as they suggest that landslides in frozen soils can be analysed in terms of conventional practice.

It must be re-stated that this thesis has concentrated on mass-movement mechanisms peculiar to periglacial regions. For this reason, no special note has been made of processes which can also be found in more temperate regions.

BIBLIOGRAPHY

Aitken, G.W. 1964. Ground temperature observations, Galkana, Alaska. TR 106, U.S. CRREL, Hanover, N.H.

Aitken, G.W. 1965. Ground temperature observations, Barrow, Alaska. TR 105, U.S. CRREL, Hanover, N.H.

Akili, W. 1971. Stress strain behaviour of frozen fine-grained soil. H.R. and R. No. 360, p.1-8.

Anderson, D.M. and Morgenstern, N.R. 1973. Physics, physical chemistry and mechanics of frozen ground. Proc. 2nd Int. Conf. on Permafrost, Yakutsk, USSR.

Anderson, D.M., Reynolds, R.C. and Brown. 1967. Bentonite debris flows in Northern Alaska. Sci. Vol. 164, p.173-174.

Arvidson, W. 1973. Water flow induced by soil freezing. Unpub. M.Sc. Thesis. U. of Alberta, Edmonton, Alberta.

Balduzzi, F. 1959. Experimental investigation of soil freezing. Trans. from the German. NRC, TT 912, 1960.

Barnett, D.M. 1966. Preliminary field investigation of movements on certain Arctic slope forms. Geo. Bull., Vol.8, No.4, p.377-382.

Benedict, J.B. 1970. Downslope soil movement in a Colorado Alpine Region. J. of Arctic and Alpine Res., Vol.2, No.3, p.165-226.

Beskow, G. 1935. Soil freezing and frost heaving. Swedish Geol. Soc. Ser. C. 26th Year Book, No.3, Translation by J. Osterberg, Illinois.

Bird, J.B. 1967. The physiography of Arctic Canada. The John Hopkins Press, Maryland.

Bishop, A.W. 1955. The use of the slope circle in the stability analysis of slopes. Geotechnique 5, p.7-17.

Bishop, A.W. and Henkel, D.T. 1957. The measurement of soil properties in the triaxial test. Edward Arnold, London, UK.

Brazel, A.J. 1970. Surface heat exchange at the Chitistone Pass, Alaska. Proc. of Assoc. of Am. Geogr., Vol.2, p.26-30.

Brown, R.J.E. 1970. Permafrost in Canada. U. of Toronto Press, Toronto.

Capps, S.R. 1919. The Kantishna Region, Alaska. US Geol. Survey Bull. 687, p.7-112.

Capps, S.R. 1940. Geology of the Alaska Railroad. US Geol. Survey Bull. 907, p.1-197.

Carslaw, H.S. and Jaeger, J.C. 1947. Conduction of heat in solids. Clarendon Press, Oxford.

Carson, M.A. and Kirkby, M.J. 1972. Hillslope form and process. Cambridge Univ. Press, London.

Castro, G. 1969. Liquifaction of sands. Unpub. Ph.D. Thesis. Harvard University, also Harvard SM Series No.81.

Chamberlain, E. 1969. Some triaxial shear strength tests on frozen soil and ice. Interim draft report, US CRREL, Hanover, N.H.

Chamberlain, E., Groves, C. and Perham, R. 1972. The mechanical behaviour of frozen earth materials under high pressure triaxial test conditions. Geotechnique, Vol.22, p.469-484.

Chandler, R.J. 1970. Solifluction on low angle slopes in Northamptonshire. Q.J. of Eng. Geol., Vol.3, No.1, p.65-69.

Chandler R.J. 1972. Periglacial mudslides in Vestspitsbergen. Q.J. of Eng. Geol., Vol.5, No.3, p.223-242.

Colbeck, S.C. and Evans, R.F. 1973. A flow law for temperate glacier ice. J. of Glaciology, Vol.12, p.71-86.

Corte, A.E. 1963. Experiments on sorting processes and the origin of patterned ground. Proc. 1st Int. Permafrost Conf., p.130-135.

Drew, J.V., Tedrow, J.C.F., Shawks, R.E. and Koranda, J.J. 1958. Rate and depth of thaw in Arctic soils. Trans. Am. Geo. Union. Vol.39, No.4, p.697-701.

Eakin, H. 1919. The Cosna Nowitna Region, Alaska. US Geo. Survey Bull. 667, p.5-53.

Embleton, C. and King, C.A.M. 1958. Glacial and periglacial geomorphology. St. Martin's Press, N.Y.

Frost, R.E. 1960. Aerial photography in arctic and sub-arctic engineering. JASCE, ATD, Vol.86, p.27-65.

Geiger, R. 1965. The climate near the ground. Harvard Univ. Press, Cambridge, Mass..

Gill, D. 1971. Vegetation and environment in the Mackenzie River Delta. Unpub. Ph.D. Thesis, Dept. of Geog., UBC., Vancouver, B.C.

Gill, D. 1972. Modification of levee morphology by erosion in the Mackenzie River Delta, NWT., in Polar Geomorphology, Price, R.G. and Sugden, A. editors. Inst. of Brit. Geog. Spec. Pub. #4, p.123-138.

Glenn, J.W. 1955. The creep of polycrystalline ice. Proc. of the Royal Soc., Ser. A, V.228, N.1175, p.519-538.

Gold, L.W. and Lachenbruch, A.H. 1973. Thermal Conditions in permafrost - a review of North American literature. 2nd Int. Conf. on Permafrost, Yakutsk, Siberia, p.3-27.

Haefeli, R. 1962. Observations of tunnels in ice and the flow of ice. In Ice and Snow: properties, processes and application. W.D. Kingery, editor, Proc. of Conf. at MIT, Feb., 1962. p.162-186.

Hardy, R.M. and Morrison, H.A. 1972. Slope stability and drainage considerations for arctic pipelines. NRC Tech. Memo. 104 p.249-267.

Harris, C. 1972. Processes of soil movement in turf-banked solifluction lobes, Okstindan, Norway. In Polar Geomorphology, Price, R.G. and Sugden, A., editors. Brit. Inst. of Geog., Spec. Pub. No.4, p.155-173.

Heginbottom, J.A. 1971. Erosion in a permafrost environment. Geol.Surv.,Can. paper 71-1, pt.A, Report of Activities, p.185-186.

Heginbottom, J.A. 1973. Some effects of surface disturbance on the permafrost active layer at Inuvik, NWT, Canada. 2nd Int. Conf. on Permafrost, Yakutsk, Siberia, p.649-658.

Higashi, A. and Corte, A.E. 1971. Solifluction: A Model Experiment. Science, Vol.171, p.480-482.

Higginbottom I.E. and Fookes, P.G. 1970. Engineering aspects of periglacial features in Britain. Q.J. of Eng. Geol. Vol.3, No.2, p.85-118.

Holmes, G.W. and Lewis, C.R. 1965. US Geological Survey Bull. No. 1201-B.

Hooke, R.L., Dahlin, B.B. and Kanper, M.T. 1972. Creep of ice containing fine sand. J. of Glaciology, Vol.11, No.63, p.327-336.

Hughes, O. 1970. Quaternary reconnaissance, Northwest District of Mackenzie. Geol.Surv.,Can. Report of Activities Paper 70-1, Pt.A, p.178-179.

Hughes, O., Hodgson, D.A. and Pilon, J. 1972. Surficial Geology and Geomorphology Maps. Geol.Surv.,Can., open file 97,108.

Hutchinson, J.N. and Bhandari, R. 1971. Undrained loading, a fundamental mechanism of mudflows and other mass movements. Geotechnique 21, p.353-358.

Isaacs, R.M. and Code, J.A. 1972. Problems in engineering geology related to pipeline construction. NRC Tech.Memo. 104, p.147-179.

Jahn, A. 1960. Some remarks on the evolution of slopes on Spitsbergen. Z. Geomorph. NF. Suppl. Bd. 1, p.49-58.

Jahn, A. 1961. Quantitative analysis of some periglacial processes in Spitsbergen. Uniwersytet Wroclawski in Boleslawa Bieruta Zeszyty Nankowe Nanki Przyrodnicze, Vol.2, Ser.B, Nr.5: p.1-54.

Jahn, A. 1970. Soil movements under the influence of freezing. Ecology of the Sub-arctic Region. Proc. of the Helsinki Symposium, UNESCO, Paris, p.119-123.

Johnson, A.M. 1970. Physical processes in geology. Freeman, Cooper and Company. San Francisco, Calif.

Judge, A. 1973. The prediction of permafrost thickness. C. Geot. J. 10, p.1-12.

Kaye, B.H. and Boardman, R.P. 1962. Cluster formation in dilute suspensions. Proc. Symp. on the Interaction of Fluids and Particles, London, p.17-21.

Kelley, J.J. and Weaver, D.F. 1969. Physical processes at the surface of the arctic tundra. Arctic, Vol.22, No.4, p.425-437.

Kerfoot, D.E. 1969. The geomorphology and permafrost conditions of Garry Island, NWT. Unpub. Ph.D. Thesis. UBC, Vancouver, B.C. 308 pp.

Kerfoot, D.E. and Mackay, R.J. 1972. Geomorphological Process Studies, Garry Island, NWT. Mackenzie Delta Monograph, D.E. Kerfoot, editor. Brock University, Ont. pub. for the 22nd Int. Geog. Congress, p.115-130.

Kersten, M.S. 1949. Laboratory research for the determination of the thermal properties of soils. Final Report. Eng. Exptl. Stn. Minnesota University, Minn., USA.

Khakimov, K.R. 1957. Artificial freezing of soils. Trans. from the Russian, Israel Program for Sci. Trans., 1966.

Kynch, G.J. 1952. A theory of sedimentation. Trans. Faraday Soc. 48, p.166-176.

Ladanyi, B. 1972. An engineering theory of creep of frozen soils. C. Geot. J. No.9, p.63-80.

Lamothe, L. and St. Onge, D. 1961. A note on periglacial erosional processes in the Isachsen Area, NWT. Geog. Bull. No.16, p.104-113.

Linell, K.A. 1973. Long-term effects of vegetative cover on permafrost stability in an area of discontinuous permafrost. 2nd Int. Conf. on Permafrost, Yakutsk, Siberia, p.688-693.

Lotspeich, F.B. 1971. Environment guidelines for road construction in Alaska. Environmental Protection Agency, College, Alaska.

Macar, P. and Pissar, A. 1964. Etudes recentes sur l'evolution des versant effectuees a l'Universite de Liege. Z.f. Geomorph. Supplementband 5, (1964), p.79-81.

Mackay, J.R. 1966. Segregated epigenetic ice and slumps in permafrost, Mackenzie Delta Area, NWT. Geo. Bull. No.8, p.59-80.

Mackay, J.R. 1971. The origin of massive icy beds in permafrost, western Arctic coast, Canada. C.J. Earth Sc., Vol.8, p.397-422.

Mackay, J.R. 1972. Permafrost and ground ice. NRC Tech. Memo. 104, p.235-249,

Mackay, J.R. 1973. The growth of pingos, western Arctic coast, Canada. C. J. Earth Sc., Vol.10, No.6, p.979-1005.

Mackay, J.R. and Mathews, W.H. 1973. Geomorphology and quaternary history of the Mackenzie River Valley near Fort Good Hope, NWT, Canada. C. J. Earth Sc., Vol.10, No.1, p.26-41.

Mather, J.R. and Thornthwaite, C.W. 1958. Microclimatic investigations at Point Barrow, Alaska. Pub. in Climat., Vol.9, No.1, Drexel Inst. of Tech., Centerton, N.J.

Meier, M.F. 1960. Mode of flow of Saskatchewan Glacier, Alberta, Canada. US Geol. Survey. Prof. Paper 351.

Mellor, M. and Testa, R. 1969. Creep of ice under low stress. J. of Glaciology, Vol.8, No.52, p.131-145.

Morgenstern, N.R. 1967. Submarine slumping and the initiation of turbidity currents. Marine Geotechnique, University of Illinois Press, Urbana, Editor: A.F. Richards, p.189-220.

Morgenstern, N.R. and Nixon, J.F. 1971 One-dimensional consolidation of thawing soils. C. Geot. J., 10, p.558-565.

Morgenstern, N.R. and Price, V.E. 1965. The analysis of the stability of general slip surfaces. Geotechnique 15, p.79-93.

McRoberts, E.C. 1972. Discussion. NRC Tech. Memo. 104, p.291-295.

Nakano, Y, and Brown, J. 1972. Mathematical modeling and validation of the thermal regimes in tundra soils. J. of Arctic and Alpine Res., Vol.4, No.1, p.19-38.

Neuber, V.H. and Wolters, R. 1970. Zum mechanischen verhatten gefrorener lockergesteine bei droixialer druckbelasting. Fortshr, Geol. Rheinld. u Westt. 1 Taf., 20 Abb., p.499-536

Nixon, J.F. 1973. The consolidation of thawing soils. Unpub. Ph.D. Thesis. U. of Alberta, Edmonton, Alberta., p.300

Nixon, J.F. and McRoberts, E.C. 1973. A study of some factors affecting the thawing of frozen soils. In press, C. Geotech. J.

Paterson, T.T. 1940. The effects of frost action and solifluction around Baffin Bay and in the Cambridge District. Geol. Soc. London. Q. J., Vol.96, Pt.1, p.99-130.

Powell, J.M. 1961. Operation Hozen. McGill Univ. Arctic Met. Res. Group. Pub. in Meteorology, No.38.

Rapp, A. 1960. Recent development of mountain slopes in Karkevagge, Scandinavia. Geogr. Annaler, Vol.42, p.2-3.

Rapp, A. 1962. Karkeragge: Some recordings of mass movement in the Northern Scandinavian Mountains. Biul. Peryglac., No.11, p.287-304.

Rapp, A. and Rudberg, S. 1964. Studies on periglacial phenomena in Scandinavia. Biul Peryglac., No.14, p.75-89.

Richardson, J.F. and Zaki, W.N. 1954. Sedimentation and fluidizaion: Part 1. Trans. Int. Chem. Eng., Vol.32, p.35-53.

Robitaille, B. 1961. Jacobsen-McGill arctic research expedition to Axel Heiberg Island. Prelim. Report 1959-1960. McGill University, Montreal.

Rouse, W.R. and Kershaw, K.A. 1971. The effects of burning on the heat and water regimes of lichen-dominated sub-arctic surfaces. J. of Arctic and Alpine Res., Vol.3, No.4, p. 291-305.

Rudberg, S. 1964. Slow mass movement processes and slope development in the Nora Storfjall area, Swedish Lapland. Z.f. Geomorp. Supplementband 5, p.192-203.

Rutter, N.W. and Minning, G.V. 1972. Surficial geology and land classification, Mackenzie Valley transportation corridor. GSC. paper 72-1, Pt.A, Report of Activities, p.178.

Sanger, F.J. and Kaplar, C.W. 1963. Plastic deformation of frozen soils. Proc. 1st Int. Conf. on Permafrost, Washington, D.C., p.305-314.

Savel'yev, V.S. 1972. Effect of ground water on stability of slopes and structures erected on them on thawing of frozen soils. US CRREL, Draft Translation 369, Hanover, N.H.

Sayles, F.H. 1968. Creep of frozen sand. TR 190, CRREL, Hanover, N.H., USA.

Sayles, F.H. 1973. Triaxial constant strain rate tests and triaxial creep tests on frozen Ottawa sand. Reprint, Proc. 2nd Int. Conf. on Permafrost, Yakutsk, USSR.

Scott, J.S. 1972. Personal communication.

Shannon, P.T., Stranpe, E., and Tory, E.M. 1962. Batch and continuous thickening. I. and E.C. Fund. Vol.2, p.203-211.

Shumskii, P.A. 1964. Principles of structural glaciology. Trans. from the Russian. Dover Press, p.497.

Sigafoos, R.S. and Hopkins, D.M. 1952. Soil unstability on slopes in regions of perennially frozen ground. In: Frost Action in Soils, H.R.B. Spec. Rep. No.2, p.176-192.

Siple, P.A. 1952. Ice-blocked drainage as a principal factor in frost heave, slump and solifluction. In: Frost Action in Soils, H.R.B. Spec. Rep. No.2, p.172-175.

Skempton, A.W. and Hutchinson, J.N. 1969. Stability of natural slopes and embankment foundations. Proc. 7th Int. Conf. S.M. and F.E. State of the Art Vol. p.291-340.

Smith, J. 1960. Cryoturbation data from South Georgia. Biul-Peryglac., Lodz, Vol.8, p.73-80.

Smith, L.B. 1972. Thaw-consolidation tests on remoulded clays. Unpub. M.Sc. Thesis. U. of Alberta, Edmonton, Alberta.

Smith, N. and Berg, R. 1972. Observations along the pipeline construction haul road, Alaska from April, 1970 to August 1971. Special Report, CRREL, Hanover, N.H., U.S.A.

Steinmann, S. 1958. Experimentelle urtersuchwagen zur plastizitat von eis. Bertrage zur Geol du Schweig. Geotech. Serie. Hydrologies, Nr.10.

Steinour, H.H. 1944. Rates of Sedimentation; collected papers. Industrial and Eng. Chem., Vol.36, P+1, p.618-624, 840-847, 901-907.

Strang, R.M. 1972. Personal communication.

Straw, A. 1966. Periglacial mass movement on the Niagara Escarpment near Meaford, Grey County, Ont., Geo. Bull. Vol.8, No.4, p.369-376.

Swinzow, G.H. 1962. Investigation of shear zones in the ice margin sheet, Thule Area, Greenland. J. of Glaciology, Vol.4, No.32, p.215-229.

Taber, S. 1930. The mechanics of frost heaving. Jour. Geol., Vol.38., p.303-317.

Taber, S. 1943. Perennially frozen ground in Alaska. Geol. Soc. Am. Bull. 54, p.1435-1548.

Terjung, W.H., Kickert, R.N., Potter, G.L., Swarts, S.W. 1969. Energy and moisture balance of an alpine tundra in mid-July. J. of Arctic and Alpine Res. Vol.1, No.1, p.247-267.

Thompson, E.G. and Sayles, F.H. 1972. In-situ creep analysis of a room in frozen soil. J.S.M. and F.D., ASLE, 98, p.899-916.

Townsend, D.L. and Csathy, T.I. 1963. Soil type in relation to frost action. Joint Report: Queen's University, Ontario Dept. Hwys. Rep. No.15.

Varnes, D.J. 1958. Landslide types and processes. In: Landslides and Eng. Practice. Ed. Ecket, E.B. HRB Spec. Rep. No.29, p.20-45.

Vialov, S.S. 1955. Creep and long-term strength of frozen soils. Defense Research Board Dir. of Sci. Info. Services. Trans. 203R, p.5-9.

Vialov, S.S. 1965. Strength and creep of frozen soils and calculations for ice soil retaining structures. Trans. No.76, CRREL, Hanover, N.H.

Wahrhaftig, C.A. and Birman, J.H. 1954. Stripping coal deposits on Lower Lignite Creek, Alaska. US Geo. Sur. Circular No.310.

Wahrhaftig, C. and Black, R.F. 1958. Engineering geology along part of the Alaska Railroad. US Geol Sur. Prof. Paper 293, p.69-118.

Wahrhaftig, C. and Cox, A. 1959. Rock glaciers in the Alaska Range. Geol. Soc. Am. Bull. Vol.70, p.383-436.

Walker, H.J. and Arnborg, L. 1963. Permafrost and ice wedge effect on river bank erosion. Proc. 1st Int. Permafrost Conf. p.164-171.

Washburn, A.L. 1947. Reconnaissance geology of portions of Victoria Island and adjacent regions. Geol Soc. Amer. Mem. 22.

Washburn, A.L. 1956. Classification of patterned ground and review of suggested origins. Geol. Soc. Am. Bull. 67, p.823-866.

Washburn, A.L. 1967. Instrumental observations of mass-wasting in the Mesters Vig District, Greenland. Medd om Gronland, 166(4), p.1-297.

Weeks, A.G. 1969. The stability of natural slopes in south-east England as affected by periglacial activity. Q.J. Eng. Geol., Vol.2, No.1, p.49-63.

Williams, P.J. 1959. An investigation into processes occurring in solifluction. Am. J. Sci. 257, p.481-490.

Williams, P.J. 1962. Quantitative investigation of soil movements in frozen ground phenomena. Biul. Peryglac. No.11, p.353-362.

Williams, P.J. 1966. Downslope soil movements at a sub-arctic location with regard to variations with depth. C. Geot. J. No.3, Vol.4, p.191-203.

Williams, P.J. 1967. Properties and behaviour of freezing soils. N.G.I. Pub. No.72.

Williams, R.B.G. 1965. Periglacial erosion in England. Biul. Peryglac. No.17, p.311-330.

Wissa, A.E. and Martin, R.T. 1968. Behaviour of soils under flexible pavements; development of rapid frost susceptibility tests. MIT Dept. of Civil Eng., RR.68-77, Soils Pub. 224.

Zaruba, Q. and Mencl, V. 1969. Landslides and their control. Elsevier Press, New York.

APPENDIX A

FIELD OBSERVATIONS

Page

A.1 Observations on Landslides in the Vicinity of the Mackenzie River Mile 205 to 660 249

A.2 Observations on Permafrost Conditions in Relation to Landslides 275

A.1 OBSERVATIONS ON LANDSLIDES

MILE 205 TO 285*

A map of this section is given in Fig A.1 and specific mileages of special interest are indicated. Detailed observations along this section follow below.

Mile 207 to 219:

The south bank of the Mackenzie in this reach contains many active flows. They are generally bi-modal, with lobe angles of from about 7° to 10°, and are seated in clayey silts. One interesting flow at Mile 219, seated in clayey silt, is perched about 50 ft above river level over a dense till.

Mile 218:

The Mile 216 flow is unique among the range of smaller scale bi-modal flows observed. A typical overall bi-angular profile with a steep head scarp and a 7° lobe was noted; but, the flow is singular in that the head scarp has failed as a rotational slide with backward tilting of the slump mass. The soil profile at the head scarp is 20 ft of sand over clayey silt. No frozen ground was found in the slumped colluvium on a cursory inspection. A small rivulet flowing with no obvious source from between the slump blocks may indicate the presence of melting permafrost.

---

* Mileages are approximate distances from the head of the Mackenzie River.

Mile 221:

The landslide at Mile 221, classified as an MR flow, is at least 25 years old as it appears on 1947 aerial coverage. This flow, seated in a bank some 180 ft high, is 2300 ft long with an overall angle of 4.5° and has a steep head scarp. Adjacent bank angles are in the vicinity of 10°. A series of ridges are contained within the bowl of the flow and were inspected during a foot traverse. These ridges consist of a silty clay of considerable dry strength. They have a symmetrical appearance as both the up and down slope scarps of an individual ridge stand at approximately the same angle. The ridges appear to have been derived from the head scarp. On the traverse up the centre of the landslide small tension cracks and steps indicate that some movement is still occurring.

Mile 225:

An exceedingly large MR flow is seated in a bank some 180 ft high. This landslide, some 10,000 ft long by 2,000 ft in depth, lies at an overall 4.7° slope. Adjacent banks stand at angles of up to 30° as measured on 1:50,000 maps.

Mile 226 (Fort Simpson Landslide); Fig A.2, A.3, Plate 1:

A large MR flow is located at Mile 226 on the south bank of the Mackenzie. This landslide is less than 12 years old as no evidence of it exists on the 1960 photo coverage. Mackay J.R. (1972)* suggests that the flow began shortly before 1970 and dendrochronological investigation on white spruce at this site (Mackay D.M., 1973)* indicates that large movements first began in 1965 and have continued until the present. This flow is still active and is currently degrading under the action of several processes.

The flow area is bounded on the west by a prominent gully that parallels the west side of the head scarp and exposes some 150 feet of silty clays and silts. This gully predates the flow and is visible on the 1960 coverage. The west scarp of the flow is steep, bare of vegetation, and apparently stable. Probing located frozen ground under the spruce on the top of the ridge between the west scarp and the gully and which may be seasonal frost.

When visited, the head scarp west of centre was failing by surface flow of thawing soil out from underneath the organic cover. Slope angles of the scarp in this section average about 20°. Frozen ground was encountered in test pit, TP1, dug some 100 ft back from the head scarp and a frozen loam encountered about 6 inches below a 9 inch organic mat. East of centre a rotational slide rings the head scarp. Test pit, TP2, dug at the base of the intact head scarp bared by the rotational failure revealed frozen ground some 2 feet below thawed soil. Two auger holes were advanced to 11 feet in the slumped block. The first was driven in the centre of the back tilted block and the second hole was located in the centre of the forward slope of the slumped mass. Both holes encountered a thawed clayey silty sand.

---

* Personal communication

Unlike the west side of the flow which extends back perpendicular from the river the east side runs at an angle from the head scarp down to the river. The east side of the flow consists of a series of steep melting scarps. There is no evidence of rotational failure and the slopes are failing by the continuous melting and subsequent rapid downslope movement of soil. In one location ice lenses, 5 to 7 inches in thickness, were noted on an almost vertical scarp at least 70 feet high. Well developed melt streams indicate a relatively great percentage of water and a blue-grey clayey silt is found in conjunction with the ice lenses. The lower part of the east scarp was visited twice over a 6 week period (12 June to 26 July 1972) and at least 10 feet of back sapping was apparent in a melting scarp about 5 to 8 feet high.

A series of tension cracks were observed along the upland behind the east scarp during May 1973 (Roggensack, 1973)*. These cracks rim the ablating scarp and in one instance a tree trunk split between both sides of a crack witnesses the movements that have occurred. These features have not been observed by the author and Mackay J.R. (1972)* suggests that they may be melt features.

Photographs (transmitted to the author by Mackay D.M., 1972)* taken in June 1970 reveal that fall landslides are also possible along the east scarp. The photographs show that differential melting occurs on scarps some 20 feet high because moss overhangs drape down over the top few feet and depress the ablation rate. Thus a thermal notch is created and a cantilevered block can be broken off.

Contained within the central part of the Fort Simpson Landslide and bounded by the west scarp and a line extending at right angles from the eastern edge of the head scarp are a series of arcuate ridges. The ridges are concave downslope, are some 10 to 15 feet high, and have a frequency of about 75 feet. Along any transect down the slope one encounters forward, backward, then forward thrown trees in conjunction with the ridges. As the ridges are derived from mass wasting processes along the head scarp and as different failure mechanisms are apparent along the head scarp this cyclic repetition of the direction of tree falls may admit to a cyclic repetition of distinctly different failure modes in the head scarp.

---

* Personal communication

In the lower third portion of the flow mass the arcuate ridges give way to a denser cover of spruce. The cover is partly undisturbed and there is a tendency towards growing upright trees. This portion of more intact cover may be the relict of the initial failure of the landslide. The toe of this landslide is thrust well out into the river. Although there was no direct evidence apparent in the field the impression was gained that the toe had undergone some degree of uplifting as the soil along the toe appeared to have been thrust upwards.

The pre-failure geometry can be approximately reassembled from maps and aerial photographs. The bank along which failure occurred stands at angles ranging from 17° to 26° with an angle of 19° being a reasonable average. The pre-failure slope is quite smooth and appears to rise as a tilted plane from the trim line to the top of the bank. The bank is covered with white spruce of which the earliest pith date reported is 1841 (Mackay D.M., 1972)*. The length of the bank along the slope is about 550 ft and the approximate length of the more undisturbed toe area which may be the remains of the initial failure is about 520 ft.

Mile 241:

Downstream from Trail River on the north bank of the Mackenzie several MR slides are visible from the air. These slides have no surface expression along the river, the head scarps are grown over, and the slides are stabilized.

Mile 258 to 260:

The morphology of landslides in the reach on the south bank change abruptly. At Mile 258 banks are low along the river and frequent small flows occur. Several of these flows were inspected and all revealed ice rich frozen silty clay at the head scarps. Generally, one could find ice and frozen ground immediately beneath the organic covers that overhang the melting head scarp. It became standard practice, on looking for ground ice exposures, to locate a well developed organic mat overhang at the head of a flow. This organic mat was then cut away, by axe, to reveal ground ice.

In one of the small flows in this section an overhanging mat covered the entire head scarp and evidence of movement could be seen by the grooves in the surface soil moving out from beneath the overhangs. The soil flow was grooved by irregularities in the moss cover. When the moss cover was cut into a large air void was encountered between the base of the organic cover and the frozen, covered over, head scarp. The air smelt dank and obviously was "dead air" and as such formed an effective insulative barrier. This flow was flown over about 10 days later and considerable back sapping had resulted in the section where the moss overhang had been removed. In the lobes of these small flows frozen ground was encountered by probing at depths of about 3 feet.

---

* Personal communication

Downstream from this section the banks become steeper and higher. Viewed from the air traces of old MR slides could be seen as fine scarps running parallel with the river. It is not clear if some of the mass movements in this reach should be classified as MR flows or slides. Opposite the west end of Burnt Island a large MR flow is still active as indicated by the bare, sandy head scarp. Active sand dunes are being formed from the colluvium in the landslide area. Silty clay was noted in the toe of this flow during the river based survey. Immediately downstream from this flow and on to Mile 260 the sand member of the sequence becomes considerably thicker. The banks are now much steeper and failure leaves a scalloped appearance. The landslides are classified as bi-modal flows; however, they have not been studied in any detail.

Mile 262 to 270:

The traces of many landslides are visible from the air in this reach. Outcrops of silty clay are common at river level. These landslides appear as a series of arcuate ridges in the head scarp regions but as there is little evidence of movement along the toes they appear to be presently inactive.

Mile 265 (Cameron Point Landslide):

A large MR flow at Mile 265 is marked on the navigation maps as having occurred in 1960. The head scarp has recently failed as a rotational slide, with substantial back-tilting, and with movement apparently seated in a sandy soil. Backward thrown trees associated with older scarp failures further down the flow indicate that rotational failure at the head scarp is common. The flow is located in a bank 125 ft high, is 1100 ft long, and has an overall angle of 6.5°. Pre-failure photography indicates that the landslide developed between two large gullies that can be seen either side of the active flow but which were not involved in movement.

Mile 275:

A series of block slides seated in banks about 120 ft high have failed with little backtilting of the slump block. Some blocks which have moved down at least 100 ft show no evidence of rotational ground movements. Immediately downstream from the slides the banks are steep and intact. These banks appear to represent the bank profile before initiation of slide activity and they appear to represent the terminal stage in a cycle of degradation.

MILE 285 TO 313

A map of this section is given in Fig A.4 and specific mileages of special interest are indicated. Detailed observations along this section follow below.

Mile 293:

A recent MR slide with a degree of backtilting of some of the slump masses is located on the 120 ft high west bank at Mile 293. The slide is seated in silty clay and sand is visible at the recently exposed head scarp. Small muddy creeks flow out at each side of the main slide area.

Mile 300:

At Mile 300 an MR slide seated in silty clay demonstrates a definite backwards rotation of the slump blocks immediately adjacent to the river.

A small cirque-shaped failure is contained within the first slump block. The bowl or flat portion of the circular cavity which extends back some 30 feet from the river is filled with sand sloughed down from above that quicks when a small excavation is made into the underlying silty clay. Water is observed seeping out at the head of the flat portion. A small 1/2" diameter probe reached refusal at about 3 1/2 feet in the lobe. No definite indications of frozen ground were noted by hand but the personnel engaged in these activities noted the extreme cold of the water in the lobe and the underlying silty clay. The small springs issuing from the head scarp are either ground water discharges or are due to melting ice.

Mile 298 to 302 (Mackenzie River West Bank):
306 to 310 (East Bank, MacGern Island):

In both these sections frequent changes in the altitude of the silt and sand interbedding was noted. Generally, the silt-sand sequences are flat lying. However, frequent observations were made of interrupted attitudes by apparent dips of up to 15° as exposed parallel to the river. Small anticlinal features were also, occasionally, observed. In all cases the overall soil profile is interbedded sands and silts overlying grey-blue silty clay.

MILE 313 TO 355

A map of this section is given in Fig A.5 and specific mileages of special interest are indicated. Detailed observations along this section follow below.

Mile 332:

At the River Between Two Mountains a till section some 200 feet thick is exposed in a north facing cut bank about 1 mile up river. This till is compact with bouldersto 1 foot diameter.

Mile 340 to 345:

Remnants of old MR slides in till are present. Till outcrops are common in this vicinity. At Mile 340 a bare head scarp is visible from the river.

Mile 350:

A large MR slide near Mile 350 has several small bi-modal flows contained within the main slide mass. One flow, similiar to those within the MR slide, was inspected just downstream of the slide. This flow had exposed ice rich clayey silts in its head scarp and ice lenses to 1 inch in thickness were noted in an exposure of some 15 ft of ice rich soil based 30 ft above river level.

Mile 351:

A vast bi-modal flow can be found adjacent to Smith Creek, Mile 351, near Wrigley. The overall profile of 3° can be estimated off topographic maps and lobe angles of 4, 4 1/2° were measured in one portion of the flow. The flow is quite old as both the head scarp and lobe areas are well vegetated with spruce.

Root River Flows:

Large ribbon-like skin flows were observed on the steep north facing slopes of the foothills of the Camsell Range near the Root River. At one location some 10 flows have occurred on a relatively steep hill-side, estimated at between 23° to 33°. The flows appear to be seated in colluvium derived from insitu weathering of shales. These flows have occurred frequently in the past as marked strips in the form of changes in vegetation cover the north facing slopes in this area are witness to past movements of the same type. These flows are in the order of 1000 ft long, 50 to 75 ft wide, and from 1 to 3 ft deep. In all cases a large mound of colluvium and vegetation is piled up at the toe of the flow. A cross-section along a typical skin flow has a steep head scarp section and a more shallow run-off section.

Wrigley River Flows; Plate 2:

Well developed skin flows were noted on some small tributaries of the Wrigley River. These flows may be seated in till. The flows occur on the south facing slopes which have recently been burnt over. Long finger-like flows co-exist with sections that have coalesced into broader sheets. Slope angles can be estimated to be from 14° to 16° for north banks and from 9° to 10° for south banks which, although burnt, have not failed.

MILE 355 TO 394 AND 394 TO 426

Maps of these sections are given in Fig A.6 and A.7. From Wrigley at Mile 355 to the Dahadinni River at 417 the Mackenzie River flows in a single channel of fairly regular width with little sign of lateral shifting or bank instability. There are very few islands and a well defined trim line appears to demarcate the average annual flood level. Beaches are well cobbled.

Opposite the Johnson River at Mile 394 a series of small inactive landslides are apparently seated in till. In the reach from

355 to 417 outcrops, where visible, are of till or bedrock. At Mile 426 outcrops of shale and interbedded sandstone dip 1 1/2 ft to 2 ft in 100 ft downstream.

MILE 440 TO 491

A map of this section is given in Fig A.8 and specific mileages of special interest are indicated. Detailed observations along this section follow below.

Below the Dahadinni and to the Redstone the Mackenzie flows in a straight reach with little bank instability but frequent sand bars and small islands. The character of the river then changes at about a point marked by its confluence with the Redstone at Mile 443. From here, and until Police Island, Mile 500, where the river changes course to the west the river is characterized by sinuous channels and many islands formed from recent fluvial deposits. There is frequent channel splitting around sand bars and wooded islands. The nature of the banks also change and frequent landslides occur. Although the left or west bank is seated in low lying and apparently easily erodible recent fluvial deposits instability is wholly restricted to the east bank.

A primary cause of instability in this area seems likely to be the inflow of coarse bed load from the Keele and the Redstone Rivers. These braided gravel tributaries dump, during flood stages, large amounts of bed load into the Mackenzie. The Mackenzie, in turn, cannot carry these imposed loads and deposits them in the form of islands around which it must pass.

It is clear, however, that the formation of islands and their influence on lateral channel shifting while being a necessary is not a sufficient condition for instability. It can be seen that the conditions downstream from the Dahadinni would also favour landslides as it is also a braided gravel river and many islands and sand bars are contained in the Mackenzie downstream from this confluence. The banks however are seated in tills and bedrock with the result that instability is generally absent.

The widening of the river channel below the Keele is a direct consequence of the bank stratigraphy in this reach. Massive deposits of GLB silty clays overlain by sands outcrop along the east bank. These glaciolacustrine deposits are very erodible and on the basis of experience in other regions of the study area likely contain massive ice lenses.

As will be pointed out in the detailed observations that follow the situation is, however, not entirely clear even in the reach from Mile 457 to 480. Frequent till exposures daylight at river level from Mile 457 to about 469. These till deposits influence the landslide morphology in this reach. Below Mile 469 no till was noted at river level and the slides are seated in silty clay. This observation may in part explain the comparatively great width of the river between Mile 469 to 480 in relation to the reach immediately upstream.

To facilitate an appreciation of the many features along this reach, more detailed plans for Miles 455 to 470 and Miles 470 to 488 are given in Figs A.9 and A.10 respectively.

Mile 440 to 470:

Till exposures are common along the east bank from Mile 440 to 470. Above Mile 457 the banks are almost entirely till while below Little Smith Creek the till is lower although it may reach as high as 80 ft above river level, locally. The till has an effect on the geomorphology of the landslides and although there appears to be some slides the overall impression is one of flow dominated movement. Within any landslide upright vegetation is absent and there is a high degree of mobility. In active landslides the overlying silty clay can be seen to have sloughed out and over the underlying till. In other locations the Mackenzie has eroded away colluvial debris truncating the toe portion of landslides and clearly revealing the soil stratigraphy. Inspection of these areas is difficult as banks are almost vertical, the current swift and seething, and there are few locations where boats may be moored. However, a typical site was observed in a cut bank some 1500 ft up Little Smith Creek. Here, clayey silt had flowed out and over the underlying till and it could be seen where the colluvial material remained dried onto the till banks. These perched landslides are classified as bi-modal flows although they may, in places, partake of more of an MR flow appearance. There is no evidence to suggest whether or not the underlying tills undergo slide or flow movements or if they are eroded and removed by direct river action and by fall landslides

At Mile 465 fluvial deposits choked up between islands have diverted the river from beneath the steep east bank. Where there is no active toe erosion banks are stable.

At Mile 469 a large mass of frozen silty clay was observed at river level. This soil had apparently slumped down from higher up and on June 16, 1972, ground ice could be seen where the block had been undercut by the river. By July 16 no trace of this block could be found.

Mile 470 to 480:

Below Mile 470 the till, which has been dipping down river, is now absent. Soil stratigraphy from Big Smith Creek, Mile 471, Fig A.11, Plate 3, and Old Fort Point, Mile 480, Figs A.12 and A.13, Plate 4, have been classified as bi-modal flows. While the lobe angles are steep compared with other bi-modal flows there is a strong bi-angular profile. At first sight, these landslides and others in this reach seem to be some form of block slide as they would appear to have undergone rotational displacements. There are, however, certain distinctions that separate these landslides and the block slides classified elsewhere. At both sites the top of the landslide mass that resembles a block is utterly devoid of upland vegetation. An inspection of both landslides revealed many spruce trunks buried or partly buried in colluvial debris. At the Big Smith Creek site, Plate 3, a single line of upright spruce can be seen bordering the base of the head scarp.

While there may be slide movements occurring within the tongue portion of the two landslides the overall impression is one of flow dominated movements. Bi-modatily is also introduced into the classification of these landslides by the different failure modes apparent. Close inspection of the smooth, steep head scarps at the Old Fort Point site has revealed that ongoing processes involve the detachment of a slab of insitu thawed soil that flows down-scarp ending at a bump at the break in slope and adding mass to the block-like central portion of the flow, Plate 4. The single row of trees at the Big Smith Creek site indicates a similar failure mode.

It is likely that the Old Fort Point and Big Smith Creek Landslides represent an earlier stage in the development of more mature bi-modal flows that are found close-by. None of these profiles have been surveyed but bi-angular profiles of 5^{o} lobes up to 1000 feet long with 35^{o} head scarps are reasonable estimates based on aerial observation and photographs. These flows are mature and partly stabilized with second growth vegetation and are common in the river bends at Mile 472 and Mile 480.

Mile 472 (Ice Buttress Landslide); Plate 5:

A bi-modal flow, at Mile 472, has a distinctly bi-angular profile with a steep scarp and low angle frontal area and when first encountered exhibited one feature of great interest. On June 16, 1972, a massive buttress of frozen sand at the top of a bare head scarp was observed cantilevered out over thawing clayey silt. By July 15 the buttress had diminished considerably and by July 30 it had almost vanished. When first observed its estimated dimensions were 25 feet deep with a 20 foot extension. Ice was clearly visible in ice wedges within the frozen sand. The sand continually thaws and spills off the buttress in small pieces. Depending on the initial position spalled sand either fell to the bottom or was collected on the scarp. This collected material then reached a critical height and flowed in a surge down to the main lobe of what is classified as a bi-modal flow.

Immediately downstream of this flow the banks have a distinctly bi-angular profile and are similar to bi-modal flows elsewhere, (for example; the Fort Norman Landslide, Mile 517), except that they have coalesced into a broad front.

Miles 475 and 484:

Large MR slides at these locations, Fig A.10, are found as isolated features in this section of the Mackenzie. The MR slide at Mile 475 is visible on the 1947 aerial coverage but is still active as a prominent toe has been recently thrust up into the river.

Immediately downstream of Mile 475 the river is not actively eroding the GLB scarp and sand bars are found along the toe of the scarp. There is an absence of any instability.

Mile 440 to 480 (Summery of Observations):

The morphology of the landslides in this reach change as the stratigraphical sequence changes. The interpretation of the relative influence of till level is complicated by the apparent conclusion that some of the landslides noted are at different stages in a cycle of degradation.

Above Big Smith Creek instability appears to be restricted to the silty clays overlying till. In some sections this clay has slumped out over the till sequence masking it and movement has occurred at a faster rate than the rate at which the Mackenzie can remove the colluvial debris. Given the velocity of the Mackenzie River and its apparent erosive power in this reach it appears that mass movements are large and catastrophic in nature. When viewed on aerial photographs the landslides have a much more truncated appearance than do those downstream of Mile 470. This is because for the same overall bank height the flows perched on the till cannot extend as far back as the flows seated at river level.

Below Big Smith Creek, Mile 470, no till outcrops were seen. Stabilized landslides with vegetated head scarps have a distinctly bi-angular cross-section with low angle bowls and steep head scarps. More recent landslides such as the Old Fort Point Landslide and the Big Smith Creek Landslide have a steeper overall cross-section. Although these two landslides have a blocky appearance the apparent top of the block is denuded of any upland vegetation. True block slides noted elsewhere have identical vegetation covers to that which is established on the terrain above the head scarp.

At Mile 475 and near Mile 484 certain multiple retrogressive features are noted. These slides are relatively old as they appear on the 1947 photo coverage. They are, however, different in morphology from the more cirque-like landslides common below Mile 470.

MILE 497 TO 565

A map of this section is given in Fig A.14 and specific mileages of special interest are indicated. Detailed observations along this section follow below.

Mile 500:

There are many scars of old landslides along the right bank of the Mackenzie River on the great bend at Police Island. Above Mile 500 there are occasional active flows. Although no bedrock was observed at river level above Mile 500 the morphology of the flows indicate that the glacial lake sediments form only a veneer over till and bedrock. The flows appear to be failing along steep slopes in the tongue portion. It is likely that the flows have slumped out over more resistant sediments. Below Mile 500 bedrock was visible and the flows in this reach are perched about 40 feet above river level.

Mile 507:

A large rock landslide in Tertiary sediments is seated on the north bank. Below Mile 507 and to Fort Norman there are many exposures of Tertiary sediments. Burning coal seams and consequent red staining is common in this reach. Near Fort Norman ice wedges were observed in drift overlying Tertiary deposits.

Mile 513 to 516:

A sequence of large slides seated in glaciolacustrine silts and silty clays are found along the south bank of the Mackenzie just downstream from Fort Norman. Slope instability processes have been active in the past as the river is very wide in this reach. In this reach the stratigraphy consists of sand overlying silt-sand rhythmites in turn overlying silty clay. On the helicopter survey it was noted that most slides involve movement of a single block although occasional multiple retrogressive features are present. Inspection of aerial photographs confirms that most failures have a blocky form.

Slump blocks are commonly flat-lying although some back-titled slumps have been noted, particularly in those blocks that have moved down almost to river level. Just downstream from Mile 513 a large gully lying perpendicular to the river exposes a cross-section where both forward and backward tilting of the silt-sand rhythmites was observed. Along or parallel with the river exposed silt-sand layers are generally horizontal. However in some places abrupt changes may occur. Dips were never greater than about 15°.

Well-developed gullying is associated with these slides. Gullies first develop at right angles to the river. They are V-notched with steep sides and do not extend much backward of the slide areas. Frequent extensions to the gullies occur at right angles to the perpendicular gullies and run parallel with the river. Sand has fallen down and covered over the sedimentary sequence in many of the gullies. However the depth of the gullies suggests that the sandy-silt facies of the GLB sequence extends almost to river level. Blue silty clay was noted at river level in this reach.

Mile 517 (Fort Norman Landslide); Fig A.15, Plate 6:

A large bi-modal flow called the Fort Norman Landslide, Mile 517 was the subject of relatively extensive investigation. The headscarp, standing at a steep 36° angle, has a relatively smooth face and a classic semi-circular shape. A test pit was dug at the base of the head scarp just east of centre. At a depth of some 18 inches horizontally into the bank a frozen silty clay with vertical and horizontal ice lenses was encountered. This silty clay extends to within 20 ft of a 110 ft scarp and is overlain by silty sand. A series of V-shaped gullies ring the top of the head scarp and are covered over with draped vegetation. These gullies may result from melting of ice wedges. Frozen ground was encountered by probing on the upland behind the head scarp, and thawed soil was found flowing out from beneath vegetation covers in a small ravine halfway down the east scarp.

The lobe area lies on a low 3^{o} angle overall and smaller lobate features can be found superimposed on the lobe near the toe, Towards the head scarp on the east side larger lobes some 5 to 10 ft high appear to be the remnants of material derived from the head scarp. Two small streams are also contained within the flow.

A large silt run extends over an area of some 5,000 sq ft at the base of the head scarp just east of centre. The run consists of a colluvial silt and clay mixture and lies at an angle of 3.5^{o}. Small mud boils, up to 3 inches in diameter, pit the surface of this silt run and water can be seen slowly weeping out from their craters. On June 17, the transducer piezometer was pushed to the thaw interface at locations P1, P2 and P3, Fig 2.3 and excess pore pressures measured. A further test, P4, was made on June 23, 1972, and a Geonor open standpipe test was made at location G1. About 1/2 hour after the piezometer was withdrawn from test P1 a mud boil began to form in the hole vacated by the probe. A plopping noise could be heard and once the silt settled in the small puddle a mud boil was found.

The Fort Norman landslide appears on both the 1950 and 1961 aerial photography of this area. Comparative measurements of the location of the head scarp with upland features suggest that some 120 feet of movement has occurred in 11 years.

Mile 518 (Little Norman Landslide); Fig A.16:

A smaller bi-modal flow called the Little Norman Landslide, Mile 518, is found one mile downstream. This flow is now well stabilized and the bowl treed, although the 1950 coverage indicates activity. Inspection of the banks immediately upstream indicates that the silty clay occurs much lower down at this site than at Mile 517. Sand and silty sand interbeds were noted almost to river level where a blue-fissured silty clay had been exposed in a recent wave cut platform. Probing at various locations down the thickly vegetated head scarp encountered frozen soil and a test pit advanced at the base of the scarp encountered frozen soil beneath a thawed sandy silt.

Mile 551:

For about one mile above and below Mile 551 frequent bi-modal flows are encountered, some with a changing morphology that reflects different stages in development. More mature flows are only marginally active, partly overgrown with small birch and poplar, and have a truncated appearance. These bi-modal flows are older flows that have reached some sort of equilibrium at the headscarp and are now having the greater portion of their tongues eroded away. Towards Mile 550 more recent flows are noted with low angle lobes of 7^{0} to 8^{0} starting at the trim line.

Mile 530 to 535 (Halfway Island Landslides):

Bi-modal flows partly controlled by bedrock elevation are found opposite Halfway Island, Mile 530 to 535. From Mile 530 and to about halfway around the bend, bi-modal flows are seated at river level. Below this point bedrock starts to rise and flows seated in clayey silt spill out and over almost vertical rock exposures.

Mile 556:

A steep exposure of GLB sands and silt with blue silty clay at river level is found in a headland being actively eroded by the river. No landslides occur in this reach although abrupt changes in the dips of originally horizontal sand-silt layers were noted. Inspection of aerial photographs indicates that an old flood plain terrace is seated on top of the bank in this section

MILE 621 TO 660

A map of this section is given in Fig A.17 and specific mileages of special interest are indicated. Detailed observations along this section follow below.

Mile 621 (Axel Island Landslide):

A large MR slide is seated in the north bank of the Mackenzie opposite Axel Island. Bank heights range from 185 to 235 ft and the overall angle of active areas of instability range from 9.5° to 14°. Adjacent banks stand at angles up to 23°.

Many arcuate ridges stepped back en-echelon from the river were noted. The slide was flown over and a rotational aspect of failure of the head scarp was apparent. Extensive exposures of silty clay along the toe were noted and small bi-modal flows contained within the toe attest to frozen ground. This landslide might be considered to be an MR flow.

Upstream of this landslide frequent bi-modal flows have occurred in a recently burned-over area.

Mile 635 (Hanna Island Landslide); Fig A.18, Plate 8:

The Hanna Island Landslide, Mile 635, presents many of the features typical of the bi-modal flows of the Sans Saults Rapid area. The head, left and right scarps are all steep and have, here and there, organic mats draped down over the scarps. The lobe is devoid of living vegetation and several smaller lobes are contained within the main area. This flow was visited twice in a 2-week period and evidence of movement could be seen in the change in altitude of a series of arcuate thrust ridges at the toe of the lobe. Upslope, and at either side, of the flow burned-over spruce indicates that a fire has recently gone through the area. Upslope from the flow, tension cracks parallel the headscarp and many are likely due to the severe desiccation of the organic mat after the fire. However, one crack has split a 16 inch diameter stump.

A test pit was cut into the right or north scarp beneath an overhanging moss cover. A plastic blue fissured clay was encountered and at about 18 inches into the scarp frozen soil with both vertical and horizontal ice lenses up to 1/8 inch was revealed.

Mile 642:

This landslide has a steep head scarp of 28°, a relatively steep lobe of 13°, and a steep toe falling over the trim line and on down to the river. As such it is a bi-modal flow.

The head scarp is melting and ground ice with lenses up to 6 inches thick is exposed. A silty colluvium flows in pulses down to the break in slope at the lobe. On the head scarp soil undercut by melting ice or thawed soil falls down and collects in small pockets or "pools". At a certain critical point this aggradation of colluvium then flows down-slope carrying contained clods of intact soil and any other debris that it has collected. Movement also occurs by gravity fall of large blocks of dried silty clay which were observed rolling down the 28° head scarp and coming to comparative rest in the bowl. Upon reaching the lobe the pulse breaks up and moves out on a slope of about 6 1/2° to 7 1/2°. Angles were taken with a Brunton compass by floating a plywood board on the lobe. The flows are quite liquid with hard crumbs of soil and small pebbles and sand (from the overlying sand strata) contained in them.

The transducer piezometer was placed in the lobe below the break in slope andat 2.05 ft a pore pressure reading of 2.3 feet was obtained.

This site was visited twice in 2 weeks and on the second visit it was apparent that lobes of soil some 1 foot thick had moved down the bowl of the flow.

Mile 642 to 653:

Frequent landslides occur along the west bank of the Mackenzie seated in GLB soils. In this reach the sand and sandy silt member of the sequence is relatively thick although it appears to thin to the north. Frequent sightings of the blue silty clay were found at river level along the banks.

Immediately downstream from Mile 642 and to Mile 646, the landslides have a tendency towards a bi-modal flow type with steep head scarps and lower angle bowls. The angles in the bowls, however, are typically greater than about 15°. It is not clear if these landslides represent a later stage in the development of the block slides found downstream or if they manifest changes in stratigraphy. No discernible changes in soil composition were noted but as the landslides are either partly stabilized and vegetated or well covered over with sandy colluvium from above, the stratigraphy is not clear.

Below Mile 646 and to Mile 655, block slides are common along the west bank of the Mackenzie. At one site, Mile 658, a large intact block of frozen sand and silty clay some 40 ft high and 500 ft long by 200 ft deep is being undercut by the river, Plate 7.

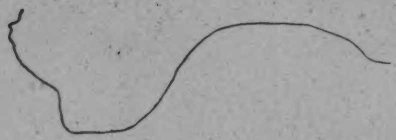

The block has apparently slumped down about 170 ft to its present location and is covered with vegetation identical to stands on the head scarp. Although there is some localized back-tilting of sand-silt layers near the toe the block itself has moved with little apparent rotational movement. The block itself is frozen and well developed ice wedges could be seen along the front of the block.

The landslides in the reach from about Mile 642 and on are associated with severe gullying. This gullying complicates the interpretation of the bank morphology as in some places it appears that the profiles attributed to block slides may have been caused by erosion. When inspected on aerial photographs there appears to be clear evidence of slide activity.

Below Mile 642, bi-modal flows cohabit with block slides and may represent a later stage in a cycle of degradation.

Mile 653:

At Mile 653 the high bank that has been following the shore of the Mackenzie from Mile 642 turns inland along an old abandoned river channel. The old scarps along the west side of the channel have a low angle slope and knobby appearance apparently characteristic of old GLB scarps. The same feature can also be found on the east bank of the Mackenzie opposite the confluence with the Hume River.

Carcajou River (Site C1):

A series of perched bi-modal flows at this site have been inspected from a helicopter and on aerial photographs. The flows occur along the 200 ft high west bank of the Carcajou over a 2 mile reach, and are seated in GLB soils over cretaceous bedrock. As one proceeds up-river the elevation of the bedrock rises and instability is, therefore, seated higher and higher up the bank. Bi-modal flows appear to be active and in one instance a tongue has spilled out and over the bedrock. One large landslide at the beginning of the sequence has elements of slide movements and on aerial photographs the suggestion of a slab-like failure exists.

Mountain River Landslides:

(i) Mountain River (Site M1); Fig A.19, A.20, Plate 9:

A series of MR slides occur on the south bank of the Mountain River at the first bend that is seated in GLB soils. These landslides are deep-seated, exhibiting some degree of back-tilting and have progressed backwards into the GLB upland by a series of retrogressive failures.

A borehole advanced some 400 ft behind the headscarp revealed a soil profile made up of glacial-lake deltaic fine sands and gravels overlying interbedded sands, silts and silty clay. An unfrozen loose sandy silt was encountered at 156 ft below the permafrost table. The detailed borehole log is given in Appendix B. Observations made during the summer 1972 noted gravel up to 3" in diameter in thin seams, and cross bedded and delicately laminated structures in the sands and silts. This soil sequence of sands and interbedded silts and minor clay is, in turn, underlain by a more extensive deposit of blue silty clay.

A tour of the toes of the slides was made by foot, during July 1972, and frequent exposures of Mountain River Blue Clay were noted. In one outcrop it appeared that a once horizontal seam of clay had been squeezed up and out as a sweeping curve of clay protruded above river level. The clay projected out almost at right angles to the bank and then curved upstream. In the area where the blue clay was sampled, a well-developed macrostructure of both vertical and horizontal fissures was observed. Although no ground ice was observed in the blue clay along the landslide toes the well-developed fissuring suggests a former frozen state. The results of the drilling programme show that the undisturbed clay at river level should be found in an unfrozen state.

Recent river action, (July 1972), at the downstream part of the bend has sliced away an excellent exposure of a slump block. Exposed along this cut is a seam of blue fissured clay. In fresh exposures ice lenses could be seen contained along both horizontal and vertical fissures. These lenses appeared to be very thin surface coatings in some instances. No samples could be taken. The clay seam was some 2 ft thick and the fissure system split the clay into blocks some 4 to 8 inches square although much finer features were also evident. It is noteworthy that many vertical veinlets of ice disect the clay. This cutting had also bared a good profile of massive ground ice. On the second visit to this site some 12 days later much of the original exposure had been melted away and a large block of frozen ground had failed in tension due to the severe undercutting during the preceding fortnight. Behind this block the glimmer of massive ground ice could be made out when viewed (in the helicopter) from above. This feature had disappeared completely when the site was visited during March, 1973. The frozen clay found in this section has apparently moved down from higher up in the bank due to landslide movements. The same type of frozen, fissured clay was not encountered in the borehole, M1.

The landslides at this site are characterized by both blocky failures and more multiple forms. Slide blocks exhibit varying degrees of backtilting which becomes more marked as the slide masses fall to near river level. The surface of the slide blocks; that is, the old glacial lake plain surface, are covered with stands of spruce identical to the upland spruce in undisturbed areas. When viewed from the air some of these stands are vertically upright while others are inclined perpendicular to the non-horizontal surface of the slide blocks.

Well-developed gullying is found in conjunction with these slides and commonly extends further back into the upland than do the mass movement features. These gullies are V-shaped, deep seated, and suggest that easily erodible soils make up the bulk of the cross section. These gullies are rimmed along their tops by heavy spruce covers which are commonly forward tilted with vegetation overhangs draped down and over the steep sand slopes of the gullies. These features, in conjunction with recently deposited trees found along the gully floors, suggest that the sand banks are actively melting and that, seasonally, an active layer skin of sand thaws and detaches itself.

Samples were obtained at various depths in boring M1 using a 1-1/2 inch diameter spoon and a 3 inch diameter thick-walled Shelby tube. Full recovery was generally obtained, however, the ends of the Shelby tubes were always buckled. The results of the drilling operations and all pertinent information is presented in Appendix B.

An unnamed MR slide was observed some 2 miles upstream from site M1, Fig A.17, during the aerial reconnaissance of September, 1971. In this slide recent failures near the head scarp have resulted in large tension cracks and tears developing in the slump block near the head scarp.

(ii) Mountain River (Site M2); Fig A.19, Plate 10:

At at least 4 sweeping bends near the mouth of the Mountain River the river is actively eroding fluvial deposits. These deposits are recent in that they are not GLB silts or clays but rather sediments laid down in the flood plain of the Mountain River. When inspected during June, 1972, the bank appeared to be in the order of 15 ft high but at low winter water level they are some 30 ft high. Banks are made up of dark brown silts and sands overlying gravel at river level.

The silts and sands, and likely the gravels, are frozen. Ice lenses were noted at some locations. The action of the river is to erode away and melt out the gravels and some of the silts leaving a slab of frozen silt and sand cantilevered out over the river. As the top of the slab is still covered by the usual organic cover the mass of frozen ground ablates from only the front and the bottom. In some instances the rate of lateral erosion at the bend in the river is such that the tensile strength of the frozen ground is exceeded and a large block falls into the river. The rates of lateral erosion have been estimated by comparing the relative position of the river bank, for the three sites noted on Fig A.19, on aerial photographs taken in 1950, 1967, and 1971. For site M2-1 erosion totalled 210 ft from 1950 to 1967 and 150 ft from 1967 to 1971. For site M2-2, erosion of 160 ft and 300 ft occurred, and for site M2-3, a total of 780 ft was measured between 1950 and 1971.

(iii) Mountain River (Site M3):

The remains of a large, ancient, bimodal flow were noted perched some 50 to 75 feet above bedrock on the right or south bank of the Mountain River, Site M3, Fig A.17. A volume of material in the order of 3×10^8 cu yd has been moved out of the flow area and into the Mountain River. No trace of recent activity is evident.

Hanna and Hume River Landslides (General Observations):

Both the Hanna and the Hume Rivers were inspected by helicopter and water based operations and one site described in the next section was the subject of a winter drilling programme. These two rivers are very similar and develop identical types of landslides.

The Hanna and the Hume meander in a wide channel entrenched up to 100 ft into the surrounding GLB upland. Well-developed thermokarst features pit this upland and extensive frozen ground conditions can be expected. As the rivers meander in their entrenched channels the bends in the river come into contact with, and erode, GLB scarps. The greater percentage of active bends abut this upland and the straighter reaches are cut through recent fluvial deposits.

The frequency and extent of flow landslides along the Hume and the Hanna is striking. A forest fire has recently swept through both areas and the effects of fire coupled with intense river erosion has resulted in active instability.

The landslides observed along the Hanna and the Hume fall into the following types:

(i) Skin Flows

Skin or long ribbon-like flows occur on slopes from 6° to 9°. Movements are shallow and involve the downslope displacement of mineral soil and vegetation covers. These flows occur frequently in burned over areas and they may coalesce to form a large sheet of instability.

(ii) Bi-Modal Flows

Bi-modal flows are common along the banks of both the Hanna and Hume Rivers and are found mainly at river bends. They appear with greater frequency in recently burned over areas. Characteristically, lobe angles of about 6° were measured and even lower angles were noted on aerial surveys. Head scarps range from 12° to steep, about 25° to 30°, inclinations. Although more than one bi-modal flow may be found at any given location each flow has its own circular head scarp. Rapid movements are evident and in many instances terminal zones are thrust out into the river causing a sharp detour of the channel and, in areas, damming the river and hindering boat movement.

(iii) Rotational Slides

Small rotational slides are found in fluvial deposits which are likely unfrozen as they occur immediately adjacent to the river. They rarely extend much behind the trim line. These rotational slides have only been observed along the straighter reaches of the Hanna and may be associated with rapid drawdown conditions due to fluctuating river levels in the Mackenzie or to river erosion. Their proximity to the river and evident rotational aspect suggests that the slides are not associated with frozen ground.

These rotational slides can also be found on the banks opposite bi-modal flows. As the toe of a typical bi-modal flow juts out into the river, the river must rapidly change direction around the toe and in doing so erodes the opposite bank. As bi-modal flows are seated in the GLB upland the opposite bank is made up of recent fluvial deposits.

(iv) Falls

Fall landslides are, however, more common opposite bi-modal flows. The fluvial deposits that are being actively eroded are frozen and well developed ice wedges which have been noted in one clear exposure attest to this condition. Depending on the relative rates of river erosion and thermal degradation a rotational slide may not develop. Instead, extensive thermal and physical erosion results inthe formation of a thermal erosion niche and the failure in tension of a block of frozen ground. This failure mode is referred to as a fall. These falls are seated in fluvial deposits and the consequences of small fall landslides do not seem to be severe because although up to 25 feet of frozen ground may be exposed flow landslides do not develop.

Evidence of small falls can also be seen seated in GLB soils. These falls occur along the top of the trim line in areas where there is little or no protection from erosion by a protective buffer of willows and low brush. Forward tilted trees are considered to be an indicator of these small falls.

Hanna River (Site H1); Fig A.21:

A piezometer test, H1, was made at the base of the head scarp of a bi-modal flow, Fig A.21. An excess pore pressure discussed elsewhere was measured. It should be noted that a series of slope profiles taken of flows along the Hanna River are reported in Tables 2.1 and 2.2.

Hume River (Site HU1); Figs A.17, A.22, A.23, Plates 11, 12:

A series of bi-modal flows can be found at the bend of the Hume River located on Fig A.17. Historically, landslide activity apparently began at the bend in the meander but has since migrated some 2,000 ft downstream along the north-facing bank which is seated in GLB soils. When viewed on 1944 aerial coverage the bi-modal aspect of these flows was evident as the most easterly flow was still active and a steep headscarp region could be seen to be melting. In 1944 an extensive tongue reached out into and crossed the 250 ft wide channel causing severe erosion of the opposite bank and a sharp detour of the river. This most recent flow has now receeded back from the river as far as it can go and there is no evidence of headscarp activity. The bowl of the flow is treed with light brush and the prominent 1944 tongue has been almost eroded away. The large cut made in the opposite north bank is partly infilled. This cycle of cutting and infilling has also occurred in the past along the north bank as evidence of a slip-off slope and a refilled channel section can be seen upstream of the present cut.

The bowl of the most recent flow now lies at an angle of about 4° overall compared with the average 12.3° slope of the south bank immediately downstream. Downstream from the flow and along the toe of the relatively undisturbed bank some form of instability process is indicated by instability in a row of large spruce bordering the bank.

A series of borings were advanced in an undisturbed portion of the glacial lake scarp downstream from the most recent flow in order to re-create pre-flow conditions. Boring HU1-2 was located within 100 ft of the Hume River and was only advanced 57 ft. No boring was made in the centre of the river and, therefore, it is not known if permafrost will be found beneath the river. However, it is expected that the Hume River will not freeze up completely during the winter months and by maintaining an average temperature greater than 0°C will not have permafrost beneath it. Furthermore, as neither boring HU1-1 or HU1-3 penetrated the permafrost table the exact position of the 0°C isotherm is unknown. The most likely position is shown in Fig A.23

The borings advanced at the Hume River site were drilled up to a depth of 150 ft using air return. No difficulty was experienced with clogging and frozen clay chips were brought to the surface. Sampling using thick-walled 3" Shelby tubes was attempted but the tubes buckled on insertion and sampling was limited to the 1-1/2 in and 3 in split spoon samplers.

The borehole logs are given in Appendix B as are plots of water (ice) content with depth. It should be noted that the water (ice) contents in hole HU1-2 are higher in the first 20 ft than in the other 2 borings. These higher water contents reflect the difference in sampling technique as large bags of chip samples were taken in HU1-2 while water content samples were taken from the split spoons for the other 2 borings.

Atterberg liquid and plastic limits are also shown in Appendix B in relation to the water (ice) contents. It can be seen that the limits are essentially constant over the entire depth.

The soil encountered in all borings is a brown silty clay, CL, with the exception of a lense of brown clayey silt, CL, found at 6 - 8 ft in HU1-1. This conclusion is, however, not based on continuous sampling.

The ground ice conditions at the Hume River site have been logged according to the NRC classification. The dominant ice type is classified as Vr which occurs in sub-horizontal and sub-vertical lenses of varying thickness up to about 1-1/2 inches. The ground ice encountered appears to make up a lattice-like structure surrounding large masses of overconsolidated silty clay with water contents as low as from 19.1% to 21.0%.

Hume River (Site HU2); Fig A.24:

A series of bi-modal flows located at the northernmost bend in the Hume River are sketched on an overall plan, Fig A.24. Seen on low altitude 1944 aerial coverage steep head scarps are evidently melting and large amounts of thawed soil are being deposited in the Hume River. Active flows have caused the river to detour around the toe and to actively erode the opposite banks. Scars of many older flows line steeper scarps abutting the GLB upland and the only sections in which evidence of movement is absent is along low lying terrace scarps.

The rate of back-sapping of the head scarp of one of the bi-modal flows noted on Fig A.24 can be calculated by comparing 1944, 1950 and 1971 aerial photography. The scarp has moved back 250 ft from 1944 to 1950 at an average rate of 40 ft/yr. From 1950 to 1971 the total movement was another 250 ft but by 1971 the landslide was stable and inactive and the prominent toe partly eroded away.

Hume River (Site HU3); Fig A.17:

A series of MR slides are seated along the east bank of the Hume River as located on Fig A.17. The bank heights in this reach are estimated to be at least 150 ft. Probably soil stratigraphy is sand over clay at river level. Sand is expected in the sequence as there are several deep-seated gullies in association with these slides.

A. 2 OBSERVATIONS ON PERMAFROST CONDITIONS

Ice-rich soil has been found in the headscarps of bi-modal flows in all parts of the study area. Although many of the smaller bi-modal flows found throughout the study area were not studied in any detail, well-developed ground ice was always found in the headscarps of those flows that were investigated. The ice encountered appeared to be of the segregated variety and was seen as frequently spaced rhythmically banded lenses of approximately 1/16 to 1/8 inch in thickness and with a frequency of 1/4 to 1/2 inch. In some instances these closely spaced lenses graded into frozen soils with more or less uniform conditions separated by thicker ice lenses of clear ice, sometimes with soil inclusions, of from 1/2 to 2 inches in thickness. A similar distribution of ice forms was found along the east scarp of the Fort Simpson Landslide where the gradation of fine rhythmically banded ice into more massive ice lenses of up to, at least, 5 to 10 inches in thickness was observed in a scarp some 70 feet high. It can also be noted that the matrix of frozen soil contained within the thicker ice lenses is sometimes laced with a renticular network of sub-vertical and horizontal ice veinlets. The renticular, three-dimensional, ground ice form was found in test pits dug at the head scarp of the Fort Norman Landslide, Fig A.15, and at the Hanna Island Landslide, A.18, although the thicker lenses were not observed. This lattice ice is usually from 1/8 to 1/4 inch in thickness and splits the soil mass into a series of blocks or lumps.

Segregated ice was also found in the headscarps of bi-modal flows seated in GLB soils near Mile 350 and in one flow investigated at Mile 642 but was not logged in any detail. Frozen ground was encountered in a test pit dug at the base of the headscarp at the Little Norman Landslide, Fig A.16, but may have represented yet unthawed seasonal ice.

Frozen ground conditions have also been found in the lobes of many bi-modal flows. Hand probes made in the lobe of the Fort Norman Landslide, Fig A.15, encountered frozen soil and a smooth thaw interface at depths of from 1.6 to 3.1 ft and at 1.5 ft in the Hanna River Landslide, Fig A.21. Probing with a 1/4 in metal rod has confirmed frozen conditions in the lobes of many of the smaller flows (see Sec 2.1.2). Frozen conditions were confirmed by driving the steel probe into the frozen layer with a hammer and assessing the resistance to torque once it has firmly seated.

Ground ice has also been found in conjunction with the bi-modal flows found along the Mackenzie, from Mile 440 to 480. These ground ice conditions were not investigated in detail at any particular site but, on the basis of observations made at chance exposures, a composite picture emerges. At Mile 470 a large mass of frozen slumped silty clay was observed at river level. Ground ice could be seen on June 16, 1972, where the block had been undercut by the river but by July 16, 1972, no trace of the block remained. Lattice ice in the form of vertical veinlets and horizontal lenses contained in a matrix of fissured silty clay was observed. Thermal erosion niches at river level are common and are associated with frozen ground conditions. At one location, just upstream from Mile 480, a very recent exposure some 20 to 25 ft high of colluvial material revealed small ice lenses. In the reach from Mile 440 to 480 small bi-modal flows, elsewhere associated with melting ground ice are common in spruce covered banks that are not otherwise failing and seeps noted in the tongue area of the Old Fort Point Landslide may be derived from melting ice.

The clearest evidence of permafrost conditions were presented at the Ice Buttress Landslide, Mile 473, Plate 5, where a large block of frozen sand was found cantilevered out over silty clay GLB soils. Small ice wedges could be seen in the frozen sand which was continuously melting and spalling off.

Frozen ground conditions have been found in conjunction with the block and MR slides classified in the study area. The best evidence was found at Mile 565 where a large block slide has moved down some 170 ft and has been undercut about 10 to 15 ft in along the toe.

Well-developed ice wedges exposed along the block face and the magnitude of the undercutting attest to the presence of frozen conditions. As the block sits out in the river it is exposed in all dimensions. On the upstream side of the block a large crack infilled with roots and ground ice can be seen running into the block parallel with the river. This crack is not an ice wedge and none of the ice wedges along the toe exhibited similar features. This large crack appears to be a tension crack feature associated with instability in the block slide and the ground ice encountered can be classified as tension crack ice (Mackay, 1972).

River action has sliced away an excellent exposure of frozen soil in the toe of one of the MR slides found on Mountain River. Exposed along this cut is a seam of Mountain River Blue Clay and in fresh surfaces lattice ice could be seen which, in some instances, appeared as very thin surface coatings. These horizontal and vertical lenses impart a fissure structure to thawed clay and split the clay into blocks some 4 to 8 inches square, although much finer features were also evident. The river action had also bared an exposure of massive ice. On the second visit to this site some 12 days later much of the original exposure had been melted away and a large fall had occurred as a result of the severe undercutting of the preceding fortnight. This fall consisted of a large block of frozen ground that had failed in tension and behind this block the glimmer of thick ice lenses could be seen when viewed from above in a helicopter.

There were a range of features observed during the survey that suggest the presence of permafrost conditions in areas of active bank instability. Although no direct evidence exists in support of some of these features there is such a paucity of information in general about permafrost conditions in the study area that it is useful to review them.

In some reaches of the Mackenzie River rapid changes in the attitudes of generally flat-lying sand-silt varves suggest conditions in which ground ice contained below the now tilted strata has melted out causing subsidence. Block and MR slides can be found in conjunction with a GLB sequence of sand over sand-silt varves over blue silty clay in certain portions of the Mackenzie River. These sand-silt varves are usually horizontal but frequent observation has been made of rapid changes in these varves resulting in apparent dips of up to 15° upstream or downstream parallel with the bank and gentle anticlinal features have also been noted. These abrupt changes in dip seldom are found along sections of bank greater than 100 to 200 ft. As these features are found in banks where block or MR slides are either active or in which older features can be seen on aerial photographs it is possible that they are caused by landslides. Areas with these features have been found at Miles 298 - 302, Miles 306 - 310 and Miles 513 - 516 and in these reaches landslides are common. However, these tilted strata have also been found at Mile 556 where a steep, 150 ft high, exposure of GLB sands, sand-silts and silty clay at river level is found in a headland being actively eroded by the river. No landslides occur in the area and a detailed inspection of aerial photographs shows no trace of any deep-seated landslides. However, a high flood plain terrace is found along the top of the bank. As the navigation channel is routed beneath the bank river erosion must be active and in any other reach of the river, block or MR slides would be expected. It is possible that historically all permafrost melted beneath the river when it occupied the terrace causing subsidence and tilting of the strata beneath. Permafrost may not have been re-established in the bank or, if it has, has not resulted in the formation of conditions that promote bank instability.

Permafrost conditions and high ice content soils can be reasonably inferred for a MR slide at Mile 350 and at Axel Island, Mile 621. In these slides bi-modal flows are common along the toe. At Mile 350 one flow was inspected in detail and segregation ice found in an exposure some 15 ft high in the head scarp of the flow. No detailed inspection was made of the bi-modal flows superimposed on the Axel Island Landslide but they are in all respects similar to flows found throughout the study area and which only occur in ice rich soils. The presence of these flows which require ice rich soils for their continued activity, therefore, strongly predict the existence of permafrost conditions within the overall slide mass. At Axel Island, permafrost conditions are also suggested by the thermokarst lakes in a GLB plain behind the head-scarp of the MR slide.

A feature resembling a bi-modal flow in profile was found in a MR slide at Mile 300. This cirque-shaped bowl is seated in silty clay and is found in the toe of an active MR slide. It may have been caused by subsidence due to melting ice in the silty clay or in the silty portions at the base of the sand-silt varves. Probing encountered what is believed to be frozen soil at 3 ft in the bowl of the depression but although the melt water found in the bowl was exceedingly cold no visual confirmation of ground ice was made.

Frozen conditions are also inferred along the banks of the Mountain and Hume Rivers where fall landslides and thermal erosion niches have been found. Although ice wedges, Table 2.6, have been found here and there in chance exposures, no other visual evidence of ground ice can be cited. However, as the sediments consist of coarse-grained sands and gravels with some silt it is quite evident that they are frozen or they would be unable to maintain their over-steepened position.

Permafrost conditions are also inferred in the headscarp of the bi-modal flow at Mile 218, Table 2.2. The headscarp of this flow has failed in a rotational fashion and a large rotational slide rings the headscarp A small rivulet with a significant flow of water issues forth from a large gully in the middle of the headscarp slide. This gully was followed to its source inside the rotational slide and a tour of the headscarp behind the slide revealed no extension to the rivulet. It is inferred, therefore, that the stream has as a source, melting ground ice.

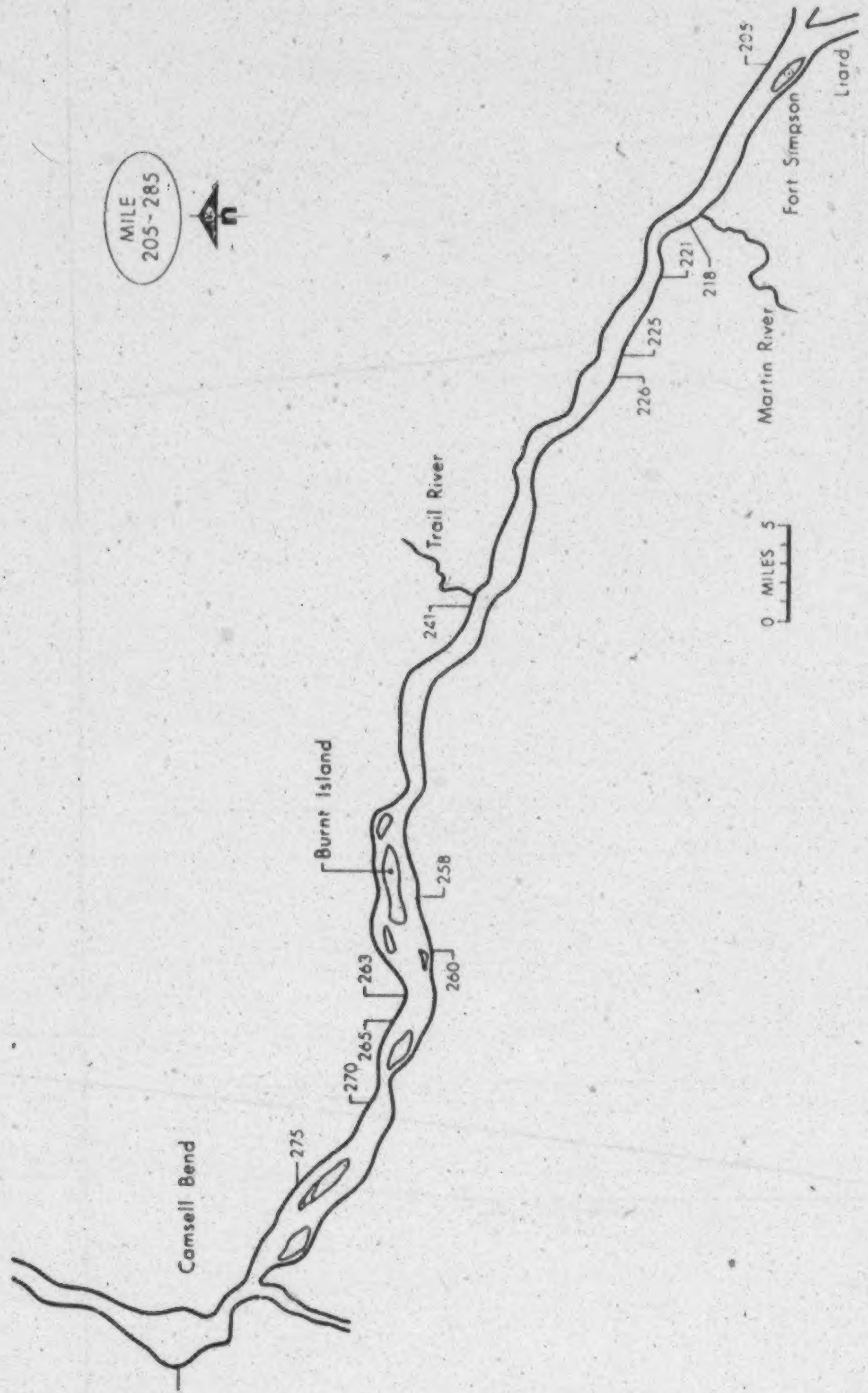
MILE
205-285
Camsell Bend
285
275
270
265
263
260
258
Burnt Island
241
Trail River
226
225
221
218
Martin River
Fort Simpson
Liard
205
0 MILES 5

Fig A.1 Mile 205 - 285

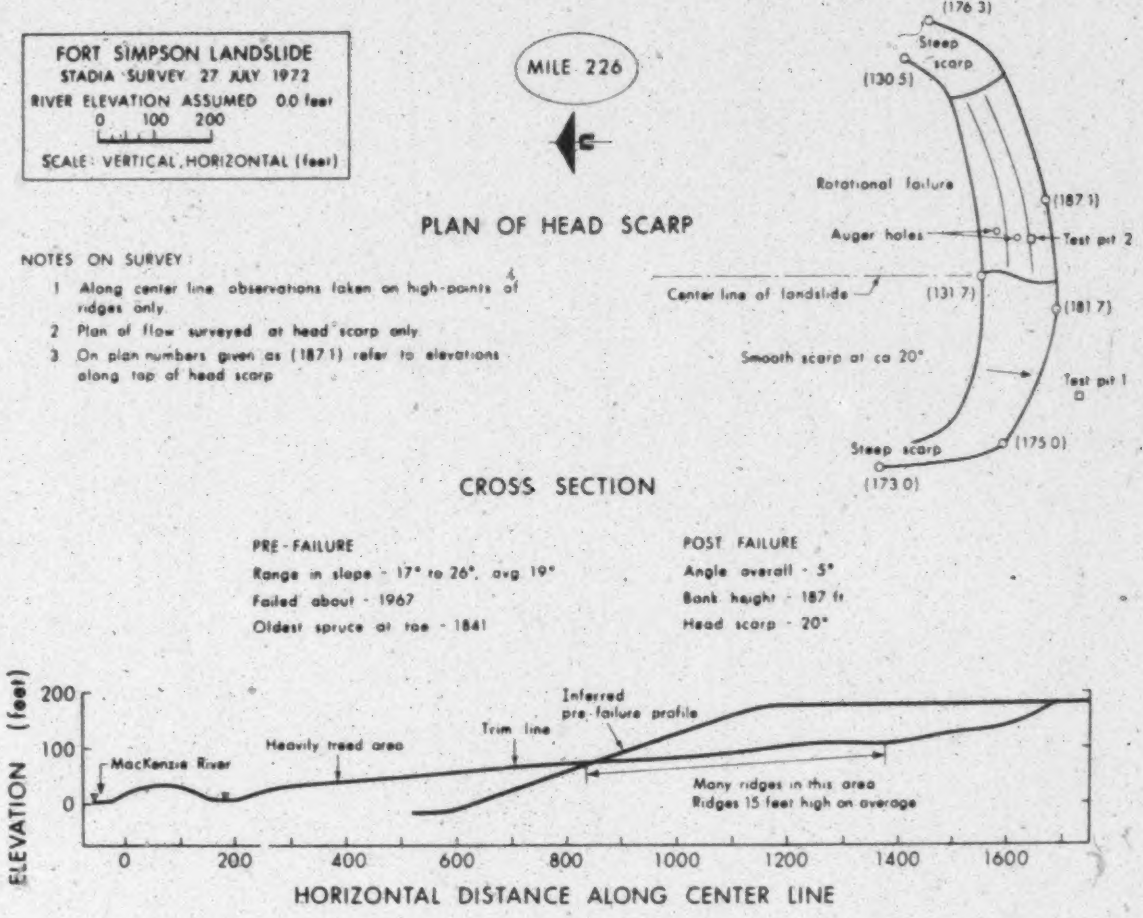
FORT SIMPSON LANDSLIDE
STADIA SURVEY 27 JULY 1972
RIVER ELEVATION ASSUMED 0.0 feet
0 100 200
SCALE: VERTICAL, HORIZONTAL (feet)
MILE 226
PLAN OF HEAD SCARP
(176.3)
Steep scarp
(130.5)
Rotational failure
(187.1)
Auger holes
Test pit 2
Center line of landslide
(131.7)
(181.7)
Smooth scarp at ca 20°
Test pit 1
Steep scarp
(175.0)
(173.0)
CROSS SECTION
ELEVATION (feet)
200
100
0
MacKenzie River
Heavily treed area
Trim line
Inferred pre-failure profile
Many ridges in this area
Ridges 15 feet high on average
0
200
400
600
800
1000
1200
1400
1600
HORIZONTAL DISTANCE ALONG CENTER LINE

NOTES ON SURVEY:

1. Along center line observations taken on high-points of ridges only.
2. Plan of flow surveyed at head scarp only.
3. On plan numbers given as (187.1) refer to elevations along top of head scarp.

PRE-FAILURE
Range in slope - 17° to 26°, avg 19°
Failed about - 1967
Oldest spruce at toe - 1841

POST FAILURE
Angle overall - 5°
Bank height - 187 ft
Head scarp - 20°

Fig A.2 Fort Simpson Landslide

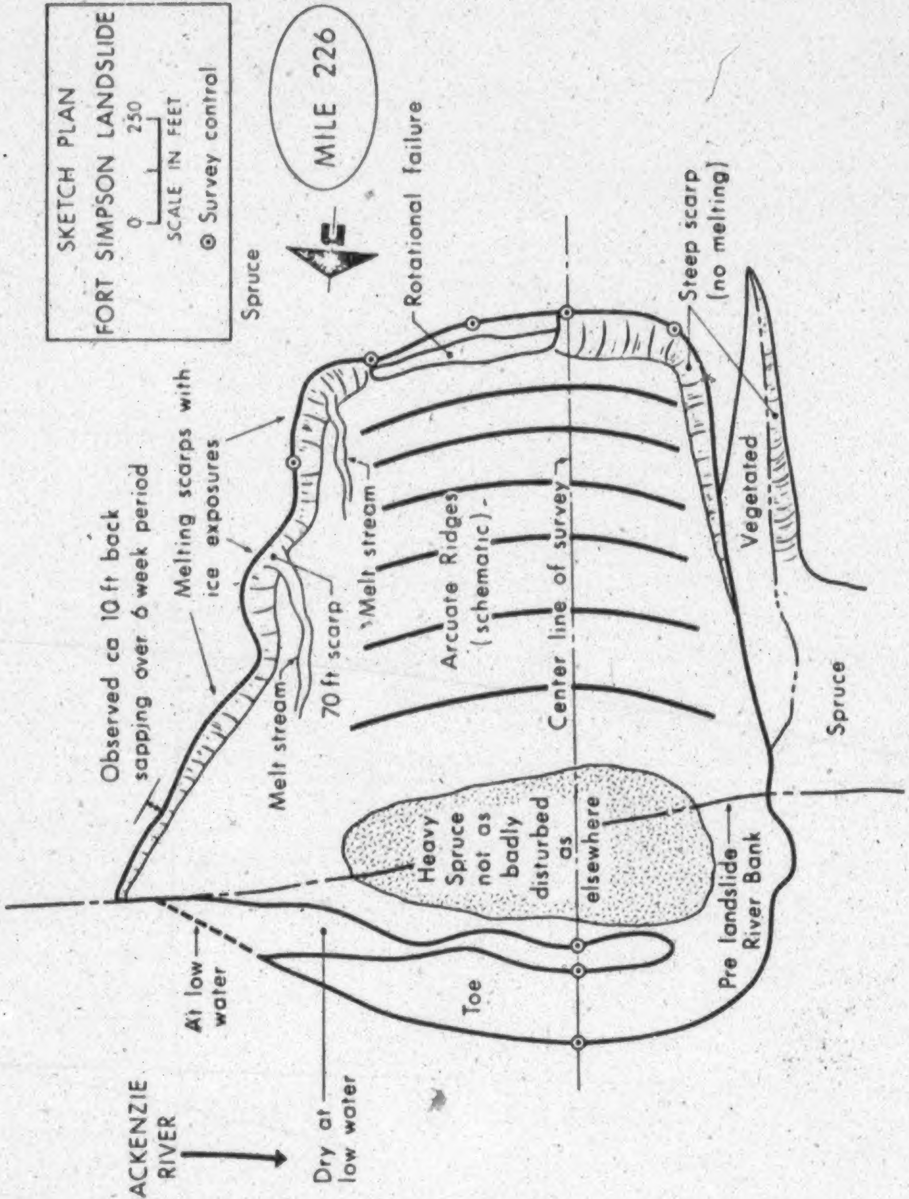
SKETCH PLAN
FORT SIMPSON LANDSLIDE
0
250
SCALE IN FEET
⊙ Survey control
MILE 226
N
Spruce
Rotational failure
Steep scarp (no melting)
Vegetated
Spruce
Observed ca 10 ft back sapping over 6 week period
Melting scarps with ice exposures
Melt stream
70 ft scarp
Melt stream
Melt stream
Arcuate Ridges (schematic)
Center line of survey
Heavy Spruce not as badly disturbed as elsewhere
Pre landslide River Bank
Toe
At low water
Dry at low water
MACKENZIE RIVER

Fig A.3 Fort Simpson Landslide

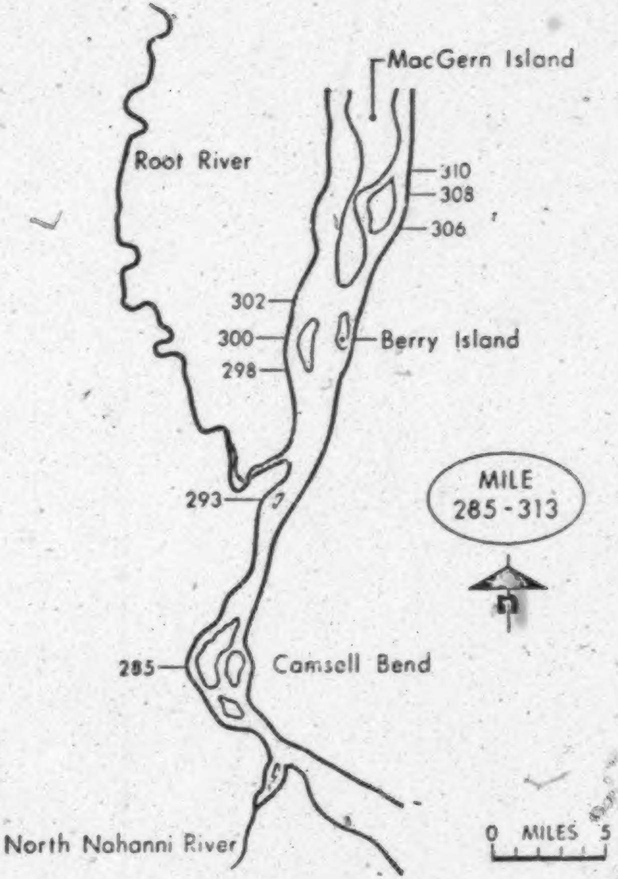
Root River
MacGern Island
310
308
306
302
300
298
Berry Island
293
MILE
285 - 313
285
Camsell Bend
North Nahanni River
0 MILES 5

Fig A.4 Mile 285 - 315

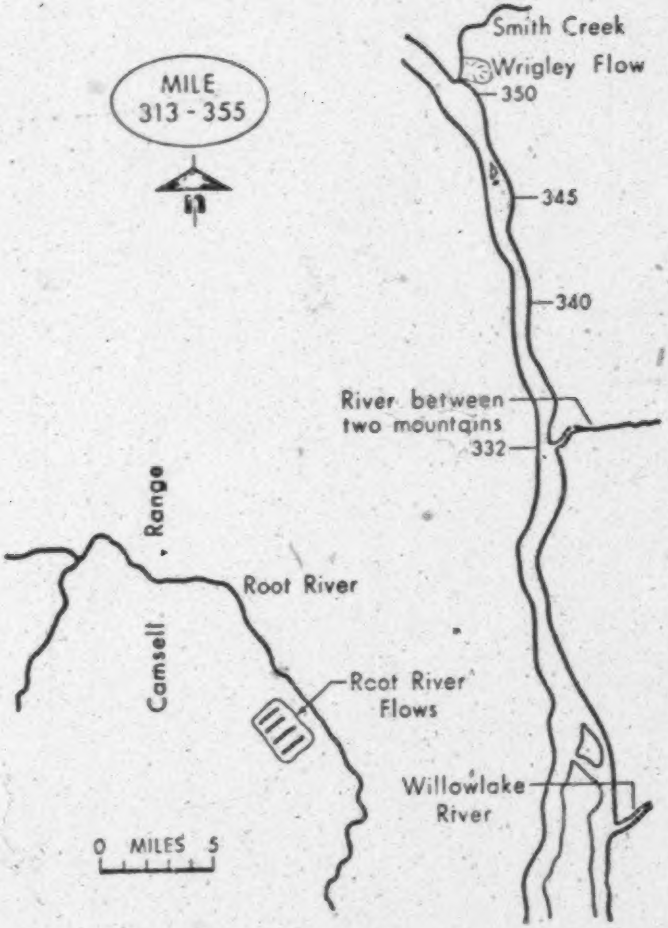
MILE
313 - 355
Smith Creek
Wrigley Flow
350
345
340
River between two mountains
332
Range
Camsell
Root River
Root River Flows
Willowlake River
0 MILES 5

Fig A.5 Mile 313 - 355

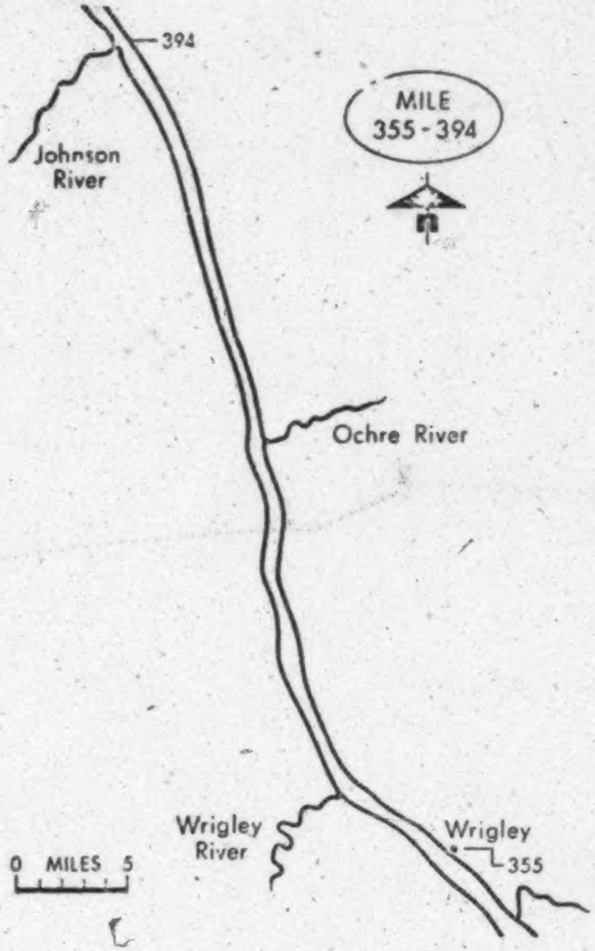
394
Johnson River
MILE 355-394
Ochre River
Wrigley River
Wrigley
355
0 MILES 5

Fig A.6 Mile 355 - 394

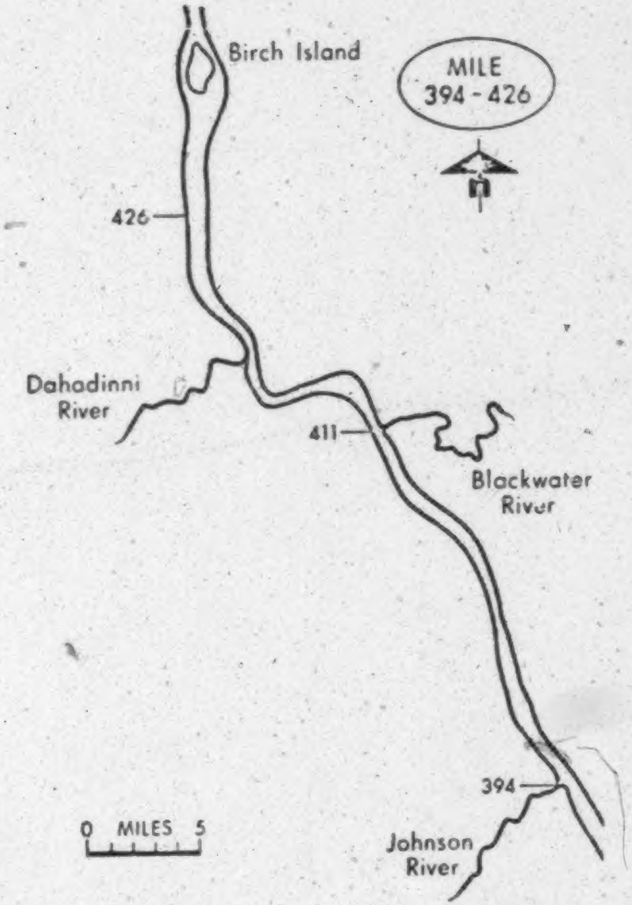
Birch Island
MILE 394-426
426
Dahadinni River
411
Blackwater River
394
Johnson River
0 MILES 5

Fig A.7 Mile 394- 426

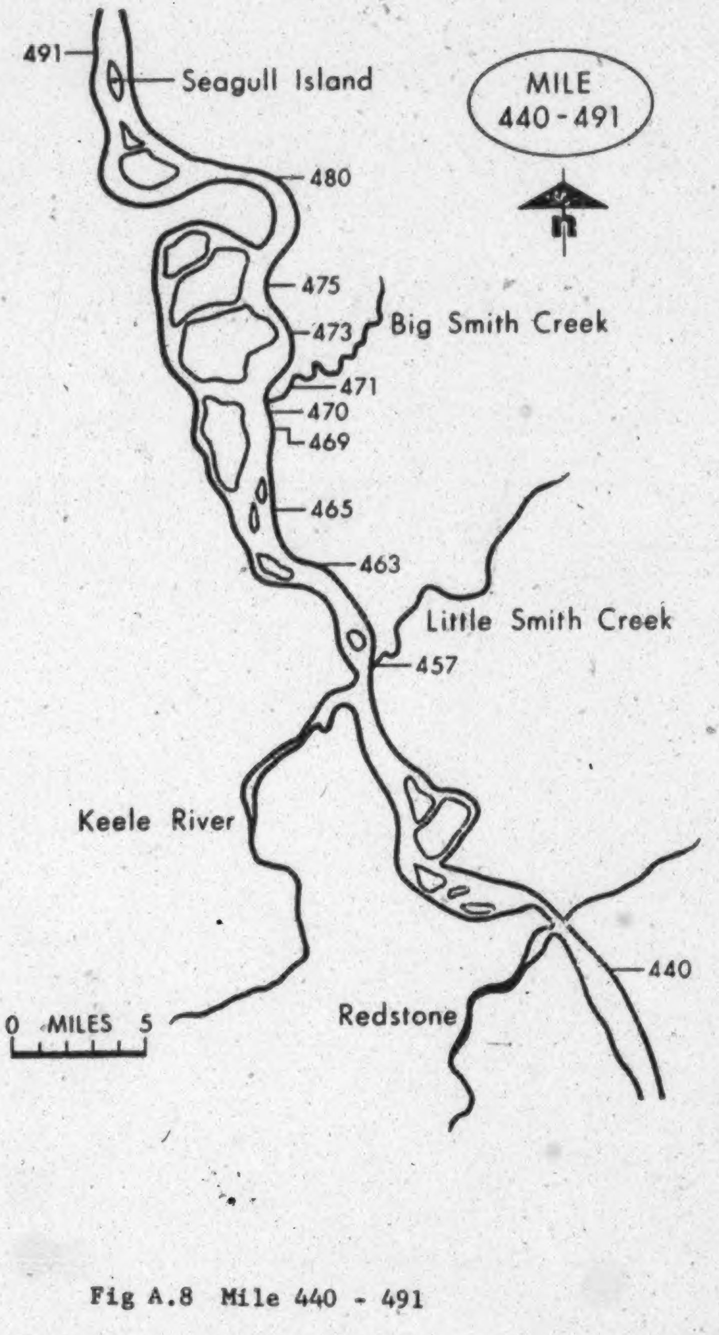
491
Seagull Island
MILE 440 - 491
480
n
475
473
Big Smith Creek
471
470
469
465
463
Little Smith Creek
457
Keele River
440
Redstone
0 MILES 5

Fig A.8 Mile 440 - 491

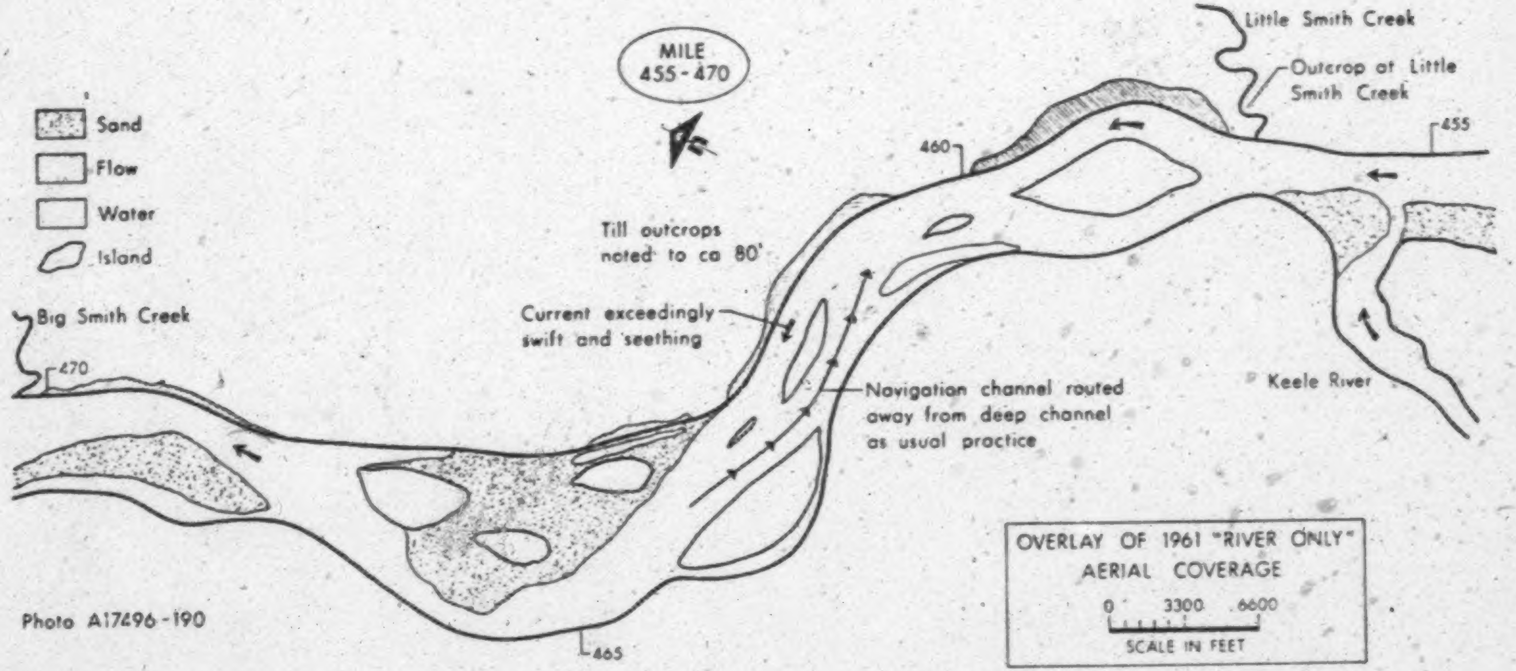
MILE
455-470
Sand
Flow
Water
Island
Big Smith Creek
470
Till outcrops
noted to ca 80'
Current exceedingly
swift and seething
Navigation channel routed
away from deep channel
as usual practice
460
465
455
Little Smith Creek
Outcrop at Little
Smith Creek
Keele River
OVERLAY OF 1961 "RIVER ONLY"
AERIAL COVERAGE
0
3300
6600
SCALE IN FEET

Photo A17496-190

Fig A.9 Mile 455 - 470

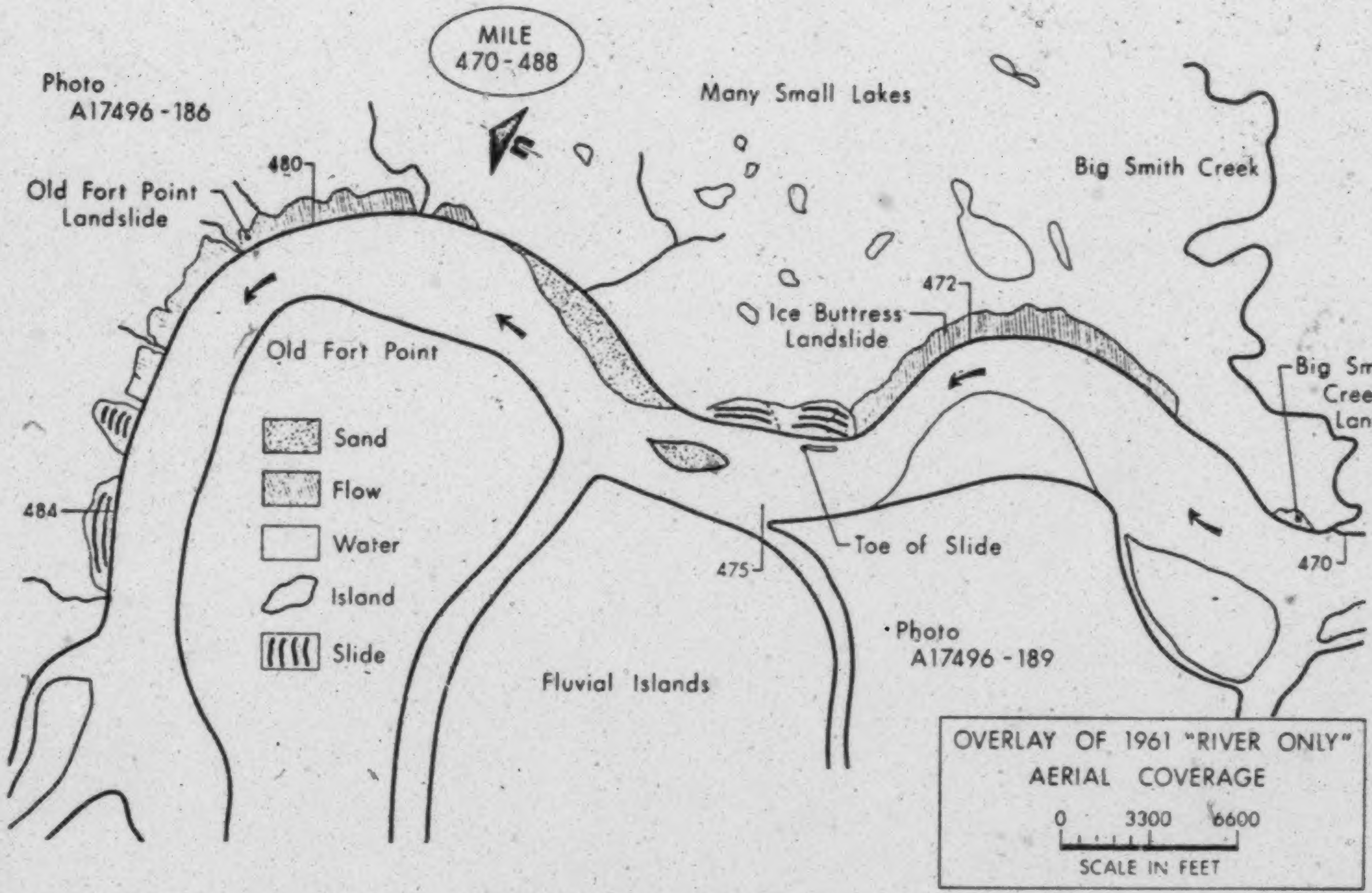
MILE
470-488
Photo
A17496-186
Many Small Lakes
Big Smith Creek
480
Old Fort Point
Landslide
Old Fort Point
Ice Buttress
Landslide
472
Big Smith
Creek
Landslide
Sand
Flow
Water
Island
Slide
484
475
Toe of Slide
470
Photo
A17496-189
Fluvial Islands
OVERLAY OF 1961 "RIVER ONLY"
AERIAL COVERAGE
0
3300
6600
SCALE IN FEET

Fig A.10 Mile 470 - 488

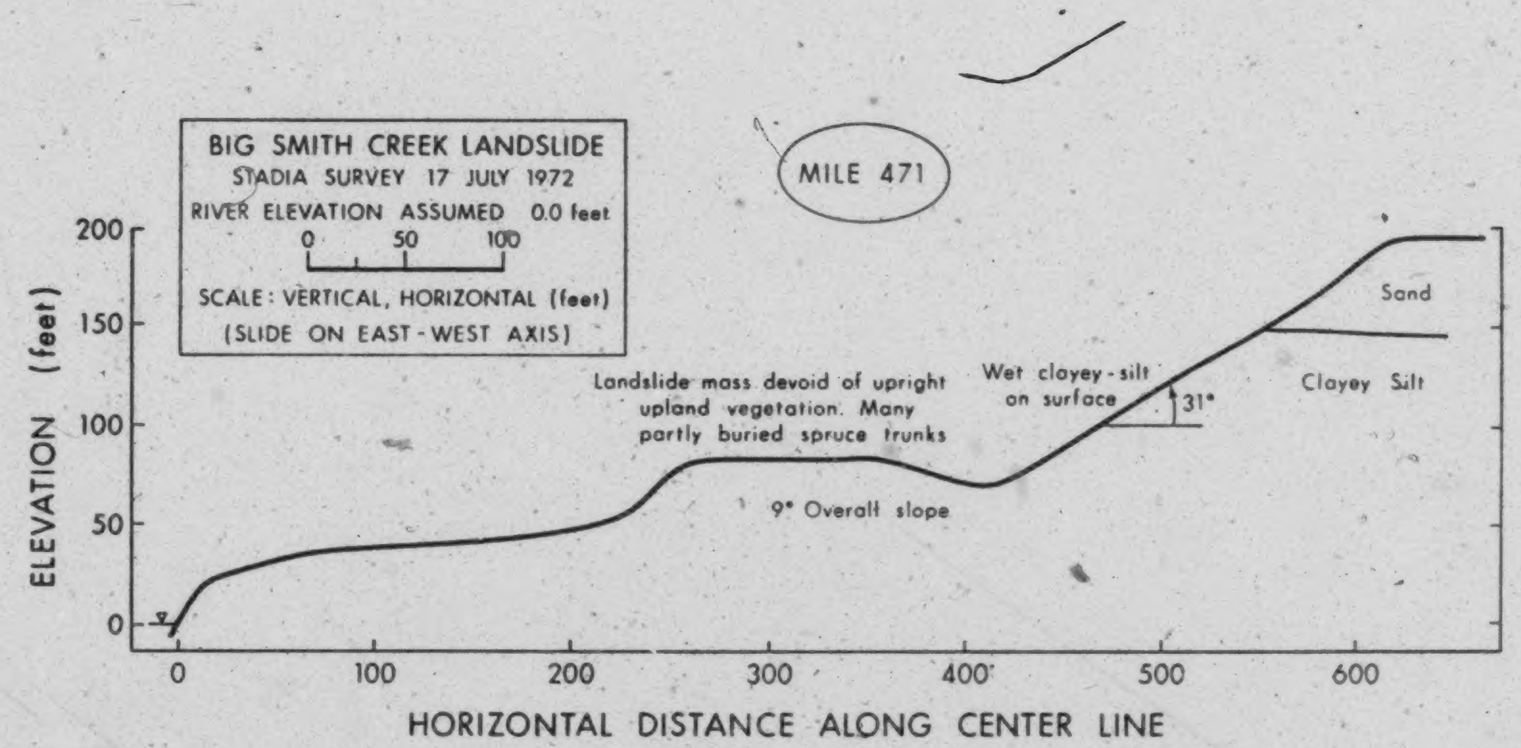

Fig A.11 Big Smith Creek Landslide

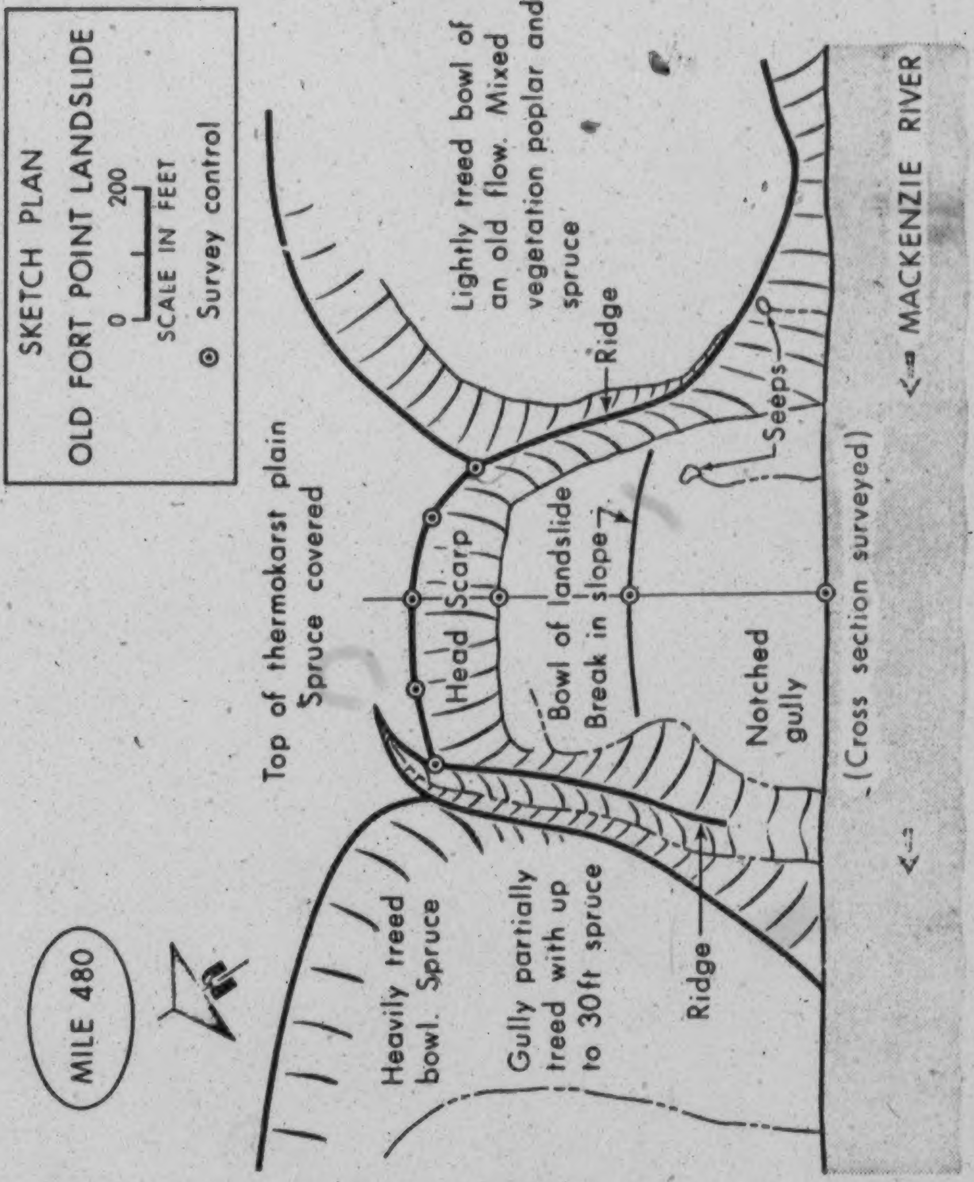
SKETCH PLAN
OLD FORT POINT LANDSLIDE
0
200
SCALE IN FEET
⊙ Survey control
MILE 480
N
Top of thermokarst plain
Spruce covered
Lightly treed bowl of an old flow. Mixed vegetation poplar and spruce
Ridge
Head Scarp
Bowl of landslide
Break in slope
Seeps
Notched gully
Heavily treed bowl. Spruce
Gully partially treed with up to 30ft spruce
Ridge
(Cross section surveyed)
MACKENZIE RIVER

Fig A.12 Old Fort Point Landslide

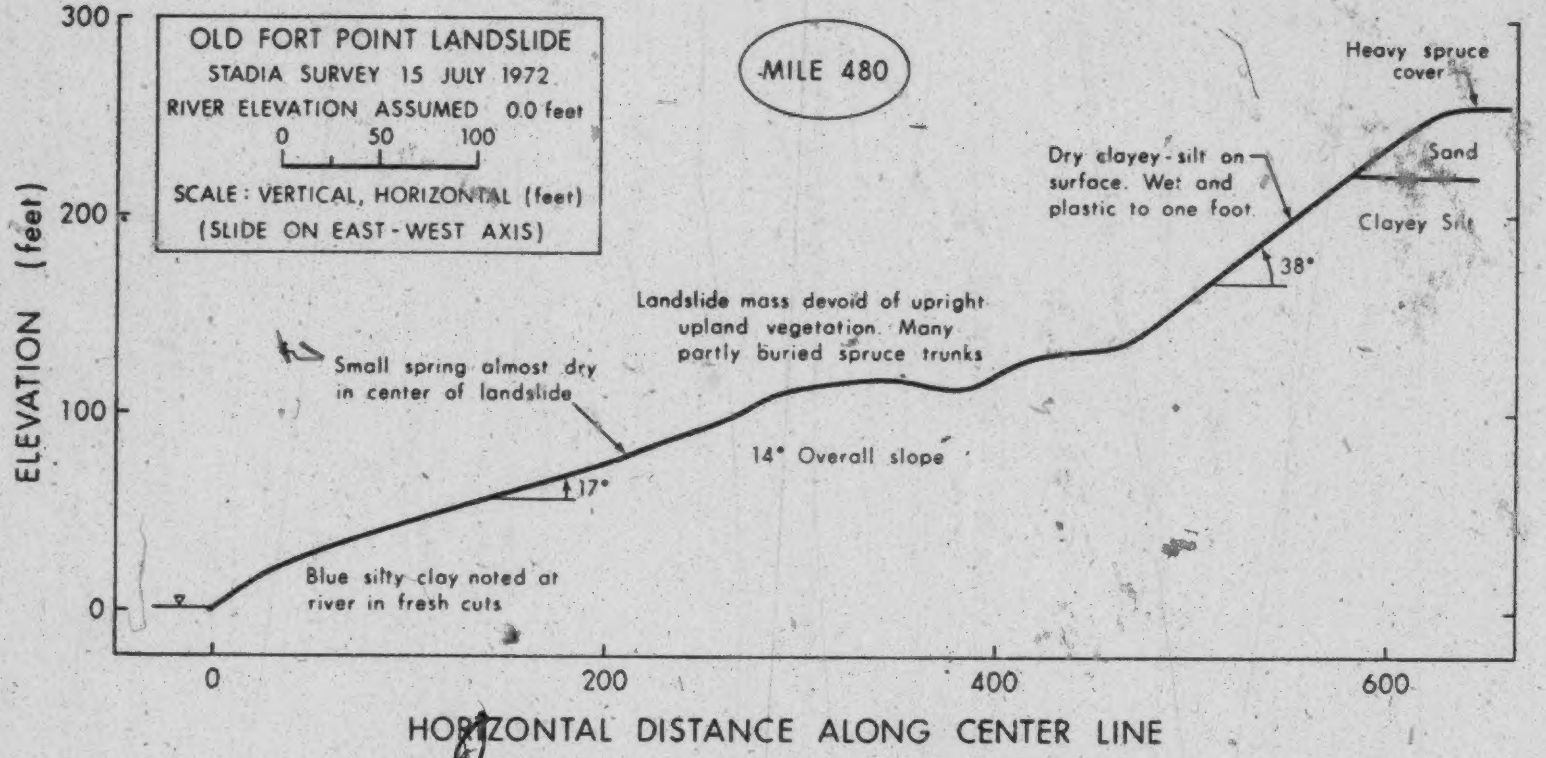

Fig A.13 Old Fort Point Landslide, Sketch Plan

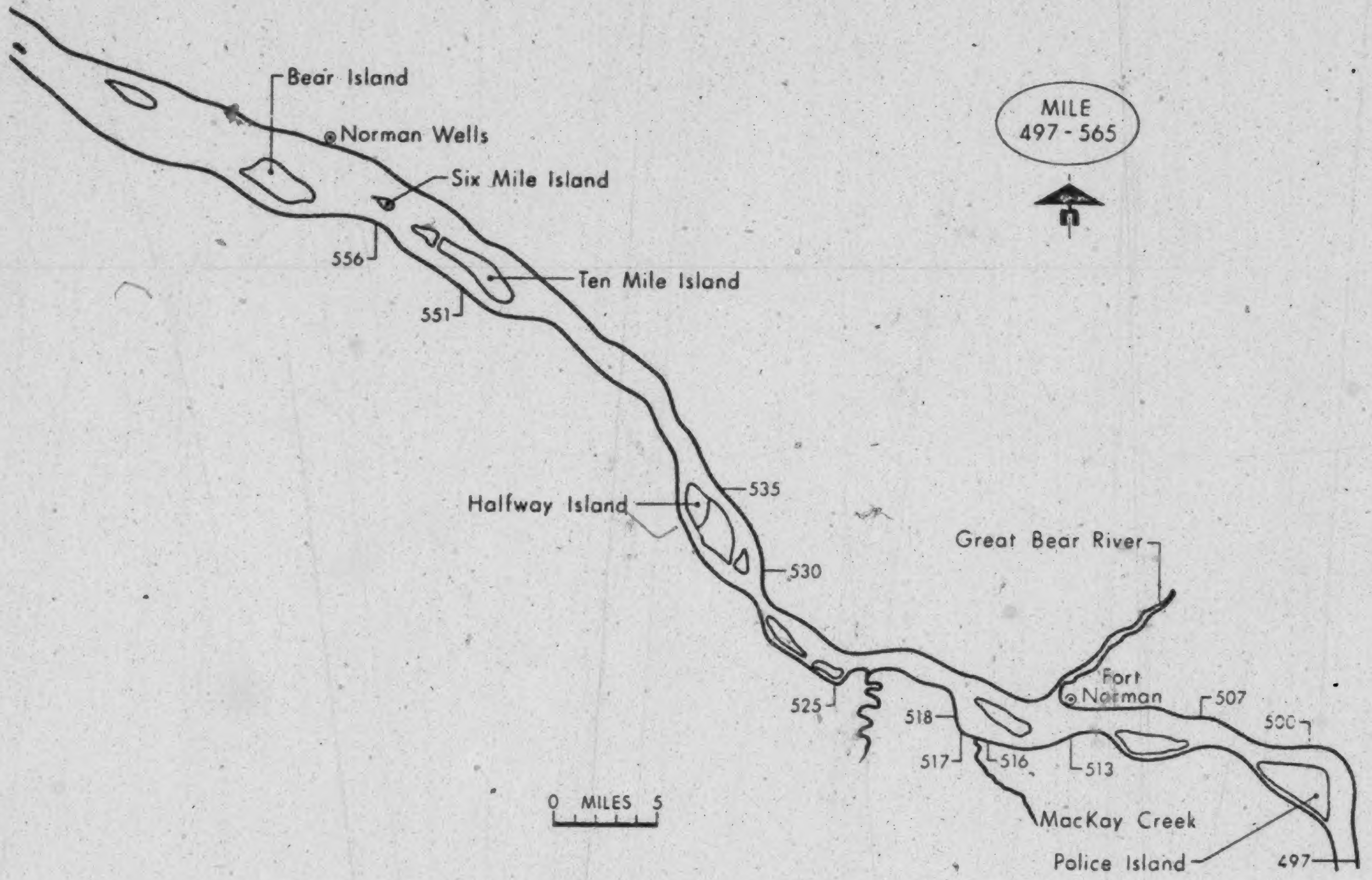
MILE
497 - 565
Bear Island
Norman Wells
Six Mile Island
556
Ten Mile Island
551
Halfway Island
535
530
Great Bear River
Fort Norman
507
500
525
518
517
516
513
MacKay Creek
Police Island
497
0 MILES 5

Fig A.14 Mile 497 - 565

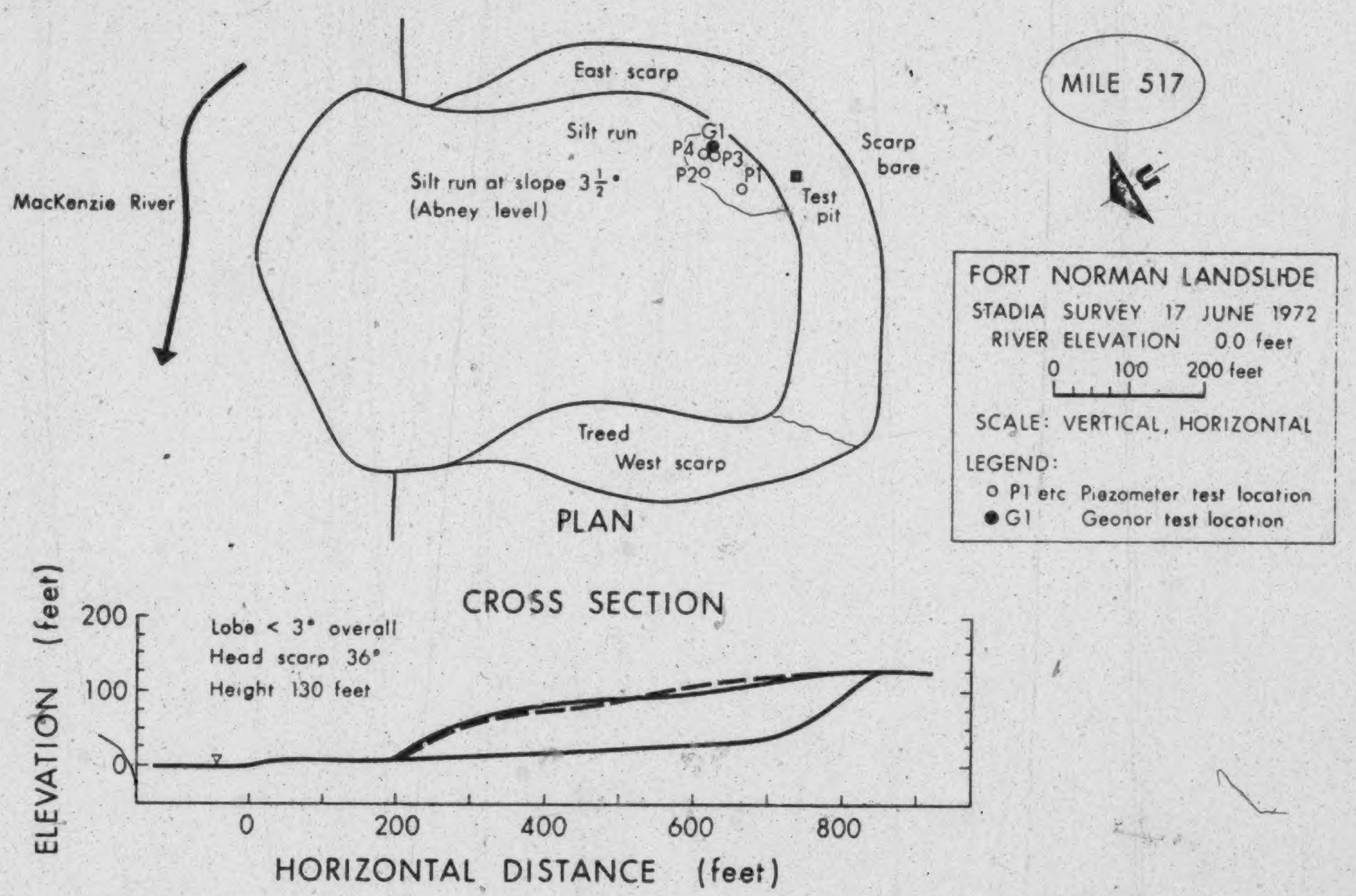
MILE 517
FORT NORMAN LANDSLIDE
STADIA SURVEY 17 JUNE 1972
RIVER ELEVATION 0.0 feet
0 100 200 feet
SCALE: VERTICAL, HORIZONTAL
LEGEND:
○ P1 etc Piezometer test location
● G1 Geonor test location
MacKenzie River
East scarp
Silt run
Silt run at slope 3½°
(Abney level)
G1
P4
P3
P2
P1
Test pit
Scarp bare
Treed
West scarp
PLAN
CROSS SECTION
Lobe < 3° overall
Head scarp 36°
Height 130 feet
ELEVATION (feet)
200
100
0
HORIZONTAL DISTANCE (feet)
0
200
400
600
800

Fig A.15 Fort Norman Landslide

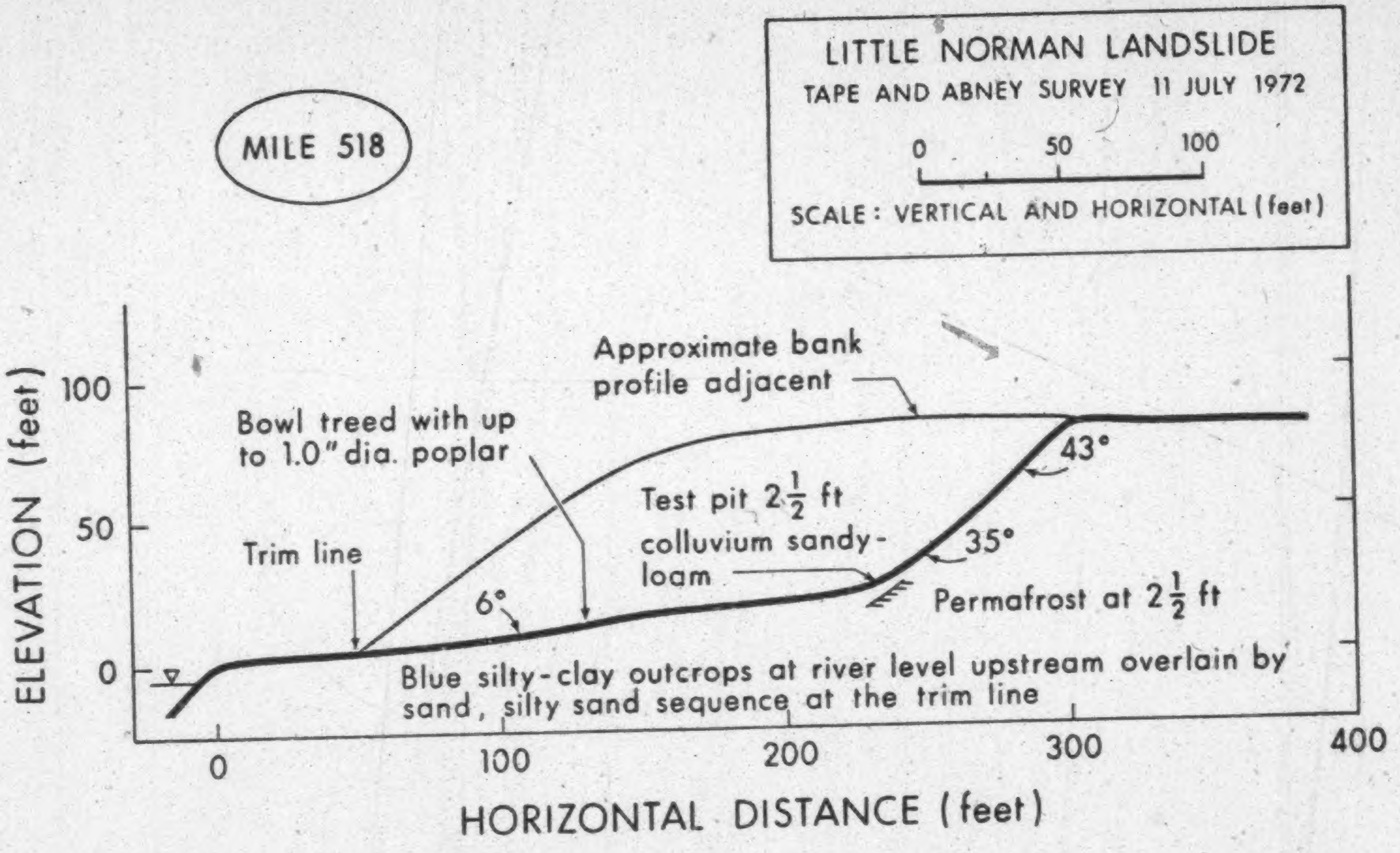
MILE 518
LITTLE NORMAN LANDSLIDE
TAPE AND ABNEY SURVEY 11 JULY 1972
0
50
100
SCALE : VERTICAL AND HORIZONTAL (feet)
Approximate bank profile adjacent
Bowl treed with up to 1.0" dia. poplar
Test pit 2 1/2 ft
colluvium sandy-loam
43°
35°
Permafrost at 2 1/2 ft
Trim line
6°
Blue silty-clay outcrops at river level upstream overlain by sand, silty sand sequence at the trim line
ELEVATION (feet)
100
50
0
HORIZONTAL DISTANCE (feet)
0
100
200
300
400

Fig A.16 Little Norman Landslide

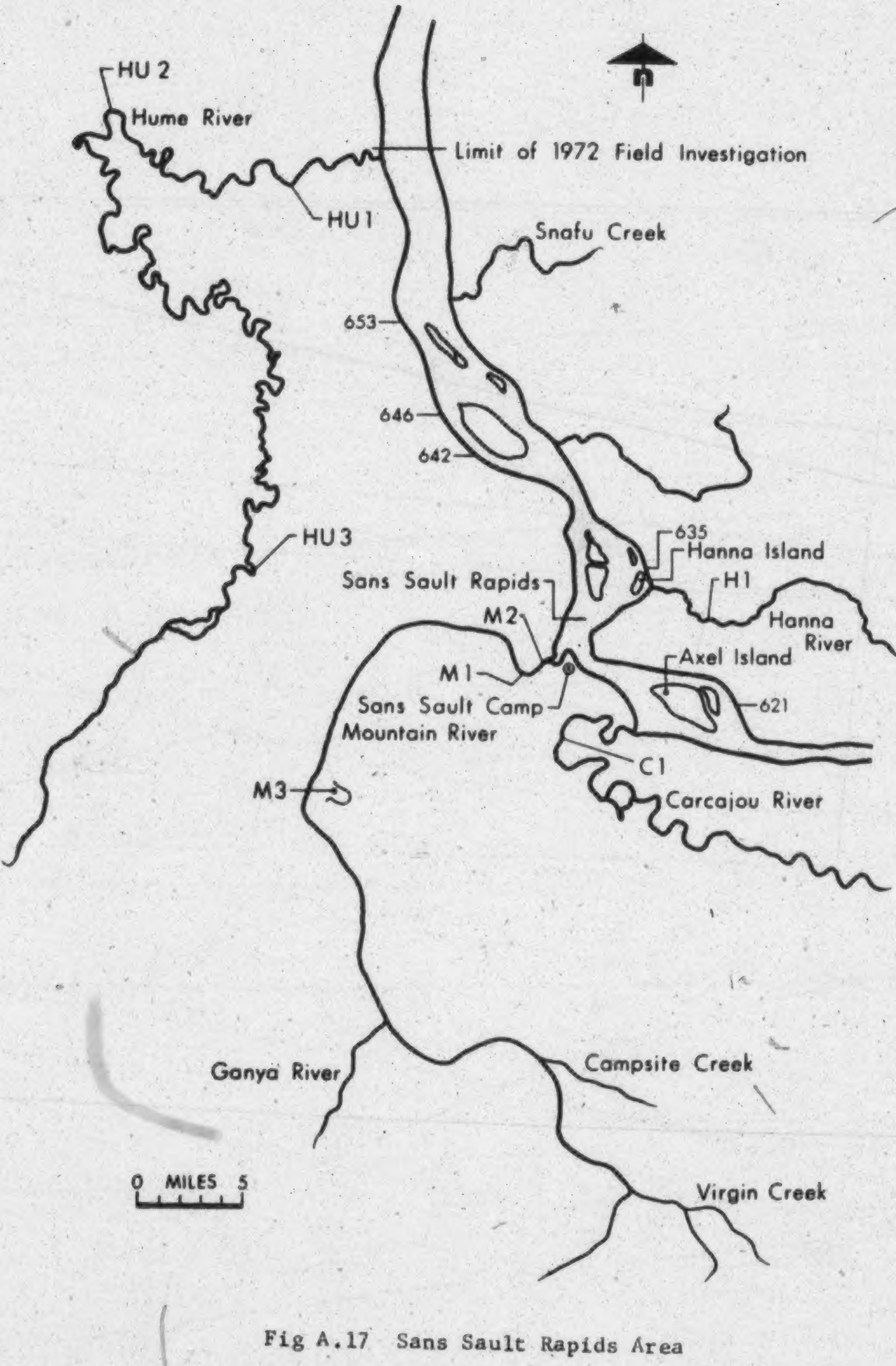
HU 2
Hume River
Limit of 1972 Field Investigation
HU 1
Snafu Creek
653
646
642
635
Hanna Island
HU 3
Sans Sault Rapids
H1
Hanna River
M2
Axel Island
M1
Sans Sault Camp
Mountain River
621
C1
M3
Carcajou River
Ganya River
Campsite Creek
0 MILES 5
Virgin Creek

Fig A.17 Sans Sault Rapids Area

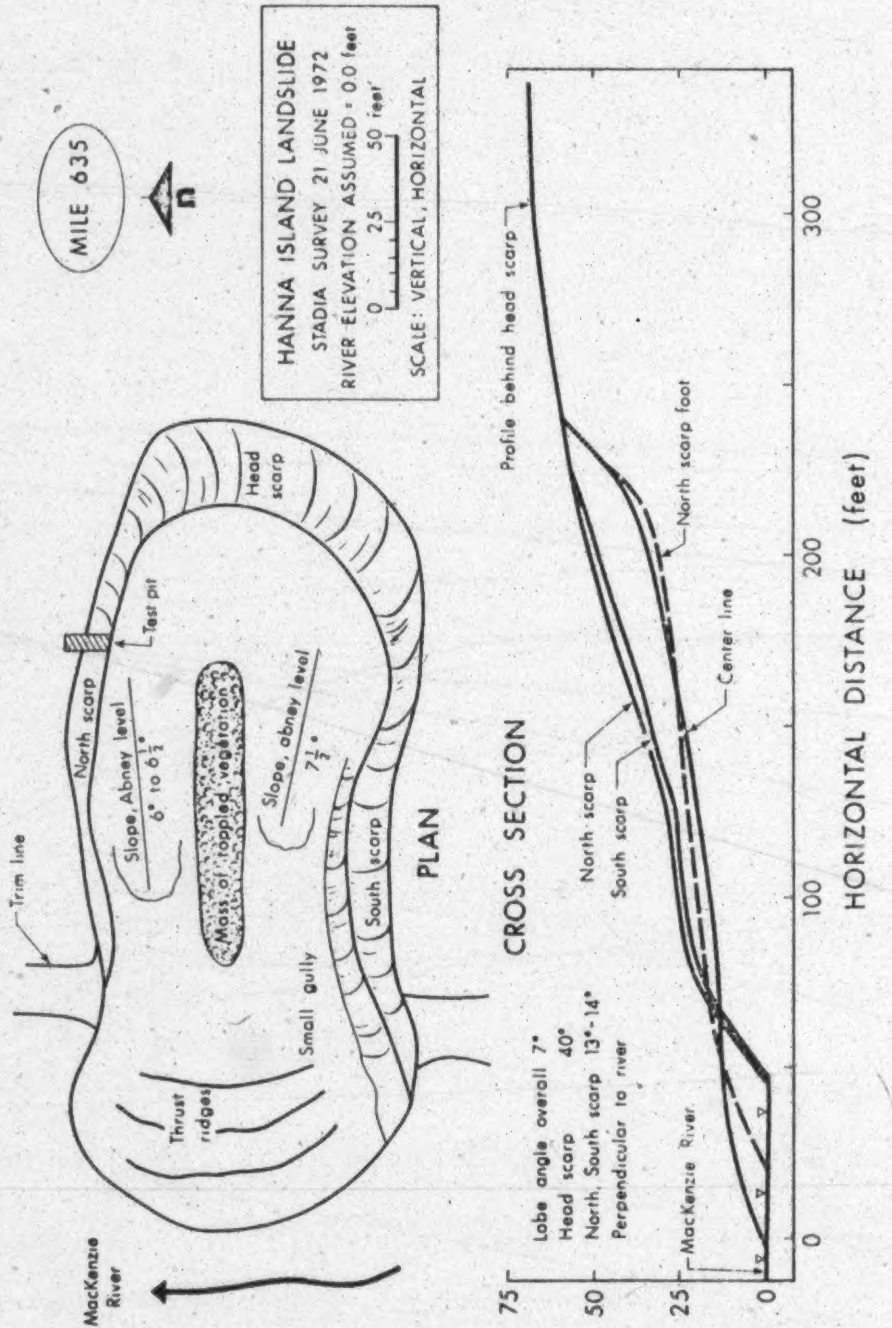
MILE 635
N
HANNA ISLAND LANDSLIDE
STADIA SURVEY 21 JUNE 1972
RIVER ELEVATION ASSUMED = 0.0 feet
0 25 50 feet
SCALE: VERTICAL, HORIZONTAL
MacKenzie River
Trim line
North scarp
Test pit
Head scarp
Slope, Abney level 6° to 6½°
Mass of toppled vegetation
Slope, abney level 7½°
Small gully
South scarp
Thrust ridges
PLAN
CROSS SECTION
Lobe angle overall 7°
Head scarp 40°
North, South scarp 13°-14°
Perpendicular to river
MacKenzie River
North scarp
South scarp
Center line
North scarp foot
Profile behind head scarp
ELEVATION (feet)
75
50
25
0
0
100
200
300
HORIZONTAL DISTANCE (feet)

Fig A.18 Hanna Island Landslide

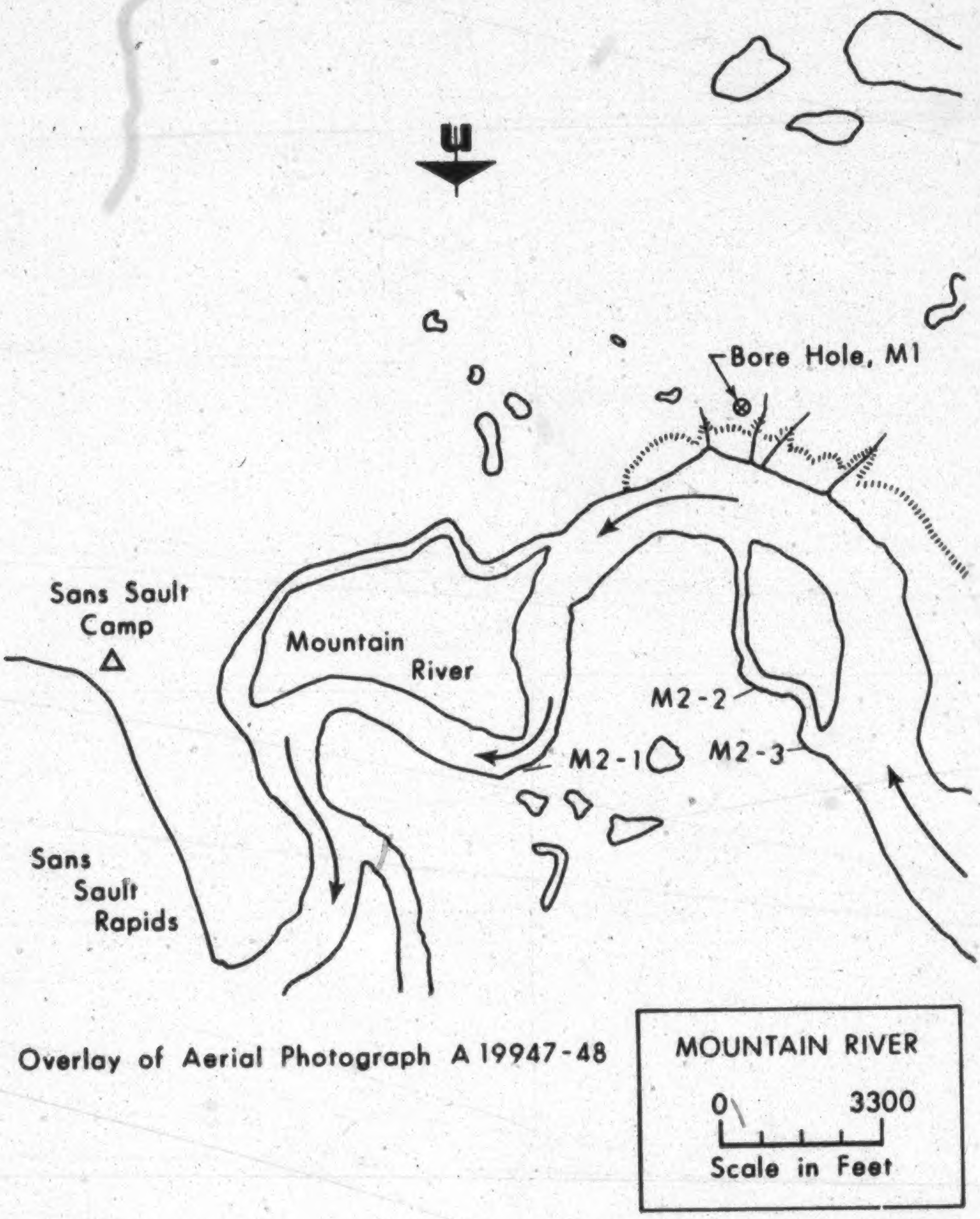
Bore Hole, M1
Sans Sault
Camp
Mountain
River
M2-2
M2-1
M2-3
Sans
Sault
Rapids
Overlay of Aerial Photograph A 19947-48
MOUNTAIN RIVER
0
3300
Scale in Feet

Fig A.19 Mountain River: Site Plan

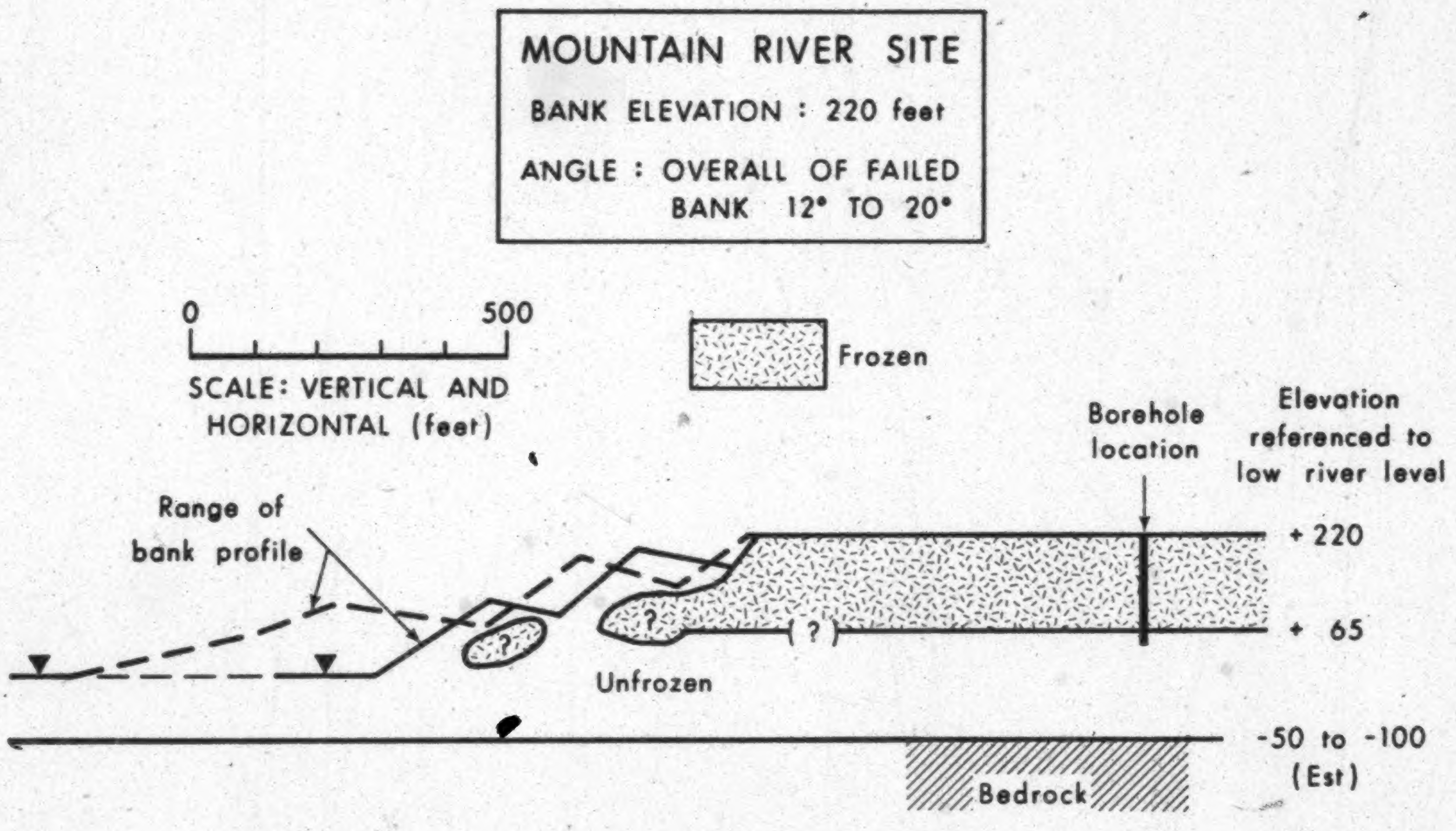
MOUNTAIN RIVER SITE
BANK ELEVATION : 220 feet
ANGLE : OVERALL OF FAILED BANK 12° TO 20°
0
500
SCALE: VERTICAL AND HORIZONTAL (feet)
Frozen
Borehole location
Elevation referenced to low river level
Range of bank profile
+ 220
+ 65
?
?
(?)
Unfrozen
-50 to -100 (Est)
Bedrock

Fig A.20 Mountain River: Profile

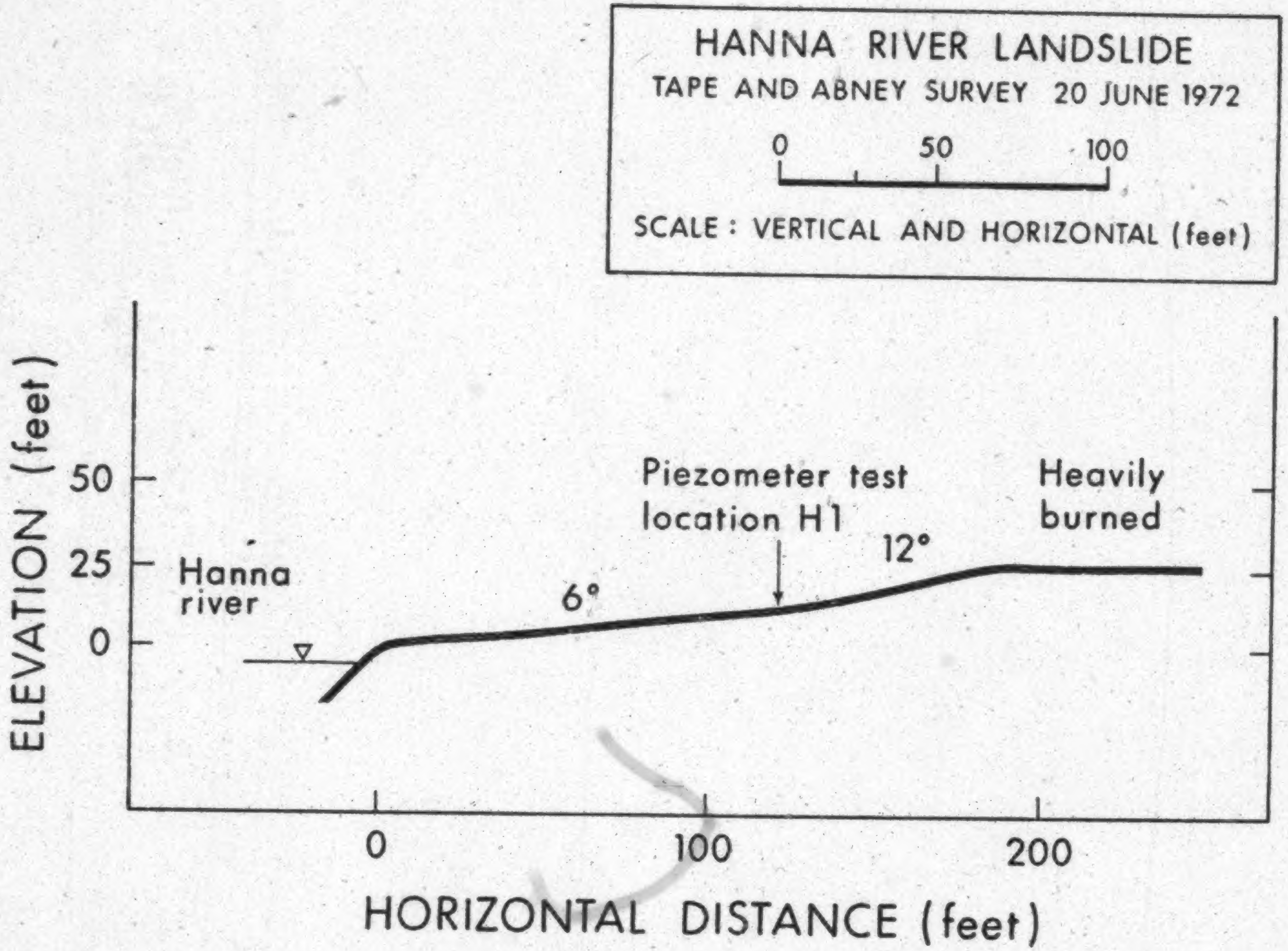

Fig A.21 Hanna River Landslide

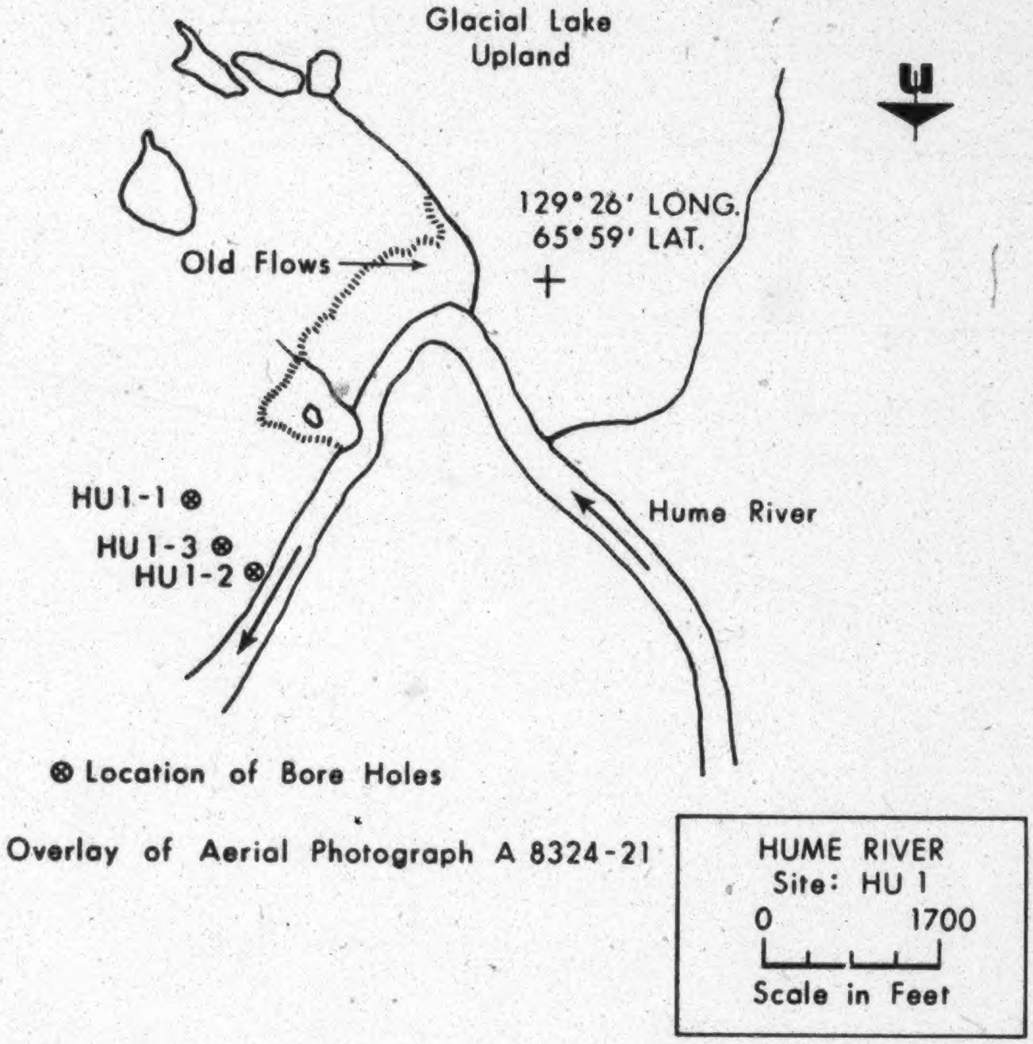
Glacial Lake Upland
129°26' LONG.
65°59' LAT.
Old Flows
HU1-1
HU1-3
HU1-2
Hume River
⊗ Location of Bore Holes
Overlay of Aerial Photograph A 8324-21
HUME RIVER
Site: HU 1
0
1700
Scale in Feet

Fig A.22 Hume River Site HU1: Site Plan

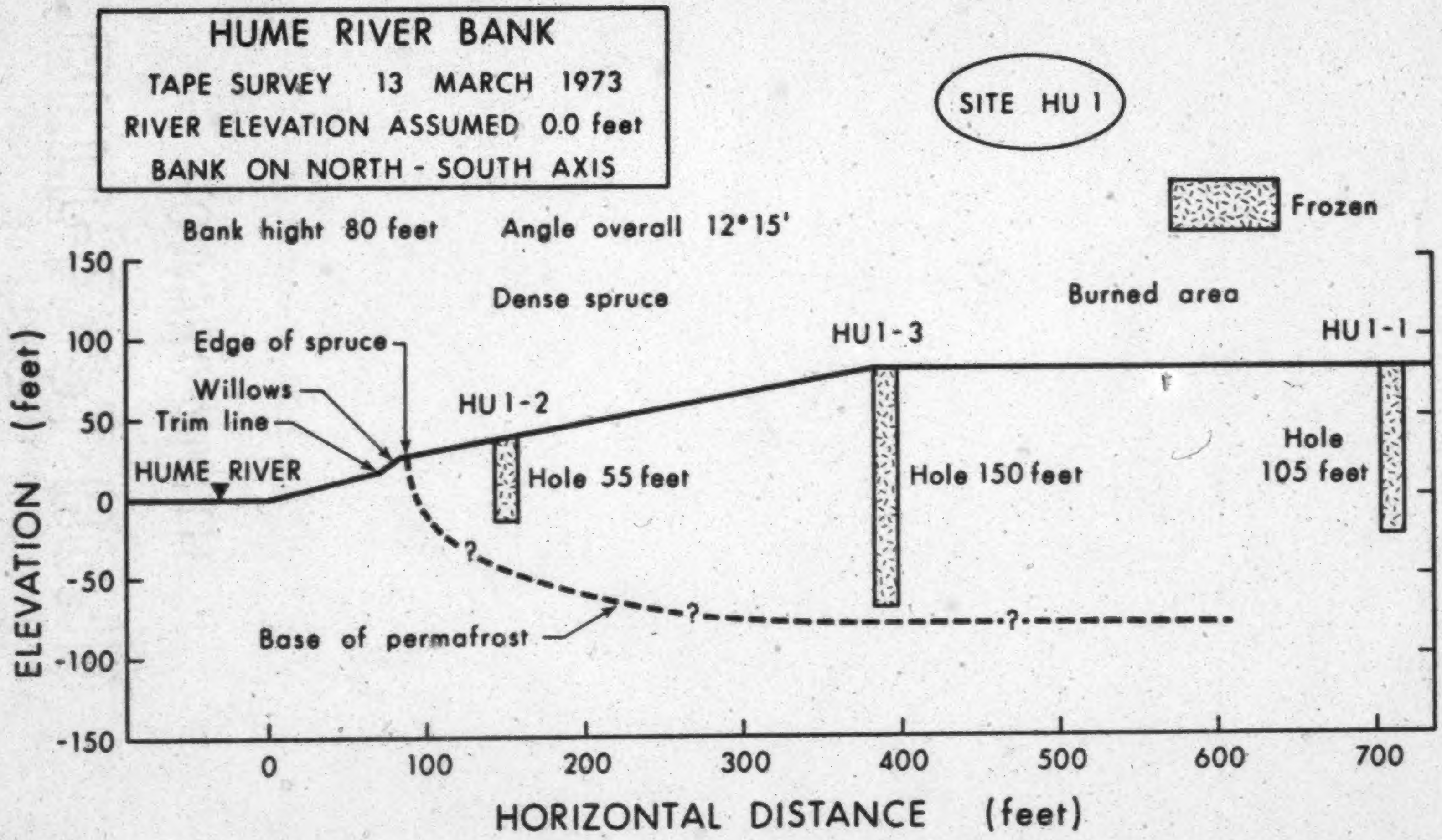

Fig A.23 Hume River Site HU1: Profile

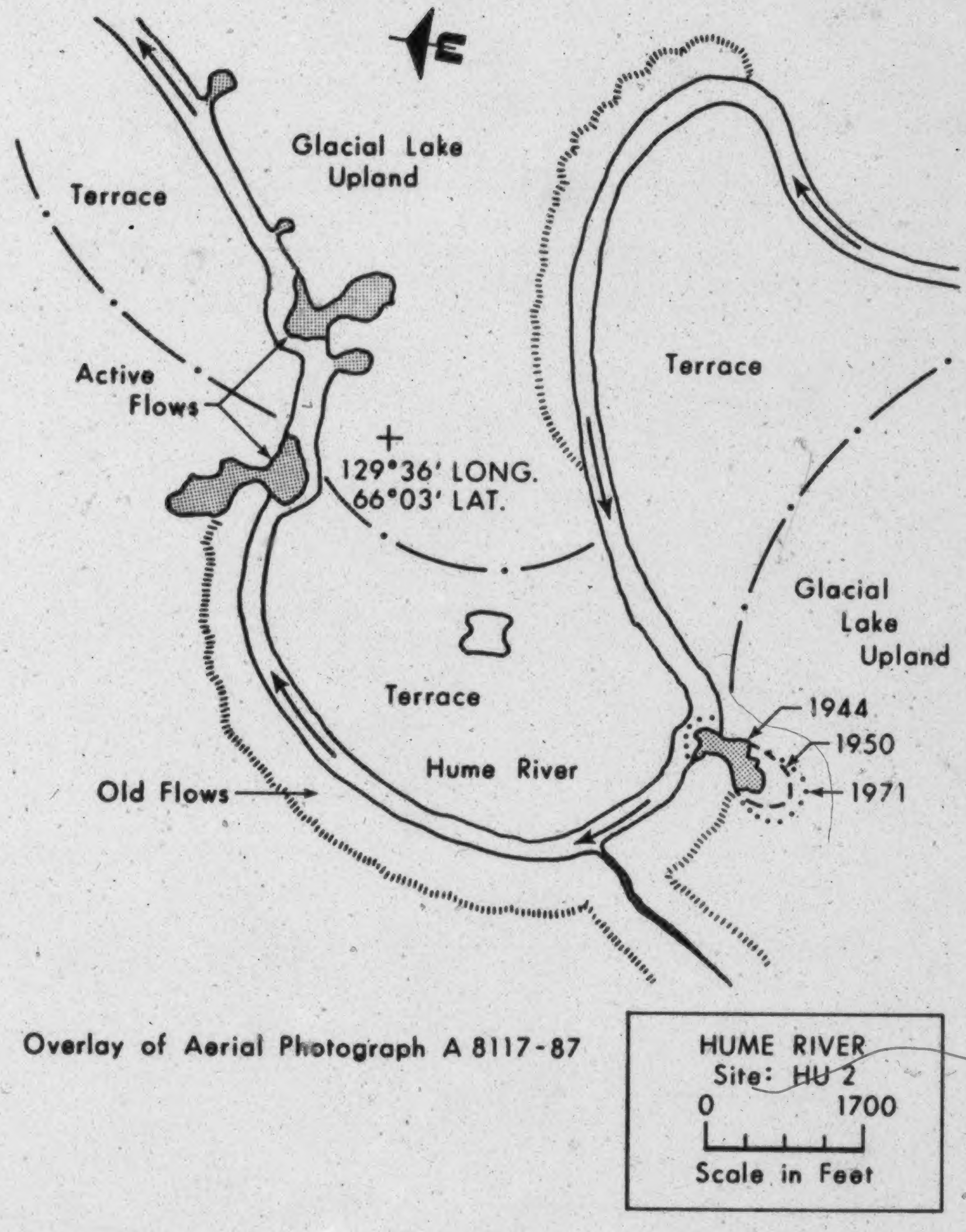
E
Glacial Lake Upland
Terrace
Active Flows
129°36′ LONG.
66°03′ LAT.
Terrace
Glacial Lake Upland
Terrace
Hume River
Old Flows
1944
1950
1971
Overlay of Aerial Photograph A 8117-87
HUME RIVER
Site: HU 2
0
1700
Scale in Feet

Fig A.24 Hume River Site HU2

UPPER: Plate 1 Fort Simpson landslide, an MR flow

CENTRE: Plate 2 Skin flows near the Wrigley River

BOTTOM: Plate 3 Big Smith Creek landslide, a bi-modal flow

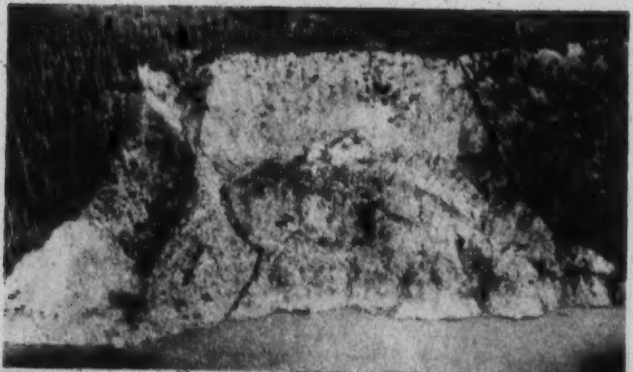

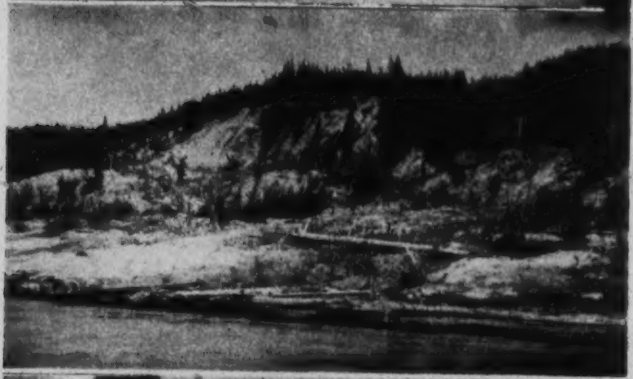

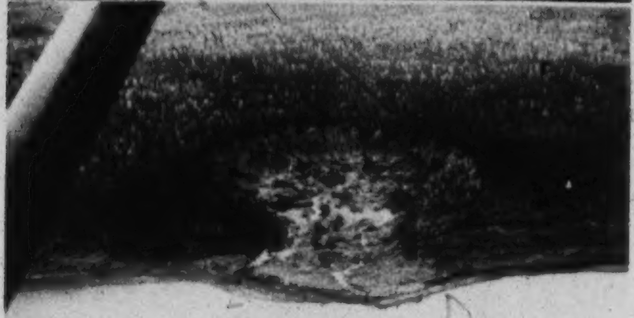

UPPER: Plate 4 Old Fort Point landslide, a bi-modal flow

CENTRE: Plate 5 Ice Buttress landslide, a bi-modal flow

LOWER: Plate 6 Fort Norman landslide, a bi-modal flow

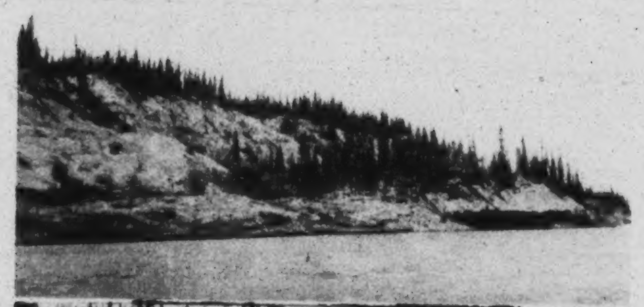

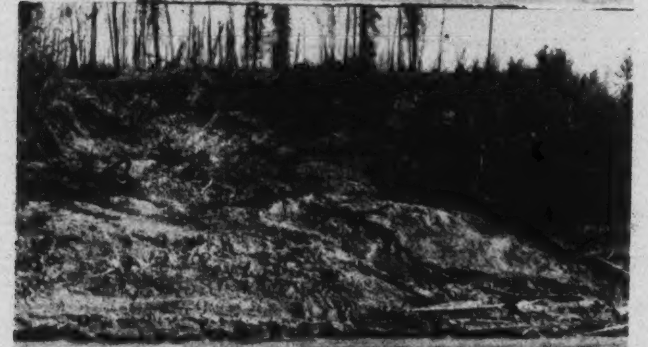

UPPER: Plate 7 Block slide at Mile 655

CENTRE: Plate 8 Hanna Island landslide, a bi-modal flow

LOWER: Plate 9 Mountain River landslide, a MR slide

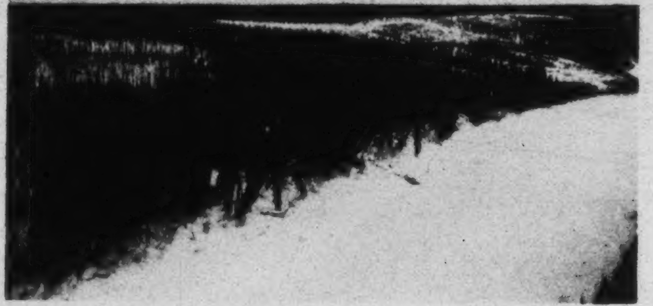

UPPER: Plate 10 Falls on the Mountain River
CENTRE: Plate 11 Hume River, site HU1-1
LOWER: Plate 12 Hume River, site HU1-1

APPENDIX B

BOREHOLE LOGS AND GEOTECHNICAL TEST DATA

TABLE B.1 INDEX PROPERTIES: SUMMER SURVEY

Sample Name	Code	River Mileage	W_L%	W_P%	I_P%	% 0.002mm	Specific Gravity	Mineralogy* I	K	C	M
Fort Simpson Landslide 1	FS1	226	26.4	20.5	5.9	20					
Fort Simpson Landslide 2	FS2	226	52.3	23.1	29.2	67	2.77	70	25	5	
Cutline	C	270	35.3	21.8	13.5	53	2.73	60	35	5	5
MacGern	M	302	39.6	19.6	20.0	47	2.72	70	25	5	5
Little Smith Creek	LS	475	43.0	21.7	21.3	47	2.76	60	30	5	5
Fort Norman	NS	517	43.3	19.7	23.6	45	2.75	60	30	5	5
Norman Landslide Silt Run	N1	517	20.5	19.9	0.6	10		65	25	5	5
Norman, Piezometer Test P1	N2	517	20.6	19.9	0.7	15		70	25	5	5
Norman, Piezometer Test P3	N3	517	20.3	19.5	0.8	11					
Mountain River 1	MR1		60.0	20.1	39.9						
2	MR2		48.3	21.9	26.4	55		60	35		5
Little Smith Creek Till	LST	457				21					
Old Fort Point Top	OFT	481	40.4	21.1	19.3						
Middle	OFM		38.0	22.0	16.0						
Norman Varve Silt	NV	516	26.0	22.1	3.9	20					
Halfway Island	HW	553	37.5	21.2	16.3						
Hanna River Clay	HR1		44.7	21.3	23.4	46					
Hanna River Clay	HR2		52.5	22.3	30.2	60					

*Mineralogy on fraction 0.002mm

I = illite,
K = kaolin,
M = montmorillonite,
C = chlorite

TABLE B.2 FIELD WATER CONTENTS: SUMMER SURVEY

Sample Number	W/C	Sample Location	Sample Description
MC1	31%	Cut Line Slide	Clayey Silt at river level. Disturbed.
MC2	31%	Cut Line Slide	
MC4	30%	Fort Norman Slide P1	Silt from piezometer test P1. Sample from interface.
MC5	31%	Fort Norman Slide	
MC6	42%	Mile 642	In flow below North Rapids
MC7	37%	Mile 642	
MC8	39%	Hanna Island Flow	Undisturbed sample of frozen silty clay.
MC9	30%	Hanna Island Flow	
M1	26%	Mountain River	From sample taken of thawed Mountain River clay,
	26%	Mountain River	
	25%	Mountain River	
	25%	Mountain River	
S1	>60%	Fort Simpson	Sample of frozen silt -clay. No wet weight in field.

TABLE B.3 SUMMARY OF GRAIN SIZE DISTRIBUTION FOR ALL BOREHOLES

Hole/Depth	% Gravel	% Sand	% Silt	% Clay
HU1-2 - 25.0			55	45
HU1[illegible] - 19.0			52	48
HU1-3 - 65.0			57	43
HU1-3 - 150.0			48	52
M1 - 16.0	41	59		
M1 - 35.0	14	80	6	
M1 - 51.0		94	6	
M1 - 57.0		98	2	
M1 -119.7			35	65
M1 -119.9		8	40	52
M1 -120.4			36	64
M1 -125.0		27	50	23
M1 -125.5		20	48	32
M1 -126.0		32	41	27
M1 -126.4		55	35	10
M1 -132.6		54	36	10
M1 -133.4		23	52	25
M1 -170.0		48	38	14

BOREHOLE M1, MOUNTAIN RIVER

DEPTH INTERVAL (ft.)	SOIL	ICE	W_N	W_L	W_P	AS NOTED
0.35- 1.35	SILT, sandy	Random ice to 1/4", V_r				
4.0 - 6.5	SILT, sandy	Horizontal ice to 1/8" at 1/2" spacing, V_s	58 53	26	NP	
6.5 - 8.0	CLAY, silty brown CL	Ice in 1/4" to 3/8" crystals, no lenses, V_x	27	43	23	γ_B = 1.87
10.0- 11.8	Four samples, W_N	Ice in 1/4" to 3/8" crystals, no lenses, V_x	26 31 33 100	49	26	
12.0- 13.6	CLAY, silty with up to 4" sandy silt lenses	Ice horizontal 1/8" to 1/4" spaced 1/2" to 3", V_s				

DEPTH	W_N	γ_b
12 - 0	26.1	1.90
12.1-12.5	24.2	1.96
12.6-13.0	34.6	1.75
13.0-13.4	53.8	1.52
13.4-13.8	28.1	1.85

DEPTH INTERVAL (ft.)	SOIL	ICE	W_N	W_L	W_P	AS NOTED
16.0- 16.6	GRAVEL, well sorted 1/2" pebbles	V_x	20.0 21.1			
16.6- 32.0	GRAVEL with plastic fines	Chips melt				
35.0- 35.9	SAND, traces of silt	V_x	23.8			
50.0- 51.0	Clay chips					
51.0- 51.4	SAND medium sand with silt lenses	V_x				
55.0- 56.1	SAND, silty with coal chips		10.1			
57.0- 59.0	SAND, medium with silt lenses, coal chips					
81.0- 81.9	SAND, silt lenses		27			γ_B = 1.92

DEPTH INTERVAL (ft.)	SOIL	ICE	DEPTH	W_N	W_L	W_P	γ_B	STRENGTH TESTS
119.5-119.5	SAND, silt lenses	No visible ice, Nb	119.7	23.6	47	18		
119.7-120.7	CLAY, silty brown CL to CH		119.9	21.5	40	19	1.99	
125.0-127.0	CLAY, silty brown with lenses of SILT, clay with laminated bedding CL	No visible ice, Nb	120.4 125.0 125.5 126.0	25.5 21.0 19.2 20.0	52 25 29 25	 16 17 16	 2.01 1.96	 M1-4 M1-1
132.6-134.4	SILT, clayey, brown with laminated bedding CL		126.4 132.6 133.4	25.1 25.3 21.0	 25	NP NP 16	1.95 1.92 1.99	M1-2 M1-5 M1-3
135 -154	SAND, silty with clay	Chips from air return 1/4" thick to 3/4" diameter contain sand and melt when heated						
155 -156	Three inch shelby easy penetration, no sample, wet soil smeared on tube							

- -

BASE OF PERMAFROST AT 155 FEET

- -

DEPTH INTERVAL (ft.)	
158.0-165.0	Drill stem fell 7.0 feet under its own weight with brake partially engaged
165.0-170.0	SAND, silty pumped from hole. Considerable quantity of water forced to surface by the air return. W_N of silty sand measured after 1/2 hour of pumping was 37%.

Fig B.1 Mountain River M1 Borehole Log

BOREHOLE HU1-1, HUME RIVER

DEPTH INTERVAL (ft.)	SOIL	ICE	W_N	W_L	W_p	AS NOTED
0.0- 1.0	Organics	Ice in 1/8" to 3/8", many lenses, V_s, plus random V_r to 1".	76			
2.0- 5.6	CLAY, silty brown CL	"	76			
6.0- 8.0	SILT, clayey, brown CL	Ice lenses to 1/4", V_r	76			
8.2- 10.2	CLAY, silty, brown CL	Ice lenses horizontal to 1/4", V_s				
10.5- 15.0		Chips ice rich				
15.0- 17.0		16.8-17.0 ICE Lenses to 1",V_r				
20.0- 21.6		Horizontal V_s at 20.2, 20.4, 21.4, 21.6 plus V_r to 1"	40			
25.0- 26.0	Refusal at 1.0'	No visible ice, Nb				
35.0- 36.3		Horizontal ICE at 35.2, 35.7, and 35.9. Thick vertical lenses, V_r				
40.0- 41.0		Horizontal ICE at 40.7, 40.9, vertical ice 3/8" 40.3 to 40.7				
45.0- 46.3		Random ice to 3/4", V_r				
50.0- 51.6		"	28			
60.0- 61.4		Random ice 3/4" to 1" Horizontal ice at 60.5, 61.2				
70.0- 71.0	No recovery					
75.0- 76.0		1 1/4" sub-vertical ice lense, ICE				
85.0- 85.5	SILT, clayey, brown CL	No visible ice, Nb	21.1			
95.0- 97.0	CLAY, silty brown CL	Lense sub-vertical along 1/2 of tube from 95.7 to 96.1	21.8			
97.0- 99.0		Chips ice rich				
105.0-109.0		Large vertical lense 105.4-106.6	24.8			

Fig B.2 Hume HU1-1 Borehole Log

BOREHOLE HU1-2, HUME RIVER

DEPTH INTERVAL (ft.)	SOIL	ICE	W_N	W_L	W_P	AS NOTED
0 - 0.5	Organic cover					
	Clay, silty, brown CL	Chips contain considerable ice				
5.0- 5.5		1.0" ice lense, ICE				
5.5- 6.0			157	40	20	
6.0- 7.0			125			
7.0- 8.0			127			
8.0- 9.0			78	42	21	
9.0-10.0			74			
11.0-12.0			47			G_s = 2.73
13.0-14.0			61	49	23	
14.0-15.0			33			
15.0-17.0		Ice lenses to 1.0". Dominant ice attitude at 45°, V_r	37			
20.0			29	45	21	
20.5-21.5		Drilling easy, pure ice				
25.0	Little recovery on 2 ft. drive. W_N on soil with no visible ice	Sample dominantly ice, ICE	29.8	45	21	
34.0-25.5	W_N adjacent to vertical ice	34.3-34.7 3/8" vertical ice V_r. 35.4-35.6 ICE with soil inclusions	29.9			
44.0-46.0	W_N adjacent to ice	44.2-44.9 ICE	21.5	43	24	
55.9-57.9		Ice sub-vertical and horizontal to 1/2" lenses, V_r	38	42	24	

Fig B.3 Hume HU1-2 Borehole Log

BOREHOLE HU1-3, HUME RIVER

DEPTH INTERVAL (ft.)	SOIL	ICE	W_N	W_L	W_p	AS NOTED
2.0- 3.5	No recovery					
5.0- 6.0	CLAY, silty brown CL	Lenses to 1" sub-vertical to sub-horizontal, V_r				
8.0- 9.0	Entire borehole	Lenses 3/4" to 1", V_r	53			
9.0- 11.0	Three samples, W_N	"	28 33 39			
15.0- 17.0	Two samples, W_N	"	45	51	25	G_s = 2.72
17.0- 19.0		17.0-17.2 ICE		51	25	
20.0- 20.5		Sample ICE with soil inclusions				
20.5- 35.0		Ice rich chips				
35.0- 35.3	Refusal at 0.3'	No visible ice, Nb	24	51	23	
50.0- 50.5		50.4-50.5, ICE	32	46	22	
65.0- 67.0		No visible ice, Nb		42	22	
80.0- 81.2	W_N above ICE	ICE at base of spoon	20.6			G_s = 2.72
	W_N including lens		24	35	22	
81.2- 82.0		Chips ice rich				
110.0-111.5	Marked sample disturbance with convoluted, distorted appearance	110.1-110.3 ICE Remainder Nb	23	41	21	
						Depth
			24.0			110.0
			43.5			110.1
			31.1			110.4
			20.4			110.5
			18.2			111.1
140.0-141.5		Ice in sub-vertical to sub-horizontal lenses to 1/2", V_r	32	49	23	
150.0-151.0		No visible ice, Nb	23.6	41	24	

Fig B.4 Hume HU1-3 Borehole Log

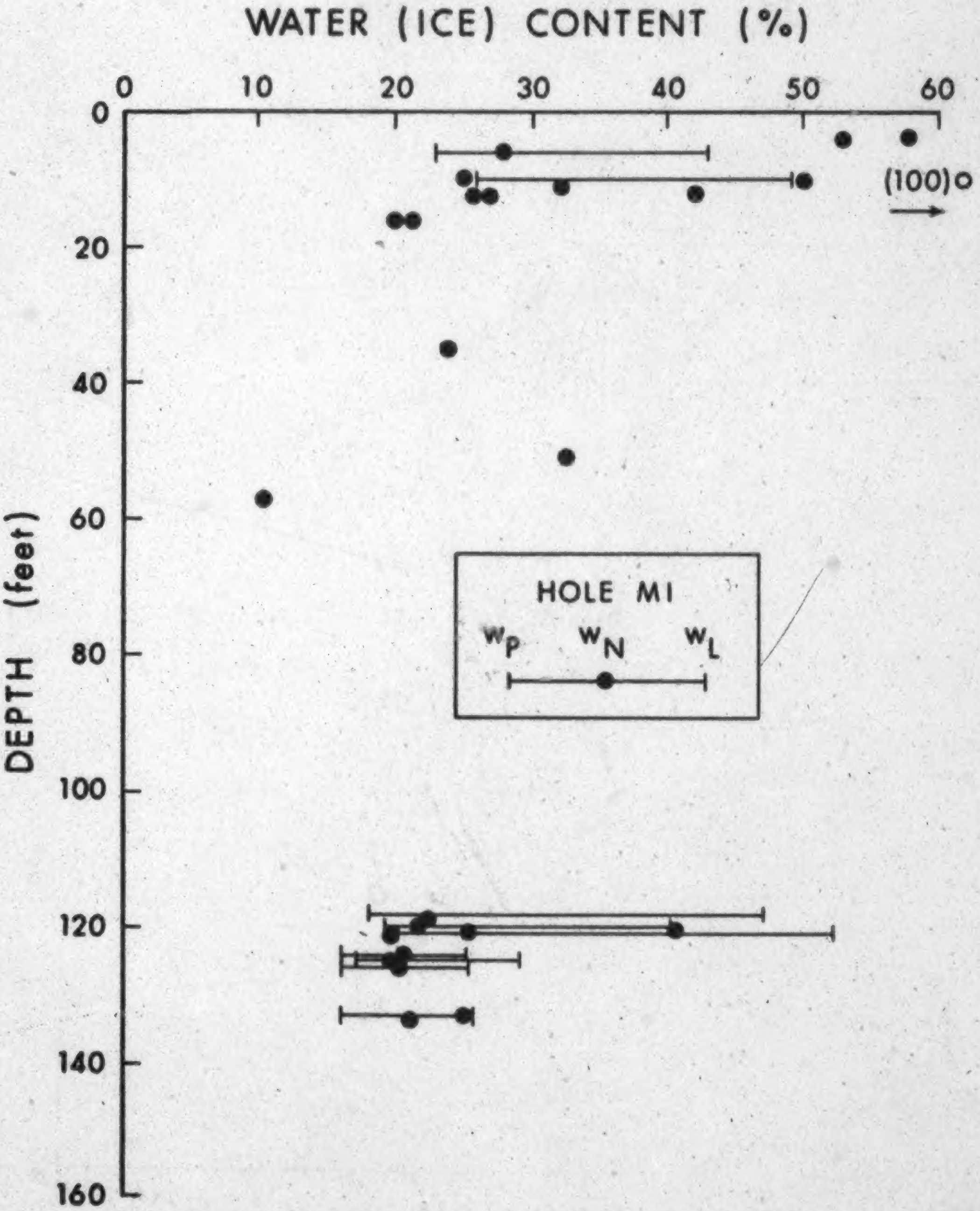

Fig B.5 Water (Ice) content versus depth for M1

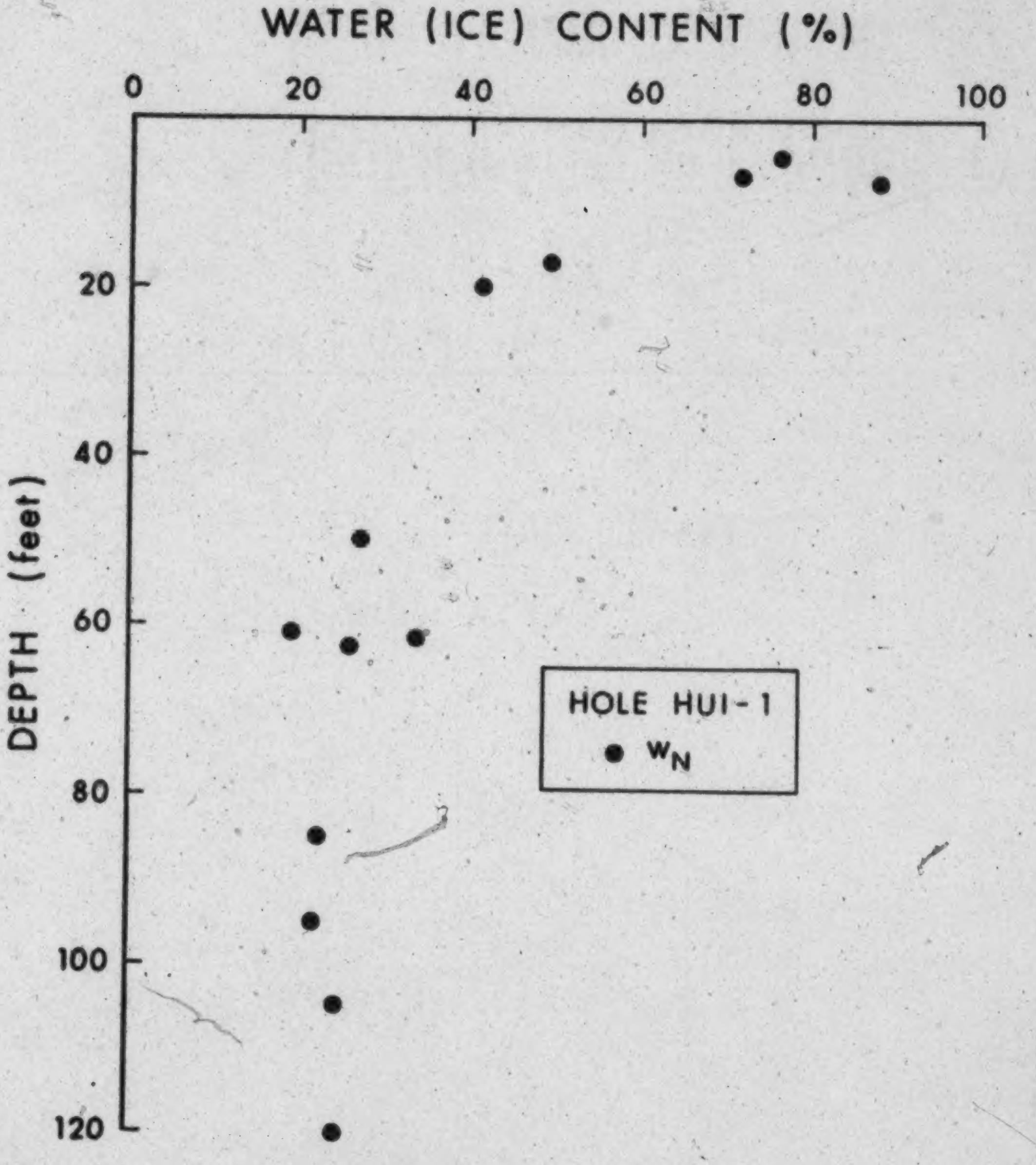

Fig B.6 Water (ice) content versus depth for HU1-1

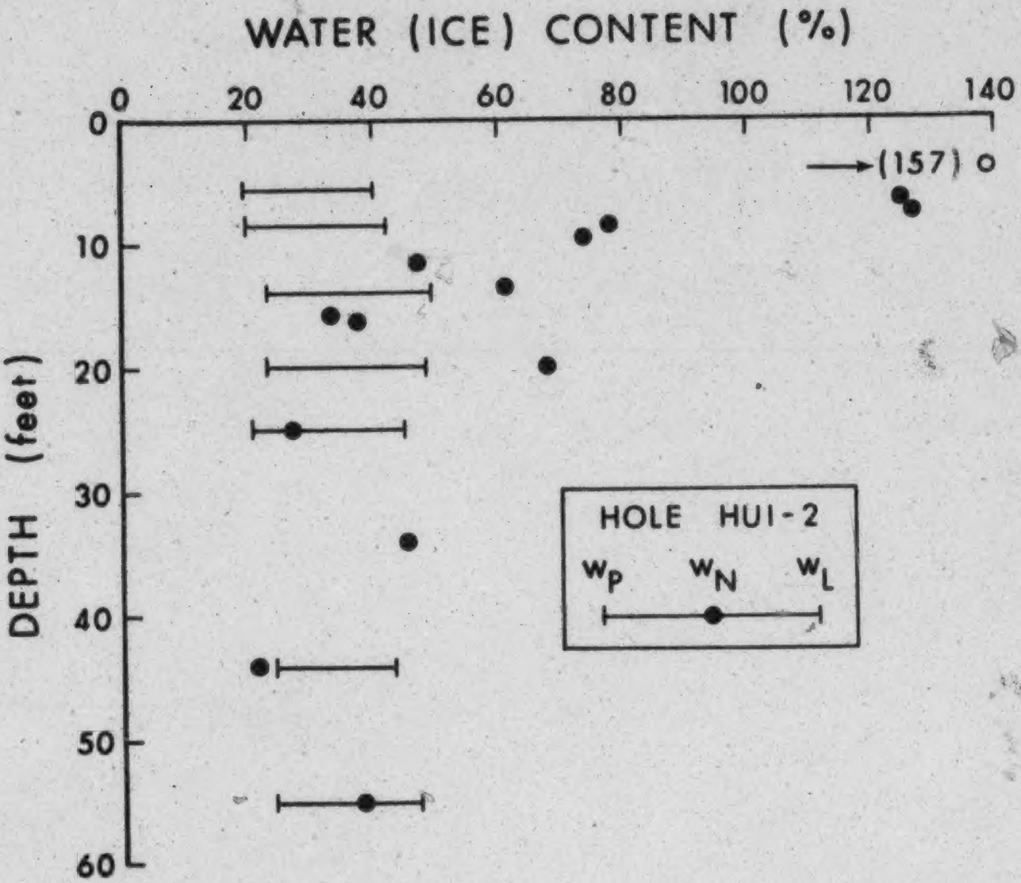

Fig B.7 Water (ice) content versus depth for HU1-2

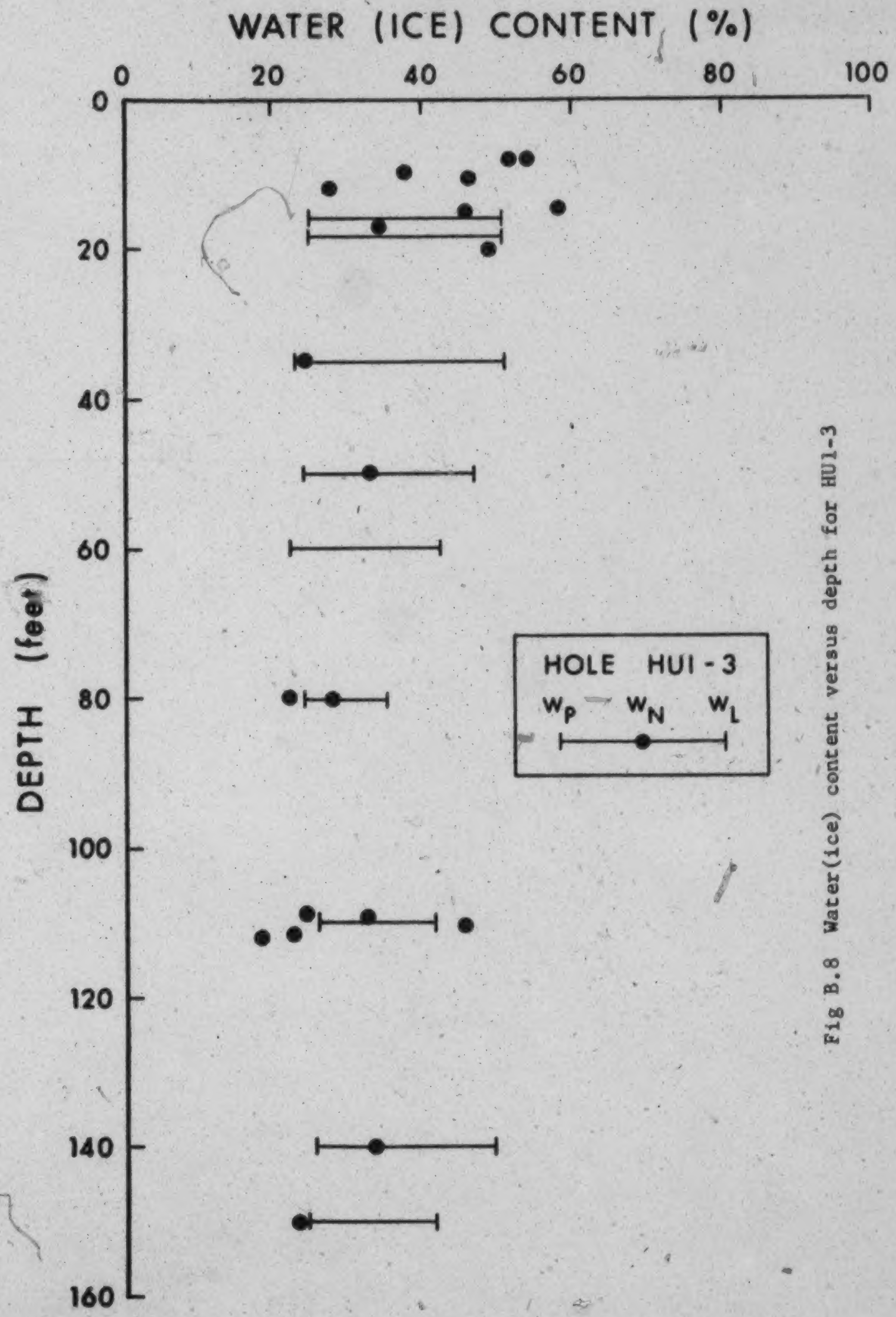

Fig B.8 Water(ice) content versus depth for HU1-3

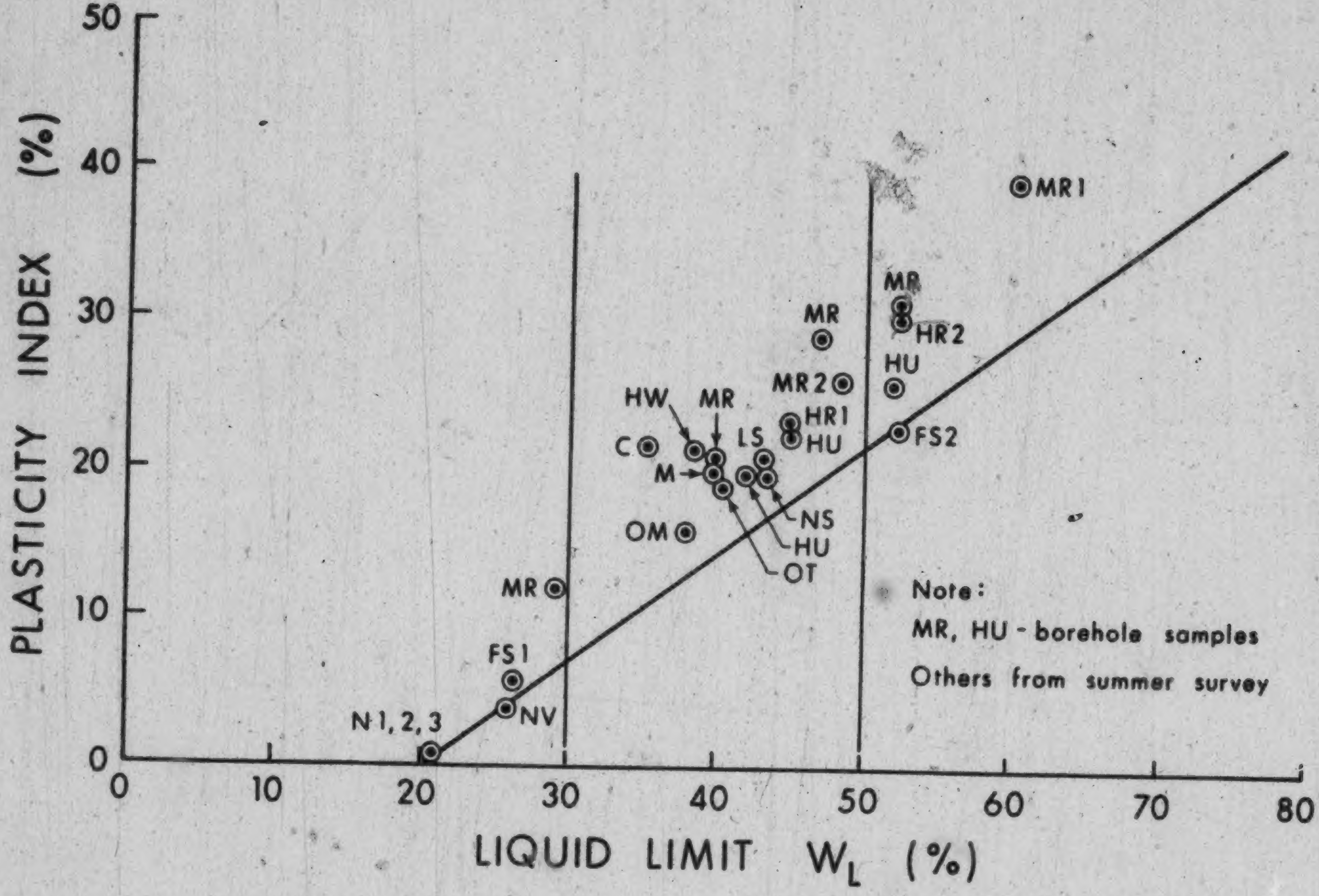

Fig B.9 Plasticity chart for Mackenzie River Clays

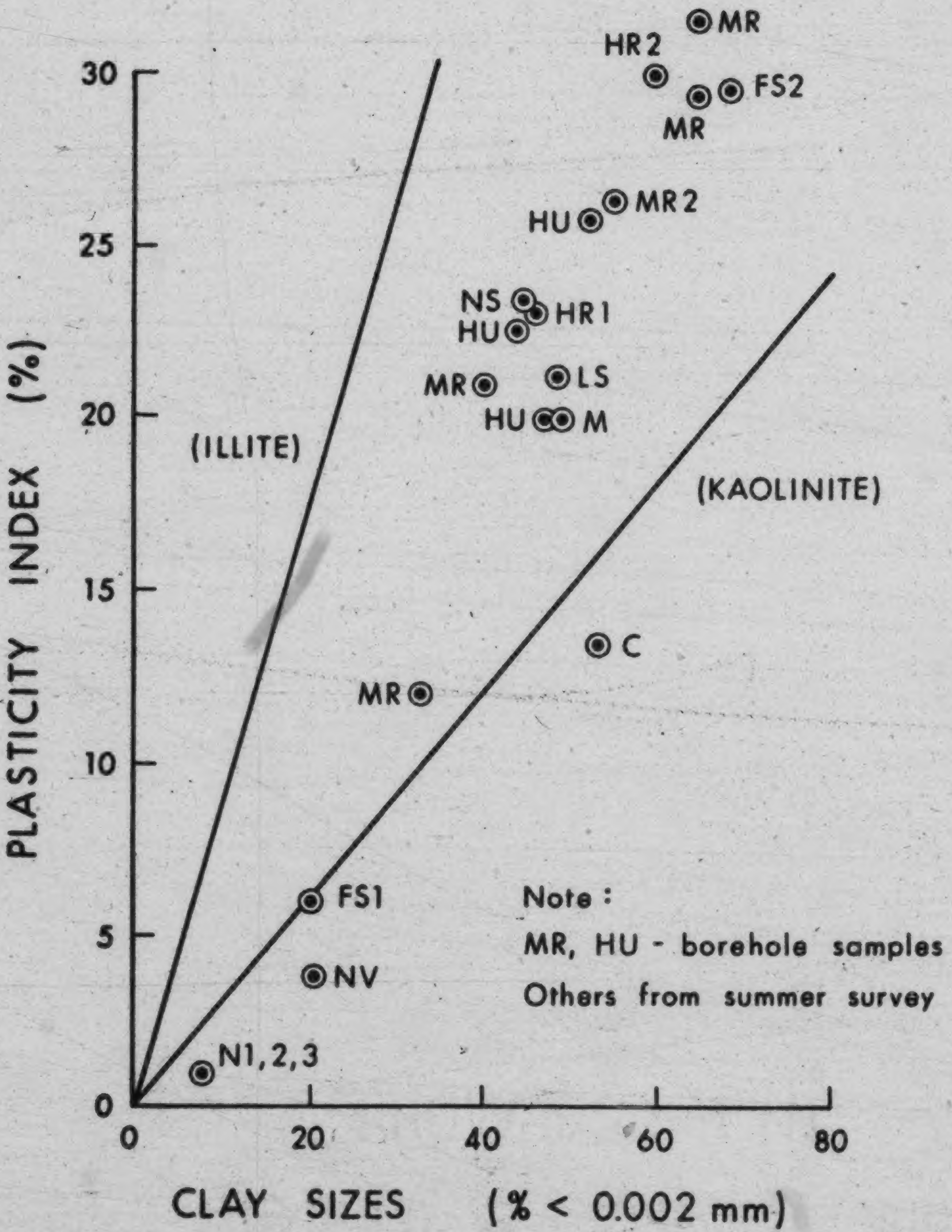

Fig B.10 Liquid Limit versus % clay fraction
Mackenzie River Clays

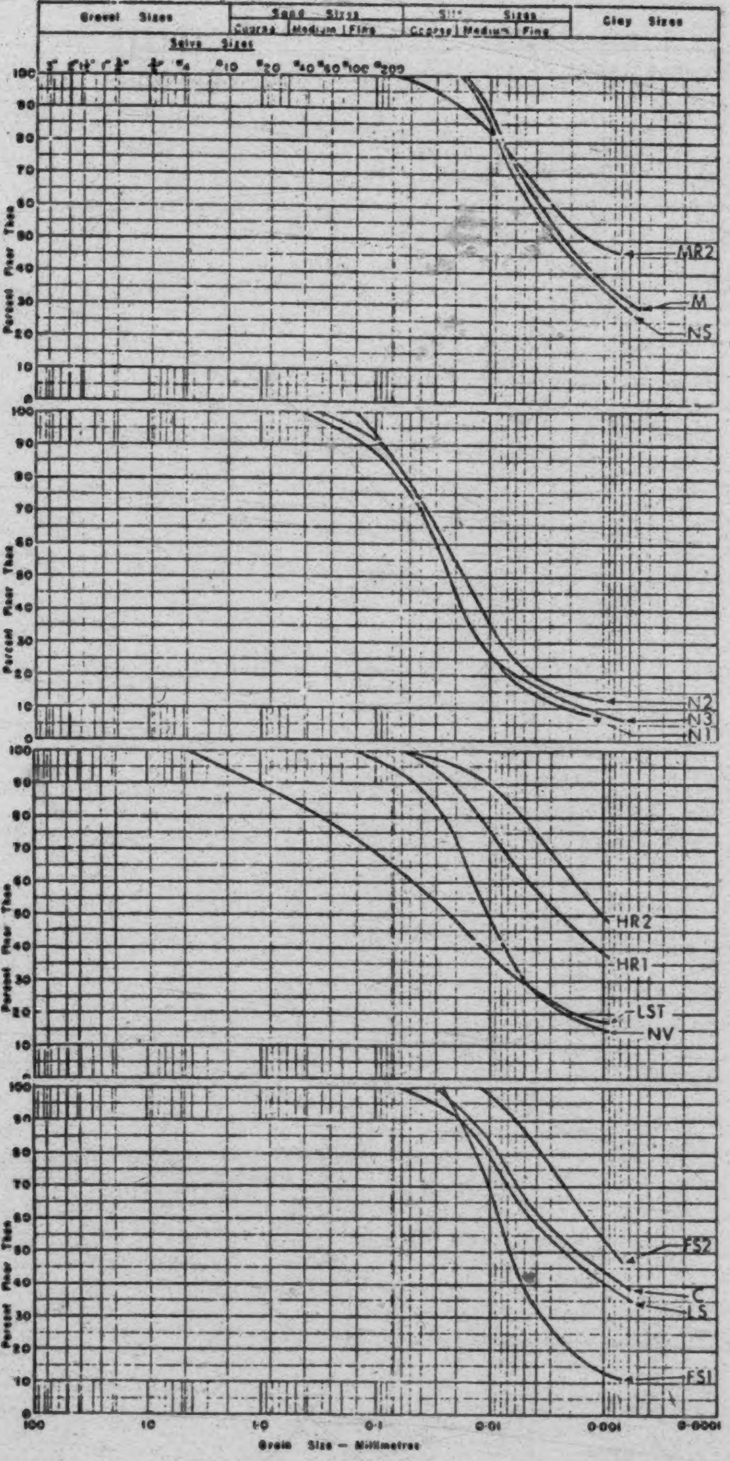

Fig B.11 Grain Size Curves: Summer Survey

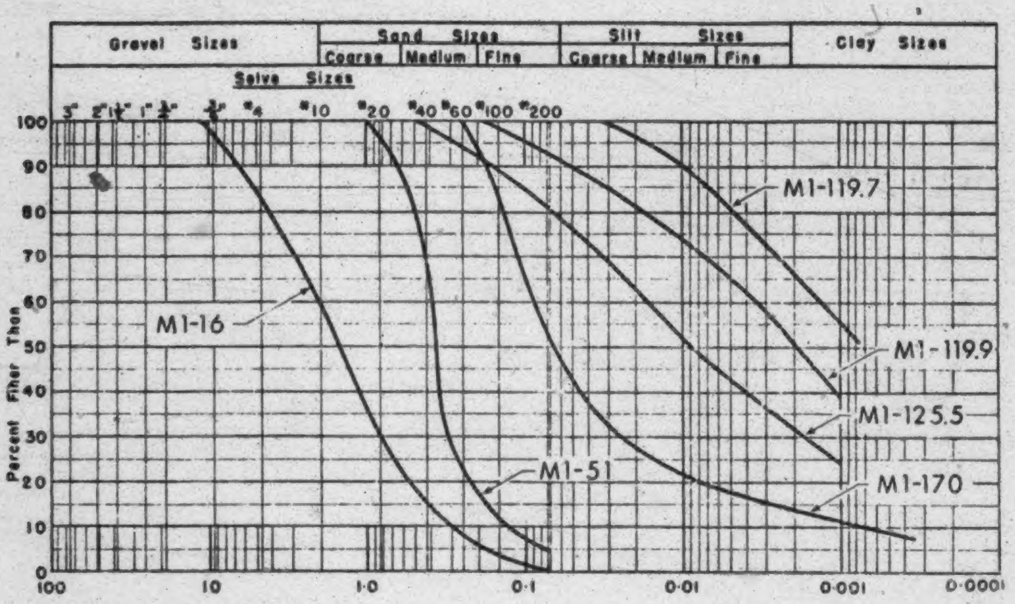

Fig B.12 Grain Size Curves:
Mountain River Site

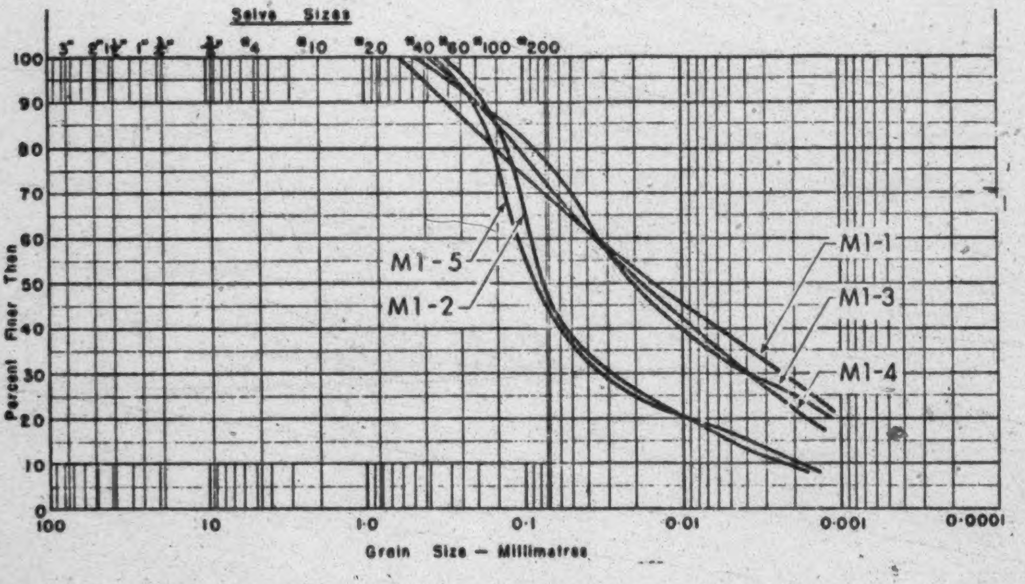

Fig B.13 Grain Size Curves:
Frozen Strength Samples

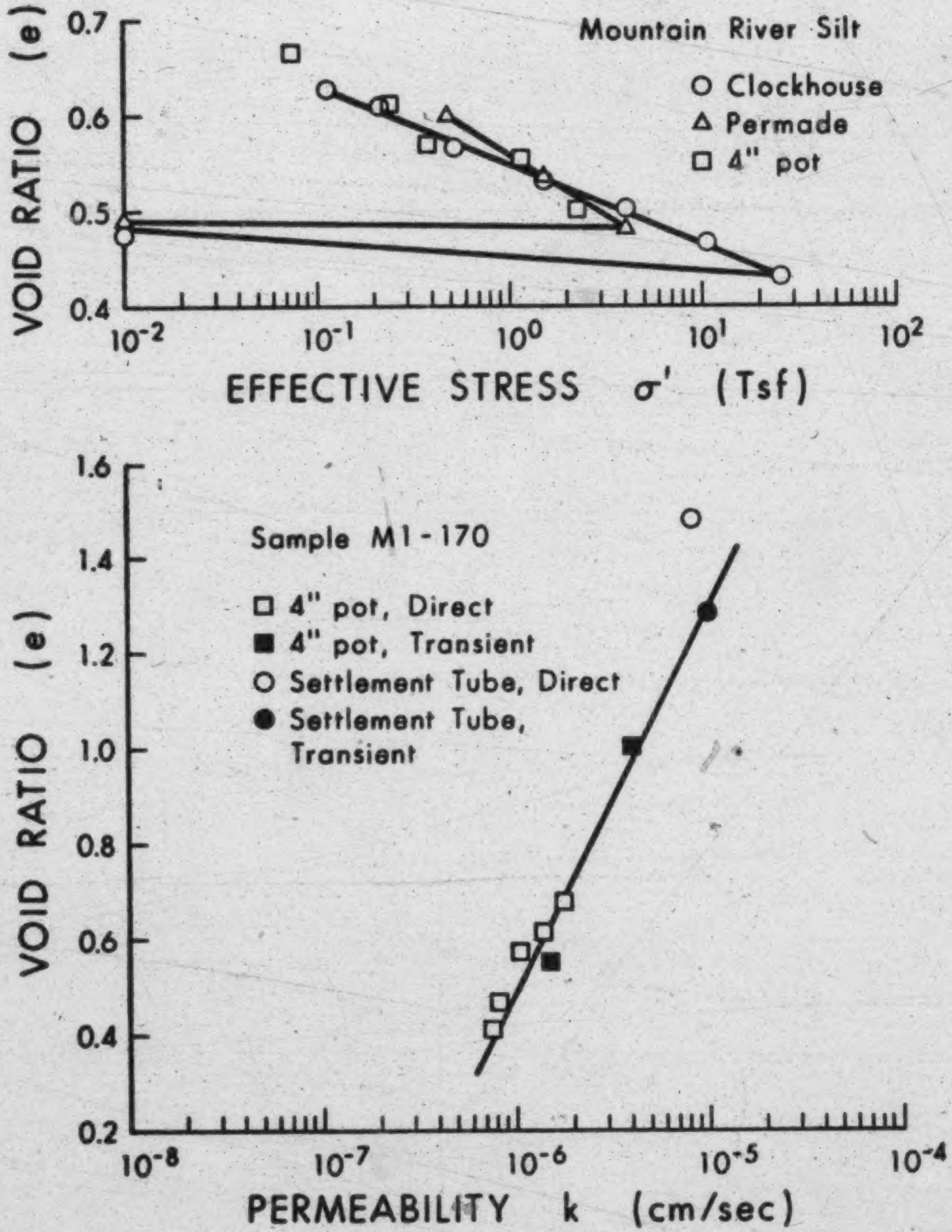

Fig B.14 Void Ratio versus permeability and effective stress for Mountain River Silt

APPENDIX C

THE SEDIMENTATION OF SOIL

		Page
C.1	Introduction	323
C.2	Development of the Theory of Sedimentation	327
C.3	Experimental Verification of Sedimentation	334
C.4	Sedimentation Consolidation	336
C.5	Thaw-sedimentation	341

C.1 Introduction

Let us follow Kaye and Broadman (1962) in observing that the behaviour of a suspension or dispersion of settling particles can be divided into four regions.

The first is a region of free settling at very low concentrations. The hydrodynamics of one particle settling through a fluid has been solved in terms of Stokes' Law

$$u_s = \frac{(G_s - 1)\,\gamma_w\,D^2}{18\,\eta} \qquad \text{C.1}$$

where u_s is the Stokes velocity

γ_w is the unit weight of water

G_s is the specific weight of soil solids

D is the particle diameter,

η is the Newtonian viscosity of the fluid

For a collection of different sized particles up to some small total concentration, each particle falls according to Eq C.1 and none influences the action of its neighbours.

With increasing concentration a dispersion enters a region of viscous interaction in which particles fall faster than their Stokes velocity. Kaye and Broadman review certain derivations by Smoluchowski who has shown that when 2 equi-settling particles move through a fluid and are separated by only a few diameters the terminal velocity of the pair exceeds the Stokes velocity for either particle. They also extend this work by showing experimentally that 4 spheres released close together fall in a cluster at greater than the individual Stokes velocity. They also present experimental data for medium sand-sized glass beads which increase velocity to 150% of Stokes between particle volume concentrations of 0.2 to 2%.

The third region at even higher concentrations is an unstable region characterized by irregular and localized return flow (Kaye and Broadman, 1962). In this region eddy currents form, disappear and reform and turbulent conditions are set up at the top of the dispersion such that a clear interface between dispersion and water cannot be maintained. A formulae, originally due to Einstein, gives the speed of fall of particles, v, as

$$v = u_s\,(1 - Ac) \qquad \text{C.2}$$

where A = a constant = 2.5 for hard spheres
c = volume concentration

and apparently has been obtained for dispersions in both regions 2 and 3 and possibly entering the last region.

The fourth region, at even higher concentrations, is a zone of hindered settling. As stated by Kynch (1952), it may be assumed that at any point in a dispersion of specified particles, in a fluid whose properties are known, that the velocity of fall depends only on the local concentration of particles. The settling process is then determined entirely from a consideration of continuity and without knowledge of the interaction of particles. That is, it is assumed that the general relationship

$$v = f\ (D,\ c,\ G_s,\ \eta\ ,\ \gamma_w) \qquad \text{C.3}$$

reduces to

$$v = v(c) \qquad \text{C.4}$$

This statement implies no segregation of different sized particles during sedimentation in the hindered settling zone.

Thus a distinction can be made between the mass movements characteristic of the hindered settling region and the particulate movements of the other three regions. At lower concentrations, sediment velocities are dominated by particle size and segregation results. Hindered settling, however, implies no segregation and a continuum exists in which although its properties may change with time they do so governed by considerations of continuity. We shall see that the process of hindered settling governs the characteristics of a dispersion before it becomes a soil.

It is useful to first consider a simple example of what is meant by hindered settling. As shown on Fig C.1 let us prepare and place a dispersion of initial uniform concentration c_i in a container such that the initial height of dispersion is H_o. If c_i is in a certain range of concentrations we will observe the following behaviour which will be later proven to be true. After some small initial time a sharp interface will form at the top of the dispersion between clear water and soil grains. This interface will settle with a constant velocity, m_2. At the base of the cylinder it can be observed that the dispersion settles abruptly into a soil of concentration, c_m, and that this interface propagates upwards with a constant velocity, m_1. At some time, t_f, the two interfaces will intersect and the dispersion, which has maintained itself at c_i, will vanish and a soil deposit overlain by water will remain.

Initially, the total stress at the base of the container equals the pore pressure and the effective stress is zero as there is no soil. At any given time the total stress at the base of the container

$$\nabla_b = m_1 \gamma t + m_2 \gamma_w t + (H_o - m_1 t - m_2 t) \gamma_f \qquad C.5$$

where (γ_w, γ_f, γ) are the unit weights of water, dispersion and soil respectively. The weight of particles plus water existing above the base of the container never changes, i.e., $d\nabla/dt = 0$, and from Eq C.5 it can be shown that

$$m_1 = m_2 \frac{(\gamma_f - \gamma_w)}{(\gamma - \gamma_f)} \qquad C.6$$

The time t_f that must elapse until all dispersion becomes a sediment is

$$t_f = \frac{H_o}{m_1 + m_2} \qquad C.7$$

and the depth of sediment formed is

$$X_f = \frac{H_o}{1 + \frac{m2}{m_1}} \qquad C.8$$

If the dispersion is made up of rigid particles the sediment formed at c_m will remain at this concentration. Furthermore, by the end of sedimentation the pore pressures at the base of the sediment will equal the hydrostatic pressure at that depth.

On the other hand, if the sediment formed contains fine-grained clayey particles the zero effective stress conditions set up at the base of the cylinder will not have been able to completely dissipate. There will then be a further post-sedimentation settlement phase as c_m is reduced and which is, of course, called consolidation.

C.2 Development of the Theory of Sedimentation

Sedimentation theory as proposed by Kynch (1952) has been developed by assuming that all particles are equi-sized. However, it seems reasonable to suggest that as the theory is valid only above some minimum concentration such that there is no segregation then the theoretical requirement for individual sized particles can be relaxed. Therefore, unlike Kynch who defines the concentration, c, as the number of particles per unit volume, c shall be used as the weight of particles per unit volume (gm/cm^3) or

$$c = G_s (1 - n) \gamma_w \qquad \text{C.9}$$

where n = porosity or volume voids per unit volume

and it should be noted that c is equivalent to γ_d the dry density.

The concept of particle flux, S, where S is the weight of particles crossing a horizontal section per unit of time is introduced where

$$S = v\ c \qquad \text{C.10}$$

and from Eq C.4 it follows that for hindered settling that

$$S = v(c) \cdot c \qquad \text{C.11}$$

or

$$S = S\ (c) \qquad \text{C.12}$$

and the particle flux (gm/cm^{2}s) at any level determines, or is determined by, the particle concentration. In general it can also be observed that the concentration at a point in a dispersion is related by the relation

$$c = c\ (x,\ t) \qquad \text{C.13}$$

Let us first consider the most simple form of sedimentation by postulating the existence of a discontinuity separating a dispersion c_1 falling at a velocity v_1 over a dispersion c_2 falling at v_2 and where $(c_1 < c_2)$. In order for the discontinuity to exist, it must have a velocity U such that

$$c_1 (v_1 + U) = c_2 (v_2 + U) \qquad \text{C.14}$$

or by Eq C. 10 we may write

$$U = \frac{S_1 - S_2}{c_2 - c_1} \qquad \text{C.15}$$

which is the assertion that a discontinuity is never at rest but moves through a dispersion with a velocity U. It should be noted that Kynch has called the discontinuity wave a discontinuity of the first kind.

The most obvious discontinuity is the top interface in Fig C.1 where

$$(S_1 = 0,\ c_1 = 0;\ S_2 = S\ (c_2),\ c_2)$$

and where

$$c_2 = c\ (x,\ t)$$

is the concentration of the dispersion immediately beneath the interface. If we anticipate later conclusions by letting

$$c_2 = c_i$$

then from Eq C.13 and Eq C.15, the velocity of the discontinuity wave between water and dispersion is

$$U = m_2 = \frac{-S(c\ (x,t)\ )}{c(x,t)} = -\frac{S(c_i)}{c_i} = -\ v(c_i) \qquad \text{C.16}$$

The second possible location of a discontinuity is at the base of the dispersion where we follow Kynch in asserting that:

> "A physically reasonable assumption about conditions at the base of a dispersion is that there is a continuous but extremely rapid increase of concentration from c_b to the maximum possible concentration c_m and that subsequently the concentration remains at c_m."

Therefore, at the base we have a discontinuity defined by

$$(S_b = S\ (c_b),\ c_b;\ S_m = 0,\ c_m)$$

where generally

$$c_b = c\ (x,t).$$

Let us again assume that

$$c_b = c_i$$

so that the velocity of the discontinuity wave between soil and dispersion is

$$U = \frac{S\ (c\ (x,t)\ )}{c_m - c(x,t)} = \frac{S\ (c_b)}{c_m - c_b} = \frac{S\ (c_i)}{c_m - c_i} \qquad \text{C.17}$$

and it is evident that velocity m_1,Fig C.1, is given by Eq C.17.

In order to prove the assertions made that the relationship

$$(c_2 = c(x,t) = c_i;\ c_b = c(x,t) = c_i\ )$$

it is necessary to return to Kynch's development and consider the existence of continuity waves. If we postulate 2 layers at heights x and x + dx above the base of a dispersion a consideration of the net accumulation of particles between these layers results in the equation of continuity as derived by Kynch (1952):

$$\frac{\partial c}{\partial t} = \frac{\partial S}{\partial x} \qquad \text{C.18}$$

On account of Eq C.10 this may be written as

$$\frac{\partial c}{\partial t} + V\ (c)\ \frac{\partial c}{\partial x} = 0 \tag{C.19}$$

$$\text{where } V\ (c) = -\frac{dS}{dc} \tag{C.20}$$

Eq C.20 can also be derived from Eq C.15 if we assume that there is a very small change in concentration across a discontinuous layer or

$$U = \frac{S_1 - S_2}{c_2 - c_1} = -\frac{dS}{dc} \tag{C.21}$$

However, as we have no knowledge of the relationship Eq C.12 it is impossible to generate a solution to the continuity equation Eq C.18 subject to the relevant boundary conditions. Thus, it is necessary to follow Kynch and consider certain characteristic solutions.

The physical meaning of Eq C.20 and C.21 is as follows. A small change in concentration dc if maintained is propagated through a dispersion of concentration c with velocity V. When considered in time and space a line of constant concentration describes a boundary between dispersions of c and c + dc and the slope of the line of constant c is given by Eq C.20. Thus Eq C.20 yields the velocity of what is called a continuity wave or what Kynch named a discontinuity of the second kind.

In order to consider the role of continuity waves, Eq C.20, and discontinuity waves, Eq C.15, we need to consider an example problem by assuming some form of Eq C.12. One possible form of the equation is that the flux plot is everywhere concave to the c axis as in Fig C.2 and this results in a characteristic sedimentation mode. Considering Case 1, Fig C.2, it can be seen that continuity waves begin to develop at velocities given by Eq C.20 in the region of the dispersion and they have all equal slopes of $+\lambda$. At the base of the container the dispersion at c_i settles discontinuously into a sediment at c_m and causes a discontinuity wave to be set up with velocity U_b. This discontinuity wave propagating up through the dispersion at a faster rate than the velocity of the continuity wave λ always overtakes and destroys the continuity waves. At the same time continuity waves are also travelling up to the top of the dispersion zone. These lines of constant c arrive at the interface and in doing so set up a discontinuity wave between water and dispersion that travels down at a constant rate. This discontinuity wave travels at a constant rate because the arriving continuity waves all have the same concentration. Thus both the top and bottom discontinuity waves trace out constant velocity paths and cause linear sedimentation modes.

In Case 2, Fig C.2, continuity waves are propagated downwards and the rising discontinuity between sediment and dispersion collides with and moves through the continuity waves.

The alternate form of Eq C.12 is that the flux plot is concave up in the region of interest, Fig C.3. For this condition a discontinuity wave is not set up at the base of the dispersion as it is possible for continuity waves to move up faster (as $U < V_B$). It can be seen that this behaviour then results in departures from linear sedimentation modes although it is to be noted that for the time ($0 < t < t_a$) the top interface does settle in a linear manner.

Before proceeding to a consideration of more general flux plots it is first necessary to investigate what Kynch has called end effects. Kynch wrongly assumes that as c approaches c_m v(c) approaches zero. The fact that the settling rate is not generally zero for a dispersion approaching c_m can be seen from a consideration of fluidization or quicking. In settling, a suspension moves through a more or less stationary fluid while in fluidization the fluid moves through a more or less stationary bed. In each case the immersed weight of the solids is supported by the fluid and the velocity with which we are interested is the relative velocity between fluid and particle. At the moment of quicking there is a certain relative velocity of water through the soil mass which is the velocity that will be approached in settling as c approaches c_m.

A useful method of both predicting the velocity at c_m and of presenting experimental data is shown by Richardson and Zaki (1954) as a result of experiments on sedimentation and fluidization. These authors found that the velocity of a dispersion could be written as

$$v = u_s \, (n)^r \qquad \text{C.22}$$

where r = a coefficient generally equal to 4.65

Eq C.22 has been found for a variety of more or less equi-sized particles from 10^{-1} to 5×10^{-2} cm in diameter. It can be noted that for a given particle size in a given fluid, Eq C.22 agrees with the basic assumption of Eq C.10.

Experimental data can be presented by preparing a plot of the log of settling velocity against the log of dispersion porosity. This plot should yield a linear relationship and it is then possible to estimate the velocity of fall at c_m by extrapolation and to then compute S_m by Eq C.10.

It can be noted that the velocity of fall can also be obtained from the analogy between sedimentation and fluidization. If the permeability, k, is known at the concentration c_m at which quick conditions are just reached in fluidization then:

$$v = k \, i = k \left(\frac{G_s - 1}{1 + e} \right) \qquad \text{C.23}$$

where e = the void ratio

and should be identically equal to the velocity predicted by Eq C.22.

If we now normalize Eq C.22 in terms of the terminal point (S_m, c_m) by combining Eqs C.9, C.11 and C.22 we can show that

$$u_s = \frac{S_m}{c_m \left(1 - \frac{c_m}{G_s}\right)^r} \qquad \text{C.24}$$

and it follows that

$$\frac{S}{S_m} = \frac{c}{c_m}\left[\frac{\frac{G_s}{c_m} - \frac{c}{c_m}}{\frac{G_s}{c_m} - 1}\right]^r \qquad \text{C.25}$$

We can now obtain the shape of the most general form of flux plot by solving Eq C.25 with the constants as noted in Fig C.4

This flux plot has been redrawn on Fig C.5 to emphasise the salient features which influence sedimentation modes. If a tangent is drawn from c_m tangent to the flux curve it defines two regions, Case 1, in which linear settling modes in all respects similar to Fig C.2 result. A second region, Case 2, is defined lying between the tangent point and the point of inflection of the curve. The characteristic sedimentation mode for this region results in a curved upper interface similar to Fig C.3. However, for Case 2 the bottom interface is a discontinuity wave defined by the departure from the flux curve at c_t as the dispersion can now settle discontinuously into c_m. The last region is defined by Case 3. While the upper surface is curved there is an abrupt change in slope as the first discontinuity wave U_b, caused by c_i settling discontinuously into c_t', arrives at the top surface.

The observation that the flux or velocity of a dispersion is not zero as c approaches c_m is important in predicting the duration of dispersion conditions in a sedimentation problem. While the velocity of the bottom interface in Fig C.5 could be easily calculated it can be seen quantitatively that the calculations required (and not presented) for Fig C.3 are more complicated as continuity waves govern the growth of the sediment-dispersion interface. However, by introducing the concept of non-zero flux conditions at the terminal concentration c_m we find, as in Fig C.5, that the growth of the sediment is always governed by a discontinuity wave and therefore moves at a constant velocity. Thus, once we know (H_o, c_m, c_i) it is an easy matter to enter the flux plot for a given soil and to calculate the time required for complete sedimentation from Eq C.7, C.8.

We are now in a position to experimentally confirm the theoretical consideration advanced above. While it is possible to re-create the entire flux plot from one sedimentation test the procedures involved are not straightforward and require a high degree of precision in monitoring the velocities of the relevant discontinuity waves. On the other hand, it is an easy matter to measure the velocity of fall of the top water-dispersion interface at a given dispersion concentration. By duplicating such tests at different concentrations and correlating results on a Richardson-Zaki diagram, Eq C.22, the normalized flux plot, Eq C.25, can then be obtained. Once the flux plot has been drawn it is then possible to predict the sedimentation behaviour for a given initial uniform concentration.

C.3 Experimental Verification of Sedimentation

Sedimentation tests were conducted by placing a dispersion of soil in a settlement tube and monitoring the fall of the top interface between water and dispersion. Samples were prepared by blender and pouring into the tube. Settlement tubes were either standard, 1 litre graduated cylinders, or a 4" diameter tube. Concentrations could be varied by syphoning off or adding a known amount of water and the tube shaken until a uniform concentration was obtained. It was impossible to shake the larger 4" diameter tube and re-mixing was attempted by stirring. However, it was found that it was impossible to obtain a uniform mix by stirring.

A summary of the soils considered is presented in Table C.1

Fig C.6 presents the weight-time relationships for the top interface of samples of Devon Sand and Fig C.7 for Grit. In Fig C.7 the slight initial departure from linear conditions is interpreted as representing the time required to accelerate to the characteristic velocity. It was not possible to trace the passage of the bottom discontinuity for Devon Sand and one attempt was made for the Grit. It can be seen that the sedimentation mode observed agrees well with the prediction of Case 1, Fig C.2.

Settlement time plots for Fort Norman Silt and Devon Silt are given in Figs C.8, and C.9. It can be seen that there is a marked linear portion for all porosities and this linear stage then grades into a curved region. This curved region may be due to the onset of consolidation effects or it may be caused by the effects noted in Cases 2 and 3, Fig C.5. However, it is not possible to discriminate between these alternatives given the accuracy the experimental techniques used. In any event, the maximum porosity, n_m, is defined by the first departure from non-linear settling using the extrapolation technique shown on Figs C.8 and C.9.

The velocity-porosity relationships for the dispersions noted on Table C.1 are then rectified according to the Richardson - Zaki correlation, Figs C.10 and C.11. It can be seen that there is a good linear fit for all seven grain-size types studied which can then be extrapolated to n_m to obtain v_m. Once v_m is known S_m can be calculated by Eq C.10 and normalized flux plots are then obtained as shown in Figs C.12 to C.14. It can be noted that the range of the exponent r of Eq C.25 is from 4.5 to 29.2.

In order to obtain a value for n_m to be used in the Richardson - Zaki extrapolation it was found necessary to take the lowest n_m predicted by the sedimentation curves. It can be seen that n_m predicted becomes lower as n_o decreases, and this effect is likely due to the marked curvature of the sedimentation modes at the lower concentrations which is, in turn, obscured by consolidation. This makes an estimate of n_m difficult.

The shape of the flux plots for Soils 3 to 7, Fig C.14, are consistent with the observed sedimentation modes for these dispersions as the linear settlement-time plots of Figs C.6 and C.7 as well as those shown by Steinour (1944) and Shannon et al (1962) are consistent with Case 1, Fig C.5.

The shape of the normalized flux plots for Devon Silt and Fort Norman Silt indicate that the sedimentation mode will vary depending on the initial concentration as in Fig C.5. Referring to Figs C.8 and C.9 it can be seen that there is a curved portion of the sedimentation curve for lower concentrations that agree in a general manner with Case 2, Fig C.5

However, it is difficult to distinguish between the possible role of initial concentration in causing deviations from non-linear settling or the effect of consolidation in the sediment. Both processes would cause the same curved settlement mode.

C.4 Sedimentation Consolidation

In the preceding development of hindered settling theory we assumed, following Kynch, that it was reasonable to assume that at the base of the dispersion that there was a continuous but extremely rapid increase of concentration from c_b to the maximum concentration, c_m. However, if the dispersion was made up of finer-grained particles it is clear that further settlements, or consolidation, will occur as concentrations are reduced below c_m in response to dissipation of excess pore pressures.

It has been shown that a uniform velocity field is maintained through the dispersion during the sedimentation process until the consolidation of the sediment starts after particle to particle contact begins at c_m. We can assume that the surface of the sediment or soil at the base of the container to be at $x = X(t)$. Assuming small strains in the soil skeleton and the maintenance of a constant flux of particles then the propagation of the surface $x = X(t)$ will be at a constant velocity, Fig C.15,

$$X(t) = m_1 t \qquad \text{C.26}$$

and for the upper surface

$$h(t) = H_o - (m_1 + m_2)t \qquad \text{C.27}$$

Thus Eq C.26 describes a region of sediment or soil which up to the termination of sedimentation at time, t_f, (Eq C.7) can be considered to be undergoing a sedimentation-consolidation process and after which enters into a region of conventional consolidation.

In writing an equation for the soil which is consolidating, the usual assumptions are made and noting that the total stress at any point in the soil remains constant the Terzaghi equation is adopted as

$$t > 0;\ \frac{\partial u}{\partial t} = c_v \frac{\partial^2 u}{\partial x^2}\ ;\ 0 \leqslant x \leqslant X(t) \qquad \text{C.28}$$

where u = the excess pore pressure

The first boundary condition for which Eq C.28 must then be solved is at the base where no flow is permitted and so

$$\frac{\partial u}{\partial x} = 0,\ x = 0 \qquad \text{C.29}$$

At the soil surface the flux of particles governs the growth of the height of the soil phase and the pore pressure at the surface $x = X(t)$ is given by the weight of dispersion and water above this point, that is

$$P_w = \gamma_f\, h(t) + (H_o - h(t) - X(t))\,\gamma_w \qquad \text{C.30}$$

where P_w = total (excess and hydrostatic) pore pressure
γ_w, γ_f = unit weight of water, fluid

and at

$$x = X(t),\ u = P_w - \gamma_w\,(H_o - X(t)) \qquad \text{C.31}$$

Thus from Eqs C.30 and C.31

$$u = (\gamma_f - \gamma_w)\, h(t) \qquad \text{C.32}$$

and from Eq C.27

$$u = (\gamma_f - \gamma_w)\,(H_o - (m_1 + m_2)\,t); \; x = X(t) \qquad \text{C.33}$$

Summarizing the consolidation problem we have:

$$t > 0 \; ; \; \frac{\partial u}{\partial t} = c_v \frac{\partial^2 u}{\partial x^2} \; ; \quad 0 \leq x \leq X(t) \qquad \text{C.34}$$

$$t > 0 \; ; \; \frac{u}{x} = 0; \quad x = 0 \qquad \text{C.35}$$

$$t > 0 \; ; \; u = (\gamma_f - \gamma_w)\,(H_o - (m_1 + m_2)t); \; x = X(t) \qquad \text{C.36}$$

$$t \geq 0 \; ; \; X(t) = m_1 t \qquad \text{C.37}$$

and where m_1, m_2, γ_f can be calculated from sedimentation theory

When the term $(H_o - (m_1 + m_2)t)$ becomes zero the sedimentation process terminates and the excess pore pressures dissipate according to the standard fixed boundary theory with $u = 0$ at $x = X_f$ where X_f is given by Eq C.8.

The solution to the above equations for the excess pore pressures in a sedimented soil at the completion of sedimentation at time t_f, has been obtained by Nixon (1972) using a finite difference technique, and is presented in Fig C.16. This solution expresses the excess pore pressure at any depth in terms of the time factor:

$$T_f = \frac{c_v \, t_f}{X_f^2} = \left(\frac{m_1 + m_2}{H_o}\right) \frac{c_v}{m_1^2} \qquad \text{C.38}$$

The theory of sedimentation-consolidation presented can be considered experimentally by modifying a settlement tube so that pore pressures can be measured at the base of the dispersion. A suitable device with a 4" diameter column was constructed and provision was also made to allow for drainage through the base of the cylinder.

Samples were prepared by mixing the dispersion in a commercial blender and storing the dispersion in a large flask. Once suitable quantities were prepared the flask was violently shaken and the dispersion poured into the tube. The height of the interface was monitored and pore pressures measured at the base of the dispersion.

The test data that can be presented in verification of the theory is somewhat meagre and the results are not conclusive. Other tests were conducted but they were incorrectly prepared. For instance, after tests DK2 and KN1 (to be considered) other concentrations were made up by adding or removing water and stirring the sediment in order to obtain a dispersion. However, this technique was later realized to be inadequate as uniform conditions could not be obtained and it is suspected that clusters of soil may have formed and which were not broken up.

Fig C.17 outlines the initial sedimentation process for a sample of Fort Norman Silt from the Fort Norman Landslide (see Appendix A), and the subsequent post-sedimentation consolidation. In the log plot the time axis was re-zero at $t_f = 3.9$ hrs corresponding to the end of sedimentation. If it is assumed that there is a triangular distribution of excess pore pressures at t_f a value of c_v can be deduced from the settlement - log t plot. This c_v can then be introduced into Fig C.16 in order to obtain an estimate of the excess pore pressures at time, t_f. The estimated $c_v = 2.6 \times 10^{-3}$ cm^2/s and as ($X_f = 18.4$ cm, $t_f = 3.9$ hrs) from Eq C.38, $T_f = 0.11$. From Fig C.16 the predicted ratio of excess pore pressure at the end of sedimentation is 0.65 compared with a measured ratio at the base of 0.39, Fig C.17.

The c_v measured during the post - sedimentation phase can also be compared with the c_v deduced from subsequent consolidation of the sample induced by a head imbalance. A total stress increment was applied by opening the drainage valve at the base of the container and a known head difference was then maintained across the sample. Fig C.18 outlines the subsequent post-sedimentation - consolidation behaviour and the value of c_v and k calculated agrees well with the values obtained in Fig C.17.

A second test on Devon Silt, Fig C.19, can also be considered although the post-sedimentation consolidation of the soil formed was not observed. A measured excess pore pressure ratio of 0.35 was noted at (X_f = 13.3 cm, t_f = 0.76 hr). The c_v during sedimentation can be estimated from a subsequent consolidation test on the same sample due to a head imbalance, Fig C.20 and is 1.37×10^{-2} cm^2/s. This c_v value results in a $T_f = 0.21$ and a predicted excess pore pressure ratio from Fig C.16 of 0.58. However, it should be noted that the c_v operative during the time up to t_f will be likely substantially different from the value deduced due to subsequent consolidation. Furthermore, as the average void ratio up to t_f is higher than for the test in Fig C.20 the actual c_v will be lower, the T_f calculated smaller and the subsequent predicted pore pressure ratio higher.

Other sedimentation tests on both Fort Norman Silt and Devon Silt were conducted but as they were the subject of certain errors in sample preparation, as discussed above, they have not been considered. One such test, KN5, Fig C.21, was made on a dispersion prepared by stirring only. The top interface underwent a more-or-less linear settling mode although the velocity increased towards time t_f. The bottom interface could be observed by noting the top of a zone in which piping began. This interface was well curved initially as coarser sediment was first deposited and then became linear as an apparently uniform and finer-grained dispersion was laid down. This separation of sizes was also seen in a tonal change in the colour of the sediment, beginning at 5 cm. Furthermore, the excess pore pressure ratios also reflect the bi-modal distribution of particles. However, even though it is encouraging to see that the experimental techniques used could pick up this process it cannot, as yet, be predicted by sedimentation theory.

The greatest shortcoming of the theory formulated in this section is that basic consolidation theory is used and small strains only are assumed in the soil skeleton. For the high void ratios encountered a non-linear theory that can cope with the large strains involved is required. This can be seen in Fig C.22 which compares the post-sedimentation consolidation of Fig C.17 with theoretical predictions. While the actual progression of settlement with time agrees well with predicted settlements the pore pressure dissipation does not.

It can also be noted that the testing technique involved here also has application in other aspects of high void ratio soils. For example, in Sec 3.3 we were concerned with the prediction of permeability of thawed Fort Norman Silt at high void ratios. The settlement tube tests of Fig C.17 and C.18 yield a prediction for k at high void ratios from consolidation theory. Furthermore, it is a simple matter to conduct a direct head permeability test, Fig C.18, in the settlement tube and the value obtained agrees well with the transient determination. It can be seen in Sec 3.3 that the high void ratio k values agree well with test data at lower void ratios.

C.5 Thaw-sedimentation

If a thaw interface is caused to advance through a frozen uniform soil it is apparent that at high enough void ratios a dispersion will be formed. Furthermore, it is possible to sustain this dispersion until the thaw rate slows down to such a point that a sediment can be formed.

If we re-derive the Kynch continuity equation consistent with having the flux S positive in the positive x direction the governing equation for the dispersion, Fig C.23 becomes

$$\frac{\partial c}{\partial t} = \lambda \frac{\partial c}{\partial x} \quad ; \quad h(t) < x < X(t) \qquad \text{C.39}$$

where $$\lambda = -\frac{dS}{dc} \qquad \text{C.40}$$

and the equation for the velocity of a discontinuity wave becomes

$$U = \frac{S_1 - S_2}{c_1 - c_2} \qquad \text{C.41}$$

It is now necessary to assume some form for the relationship $S = S(c)$ and the simplest relation which is consistent with real flux plots is, see Fig C.23

$$S = S_m + \lambda(c_m - c) \tag{C.42}$$

Let us now inspect conditions along the bottom boundary $x = X(t)$ which is a discontinuity separating a dispersion of concentration c from a frozen soil that is stationary, $S_2 = 0$, at some concentration, c_i. Thus

$$U = \frac{dX}{dt} = \frac{S(c)}{c - c_i}$$

or

$$c = c_i + \frac{S(c)}{dX/dt} \tag{C.43}$$

Substituting C.43 into C.42

$$c = c_i + \frac{S_m + \lambda(c_m - c)}{dX/dt}$$

or

$$c(X,t) = \frac{\frac{dx}{dt} c_i + \lambda c_m + S_m}{\frac{dX}{dt} + \lambda} \tag{C.44}$$

which gives c directly at the boundary $x = X(t)$ once dX/dt is prescribed.

If we now cause dX/dt to be governed by the Neumann solution then

$$\frac{dX}{dt} = \frac{\alpha}{2\sqrt{t}} \qquad \text{C.45}$$

and if we define the time t_F as the first time at which a real soil is formed then in Eq C.44 $c(X,t) = c_m$ and it can be shown that

$$t_F = \frac{\alpha^2}{4} \left(\frac{c_m - c_i}{S_m} \right)^2 \qquad \text{C.46}$$

and the corresponding depth

$$X_F = \alpha\sqrt{t_f} = \frac{\alpha^2}{2} \left(\frac{c_m - c_i}{S_m} \right) \qquad \text{C.47}$$

Eq C.47, therefore, predicts the depth to which thaw will maintain a dispersion in a fluid-like state. At depths greater than X_f effective stresses will begin to be mobilized. Typical values of X_f are presented in Chapter 3.

TABLE C.1 SUMMARY OF SOILS CONSIDERED IN SEDIMENTATION THEORY

Code	Soil	G_s	Comments	Source
1	Fort Norman Silt	2.73	Grain size curve in Appendix B	This study
2	Devon Silt	2.65		This study
3	Devon Sand	2.65	#40 to #200 Fraction of Devon Silt	This study
4	Glass Beads	2.32	0.013 mm size	Steinour (1944)
5	Emery	3.78	0.012 mm size	Steinour (1944)
6	Glass	2.45	0.067 mm size	Shannon (1962)
7	Grit	3.78	#100 to #300 sieve size	This study

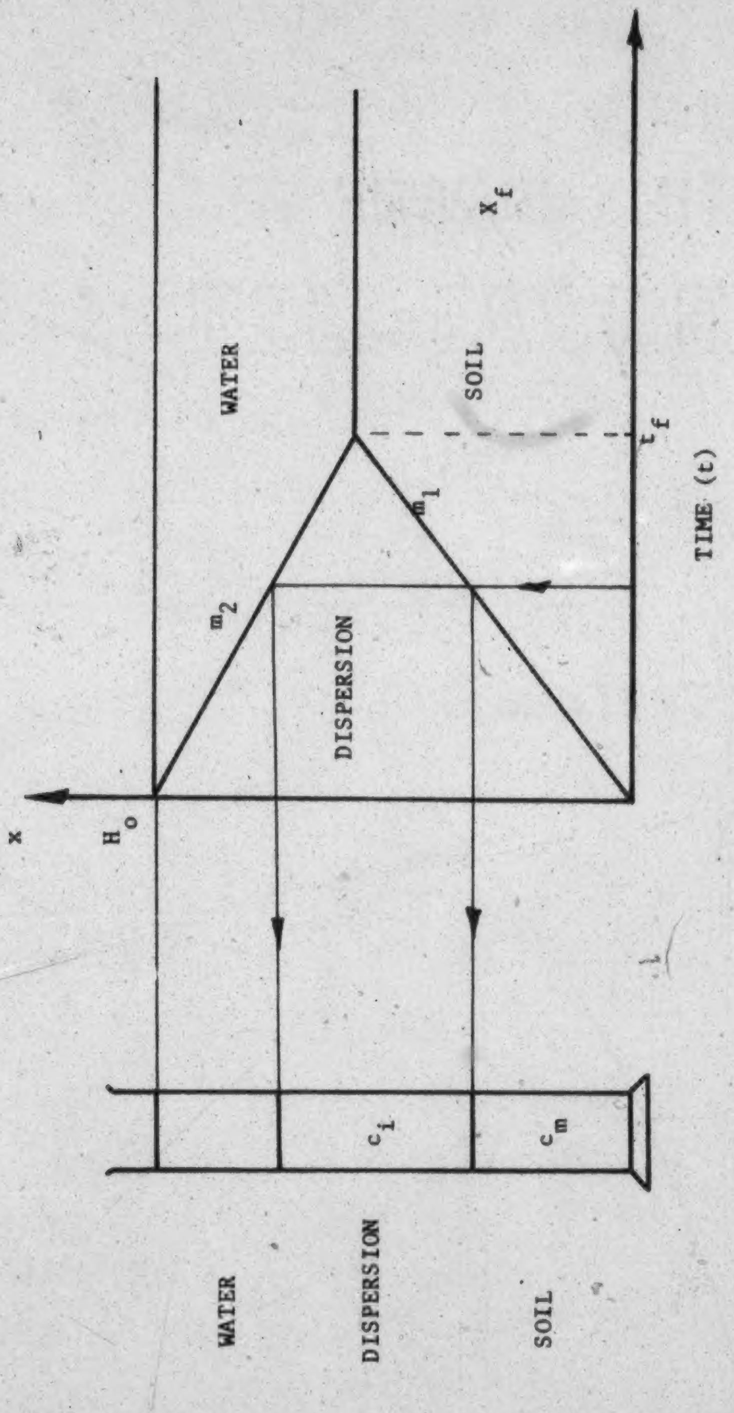
x
H_o
WATER
DISPERSION
SOIL
m_2
m_1
t_f
X_f
TIME (t)
c_i
c_m
WATER
DISPERSION
SOIL

$$m_1 = m_2\left(\frac{c_i}{c_m - c_i}\right) = m_2\frac{(\gamma_f - \gamma_w)}{(\gamma - \gamma_w)}$$

Fig C.1 Characteristics of hindered settling sedimentation

SEDIMENTATION MODE FOR CONCAVE DOWN FLUX PLOTS

FLUX PLOT: CONCAVE DOWN $\equiv \frac{dV}{dc} > 0 \equiv \frac{d^2S}{dc^2} < 0$

DISCONTINUITY $U = \frac{S_1 - S_2}{c_2 - c_1}$

CONTINUITY $V = -\frac{dS}{dc}$

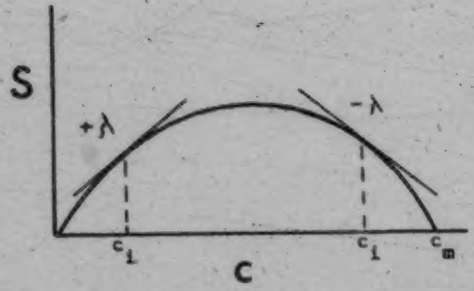

SEDIMENTATION MODE : DISPERSION AT UNIFORM INITIAL c_i

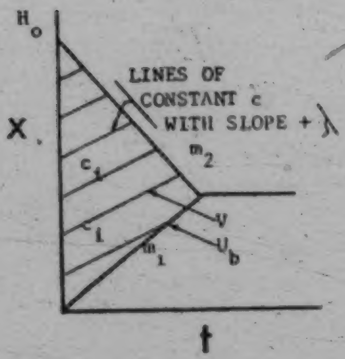
H_o
X
LINES OF CONSTANT c WITH SLOPE $+\lambda$
m_2
c_i
c_i
m_1
V
U_b
t

CASE 1: c_i SUCH THAT $\frac{dS}{dc} = -\lambda$

$$U_b = \frac{S_i}{c_m - c_i}$$

$V = +\lambda$

$U_b > V$

THEN $(m_1 = U_b \; ; \; m_2 = -v(c_i))$

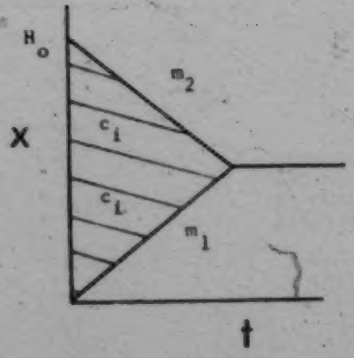
H_o
m_2
X
c_i
c_i
m_1
t

CASE 2 : c_i SUCH THAT $\frac{dS}{dc} = +\lambda$

$$U_b = \frac{S_i}{c_m - c_i}$$

$V = -\lambda$

$U_b > V$

THEN $(m_1 = U_b \; ; \; m_2 = -v(c_i))$

Fig C.2 Sedimentation Mode: Concave Down Flux Plot

SEDIMENTATION MODE FOR CONCAVE UP FLUX PLOTS

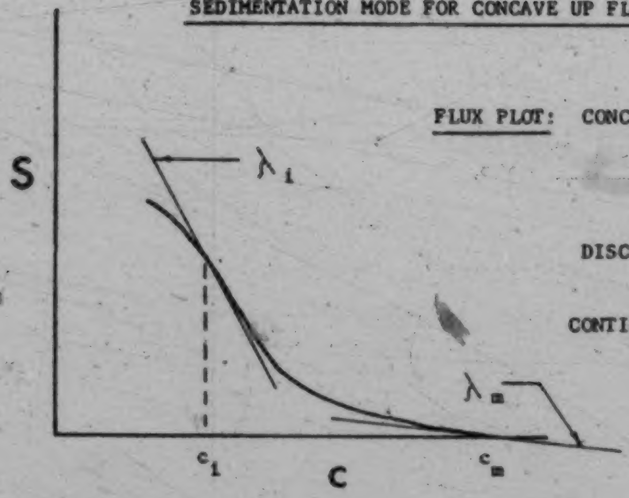
S
λ_i
c_i
C
c_m
λ_m

FLUX PLOT: CONCAVE UP $\equiv \frac{dV}{dc} < 0 \equiv \frac{d^2S}{dc^2} > 0$

DISCONTINUITY $U = \frac{S_1 - S_2}{c_2 - c_1}$

CONTINUITY $V = \frac{-dS}{dc}$

SEDIMENTATION MODE:

FOR ($x = 0$, $t = 0$)

$$U = \frac{S_i}{c_m - c_i} < V_b = +\lambda_i$$

FOR $(0 < t < t_a)$ $m_2 = v(c_i)$

$(t_a < t < t_f)$ $m_2 = v(c)$

WHERE $c = c(x,t)$

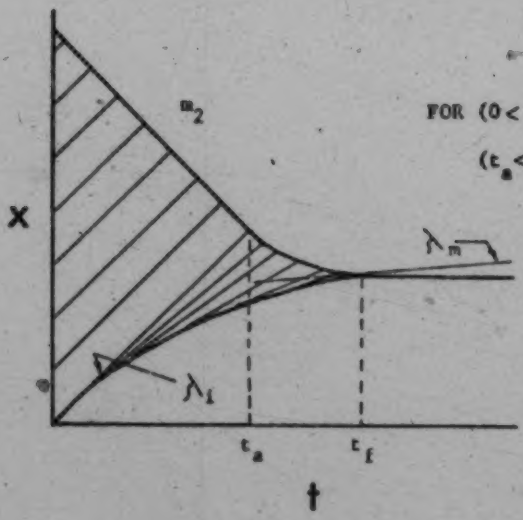
m_2
X
λ_m
λ_i
t_a
t_f
t

FOR $(0 < t < t_f)$

$V_b = \lambda_i$ to λ_m

Fig C.3 Sedimentation mode: concave up flux plot

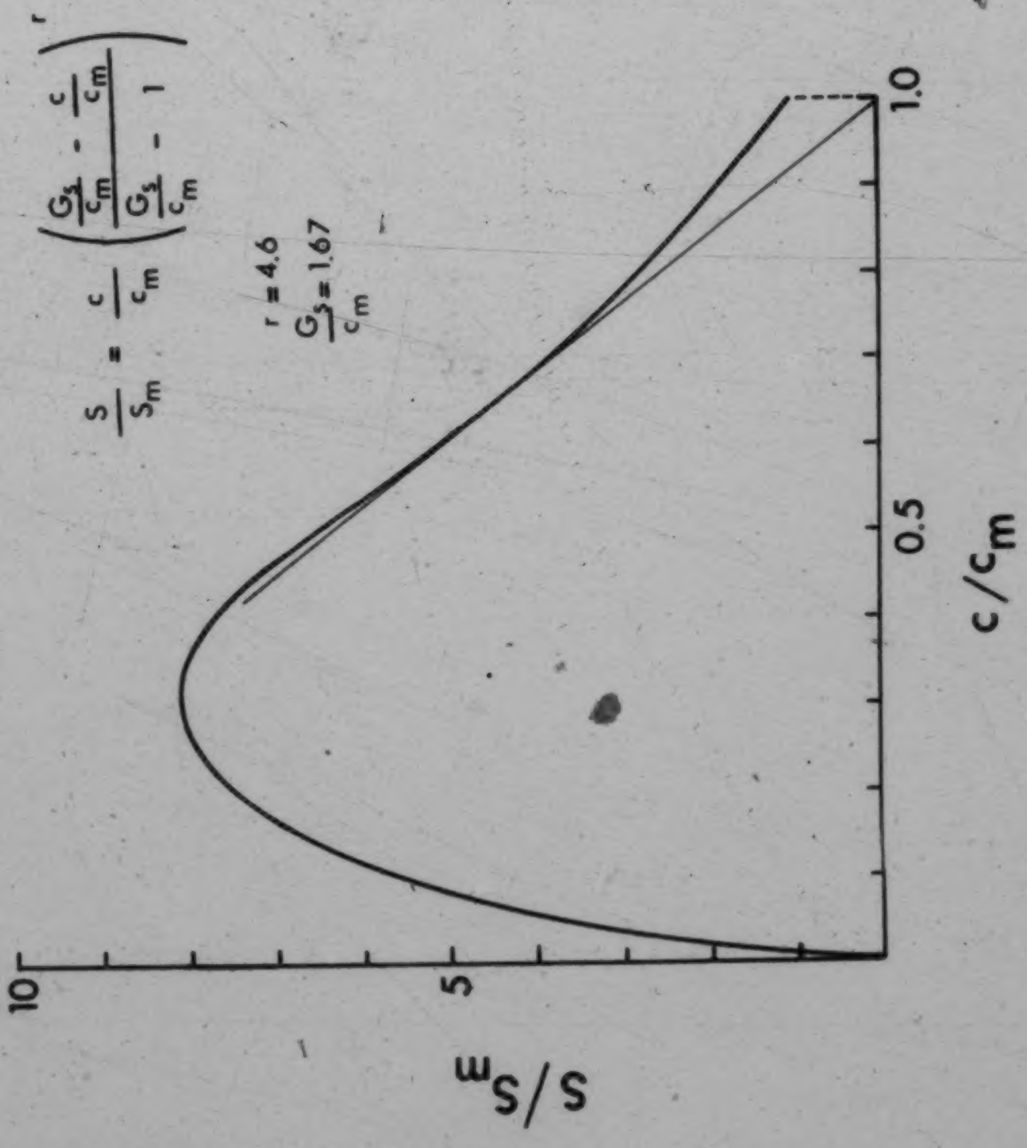

Fig C.4 Normalized flux plot: Richardson-Zaki relationship

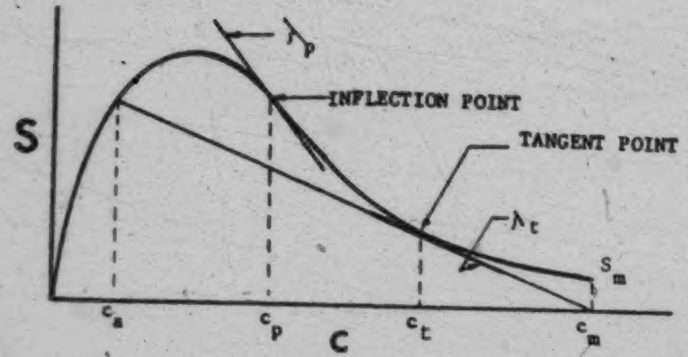

λ_p
INFLECTION POINT
TANGENT POINT
S
λ_t
S_m
c_a
c_p
c_t
c_m
C

CASE 1 $(0 < c_i < c_a \; ; \; c_t < c_i < c_m)$

FLUX PLOTS CONCAVE DOWN OR $U_b > V$ THEREFORE LINEAR SETTLING MODES

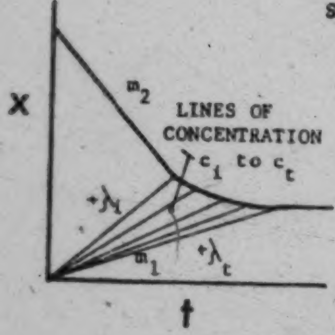

X
m_2
LINES OF CONCENTRATION
c_i to c_t
$+\lambda_i$
m_1
$+\lambda_t$
t

CASE 2 $(c_p < c_i < c_t)$

$$m_1 = +\lambda_t = -\left(\frac{dS}{dc}\right)_{c_i} = \frac{S_t}{c_m - c_t}$$

$$m_2 = -v(c_i)$$

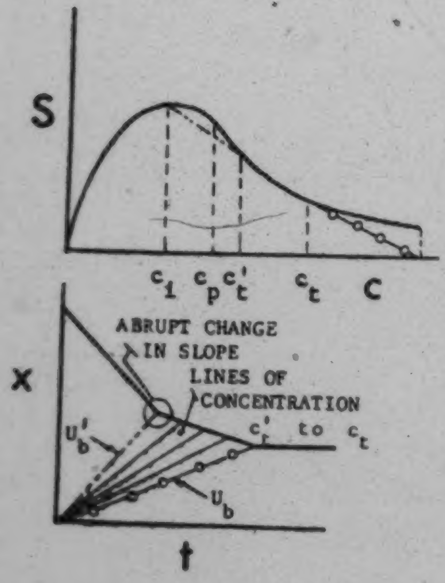

S
c_i
c_p
c_t'
c_t
C
X
ABRUPT CHANGE IN SLOPE
LINES OF CONCENTRATION
c_t' to c_t
U_b'
U_b
t

CASE 3 $(c_a < c_i < c_p)$

c_t' DEFINED BY TANGENT DRAWN FROM c_i TO THE FLUX CURVE

$$U_b' = \frac{S_i - S_t'}{c_t' - c_i}$$

$$U_b = \frac{S_t}{c_m - c_t}$$

Fig C.5 Generalized sedimentation modes for hindered settling

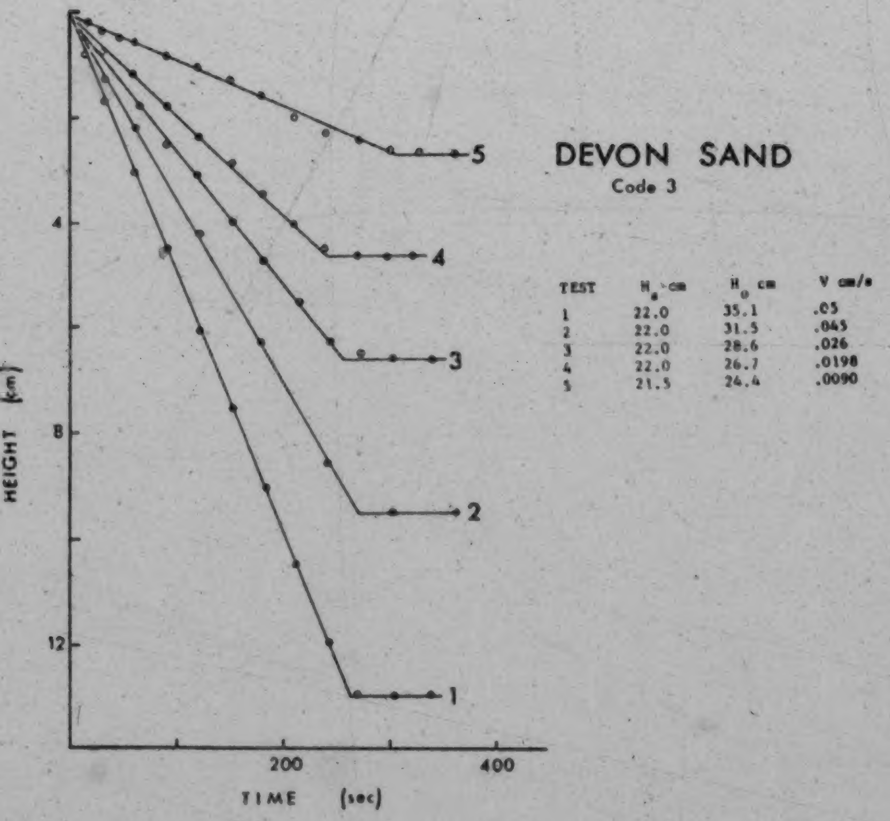

TEST	H_e cm	H_0 cm	V cm/s
1	22.0	35.1	.05
2	22.0	31.5	.045
3	22.0	28.6	.026
4	22.0	26.7	.0198
5	21.5	24.4	.0090

Fig C.6 Hindered settling for Devon Sand

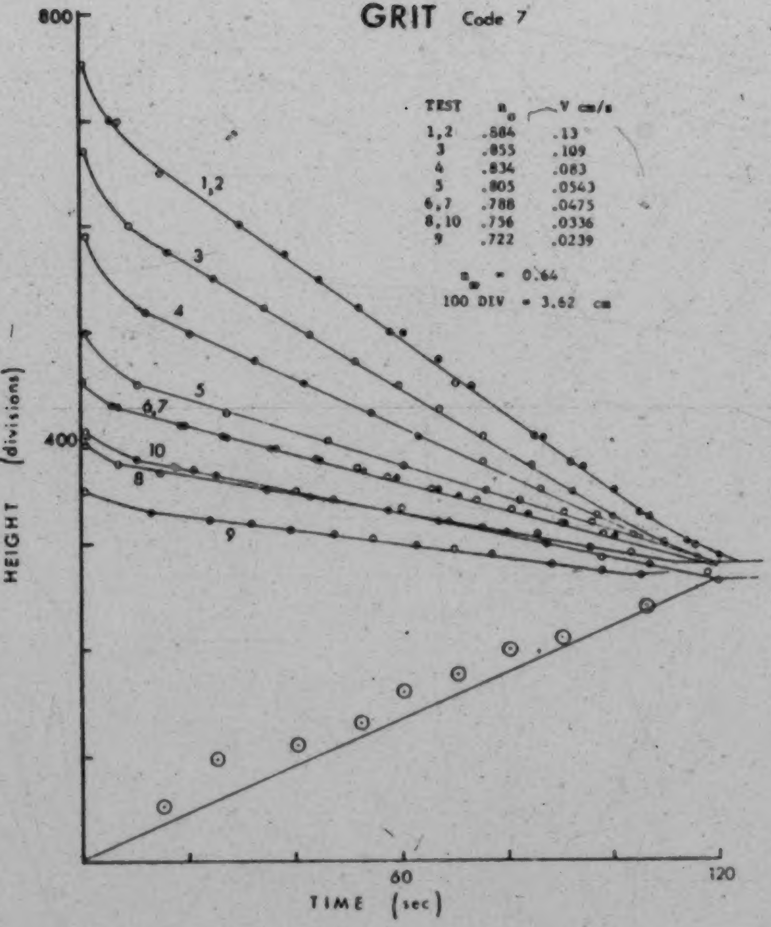

TEST	n_0	V cm/s
1,2	.884	.13
3	.855	.109
4	.834	.083
5	.805	.0543
6,7	.788	.0475
8,10	.756	.0336
9	.722	.0239

n_∞ = 0.64

100 DIV = 3.62 cm

Fig C.7 Hindered settling for Grit

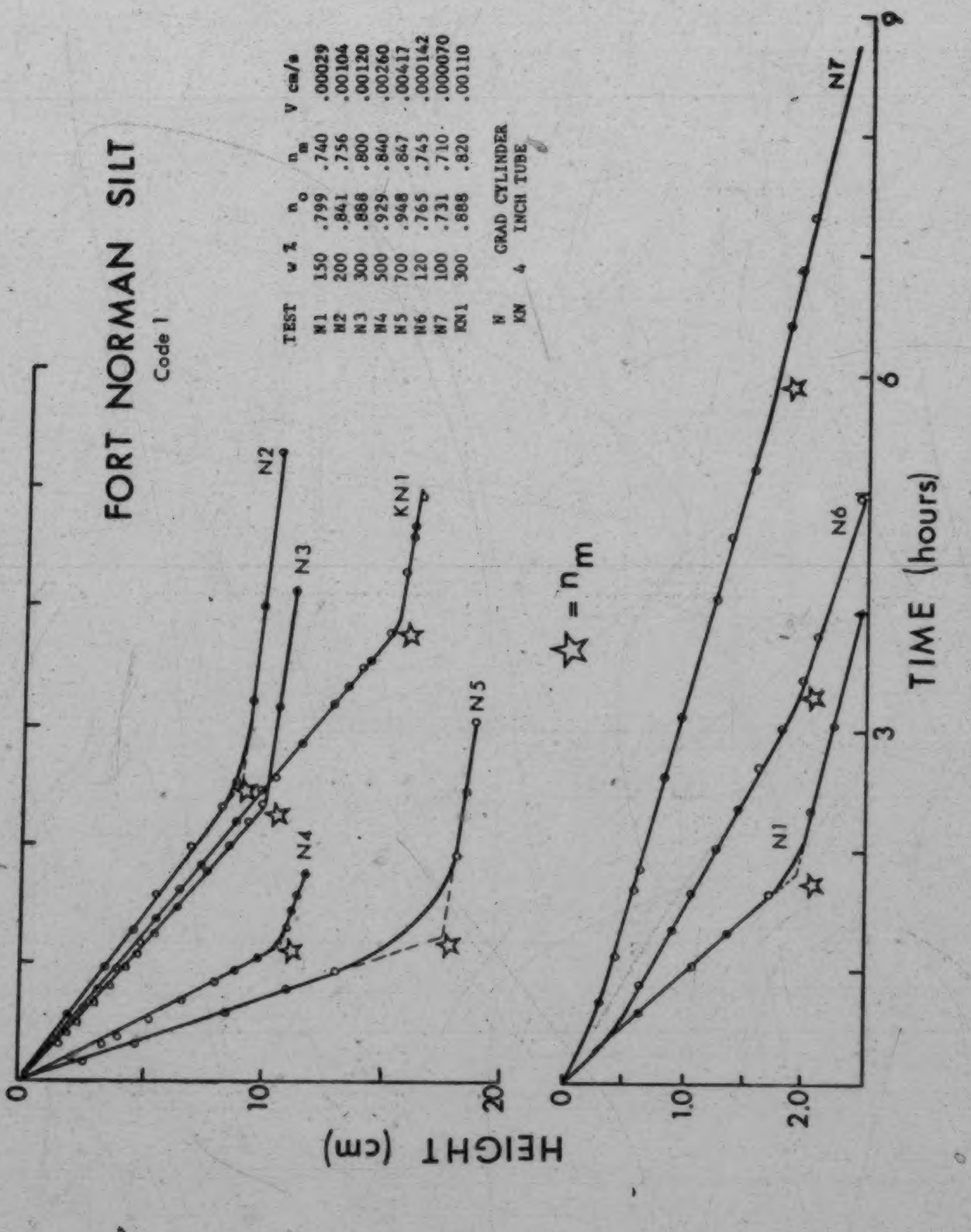

TEST	w %	n_o	n_m	V cm/s
N1	150	.799	.740	.00029
N2	200	.841	.756	.00104
N3	300	.888	.800	.00120
N4	500	.929	.840	.00260
N5	700	.948	.847	.00417
N6	120	.765	.745	.000142
N7	100	.731	.710	.000070
KN1	300	.888	.820	.00110

N GRAD CYLINDER
KN 4 INCH TUBE

Fig C.8 Hindered settling for Fort Norman Silt

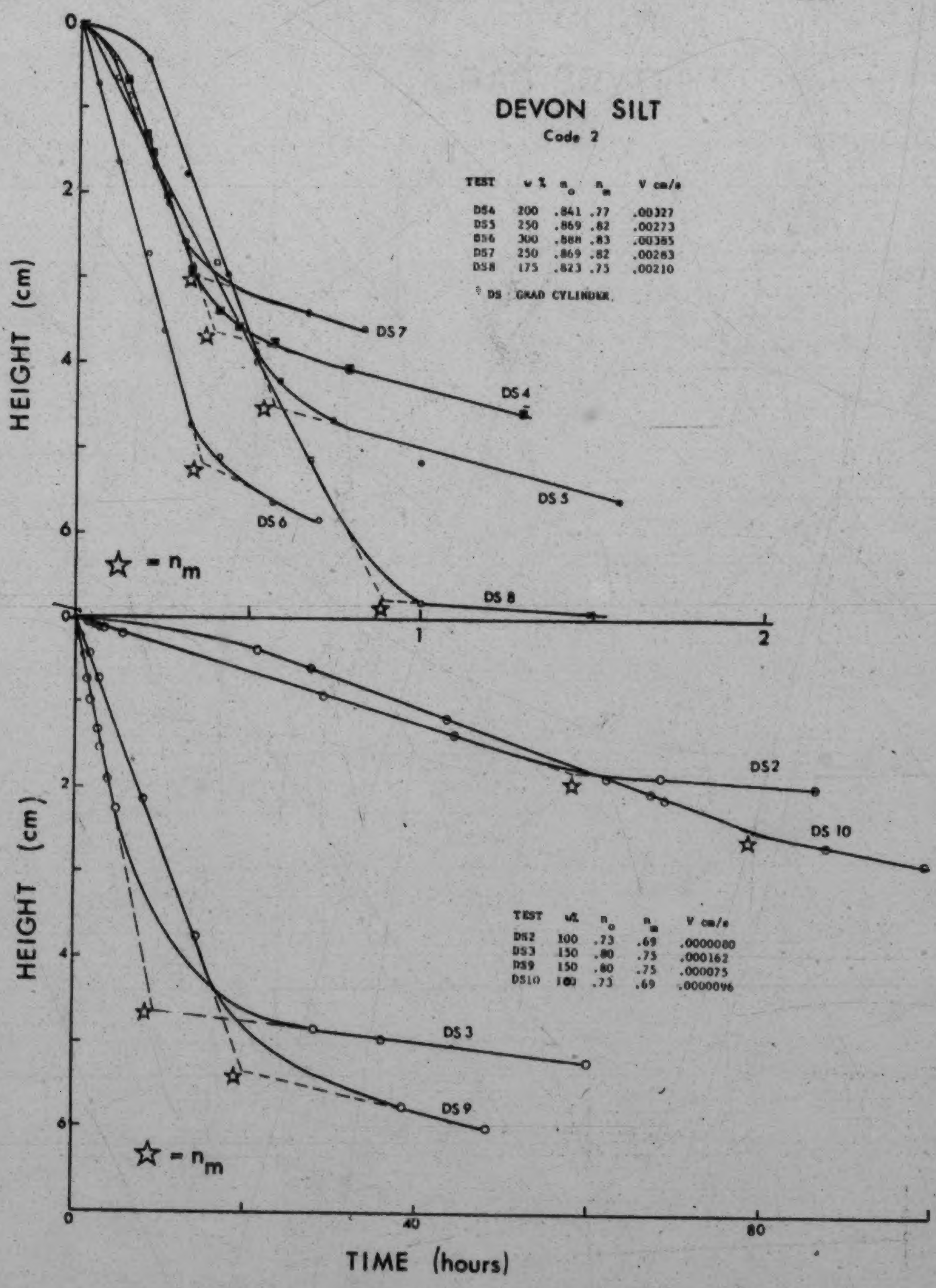

TEST	w %	n_o	n_m	V cm/s
DS4	200	.841	.77	.00327
DS5	250	.869	.82	.00273
DS6	300	.888	.83	.00385
DS7	250	.869	.82	.00283
DS8	175	.823	.75	.00210

DS : GRAD CYLINDER.

TEST	w%	n_o	n_m	V cm/s
DS2	100	.73	.69	.0000080
DS3	150	.80	.75	.000162
DS9	150	.80	.75	.000075
DS10	100	.73	.69	.0000096

Fig C.9 Hindered Settling for Devon Silt

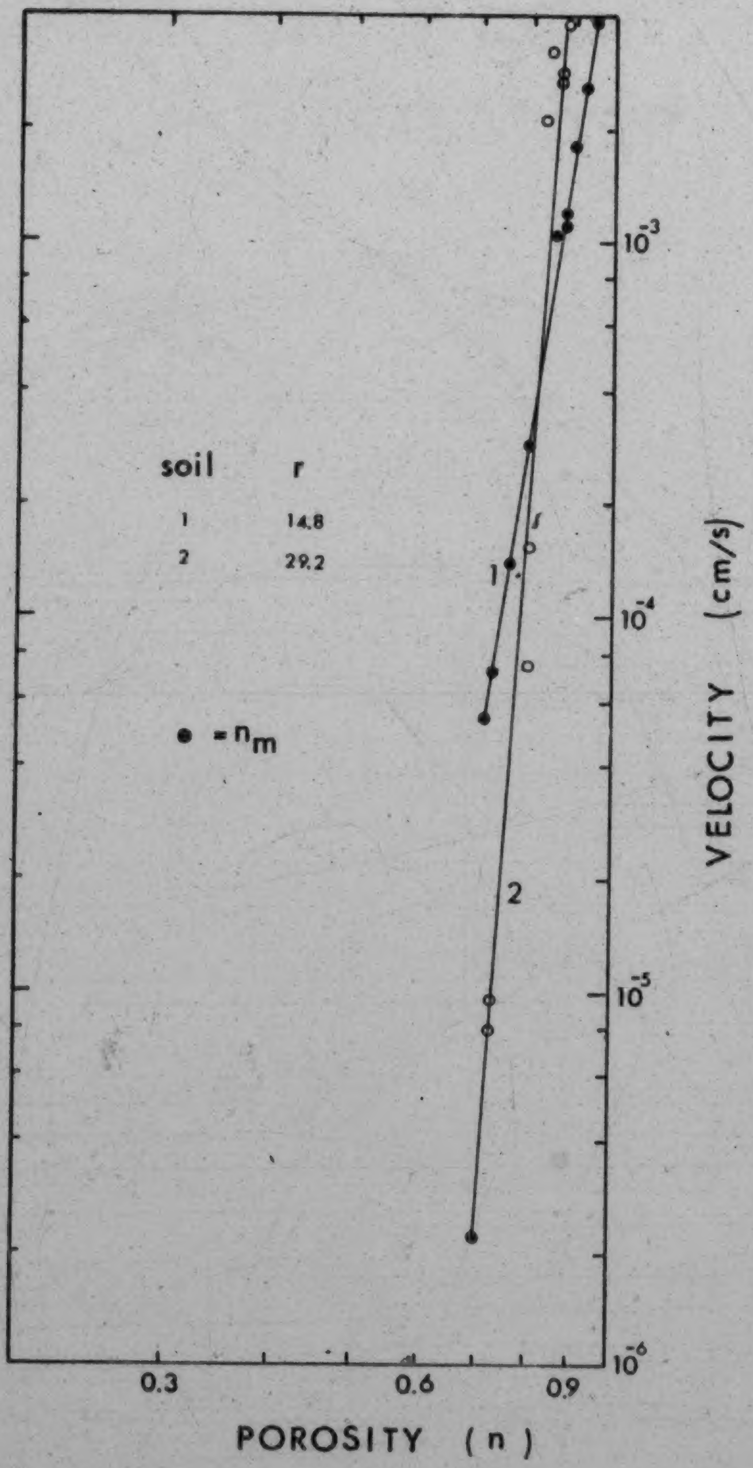

Fig C.10 Richardson-Zaki Correlations

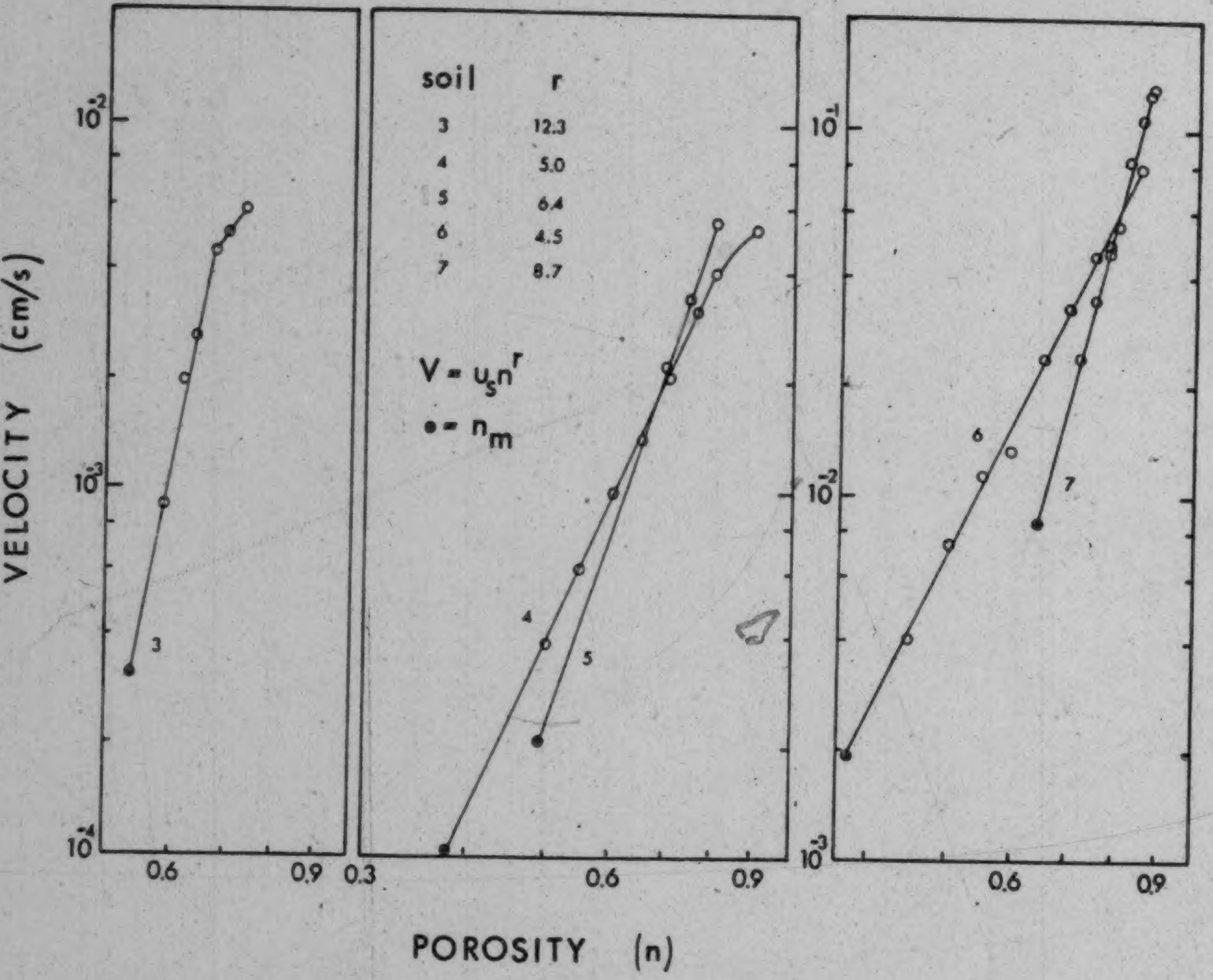

Fig C.11 Richardson-Zaki Correlations

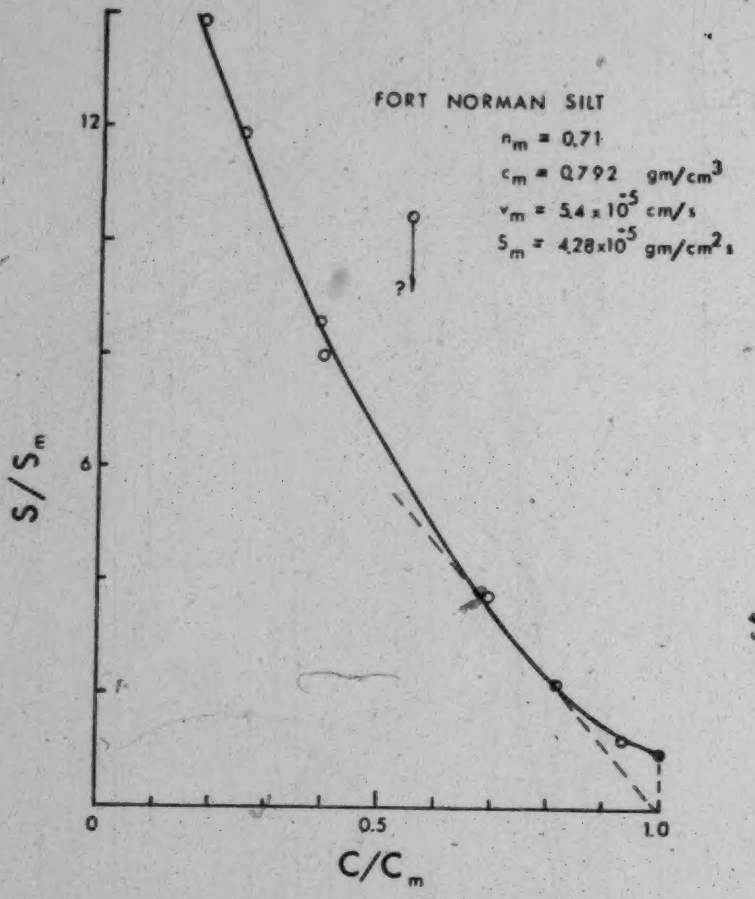

Fig C.12 Normalized flux plot:
Fort Norman Silt

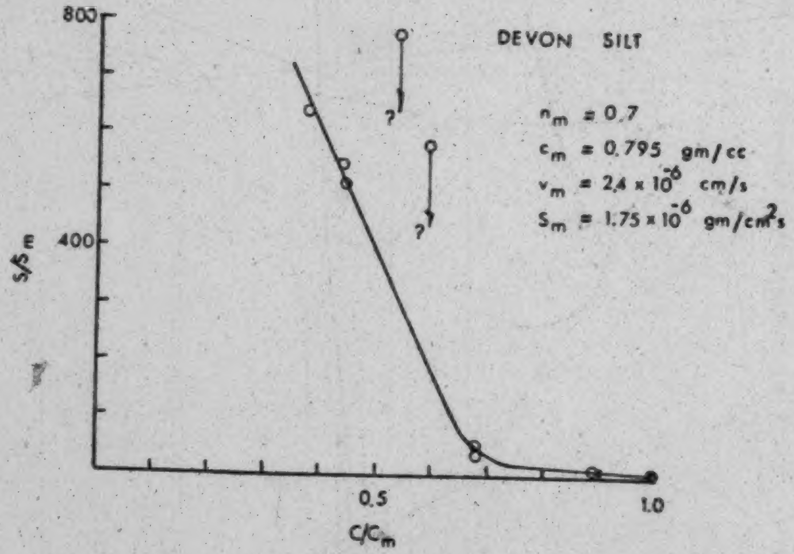

Fig C.13 Normalized flux plot:
Devon Silt

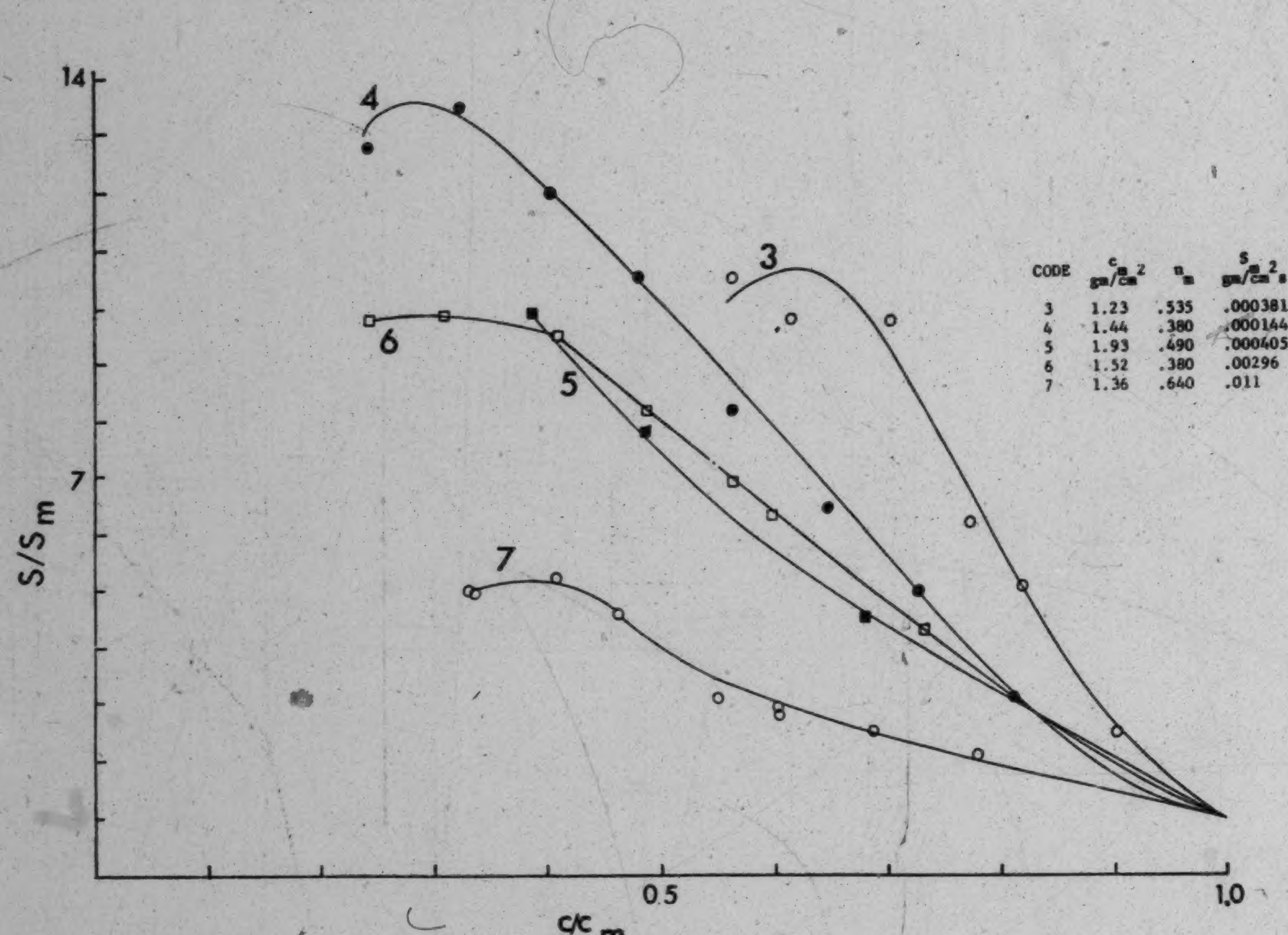

CODE	c_m gm/cm^2	n_m	S_m gm/cm^{2}s
3	1.23	.535	.000381
4	1.44	.380	.000144
5	1.93	.490	.000405
6	1.52	.380	.00296
7	1.36	.640	.011

Fig C.14 Normalized flux plots

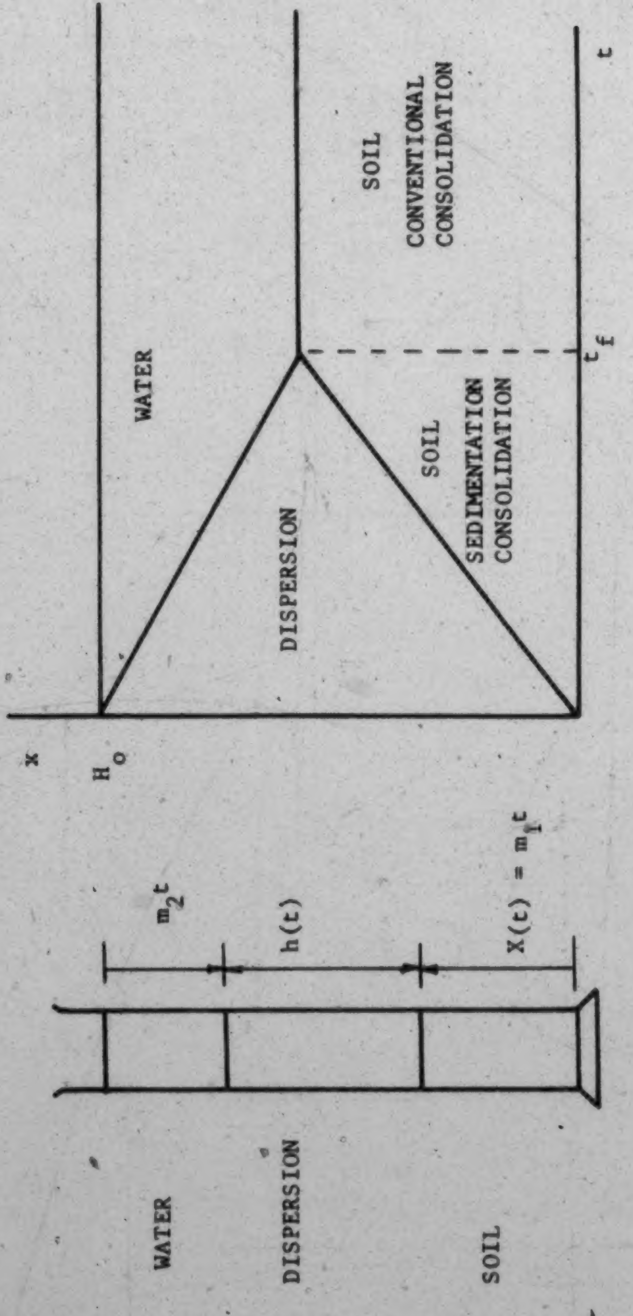
x
H_o
WATER
DISPERSION
SOIL
SEDIMENTATION
CONSOLIDATION
SOIL
CONVENTIONAL
CONSOLIDATION
t_f
t
m_2t
h(t)
$X(t) = m_1t$
WATER
DISPERSION
SOIL

Fig C.15 The sedimentation-consolidation problem

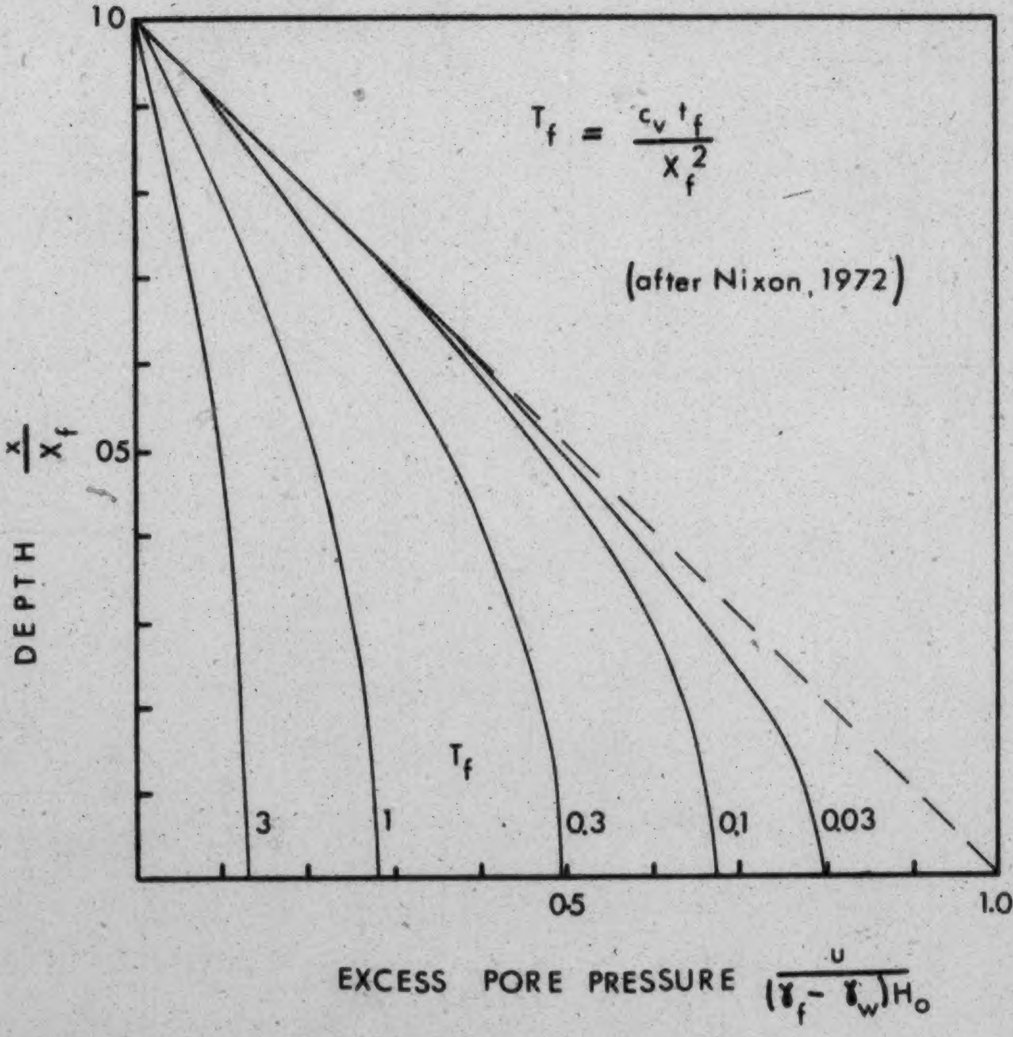

Fig C.16 Solution for the excess pore pressures in a sedimented soil at the completion of sedimentation

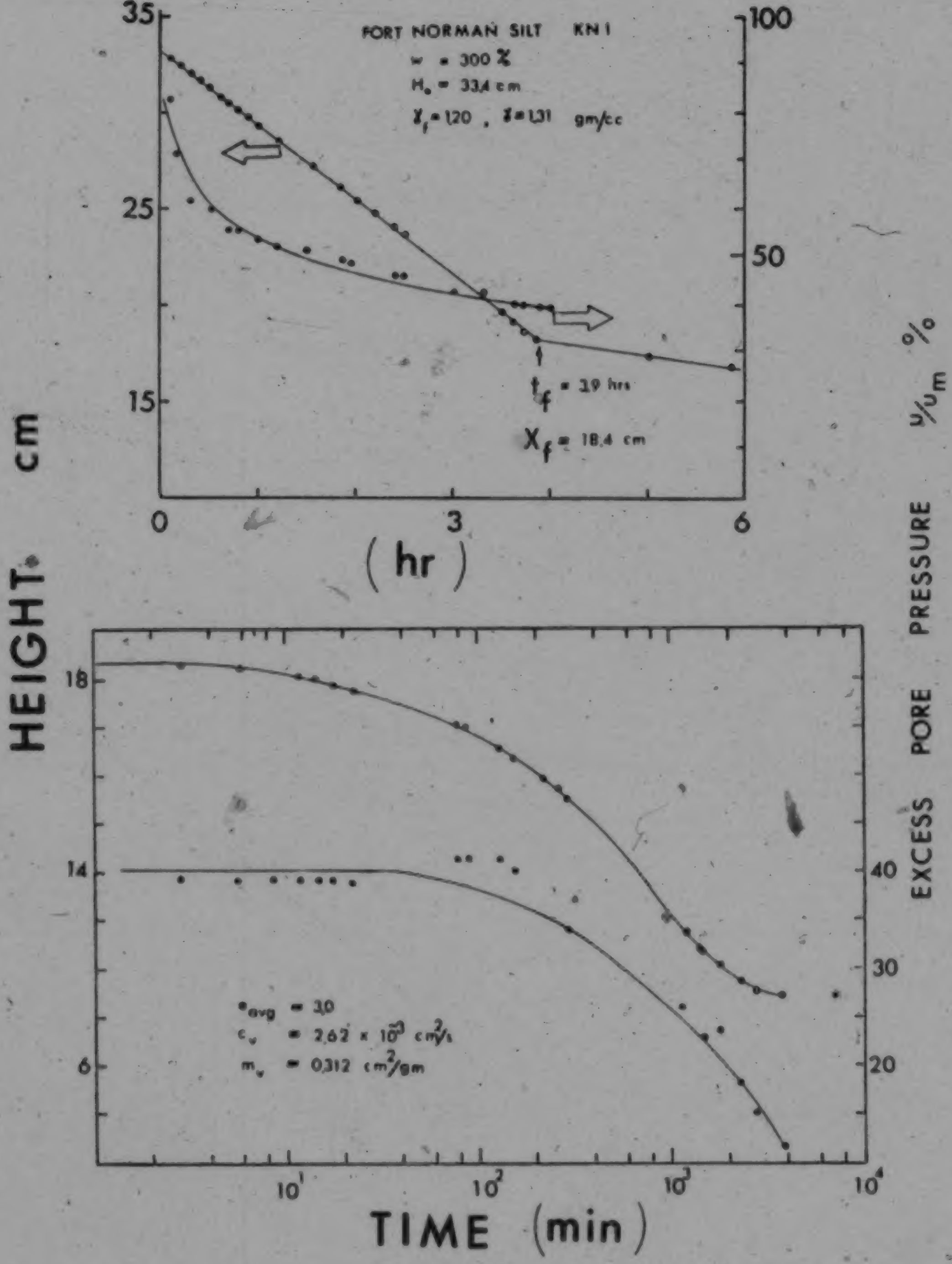

Fig C.17 Hindered settling and subsequent consolidation: Fort Norman Silt

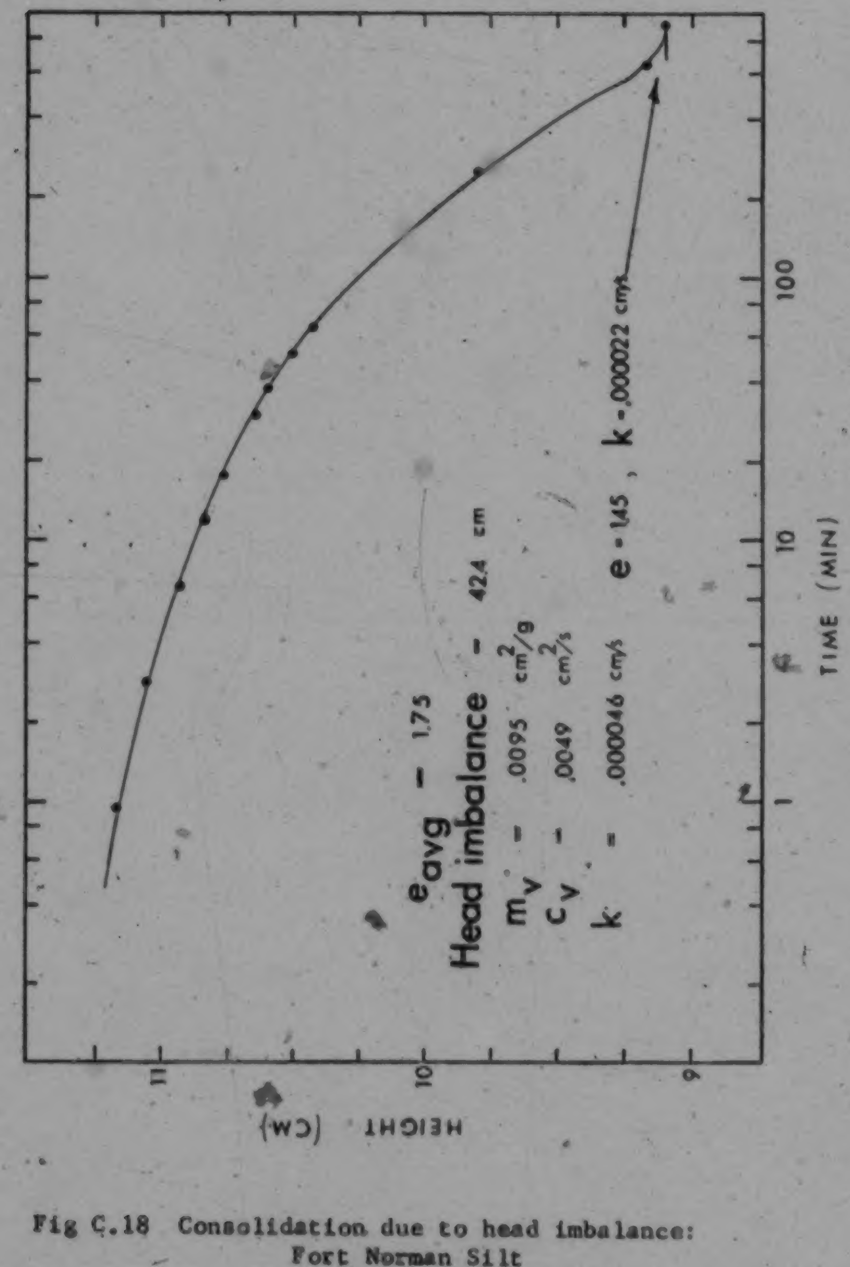

Fig C.18 Consolidation due to head imbalance: Fort Norman Silt

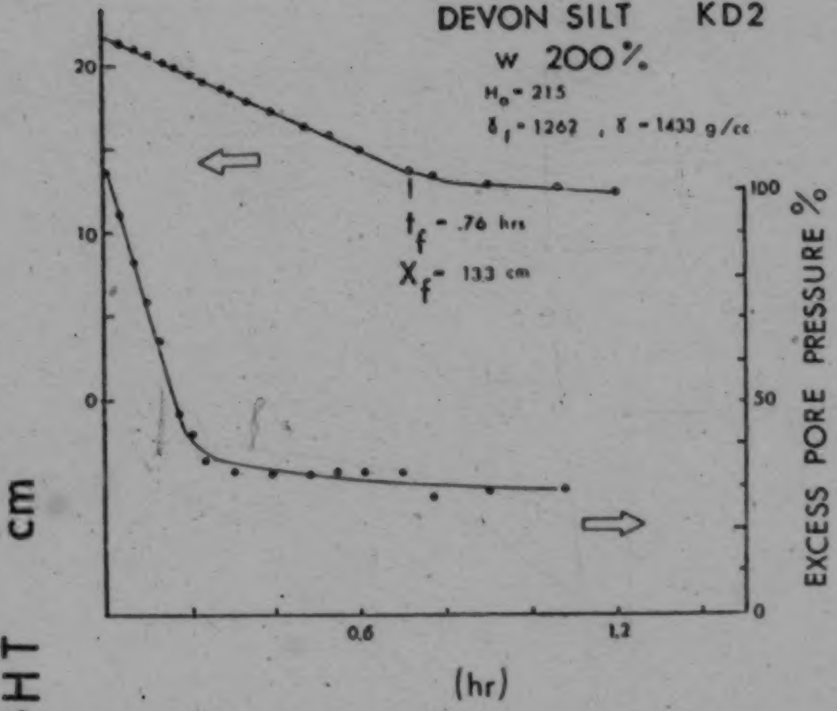

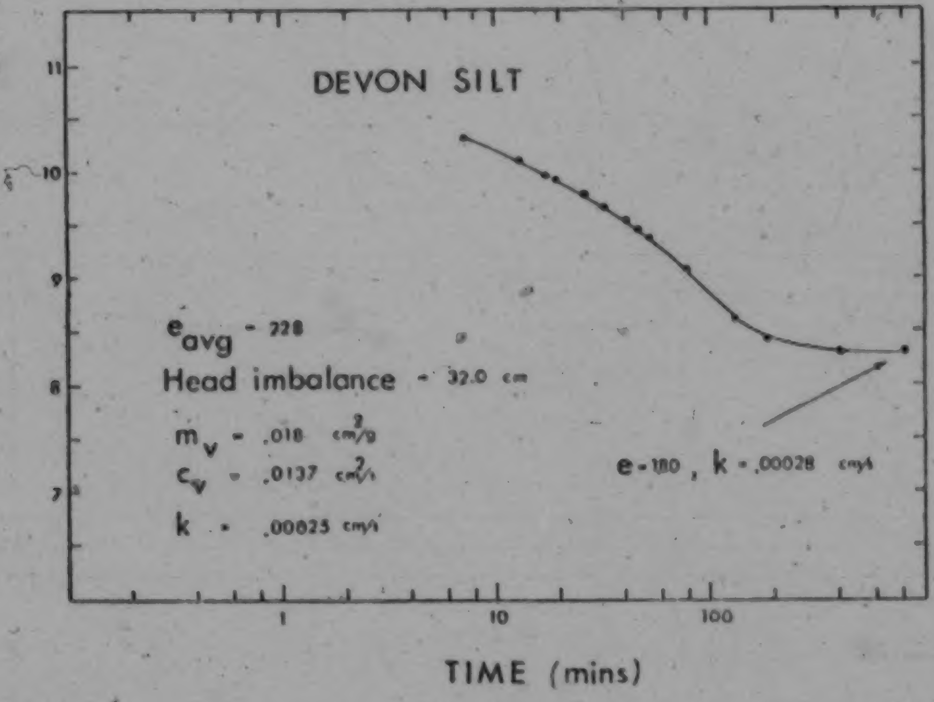

ABOVE Fig C.19 Hindered settling

BELOW Fig C.20 Consolidation due to head imbalance

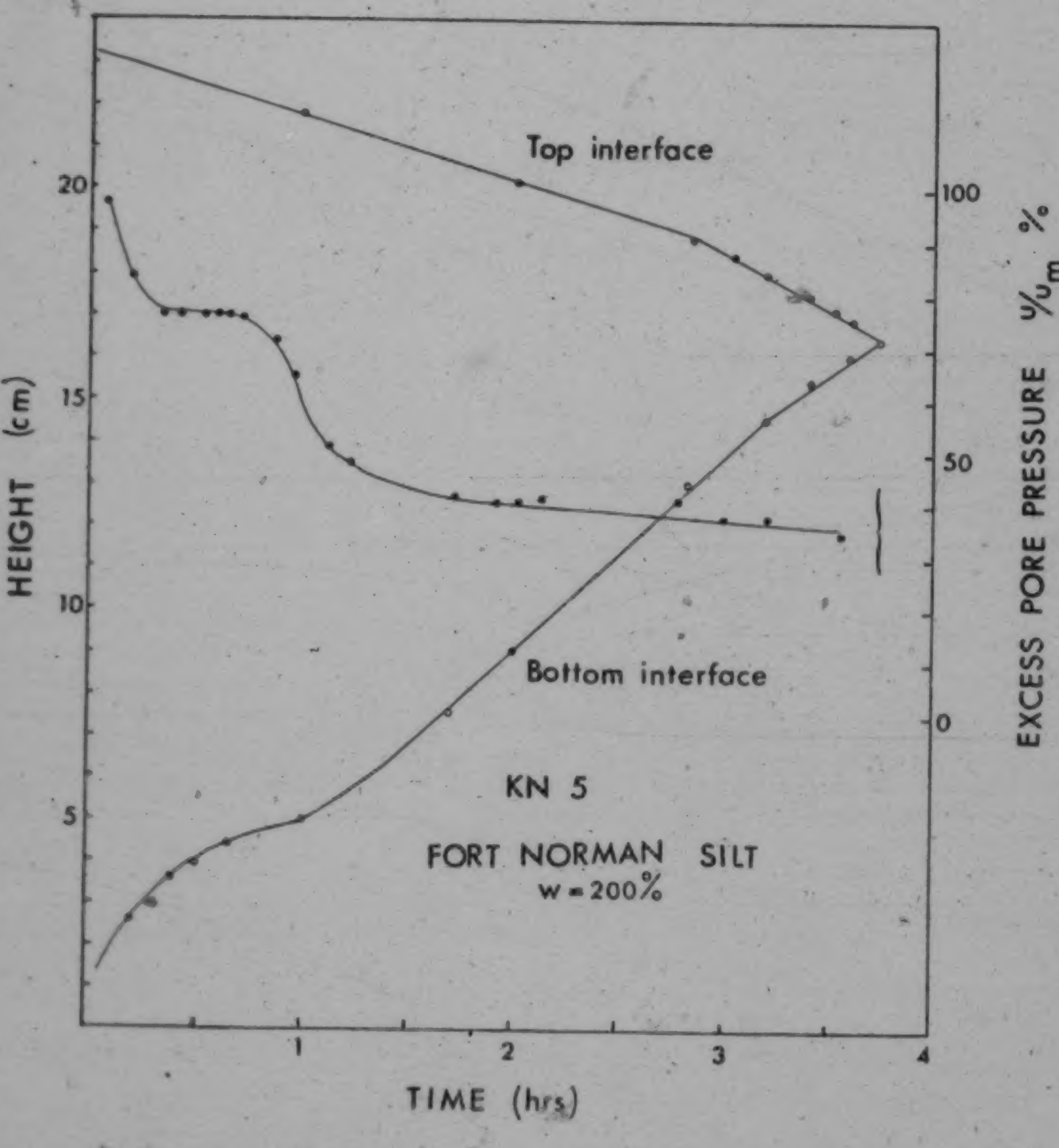

Fig C.21 Hindered settling: stirred Fort Norman Silt

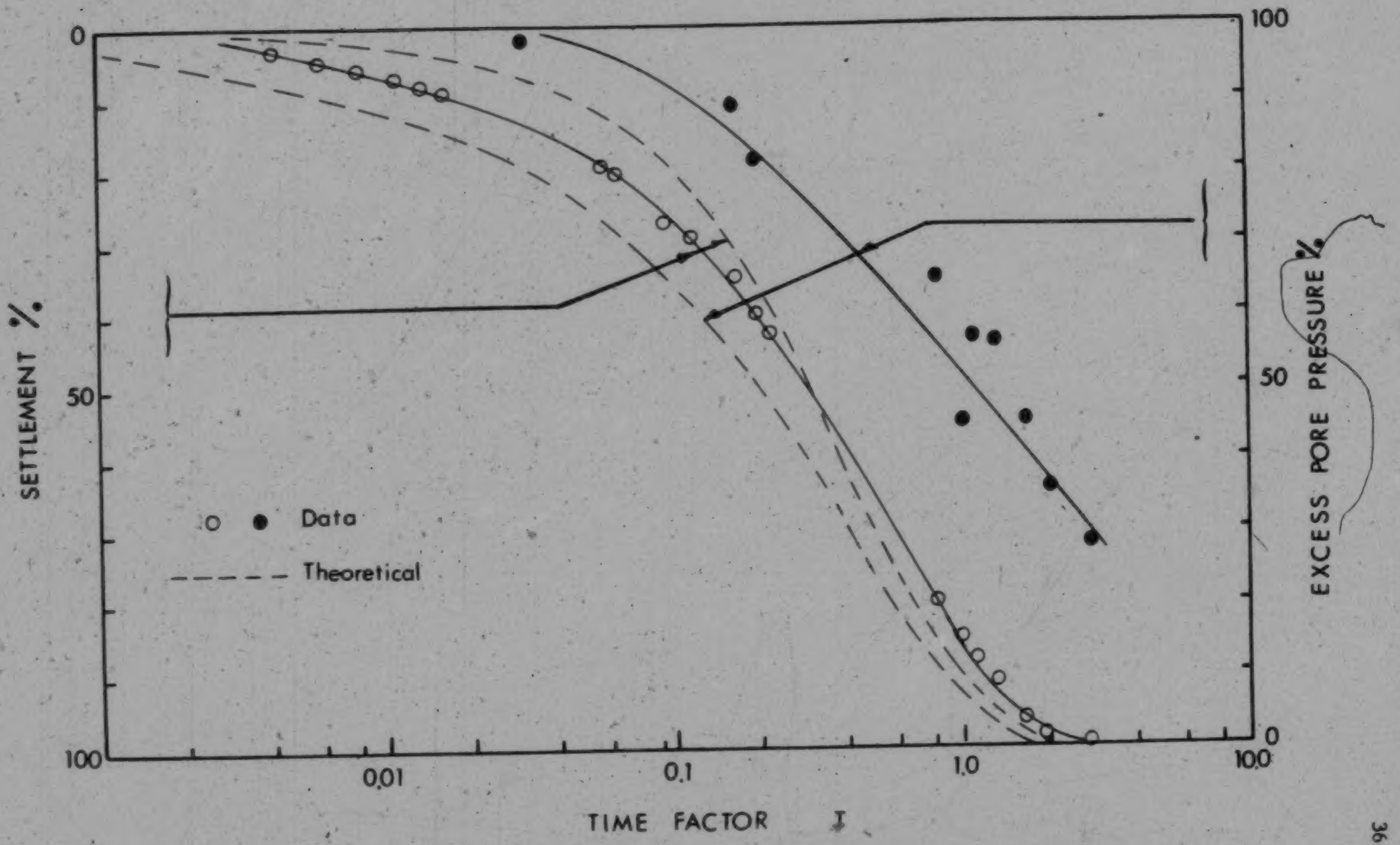

Fig C.22 Comparison of observed and predicted settlement and pore pressures, Fort Norman Silt

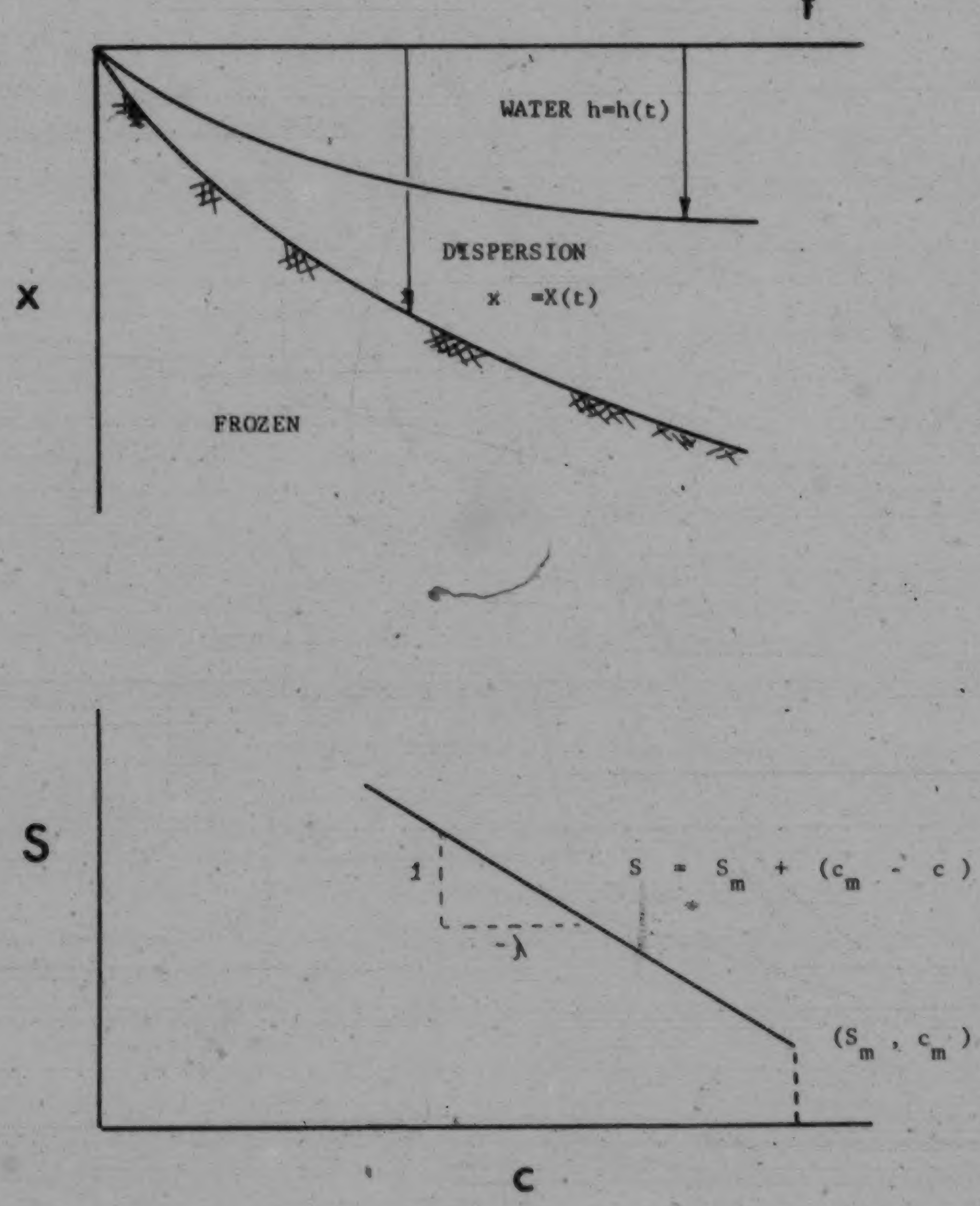
t
WATER h=h(t)
DISPERSION
x =X(t)
x
FROZEN
S
1
-λ
S = S_m + (c_m - c)
(S_m , c_m)
c

Fig C.23 The thaw-sedimentation problem

A P P E N D I X D

THE SOLUTION FOR THE FLOW SPECIFIED SEEPAGE PROBLEM

It is required to solve the Laplace equation

$$k\ (\nabla^2 \phi) = 0 \qquad \text{D.1}$$

for the problem outlined in Fig 4.2 for the following boundary conditions. Along the boundary 1 which is centreline symmetrical, it can be seen that

$$(\ x = 0,\ y\ ;\ \frac{\partial \phi}{\partial x} = 0\ ) \qquad \text{D.2}$$

and along boundary 2 which is an equipotential

$$(\ x = L,\ y\ ;\ \phi = 0\ ) \qquad \text{D.3}$$

and along boundary 3, an impervious layer

$$(\ y = 0,\ x\ ;\ \frac{\partial \phi}{\partial y} = 0\ ) \qquad \text{D.4}$$

A flow F is applied along boundary 4 so that

$$(\ y = B,\ x;\ F = \frac{\partial \phi}{\partial y}\ ) \qquad \text{D.5}$$

In the region where flow occurs

$$\nabla^2 \phi = 0 \qquad \text{D.6}$$

A solution is then sought using a separation of variables technique and assuming a solution of the form

$$\phi\ (x,y) = \phi_x\ (x) \cdot \phi_y\ (y) \qquad \text{D.7}$$

and by applying Eq D.5 we obtain

$$\phi_y \frac{\partial^2 \phi_x}{\partial x^2} + \phi_x \frac{\partial \phi^2_y}{\partial y^2} = 0 \qquad D.7$$

and we can assume

$$\frac{1}{\phi_x} \frac{\partial^2 \phi_x}{\partial x^2} = -\frac{1}{\phi_y} \frac{\partial^2 \phi_y}{\partial y^2} = -\lambda^2 \qquad D.9$$

so that the solution to the partial differential equation can now be expressed in terms of two ordinary differential equations

$$\frac{d^2\phi_x}{d x^2} + \lambda^2\phi_x = 0 \qquad D.10$$

$$\frac{d^2\phi_y}{d y^2} - \lambda^2\phi_y = 0 \qquad D.11$$

the solutions of which are

$$\phi_x = A \cos \lambda x + B \sin \lambda y \qquad D.12$$

$$\phi_y = C \sinh \lambda y + D \cosh \lambda y \qquad D.13$$

and which satisfy Eq D.6

Applying boundary conditions 1 and 3 we find that

$$B = C = 0 \qquad D.14$$

at boundary 2 we note that, applying Eq D.3

$$\phi (L, y) = (A \cos \lambda L) (D \cosh \lambda y) = 0$$

and the only non-zero term is

$$\lambda = \frac{2n - 1}{2L} \Pi = k_n \text{ for all n} \qquad D.15$$

Thus we can write

$$\phi (x, y) = \sum_{n = 1}^{\infty} E_n \cosh (k_n y) \cos (k_n x) \qquad D.16$$

Applying Eq D.5 to Eq D.16

$$F = \sum_{n = 1}^{\infty} k_n E_n \sinh (k_n B) \cos (k_n x) \qquad D.17$$

$$\text{or } F = \sum_{n=1}^{\infty} \alpha_n \cos(k_n x) \tag{D.18}$$

Multiplying both sides by $\cos k_m x$ and integrating from ($x = 0$, to $x = L$)

$$\int_0^L F \cos(k_m x)\, dx = \int_0^L \sum_{n=1}^{\infty} \alpha_n \cos(k_n x) \cos(k_m x)\, dx \tag{D.19}$$

It can be shown that the LHS of Eq D.19 is equal to

$$\text{LHS, Eq D.19} = \frac{F}{k_m} \sin(2n-1)\frac{\Pi}{2} \tag{D.20}$$

and it can be shown for the RHS, Eq D.19 that only at $n = m$ do we get non zero terms so that the RHS becomes equal to

$$\text{RHS, Eq D.19} = \frac{\alpha_m L}{2} \tag{D.21}$$

or we can write as $n = m$

$$\alpha_n = \frac{2F}{Lk_n} \sin(2n-1)\frac{\Pi}{2} \tag{D.22}$$

It follows from Eq D.17, D.18 that

$$E_n = \frac{\alpha_n}{k_n \sinh(k_n L)} \tag{D.23}$$

and substituting Eq D.15, D.22 in Eq D.23

$$E_n = \frac{8FL}{\Pi^2} \frac{\sin(2n-1)\frac{\Pi}{2}}{(2n-1)^2 \sinh\left(\frac{2n-1}{L}\right)\frac{\Pi}{2}} \tag{D.24}$$

and it follows that as ($\phi = -kH$, Eq 4.14) that from Eq D.16

$$H(x, y) = \sum_{n=1}^{\infty} \frac{8FL}{\Pi^2 k} \frac{\sin(2n-1)\frac{\Pi}{2}}{(2n-1)^2} \cdot$$

$$\cdots\cdots \quad \cdot \; \frac{\left(\cosh\,(2n-1)\,\frac{\pi y}{2L}\right)\left(\cos\,(2n-1)\,\frac{\pi x}{2L}\right)}{\sinh\,(2n-1)\,\frac{\pi B}{2L}} \tag{D.25}$$

The solution is then given by Eq D.25 which expresses the excess head required to cause flow at any point in the region of Fig 4.2. Along the top, flow specified boundary

$$H(x,B) = \frac{8FL}{k\pi^2} \sum_{n=1}^{\infty} \frac{\sin\,(2n-1)\frac{\pi}{2}\;\coth\,(2n-1)\frac{\pi B}{2L}\;\cos\,(2n-1)\frac{\pi x}{2L}}{(2n-1)^2} \tag{D.26}$$

The boundary conditions Eq D.2 to D.4 are identically satisfied by Eq D.25. For the surface (x,B)

$$\frac{\partial \phi}{\partial y}\,(x,B) = \frac{4F}{\pi} \sum_{n=1}^{\infty} \frac{\sin\,(2n-1)\frac{\pi}{2}\;\cos\,(2n-1)\frac{\pi x}{2L}}{(2n-1)} \tag{D.27}$$

It can be shown that the terms under the summation sign in Eq D.27 are identically equal to $\frac{\pi}{4}$ at (x=0,L) and, therefore, Eq D.5 is identically satisfied at (x=0,L). A computer solution summing the first 100 terms of Eq D.27 for x/L ratios from 0.1 to 0.9 showed that Eq D.5 was satisfied for all points $(0 < x < L,\ y = B)$. As it is easily shown that Eq D.25 satisfies the Laplace equation Eq D.1 and as all boundary conditions are satisfied the solution to the problem has been obtained.

By expressing the head as a normalized ratio, Eq D.25 may be written in terms of three dimensionless variables or as

$$\frac{H\,(x,B)}{\frac{FL}{K}} = \text{function}\left(\frac{x}{L}, \frac{B}{L}\right) \tag{D.28}$$

The solution for the head along the top surface $(0 < x < L,\ y = B)$ can be presented graphically in terms of these three variables, Fig 4.3. The Eq D.28 has been solved by summing the first 100 terms of the series expansion. Greater than 99.0% convergence is obtained.

A linear relation was noted between the normalized head and B/L for values of B/L greater than 10^{-1} and up to 10^{-6}. Therefore, if a solution is required for B/L ratios smaller than those presented in Fig 4.3 the indicated relation may be extrapolated as required.